THE REGULATION OF URIDINE 5'DIPHOSPHO-GLUCURONOSYLTRANSFERASE 1A (*UGT1A*) GENE FAMILY MEMBERS BY VITAMIN D RECEPTOR

Khanyile Merritt Dube

BSc (Hons) Biomedical Sciences

Research conducted within

The School of Biomedical Science

Faculty of Life and Health Sciences

University of Ulster

A thesis submitted for the degree of

Doctor of Philosophy

October 2020

I confirm that the word count of this thesis is less than 100,000 words

Contents

List of Figures

List of Tables

DECLARATION

"I hereby declare that for 2 years following the date, on which the thesis is deposited in the Research Office of the University of Ulster, the thesis shall remain confidential with access or copying prohibited. Following expiry of this period I permit

1. The Librarian of the University to allow the thesis to be copied in whole or in part without reference to me on the understanding that such authority applies to the provision of single copies made for study purposes or for inclusion within the stock of another library.

2. The thesis to be made available through the Ulster Institutional Repository and/or EThOS under the terms of the Ulster eThesis Deposit Agreement which I have signed.

IT IS A CONDITION OF USE OF THIS THESIS THAT ANYONE WHO CONSULTS IT MUST RECOGNISE THAT THE COPYRIGHT RESTS WITH THE UNIVERSITY AND THEN SUBSEQUENTLY TO THE AUTHOR ON THE EXPIRY OF THIS PERIOD AND THAT NO QUOTATION FROM THE THESIS AND NO INFORMATION DERIVED FROM IT MAY BE PUBLISHED UNLESS THE SOURCE IS PROPERLY ACKNOWLEDGED."

Acknowledgements

My first thank you goes to Dr Paul Thompson for giving me the opportunity to complete my PhD in your laboratory. The journey was not easy but through your guidance, patience and shared knowledge it was all possible. Your time, resources and the many valuable lessons are appreciated and will serve me well in my continued career as a scientist. In addition, Dr Patricia Rodriguez, thank you for the many lessons, training and the chats that kept me going. All your efforts in my journey will also be fondly appreciated.

I would also extend a thank you to my family, Mom, Dad, SJ for supporting me and putting up with the long journeys to NI. I greatly appreciate all the prayers more than anything and for being a listening ear, even though you may not have understood what I was talking about!

To my extended family at Coleraine SDA Church and London-Derry SDA Church, thank you for providing me with a home away from home. To my friends,I could not possibly name you all but I do appreciate each one of you.

My fellow NICHE colleagues, the NICHE department, Doctoral College and the Department of Education and Learning (DEL), thank you for the opportunity to complete my studies here at Ulster University.

Most important, I would like to thank God for hearing my every prayer.

Summary

UGT1A gene family members encode for phase II metabolic enzymes that play a crucial role in the biotransformation of endogenous and exogenous compounds into highly active, lower activity or inactive compounds that are easily excreted from the body. Many of these compounds include clinically administered drugs, hormones, bile acids and environmental toxins. Compromised or excess expression of the *UGT1A* genes is commonly associated with adverse consequences such as hyperbilirubinemia, cancer progression or undesired drug-drug interactions. Whilst a substantial amount of research has linked hepatic *UGT1A* gene expression to activated pregnane X receptor (PXR), upcoming research has evidenced extrahepatic UGT1A activity as very clinically relevant, although influenced by vitamin D receptor (VDR). Research in this direction is still at its infancy, the extent, clinical consequences and molecular mechanisms are not well understood. This project aims to characterize VDR in the detoxification processes, particularly, the regulation of UGT1A gene family members and the molecular mechanisms involved. Therefore, to address this issue, LS180 cells, that imitate 1,25D's colonic physiological responses were used to investigate the regulation of the entire family at mRNA, protein and functional level. A series of reporter-based assays were implemented to define a functional and VDR specific binding motif. Upon identification of *UGT1A4* as the most responsive to VDR ligands, novel tools such as CRISPRi genome editing, molecular cloning and characterization of the *UGT1A* promoter region were employed to examine putative binding motifs. To extend upon this study, novel molecular mechanisms, to investigate the reciprocal effects of cross-talk between VDR and NRF2 signalling pathways were examined. This interplay has direct implications for a range of physiological and pathological consequences, including enhanced detoxification, cancer prevention and anti-aging properties. Contrary to previous findings, we identified that VDR was in this case dependant upon intact NRF2 signalling. Furthermore, the interaction of both NRF2 and VDR signalling pathways did not significantly enhance *UGT1A* gene expression, although, surprisingly, inhibitory effects were observed. Although LS180 cells were predominantly used in our novel approaches, future studies should incooperate other cell model systems were NRF2 expression is abundant.

Collectively this study contributes towards our understanding of VDR and its co-operative activities that influence *UGT1A* gene expression and NRF2 signalling pathways. Whilst the study highlights the impact of VDR ligand co-administration with glucuronidation susceptible drugs, this study reinforces the importance of maintaining optimal 1,25D levels for chronic disease prevention, management of hereditary hyperbilirubinemia and neonatal jaundice. Perhaps, employing novel approaches using these findings will be the best advancement, where *UGT1A* expression is compromised.

ABBREVIATIONS

1,25D	1,25-dihydroxyvitamin D
25(OH)D_3	25-hydroxyvitamin D
3kLCA	3-keto-lithocholic acid
7-DHC	7-dehydrocholesterol
AhR	Aryl hydrocarbon Receptor
AKRs	Aldo-keto reductase
ALOX5	Arachidonate 5-lipoxygenase
ARE	Anti-oxidant Response Element
ARV	Antiretroviral
ATIR	Angiotensin II Type 1 Receptor
BAK1	BCL2 Antagonist 1
BBB	Blood Brain Barrier
Bcl	B-cell lymphoma 2
BIRC5	Baculoviral IAP Repeat Containing 5
BP	Blood Pressure
BTB	Blood-thymus barrier
bZIP	Basic Leucine-Zipper
cAMP	Cyclin Adenosine Monophosphate
CAP	Catabolite Activator Protein
CAR	Constitutive Androstane Receptor
CCNC	Cyclin C
CDCA	Chenodeoxycholic Acid
CDK1	Cyclin-dependant kinase 1
CDKN1A	Cyclin Dependant kinase inhibitor 1 A
cDNA	complementary DNA
CHD6	Cadherin 6
ChIP-Seq	Chromatin Immunoprecipitation -Sequencing
c-MYC	myelocytomatosis
CNC	Cap ‘N’ Collar
CNS I/II	Cigler Nigger Syndrome 1/II
CRC	Colorectal Cancer

CREB	cAMP response element-binding protein
CREB-1	CAMP Responsive Element Binding Protein 1
CRISPRi	Clustered Regulatory Interspaced Short Palindromic Repeats *interference*
crRNA	crisprRNA
CSS	Charcoal Stripped Serum
Ct	Cycle Threshold
Cul3	Cullin 3
CYP	Cytochrome P450
CYPs	Cytochrome P450s
DBD	DNA Binding Domain
DC	Dendritic cells
D-Cys	D-Cysteine
DDI	Drug-Drug Interactions
DFFB	DNA Fragmentation Factor Subunit Beta
DHEA	Dehydroepiandrosterone
DKK-1	Dickkopt WNT Signalling Pathways Inhibitor 1
DKK-4	Dickkopt WNT Signalling Pathway Inhibitor 4
DMEM	Dulbecco's Modified Eagle Medium
DMSO	Dimethyl sulfoxide
D NA	Deoxyribonucleic acid
DNA	Deoxyribonucleic Acid
dNTP	deoxyribonucleotide triphosphate
DR3	Direct Repeat motif
ECACC	European Collection of Authenticated Cell Culture
EDTA	Ethylenediaminetra acetic acid
EFSA	European Food Safety Authority
EMSA	Electronic Mobility Shift Assay
ER	Endoplasmic Reticulum
ER6	Everted Repeat
EtOH	Ethanol
FBS	Fetal Bovine Serum
FGF23	Fibroblast Growth Factor 23

FGFR	Fibroblast Growth Factor Receptors
FTH	Ferritin heavy
FXR	Farnesoid X Receptor
G6PD	Glucose 6 phosphate dehydrogenase
GADD45A	Growth Arrest and DN Damage Inducible Protein Alpha
GADD45A	Growth Arrest DNA Damage-inducible Protein Alpha
GC%	Guanine-Cytosine percentage
GCLC	Glutamate-Cysteine Ligase Catalytic Subunit
GCLM	Gamma-glutamycysteine synthetase
gDNA	genomic Deoxyribonucleic Acid
GPX2	Glutathione Peroxidase 2
GR	Glucocorticoid Receptor
GS	Gilbert's Syndrome
GSH	Glutathione
GSH	Glutathione
GSK-3	Glycogen Synthase Kinase
GSR1	Glutathione Reductase
GSTP1	Gluthathione S-transferase P1
gtPBREM	Phenobarbital-responsive enhancer module
HAT	Histone Acetyltransferase
hCAPI8	Human Cationic Antimicrobial Protein
HCl	Hydrogen Chloride
HDAC	Histone Deacetylase
Her2	Human Epidermal Growth Factor Receptor 2
HLM	Human Liver Microsomes
HMOX1	Heme Oxygenase 1
HNF1α	Hepatocyte Nuclear Factor 1 Alpha
HNL	Human Neutrophil Lipopcalin
HPRT	Hypoxanthine-guanine phosphoribosyltransferase
HSF1	Heat Shock Factor 1
HUVEC	Human Umbilical Vein Endothelial Cells
Ig	Immunoglobulin
IL	Interleukin

IOM	Institute of Medicine
IR6	Inverted Repeat sequence
IRF8	Interferon Regulator Factor 8
IU	International Units
JKN	c-JUN N-Terminal Kinase
JMJD3	Jumonji Domain Containing Protein
Kb	Kilobase
KCl	Potassium Chloride
kDA	kilo Daltons
KEAP1	Kelch-like ECH-associated protein 1
KRAS	Cellular Transforming Proto-Oncogene
LBD	Ligand Binding Domain
LCA	Lithocholic Acid
LC-MS/MS	Liquid Chromatography Mass Spectrometry
LRPS	Low Density Lipoprotein Receptor-Related Protein
LXR	Liver X Receptor
MDR1	Multi-drug Resistance-1
ME1	Malic Enzyme 1
MEM	Minimum Essential Media
MHC	Major Histocompatibility Complex
miR	micro RNA
MMP9	Matrix metallopeptidase 9
MPA	Mycophenolic Acid
MPTP	1-methyl-4-phenyl-1,2,3,6-tetrahydropyridine
mRNA	messenger Ribonucleic Acid
MRP	Multidrug Resistance-Associated Protein
MS	Multiple Sclerosis
MUT	Mutant
NaCl	Sodium Chloride
NADPH	Nicotinamide Adenine Dinucleotide Phosphate
NaOH	Sodium Hydroxide
NCBI	National Center for Biotechnology Information
NEAA	Non-Essential Amino Acids

Neh	NRF2-ECH homology
NF-E2/API	Nuclear Factor Eythroid-derived 2/Activator Protein 1
NFκB	Nuclear Factor Kappa Light Chain Enhancer of Activated B Cells
NOX	NADPH oxidase
NQO1	NAD(P)H Quinone Dehydrongenease 1
NR	Nuclear Receptor
NRF2	Nuclear Factor 2 Erythroid 2 receptor 2
NSCLC	Non-small cell lung carcinoma
OS	Oxidative Stress
P/S	Penicillin/ Streptomycin
PAM	Protospacer Adjacent Motif
PCa	Prostate Cancer
PD	Parkinson's Disease
PGD	Phosphogluconate Dehydrogenase
PMCA1b	Plasma Membrane Ca^{2+} ATPase
PPAR	Peroxisome Proliferator Activated Receptor
pRL-TK	Renilla Luciferase
PTH	Parathyroid hormone
PXR	Pregnane X Receptor
qPCR	Real Time Polymerase Chain Reaction
RAC3	Rac Family Small GTPase 3
RAGE	Receptor for Advanced glycation endpoints
RANKL	Receptor activator of nuclear factor kappa-B ligand
RDA	Recommended Daily Allowance
Rif	Rifampicin
RIPA	Radio immunoprecipitation assay
RL-D5/D6	Receptor Activator of Nuclear Factor κB ligand enhancer 5/6
RNA-seq	RNA sequencing
RNP	Ribonucleoprotein
ROS	Reactive Oxygen Species
RSAT	Regulatory Sequence Analysis Tool
RT-PCR	Reverse transcriptase polymerase chain reaction
RXR	Retinoid X Receptor

SCF	Stem Cell Factor
SDS	Sodium dodecyl sulfate
sgRNA	short guide Ribonucleic Acid
siRNA	Small Interfering ribonucleic acid
SIRT6	SIR2-Like Protein 6
sMAF	small Musculoaponeurotic Fibrosarcoma
SN-38	7-ethyl-10-hydroxy-camptothecin
SNPs	Single Nucleotide Polymorphism
SOD1	Superoxide dismutase 1
SP1	Specificity Protein 1
SRC	Proto-oncogene tyrosine kinase
SULTs	Sulfotransferases
T_4	Thyroid Hormone
TAE	Tris-acetate
*t*BHQ	*tert*-butylyhydroquione
TBT-T	Tris-buffered saline
TCDD	2,3,7,8 Tetrachlodibenzodioxin
TCF4	Transcription Factor 4
TCF7	Transcription Factor 7
TCPOBOP	1,4-Bis(3,5-Dichloro-2-pyridinyloxy)benzene
TF	Transcription Factor
TFL	Protein Terminal Flower 1
Tg	Transgenic
TID	Type 1 Diabetes
TLCA	Taurolitho-cholic acid
TLR	Toll-like Receptor
TNF	Tumour Necrosis Factor
TNFα	Tumour Necrosis Factor α
Trp53	Tumour Protein 53
TRPVs	Transient Receptor Potential Cation Channel subfamily V
TSS	Transcription Start Site
U290	UGT1A1-290bp
U2K	UGT1A1-2000bp

UDPGlcA	UDP glucuronic acid
UGT1A	UDP-glucuronosyltransferase 1 A
UVB	Ultra Violet B
V	Volts
VCAM-1	Vascular Call Adhesion Protein 1
VDBP	Vitamin D Binding Protein
VDR	Vitamin D Receptor
VDRE	Vitamin D Response Element
VEGF	Vascular Endothelial Growth Factor
WT	Wild-Type
XRE	Xenobiotic Response Element
β-Trcp	Beta-Transduction Repeat Containing E3 Ubiquitin Protein Ligase
Γ-GT	Gamma Glutamyltransferase

1: Chapter 1

General Introduction

1 Introduction

1.1 Vitamin D and its bio-synthesis

The structural characterization of Vitamin D led to the isolation of Vitamin D_2 from an irradiation mixture and Vitamin D_3 from 7-dehydrocholesterol (7-DHC) (Askew *et al.,* 1932). Holick *et al.,* (1981) revealed a new Vitamin D concept signifying that pre-Vitamin D_3 was formed in the skin via ultra violet (UVB) irradiation. To date, the skin is the most important source of Vitamin D_3, which is dependent upon UVB intensity (*290-320nm*), melanin (which blocks UVB from reaching 7-DHC), sunscreen, clothing, season and latitude (Holick, 2004). With regards to the latter, the further from the equator, the less solar exposure to produce Vitamin D_3 (Jelinek *et al.*, 2015). UVB disrupts a *b*-ring on the 7-DHC, found in the epidermal layer of the skin. This forms the thermo-sensitive pre-Vitamin D_3 (Webb *et al.,* 1989). Reacting to the 37°C body heat in a non-catalytic process, pre-vitamin D_3 isomerizes to form Vitamin D_3 (cholecalciferol) (Webb *et al.,* 1989) (See Figure 1.1). Vitamin D can also be acquired through a limited selection of dietary foods including fatty fish and UVB irradiation of the ergosterol in plants (green leafy vegetables and fungi) forming Vitamin D_2 (Holick *et al.,* 2008).

The difference between Vitamin D_3 and D_2 is that the latter has a double bond between Carbon 22 (C-22), C-23 and in addition, a methyl group at C-24 in the side chain (Hollis *et al.,* 1984). These differences affect catabolism capabilities; hence, a higher Vitamin D_2 dose is required to reach comparable amounts of Vitamin D_3 in the blood stream (Hollis *et al.,* 1984). Furthermore, Vitamin D_2 has a lower affinity for association with Vitamin D Binding Protein (VDBP) and faster clearance from the circulation (Delanghe *et al.,* 2015). A major proportion of Vitamin D is bound to the VDBP, which functions to transport Vitamin D metabolites between the liver, kidney and various other target tissue (Delanghe *et al.,* 2015).

1.1.2 Hepatic and Renal Metabolism of Vitamin D

Both Vitamin D_3 and Vitamin D_2 are not biologically active, and as such, go through a series of metabolic reactions to reach a biologically active state (Tripkovic *et al.,*

2012). Transported by VDBP, the first site of metabolism is the liver, where the hepatic endoplasmic reticulum (ER) phase I metabolic enzyme, cytochrome P450 2R1 (CYP2R1) facilitates in C-25 hydroxylation producing the 25-hydroxyvitamin D_3 (25(OH) D3), which is the major circulating form of Vitamin D, serving as a biomarker for Vitamin D status (Zerwerk, 2008). The 25(OH) D_3/VDBP complex is filtered in the kidney (glomerulus) were the VDBP binds to the lipoprotein known as megalin, resulting in the endocytotic internalization of 25(OH) D_3 (Kalousovu *et al.,* 2015). 25(OH) D_3 is further hydroxylated at the C-1 position of the α-ring by the CYP27B1 forming 1,25-dihydroxyvitamin D_3 ($1,25(OH)_2D_3$) (referred to as 1,25D hereafter), the functional form of Vitamin D, responsible for all of its biological actions (Kalousovu *et al.,* 2015) (See Figure 1.1).

1.1.3 Homeostatic control of Vitamin D

1,25D homeostatic control is facilitated by a strict balance between its 1α-hydroxylation and 24-hydroxylation, by the mitochondrial CYP24A1 enzyme (Jones *et al.,* 2011). The latter results in 1,24,25-dihydroxyvitamin D_3, a target for excretion (Jones *et al.,* 2011). Both enzymes are rigorously controlled by 1,25D, serum calcium and phosphate levels (Veldurthy *et al.,* 2016). Low calcium or 1,25D causes parathyroid hormone (PTH) secretion by the parathyroid glands (Veldurthy *et al.,* 2016). This stimulates increased expression of *CYP27B1*, resulting in 1,25D synthesis (Anderson *et al.,* 2004). On the other hand, PTH inhibits CYP24A1 enzymatic activity whilst inducing fibroblast growth factor 23 (FGF23) synthesis in osteoclast and osteocytes, causing a reduction in sodium phosphate transporters (Shigematsu *et al.,* 1986). Interestingly, FGF23 controls 1,25D levels by suppressing CYP27B1 enzymatic activity, while increasing that of CYP24A1 (Haussler *et al.,* 2012). In this case, 1,25D and calcium are reduced under hyperphosphatemia conditions. Klotho is highly expressed in the distal tubule of the kidney, and acts as an obligate co-receptor for FGF23 and as such required by FGF23 to activate fibroblast growth factor receptors (FGFRs) (Donate-Correa *et al.,* 2019). Similar to FGF23, klotho also suppress the expression of *CYP27B1* and induces *CYP24A1*, thereby inhibiting the synthesis and promoting the catabolism of 1,25D (Bachetta *et al.,* 2013). The actions of *CYP24A1* increase with age, hence the increase in 1,25D catabolism, which is a contributory factor to age –related bone loss (Bachetta *et al.,* 2013). *CYP24A1* also

mediates intracellular 1,25D as it is also expressed in cells containing VDR (Osanai and Lee, 2016). These findings have been the forefront of Vitamin D analogue design and *CYP24A1* inhibitors.

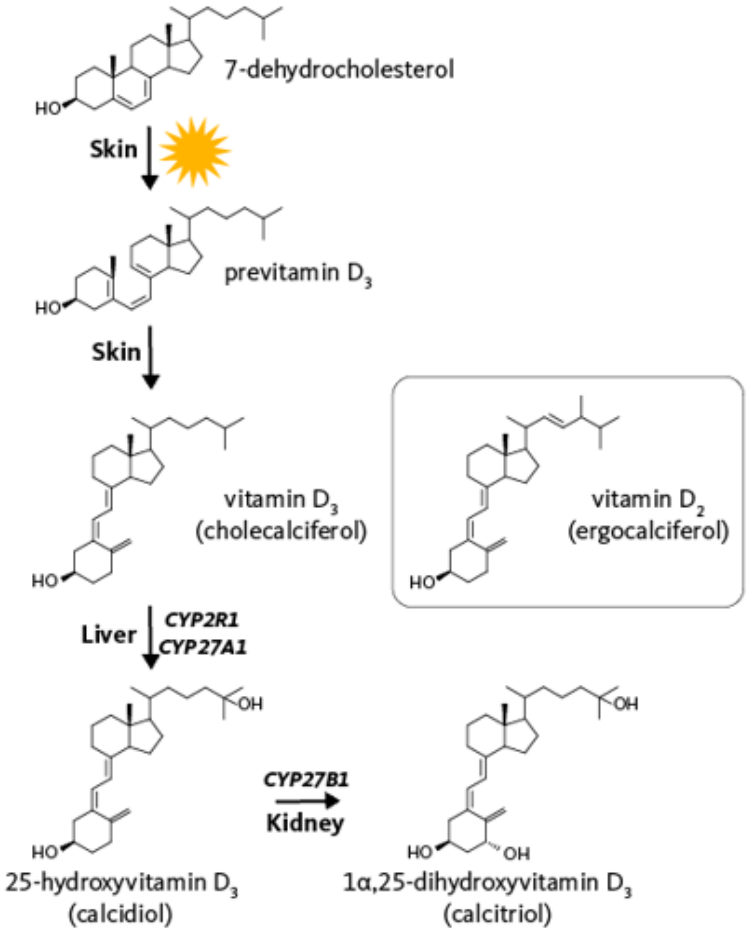

Figure 1.1: Chemical Structures and Vitamin D Biosynthesis. *Pre-Vitamin D_3 is synthesized in the epidermal layer of the skin from 7-dehydrocholesterol by the action of UVB light from sunlight. Thermal isomerization converts pre-Vitamin D_3 to Vitamin D_3 , which is transported to the liver. Hepatic CYP2R1 and CYP27A1 enzymes catalyse 25-hydroxylation of Vitamin D_3 and the plant-based Vitamin D_2. The product is further transported to the kidney for a further 1α-hydroxylation to the biologically active form, 1α,25-dihydroxyvitamin D_3 by CYP27B1. Holick et al., 1987) (Image edited from Vitamin D, 2020)*

1.2 Actions of Vitamin D

1.2.1 Regulation of Mineral Homeostasis (Classical Role of Vitamin D)

1,25D regulates calcium and phosphate levels by facilitating absorption, renal excretion and calcium bone utilization (Mundy and Guise, 1999). Diminished calcium levels lead to PTH secretion and 1,25D synthesis, resulting in the stimulation of calcium renal re-absorption (Blaine *et al.,* 2015). If the calcium levels are in excess, the parafollicular cells on the thyroid secrete calcitonin, block calcium mobilization and increase calcium and phosphorus excretion (Morris and Anderson, 2010). This process regulates calcium levels. Conversely, an increase in serum calcium levels reduces PTH secretion, 1,25D synthesis and calcium utilization (Morris and Anderson, 2010).

Additionally, 1,25D targets three tissues for mineral homeostatic control (Fleet, 2017). In intestinal tissue, 1,25D stimulates intestinal calcium absorption, though affected by intestinal solubility, diet and absorption capacity (Fleet and Schoch, 2011). Optimum calcium levels are required for trans-cellular calcium transportation (Christakos *et al.,* 2011). Hoenderop *et al.,* (2003) characterized member of the transient receptor potential cation channel subfamilies V (TRPVs) including *TRPV6* as important calcium transport channels. The expression of these and other transporters (calbindin-D9K, and Plasma membrane Ca^{2+} ATPase 1b (PMCA1b)) are highly regulated by 1,25D (Choi and Jeung, 2008). Secondly, 1,25D along with PTH induces renal distal tubule reabsorption of calcium (Blaine *et al.,* 2015). 1,25D stimulates calcium cellular influx through the apical membrane, calbamicin-mediated calcium diffusion and its transportation through the basolateral membrane (Wong and Ko, 2002). Renal phosphate reabsorption is inhibited by 1,25D (Haussler *et al.,* 2012). This is an indirect consequence of FGF23 and klotho induction in osteocytes (Haussler *et al.,* 2012).

Additionally, 1,25D mobilizes calcium from the bone through the involvement of PTH (*Gil et al.,* 2018). Diminished calcium levels lead to PTH mediated 1,25D activation (Tebben *et al.,* 2016). Vitamin D Receptor (VDR)-induced differentiation of osteoclasts then follows (Takahashi *et al.,* 2014). This initiates calcium from the bone

by stimulating the secretion of receptor activator for nuclear factor kappa-β ligand (RANKL) which acts as a precursor for osteoclasogenesis and bone resorption (Boyce and Xing, 2008). Moreover, 1,25D inhibits mineralization through the increase of pyrophosphate levels and osteopontin (Gil *et al.,* 2018). 1,25D also promotes growth and bone formation through the activation of chondrocyte differentiation and increasing serum calcium and phosphate levels (Bikle, 2013). Evidently, Vitamin D deficiency results in inadequate mineralization of skeletal bones. 1,25D defiant individuals means bone health is diminished due to calcium and phosphate depletion. 1,25D suppresses the parathyroid gene expression and parathyroid cell proliferation, again reinforcing its control of calcium regulation (Bikle, 2013).

1.3 Clinical Recommendation of Vitamin D

1,25D is implicated with numerous clinical consequences (discussed in section 1.5).Therefore maintaining optimum levels within the global population is evidently vital. What is challenging to scientists are the many factors that impact optimum 1,25D levels. Even though 1,25D has been under scrutiny for most part of the century, there is still much controversy regarding its daily-recommended allowance (RDA), because the above-mentioned factors and many others need to be considered. Prior to 2010, the recommended RDA for an adult was 200IU/day (Glerup *et al.,* 2000). However, the USA Institutes of Medicine (IOM) refuted this because it only considered optimum levels for rickets prevention and not the other physiological benefits (Holick *et al.,* 2011). The IOM then recommended 600IU/day for an average adult and at least 800IU/day for adults over the age of 70, one reason being its increased catabolism rate (Boucher, 2012). Priemel *et al.*, (2010) recommended 20ng/ml 25(OH)D_3 serum concentration for adequate physiological health. This was challenged by Garland *et al.,* (2015) who observed that 30ng/ml 25(OH)D_3 yielded a better prognosis for chronic illnesses, although a limitation to this and similar studies is they point towards higher concentrations as the minimal for physiological webb-being. Consequently, even the IOM's recommendations were suggestive as a better fit for subclinical osteomalacia prevention (Bischoff and Willet, 2010). Modern societal habits prevent sunlight exposure from which 80% of Vitamin D is derived, and as such, across all of Europe, Vitamin D deficiency prevalence rates are a great concern

(Spiro and Buttris,2014). The current European guidelines recommend 30-50ng/ml. This was also in line with the guidelines for $25(OH)D_3$ in United Arab Emirates and Gulf population (Haq *et al,* 2018). These guidelines, unlike that of IOM do consider the pleotropic actions of 1,25D (Haq et al., 2018). The challenge with setting uniform RDA guidelines on a global scale depends of several clinical and environmental factors, including skin pigmentation, latitude of residence, diet, clothing and exposure to sunlight. Table 1.1 however**,** provides the recommended 1,25D daily intake guidelines taken from the IOM, European Food and Safety Authority (EFSA) and Scientific Committee or Food (SCF) (Spiro and Buttriss, 2014). Furthermore, authorities have since based their recommendations on the following blood levels (Norman, 2008):

- Severe Vitamin D Deficiency <5ng/ml
- Vitamin D Deficiency 5-10ng/ml
- Vitamin D insufficiency 10-20ng/ml
- Sufficient $25(OH)D_3$ > 30-60ng/ml
- Risk of toxicity >150ng/ml

While there is an urgent need to combat 1,25D deficiency, the RDA guidelines are critical, as excessive intake leads to toxicity, resulting in hypercalcemia and as such, doses beyond the RDA are administered for medical treatment (Tebben *et al.,* 2016).

Table 1.1: The recommended daily intake for Vitamin D, taken from EFSA and IOM (Spiro and Buttriss, 2014)

EFSA		IOM	
Tolerable upper intake level µg/day (IU/day)		**Tolerable upper intake level µg/day (IU/day)**	
0–12 months	25 (1000)	0–6 months	25 (1000)
1–10 years	50 (2000)	7–12 months	37.5 (1500)
11 years to adult	100 (4000)	1–3 years	62.5 (2500)
		4–8 years	75 (3000)
		9 years to adult	100 (4000)

1.4 Genomic Mechanisms of Vitamin D

1.4.1 Introduction to Nuclear Receptors

The biological responses of 1,25D are mediated by its actions as a ligand to the Vitamin D receptor (VDR) (Ryan *et al.*, 2015). VDR also known as nuclear receptor subfamily 1 group 1, member 1 (NR1I1), forms part of the 49 Nuclear Receptor (NR) superfamily members that evolved from common ancestry (Krasowski *et al.,* (2005) (Examples shown in Table 1.2). NRs are divided in to seven sub-families according to their homology in the ligand and DNA binding domains (Kwasowski *et al.*, 2005). Pregnane X Receptor (PXR, NR1I2) is the closest relative to VDR. Both share a common modular structure and also derived from a duplication of a single ancestral gene following examination of the *Ciona intestinalis* gene in the genome of chordate invertebrate (Reschley *et al.*, 2006).

Table 1.2: Examples of known NRs and their prototypical ligands (Sonoda *et al.*, 2008)

Nuclear Receptor Classification	Class	Denomination	Prototypical ligands
Vitamin D Receptor (VDR)	NR1I1	Endocrine Receptor	1,25D LCA 3kLCA
Glucocorticoid Receptor (GR)	NR3C1	Endocrine Receptor	Cortisol
Estrogen Receptor (ER)α,β	NR3A1,A2	Endocrine Receptor	Estradiol
Pregnane X Receptor (PXR)	NR1I2	Adopted Orphan Receptor	Rifampicin 5β-pregnane 3, 20 dione
Retinoid X Receptor (RXR) α,β,γ	NR2B1,B2,B3	Adopted Orphan Receptor	9-cis-retinoid acid
Liver X Receptor (LXR)α,β	NR1H2,H3	Adopted Orphan Receptor	T0901317
Farnesoid X Receptor (FXR)	NR1H4	Adopted Orphan Receptor	Chenodeocycholic acid
Constitutive Androstane Receptor (CAR)	NR1I3	Adopted Orphan Receptor	3α,5α-androstanol

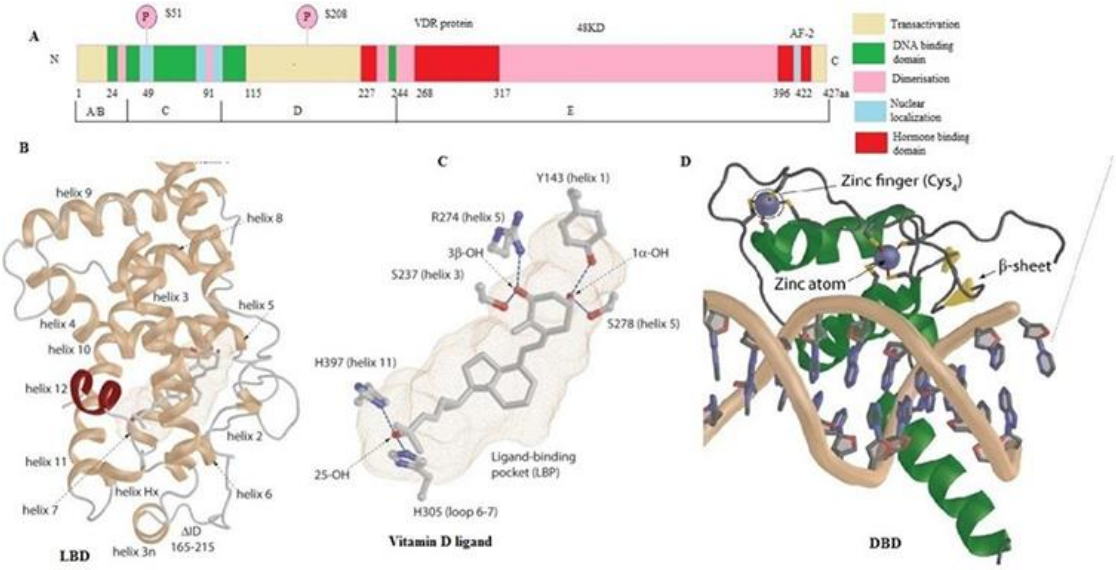

Figure 1.2: A schematic representation of VDR functional domains. *(A) VDR domains (B) Ligand binding domains (C) The binding mode of Vitamin D in the binding domain (D) The DNA binding domain of VDR. (Image from Iqbal and Khan, 2017).*

1.4.2 Vitamin D Receptor (VDR)

The past two decades of 1,25D examination have seen its influence on nearly every tissue and organ, across numerous species, including mammals, birds, amphibians, and reptiles (Krasowski *et al.,* 2011). At least all mammalian genomes analysed to date express the VDR gene (Reschly *et al.,* 2007). Human VDR expression ranges from brain, gut, skeletal muscle and immune cells. Detection in the liver and Central Nervous System (CNS) has been a challenge (Reschly *et al.,* 2007).

The 472 amino acid VDR protein encompasses two functional units, the DBD and the LBD. (See Figure 1.2) (Campbell *et al.,* 2010). Evidence from an x-ray crystallographic structure determined that the *α*-helical sandwich-like structure allows VDR surfaces to form heterodimers with retinoid x receptor- (RXRα, RXRβ or RXRγ), following its liganding with 1,25D (Dawson *et al.,* 2012). Only the liganded VDR/RXR heterodimeric complex is able to access and recognize the Vitamin D response elements (VDREs) in the DNA sequence of 1,25D target genes (Pike and

Meyer, 2010). VDREs commonly consists of either direct repeat of two half elements with three nucleotides spacers (DR3) with an AGGTCA consensus sequence (Thummel *et al.,* 2001). Everted repeat of two half-elements with 6 nucleotide spacers (ER6) are the less common responsive motifs (Thummel *et al.,* 2001). PXR also employs RXR as its heterodimeric partner. The complex also recognizes the DR3 and ER6 motifs (Wallace *et al.,* 2013). VDREs are typically positioned proximally in the promoter region of target genes, although this is not always the case (Pike and Meyer, 2010). For example, human *CYP3A4* VDRE is located close to 7.5kb upstream of its transcription start site (TSS) (Gombart *et al.,* 2012 and Thompson *et al.,* 2002). The genomic mechanism of 1,25D/VDR signaling results in either target gene transactivation or repression (Carlberg *et al.,* 2013). Following the heterodimeric complex binding to the VDRE, gene expression is mediated through the ability to recruit transcriptional complexes (Stees *et al.,* 2012). The co-regulatory complexes primarily bind to the AF-2/H12 domain of the VDR (Kraichely *et al.,* 1999). These include p160 co-activators, steroid receptor activators 1, 2 and 3 (SRC-1, SRC-2 and SRC-3) (Teichert *et al.,* 2009). SRC co-activators contain Leucine (L-xxL, x is any amino acid) motifs that facilitate binding to VDR and multiple other NRs (Teichert *et al.,* 2009). SRC co-activators recruit other secondary protein, for example, a large macromolecular co-activator complex, DRIP/TRAP, the CBP/p300 complex, SMAD-3 and NCoA62, which in addition to p160 co-activators have histone acetylase transferase (HAT) activity (Rachez *et al.,* 2000). Further emerging evidence of individual gene regulatory activities has so far detailed how the machineries operate to enhance or suppress the expression of target genes. Crystallographic analysis identified 1,25D inhabiting the hydrophobic pocket and molecular modelling identified lithocholic acid (LCA) to associate compatibly with VDR, also confirming the NR involvement in bile acid (BA) biology (Masuno *et al.,* 2013). Haussler *et al.,* (2016) further identified numerous low affinity VDR ligands including ω3- and ω6-essential polyunsaturated fatty acids (PUFAs), docosahexaenoic acid (DHA), arachidonic acid, and γ-tocotrienol (Vitamin E derivative). New knowledge on novel concepts will further the understanding of 1,25D/VDR signaling to develop sustainable nutritional solutions to prevent or treat diseases, particularly where VDR target genes are compromised.

1.4.3 Genome-wide studies of VDR/RXR binding in various cell lines

Transcriptome-wide analysis on numerous *in-vitro* and *in-vivo* models indicated more than 1000 genes are direct VDR target genes (Vukic *et al.,* 2015 and Pike *et al.,* 2016). On a genome-wide level, chromatin immunoprecipitation –sequencing (ChIP-seq) data has also expanded insight on the genomic VDR binding loci, with emerging data on B-lymphocytes, T+HP-1 monocytic cells and colon cancer cells (Meyer *et al.,* 2012). Beyond mineral homeostasis, 1,25D has been implicated with a global network of genes such as Cyclin Dependent Kinase Inhibitor 1A (CDKN1A), Glutamate-cystein ligase catalytic subunit (GCLC) in addition to the Growth arrest and DNA-damage-inducible protein (GADD45A), (involved in cell cycle, glutathione synthesis and growth regulation respectively) that function to maintain cellular as well as overall physiological health (Protiva *et al.,* 2009). Classically, much of 1,25D's physiological mechanisms have been investigated in whole organisms, however within the last decade, scientists have implemented powerful tools such as genome-wide microarrays, large-scale genome sequencing and genomic approaches for molecular characterization. Initially, the 1,25D-induced transcriptome by microarray analysis reported a small number of target genes from the colon, prostate and breast (Palmer *et al.,* 2003, Krishnan *et al.,* 2004 and Swami *et al.,* 2003). Although still in the early phase, Wang *et al.,* (2005) further identified 913 1,25D responsive genes by oligonucleotide microarray in *SCC25* cells. In the same study, a combination of 35,000 gene microarrays and genome-wide screens identified that 65% of the VDREs identified within 1,25D target genes were within -10 to 5kbp of the 5'-region (transcription start site ; TSS) of the gene. A study by Ramagopalan *et al.,* (2010) later determined 2776 VDR binding motifs in lymphoblastoid cells, with enriched sites within Cyclin-C gene (*CCNC),* the intronic region of Arachidonate 5-lipoxygenase (*ALOX5),* and *VDR* gene itself. The ChIP-seq analysis further determined significant changes in expression of genes such as Interferon regulatory factor 8 (*IRF8)* and Tyrosine-protein phosphatase non-receptor type 2 (*PTPN2)* following 1,25D exposure (Ramagopalan *et al.,* 2010). Further genome-wide investigation of 1,25D's actions was focused on osteoblasts in view of its bone anabolic activity (Meyer *et al.,* 2010). Meyer's *et al.,* (2010) ChIP-ChIP analysis refuted the tradition principle that suggests

that gene regulation occurs near the transcriptional start site (TSS). 43% binding sites occupied by VDR, RXR and H4 acetylation were distal, 44% within introns and exons (Meyer *et al.,* 2010) Only 13% motifs were proximally occupied (Meyer *et al.,* 2010) Interestingly, majority of basal VDR binding overlap those defined following 1,25D exposure, suggesting that selective occupancy by VDR does not require the ligand for activation (Meyer *et al.,* 2010). This is contrary to other TFs such as PXR where DNA binding is a principle characteristic. Another intriguing finding from the ChIP-seq data set is that RXR pre-occupies VDR binding motifs, suggesting that RXR is a good indicator of potential VDR activity (Meyer *et al.,* 2012). However, the fundamental nature of this binding is still not fully understood. *De novo* sequence motifs that represent both VDR/RXR complex binding motifs have since been implemented. The most common DR3-type VDRE consensus sequence, first identified by Kerner *et al.,* (1989) is frequently defined. In most experiments, the multiple VDREs on the genome have correlated with synergistic activation mechanism (Kim *et al.,* 2006). Additionally, Campbell (2014) suggested that the linking of distal with proximal VDREs via DNA chromatin looping creates a single platform that supports this synergistic transcriptome machinery (Figure 1.3). Chromatin configuration and the utilization of multiple VDREs works as an advantage in that, many co-regulatory complexes are recruited simultaneously, fine-tuning and contributing towards combinatorial synergistic transactivation (Campbell, 2014) Contrary to this, Onal *et al.,* (2016) suggested that unique distal enhancers are linked to transactivation. For example, enhancers RL-D5 and RL-D6, are involved in the induction of *RANKL,* but the same was not observed for RL-T1 enhancer (Onal *et al.,* 2016). More relevant to our study are genome-wide data sets from LS180 cells where 1,25D activities closely recapitulate intestinal and colon physiology (Meyer *et al.,*2012). In this study, 262 VDR binding motifs were identified under basal conditions; however, the ChIP-seq data reveals a 2209 increase following 1,25D treatment (Meyer *et al.,*2012) RXR binding also increased by 6-fold in a 1,25D dependant manner in the same study (Meyer *et al.,* 2012). RXR binding occupied over 75% VDR binding sites Meyer *et al.,* (2012). In addition to VDR/RXR binding motifs, transcription factor 7-like 2 (TCF7/L2/TCF4)/β-catenin cistromes and the genes these TFs regulate were also identified (Meyer *et al.,* 2012). Amongst these genes were c-*MYC, c-FOS* and *UGT1As,* again suggesting that the actions of 1,25D extend beyond mineral health

(Meyer *et al.*, 2010). Our laboratory and others have since defined functional VDREs within the genes' (CYP3A) promoter region. Investigations are still rudimentary; however, it is clear that 1,25D is of uttermost significance in malignancies and detoxification pathways. Altogether these and subsequent studies applying advanced molecular approaches will provide a new insight into cell and tissue specific 1,25D activity.

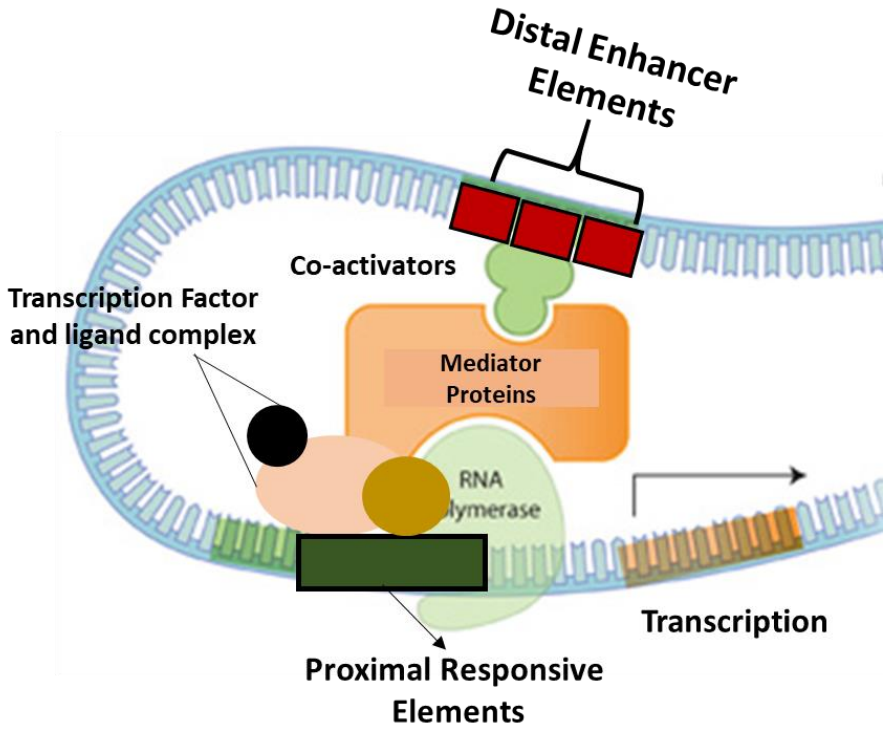

Figure 1.3: Gene transcription activity. *Gene transcription is tightly controlled. As shown here, the liganded transcription factor complex binds to proximal response elements and distal enhancers within the gene's promoter region. Co-regulatory complexes and RNA polymerase II recruitment initiate gene transactivation (Campbell, 2015) (Image edited from CNX OpenStax, 2007)*

1.5 Non-classical Roles of Vitamin D

1.5.1 Vitamin D and Immunology

Lagishetty *et al.,* (2011) identified that 1,25D stimulates innate immune responses. The first evidence being the treatment of tuberculosis with cod liver oil (Green, 2011). This involved macrophages and monocytic scavenging of *Mycobacterium tuberculosis* (Green, 2011). Additionally 1,25D regulates antimicrobial protein levels and may be crucial in infection control. These include the expression of defensin β2 (DEFB) and cathelicinin antimicrobial peptide (hCAP18) (Gombart *et al.,* 2009). Jean *et al.,* (2017) also linked low 1,25D levels to increased mortality in end-stage renal patients with severe infection. 1,25D has also proven its importance in association with influenza and allergic asthma (Ali *et al.,* 2017). Dendritic cells (DC) are also an important target for immune modulatory effects of 1,25D (Prietl *et al.,* 2013). 1,25D alters the function and morphology of DC, inducing immature DCs with decreased major histocompatibility complex (MHC) class II and co-stimulatory molecule expression that reduces antigen-presenting process (Prietl *et al.,* 2013). Animal models studies by Adzemovic *et al.,* (2013) found that 1,25D ameliorates Type 1 Diabetes (TID) and Multiple Sclerosis (MS) Furthermore, VDR knockout mice showed an increase in inflammation and development of TID and Crohn's disease, along with disturbed T-cell homing and lack of host protection from bacterial infections (Ardesia *et al.,* 2015).

1.5.2 Vitamin D and Cardiovascular Diseases

1,25D, through UVB light exposure was linked to decrease blood pressure (BP), resulting in the suppression of renin (McMullan *et al.,* 2017). Additionally, Xiang *et al.,* (2005) observed that mice with abolished VDR expression were hyperreninemic and presented with high BP and hypertrophy. Additionally Pilz *et al.,* (2009) identified 1,25D's ability in regulating BP through the prevention of secondary hyperparathyroidism. Molecular mechanisms further revealed 1,25D's inhibitory effects on the renin –angiotensin system and nuclear factor β pathway (NFKβ) which directly increase BP (Ajabshir *et al.,* 2014).

1.5.3 Vitamin D and Neurodegenerative Disorders

Adding to the on-going evidence of 1,25D's extra-skeletal roles, Littlejohns *et al.,* (2014) confirm that 1,25D deficiency is associated with a substantial increased risk of dementia and Alzheimer disease. Contrary to this finding, Olsson *et al.,* (2017) found in a cohort study that there was no association between baseline 1,25D status, dementia or cognitive impairment. Zündorf and Reiser, (2011) concluded that calcium dysregulation is influential on brain cell death , Parkinson's disease, Huntington's disease and Alzheimer's disease development.

1.5.4 Vitamin D and Malignancies

1,25D deficiency is frequently correlated with high incidence and mortality in malignancies (Grant *et al.,* 2009). As observed in numerous cancer cell types, 1,25D stimulates cellular differentiation and inhibits proliferation by regulating Cyclin dependant kinase inhibitors (CDKIs) (Jensen *et al.,* 2001). CDKI are key proteins involved in cell cycle initiation (Jensen *et al.,* 2001). Flores *et al.,* (2010) also identified that 1,25D regulates the DNA damage 45α (GADD45A) gene which induces cell cycle arrest in G0/G1. The c-MYC oncogene, whose products promote cell proliferation, immortalization and reverse differentiation, is repressed by 1,25D (Saleh-Tabar *et al.,* 2012). Additionally Levresse *et al.,* (2002) identified that in non-small cell lung cancer (NSCLC) c-JUN overexpression correlated with primary and metastatic lung tumour cases, contrary to normal tissue, which did not express c-JUN. Likewise, c-FOS was associate with high-grade lesion and poor prognosis (Liu *et al.,* 2016).

Colorectal cancer (CRC) and 1,25D have in recent years been a topic of interest, particularly because CRC is becoming a critical health problem and there is a worldwide need for effective chemopreventative/chemotherapeutic measures. With a significantly high VDR expression profile in intestines, researchers such as Ferrer-Mayorga *et al.,* (2019) have since evaluated the effects of 1,25D in CRC. So far, it is known that the Wnt/β-catenin signalling pathway, involved in CRC progression is antagonized by 1,25D through various events (Larriba *et al.,* 2013). These include TCF/β-catenin transcription complex disruption due to VDR and β-catenin binding.

1,25D also abrogates nuclear β-catenin content by promoting binding of β-catenin to E-cadherin which is regulated by 1,25D (Larriba *et al.*, 2013). Furthermore, Larriba *et al.*, (2013) noted that in CRC patients, 1,25D suppressed β-catenin whilst inducing E-cadherin. Furthermore, angiogenesis, migration and invasiveness are repressed by 1,25D through the downregulation of genes such as Dickkopf 4 (*DKK-4*) (Aguilera *et al.*, 2007). Angiogenesis is abrogated through control of vascular endothelial growth factor (VEGF), inhibitor of differentiation (ID)-1/2 and thrombospondin (TSP)-1 genes, an effect that was observed in both human *in vitro* and rat model systems (Shibuya, 2011). MicroRNAs (miR) such as miR-22 induced by 1,25D were found to be involved in antiproliferative, anti-migratory, tumour growth inhibition and suppressed invasion effects in several cancer cell lines (Alvarez-Diaz *et al.*, 2012). With the above-mentioned and many more findings associated with 1,25D and malignancies, there seems to be potential in VDR agonist use as a chemotherapeutic, or better yet, chemo-preventative measure.

1.5.5 Vitamin D and Metabolism

Xenobiotic metabolism involves a set of specialized enzymatic pathways that facilitate in the biotransformation of toxic substances such as drugs, carcinogens, environmental toxins and endogenous compounds into easily excretable forms (Penner *et al.*, 2012). There are three phases of xenobiotic metabolism, namely phase I reactions which introduce reactive or polar groups to susceptible substances. Phase II reactions catalyse conjugation reactions of phase I metabolites and Phase III transporters facilitate in the basolateral efflux of conjugated metabolites for excretion in the bile or urine (Xu *et al.*, 2005) (See Figure 1.4). The nuclear receptor subfamily 1 group I (NR1I) family members (e.g. VDR, PXR and CAR) play a central role in the xenobiotic metabolism, integrating a network of transcriptional target gene products that orchestrate the defence against toxic endogenous and exogenous substances (Prakash *et al.*, (2015). While a broad spectrum of chemicals serve as prototypical ligands for PXR, VDR agonists are restricted to 1,25D, its hydroxylated metabolites and secondary bile acids. (Khedkar *et al.*, 2017; Makishima *et al.*, 2002). We and others have defined VDR activity to induce phase I *CYP3A* expression (Maguire *et al.*, 2012, Doherty *et al.*, 2014). In expanding upon our knowledge was the earlier identification of functional VDREs within the 10kbp *CYP3A* promoter fragment

(Thompson *et al.,* 2012). Seo *et al.,* (2013) also observed VDR mediated *SULT2B1* in prostatic cancer cells, an effect thought to suppress disease progression. Shen and Kong, (2009) and our laboratory-based evidence has correlated multidrug resistant protein 1 (*MDR1)* and multidrug resistant associated protein 2 (*MRP2)* phase III transporters expression with VDR activation.

Much of our attention is on our unpublished data that links the phase II metabolic gene, *Uridine 5'diphsophoglucuronosyltransferase 1 A (UGT1A)* induction to VDR activation. Although extensive extrahepatic *UGT1A* gene profile regulation by VDR has not yet been conducted, multiple VDR/RXR binding sites have been identified within the *UGT1A* locus. Additionally, attempts by Wang *et al.,* (2016) identified 13 putative VDREs within the 10kb *UGT1A8* and *UGT1A10* promoter region. Whilst significant attempts have been employed, the regulatory mechanisms have not been examined fully; therefore, this study aims to fully characterize this at a molecular level as further discussed below.

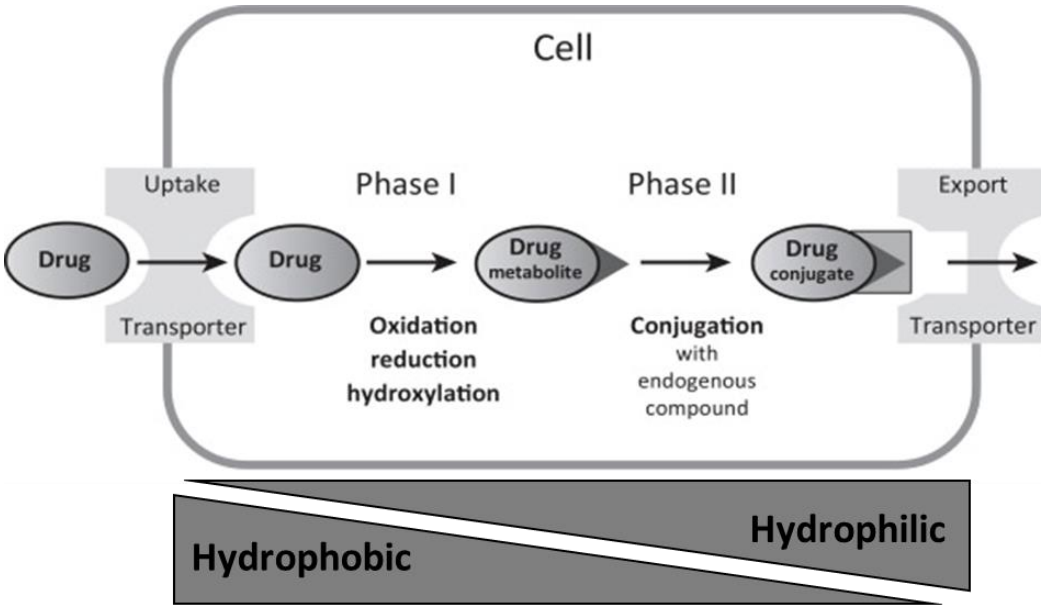

Figure 1.4: A representation of cellular detoxification. *Phase I metabolism involves oxidation, reduction and hydroxylation reactions of hydrophobic substances. The metabolites usually undergo further conjugation reactions by phase II metabolic enzymes, converting water-soluble forms that can be easily exported by phase III transporters.*

1.6 UDP-Glucuronosyltransferases 1A (UGT1As)

Of the above-mentioned phase II detoxification processes, glucuronidation, mediated by UGT1As is the most significant, representing the pathway of critical compounds, which, if disrupted leads to serious clinical consequences (Section 1.6.4). Glucuronidation occurs following transfer of the glucuronic acid moiety from a ubiquitous co-substrate uridine diphosphoglucuronic acid (UDPGlcA) to susceptible substrates, forming a glucuronide derivatives (-G) which are consequently more easily excreted from the body due to the carboxyl group's ionized state at physiological pH, thus increase water solubility of the otherwise hydrophobic substance (Mottino and Rodriguez, 1987) (Figure 1.5). The glucuronide is transported by the biliary and renal organic anion efflux system, leading to secretion in the bile and urine respectively (Fujiwara *et al.*, 2010). Glucuronidation alters the chemical structure of xenobiotics and therefore; their biological function is diminished (Fujiwara *et al.*, 2010). Glucuronidation is critical in the detoxification and clearance of endogenous hydrophobic substances including sex hormones, bile acids, bilirubin and fatty acids (Rowland *et al.*, 2013). This mechanism maintains homeostasis and regulates the biological activity of these substances. Interestingly, these substances are able to regulate the expression of *UGT1A* genes, thus generating a feedback loop and the mediation, distribution and physiological effects of the ligand (Rowland *et al.*, 2013).

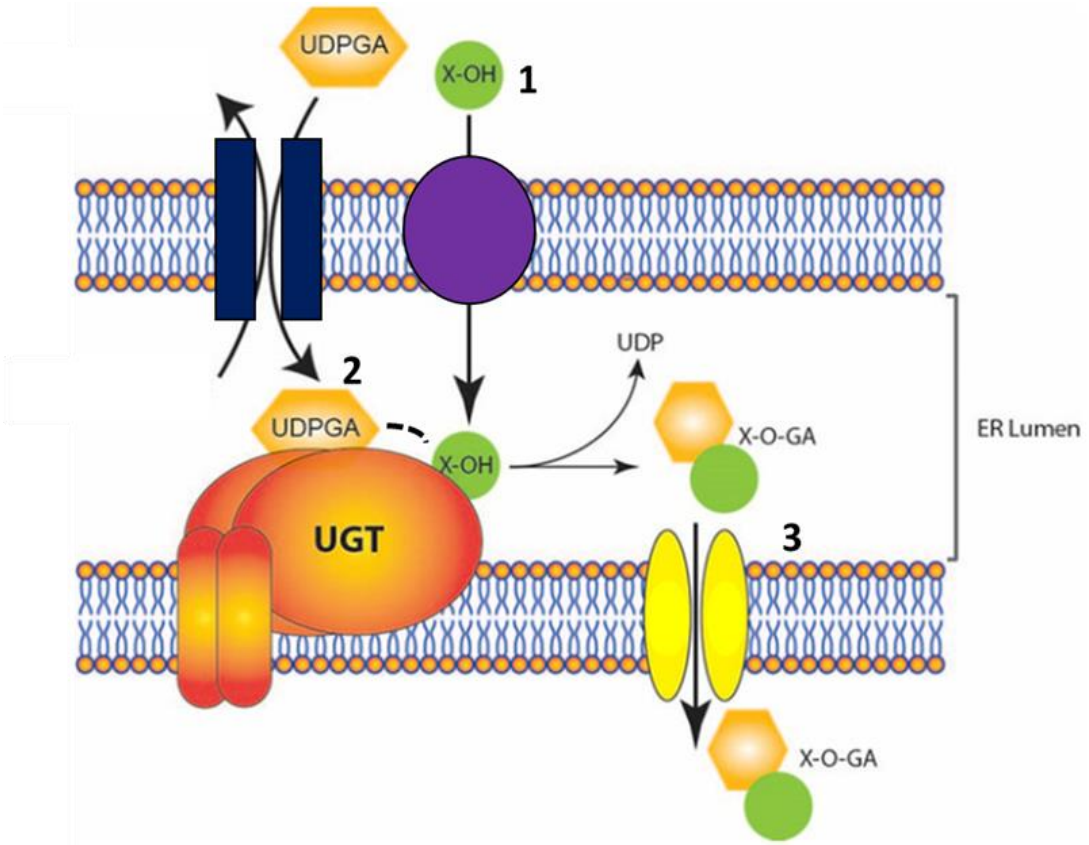

Figure 1.5: The endoplasmic reticulum (ER) glucuronidation pathway. ***1****. Substrate depicted as X-OH diffuses into the ER lumen.* ***2****. The co-factor UDPGA is also transported into the lumen and transfers a molecule of glucuronic acid (GA) to the substrate.* ***3.*** *This results in a conjugated substrate that is easily excreted by efflux transporters (Image edited from Liu and Coughtrie, 2017).*

Due to the UGT's inherent localization within the luminal side of the endoplasmic reticulum (ER) membrane, rich in UDPGla, the structural analysis of UGTs to determine catalytic mechanisms is still being researched, however UGT cDNA cloning has enabled DNA based expression of individual gene family members for substrate specificity (Liu and Coughtrie, 2017). Izukawa *et al.*, (2009) identified two UGT superfamilies, namely *UGT1A* and *UGT2.* The *UGT2* superfamily is further sub-divided into *UGT2A* and *UGT2B,* which contains three and seven individual isoforms respectively. *UGT2B* gene family members within 4q13 gene loci contain six specific exons (Strassburg *et al.,* 1997). HEK293 cells stably expressing *UGT2B* isoforms demonstrated glucuronidation towards endogenous substances including sex hormones and bile acids (Strassburg et al., 1997). Turgeon *et al.,* (2001) and Chouinard *et al.,* (2007) further evidenced that *UGT2B15* and *UGT2B17* are

significantly expressed in prostatic cancer cell lines, and mainly catalyze testosterone and dihydrotestosterone glucuronidation. These findings suggest the important role of glucuronidation in fine-tuning androgen signaling. As with endogenous compounds, *UGT2B7* metabolizes epirubicin (hepatocellular carcinoma anti-cancer drug), an effect that contributes to acquired chemotherapeutic resistance (Hu *et al.,* 2014). Nevertheless, the focus of this study, *UGT1A* gene family members encoded on chromosome 2q37.1, spans approximately 200kbp (Fujiwara *et al.,* 2016). Their N-terminal amino acid sequence contains isoform specific first exons, which exhibit significantly low amino acid sequence similarity (24-49%), and contribute towards substrate specificity (Strassburg *et al.,* 1997.) The N-terminal is spliced to the highly conserved C-terminal amino acid sequence encoded by common exons (2-5), generating nine functional isozymes (*UGT1A1, UGT1A3, UGT1A4, UGT1A5, UGT1A6, UGT1A7, UGT1A8, UGT1A9 and UGT1A10*) (Fujiwara *et al.,* 2016). (Figure 1.6). The involvement of both N- and C-terminal in substrate binding was demonstrated by Radominska-Pandya *et al.,* (2010) through a series of point mutations. The findings demonstrated abrogated affinity towards substrates and UDPGlcA (Radominska-Pandya *et al.,* (2010). Interestingly, alternative splicing of exon 5 (exon 5b) resulting in the generation of *UGT1A* variant were recently observed (UGT1A_b) which generates a shorter amino acid sequence (Girard *et al.,* 2007). Bellamare *et al.,* (2010) later identified that the UGT1A_b protein is 45kDa compared to the main variant ranging from 50-55kDa. Moreover, the alternative products interact with the enzymatically active proteins, subsequently inhibiting their *in vitro* glucuronidation (Bellamare *et al.,* (2010). However, the relative abundance activity of these variants needs further investigation to determine the extent of inhibition and its translation to physiological health.

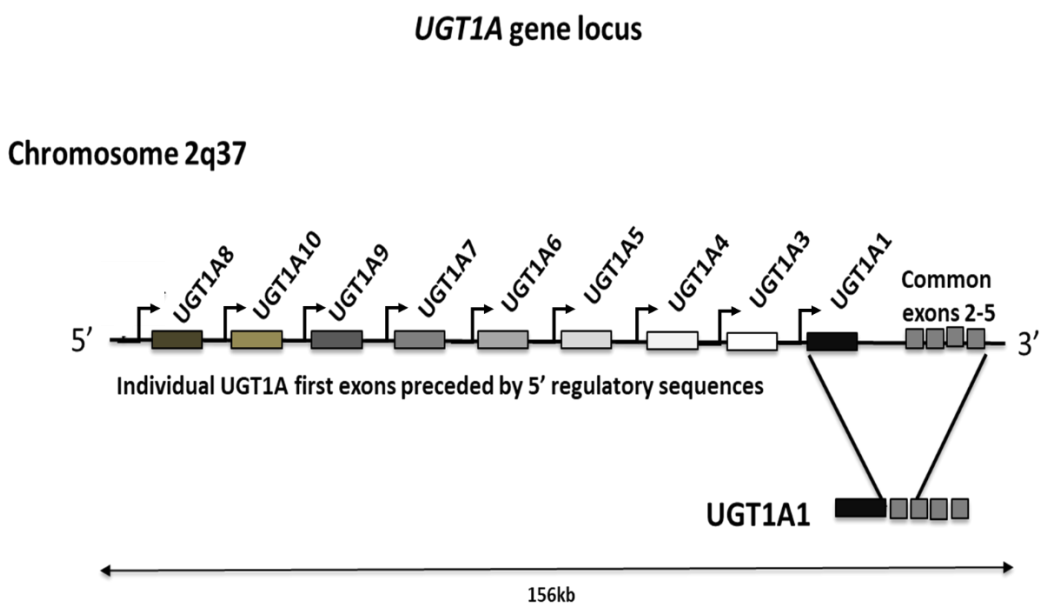

Figure 1.6: The genomic organization of the UGT1A loci on chromosome 2q37. *The locus contains 9 unique first exons that are alternatively spliced at the 5'-end of the mRNA with common exons 2-5. There is a TATA-box approximately 30bp upstream of each unique first exon sequence, which implies individual transcriptional regulation.*

1.6.1 *UGT1A* Tissue Distribution

UGT1A mRNA expression profile was first quantified in human tissue samples using conventional RT-PCR and more recently by real-time RT-PCR (Nakamura *et al.,* 2010; Cengiz *et al.,* 2015). Findings by Court, (2010) and Nakamura *et al.,* (2008) have shown a tissue specific distribution and inter-individual differences in *UGT1A* mRNA levels in various tissue types. More precisely, *UGT1A* expression was detected predominantly in the liver, a major detoxification site, but also kidney, gastrointestinal tract, pancreas, lung, breast, brain, prostate and bladder (Tang *et al.,* 2012) (Figure 1.7). Izukawa *et al.,* (2009) successfully quantified *UGT1A* mRNA transcripts, although protein expression in human liver only correlated with *UGT1A1* out of all the hepatic *UGT1As*. Nonetheless, we and others have been able to correlate *UGT1A* mRNA transcripts with protein expression in extrahepatic cell line models (Wang *et al.,* 2014 and Strassburg *et al.,* 1998). Alas, isoform specific protein expression analysis has been impossible due to *UGT1A* gene family member's high amino acid sequence similarity. Nevertheless, Sridar *et al.,* (2013) successfully measured stable

isotope-labelled peptide-based *UGT1A* expression by use of liquid chromatography-tandem mass spectrometry (LC-MS/MS). Although this methodology has proven to be better than the standard western blot, the approach does not distinguish between *UGT1A* variants that occur due to alternative splicing. So far, *UGT1A1, UGT1A3, UGT1A4, UGT1A6 and UGT1A9* expression have been detected in human liver. *UGT1A7*, *UGT1A8* and *UGT1A10* were not detected in human liver microsomes (Strassburg *et al.,* 1999 and Nakamura *et al.,* 2005). Extrahepatic exclusive *UGT1As* include *UGT1A7, UGT1A8, UGT1A9* and *UGT1A10,* although mRNA expression of other isoforms were also detected (Tukey and Strassburg, 2000). The *UGT1A6* and *UGT1A9* are predominantly expressed in the kidneys (Fujiwara *et al.,* 2007).

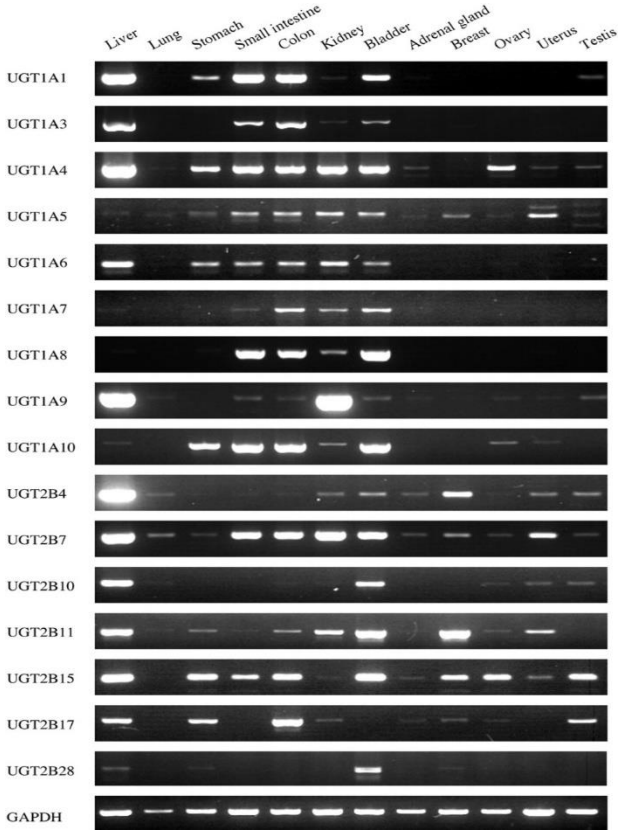

Figure 1.7: Differential expression of UGT1A and UGT2B genes in normal human tissue*. Basal UGT1A isoform expression in normal human tissue including liver, lung, stomach, small intestine, colon, kidney, bladder, adrenal gland, breast, ovary, uterus, and testis were investigated by RT-PCR. Liver, as a major glucuronidation site houses majority of expression. As shown UGT1A7, UGT1A8 and UGT1A10 are exclusive extrahepatic isoforms (Nakamura et al., 2008).*

1.6.2 Transcriptional regulation of *UGT1A* gene family members

Numerous transcription factors (TFs), are linked to *UGT1A* gene induction. For example, 2, 3,7,8-tetrachlordibenzo-*p*-dioxin (TCDD) activated Aryl Hydrocarbon Receptor (AhR), which induced *UGT1A8* and *UGT1A10* in KYSE70 (human esophageal squamous carcinoma) cell line (Kalthof *et al.,* 2010). Xenobiotic Response Element (XRE) motif mutagenesis significantly abrogated this induction (Kalthof *et al.,* 2010). Furthermore, *Ugt1a6* and *Ugt1a7* mRNA expression and glucuronidation activity acetaminophen was observed in rat brain samples in response to β-Naphthoflavone induced AhR activation (Sakakibata *et al.,* 2016). Constitutive Androstane Receptor (CAR), signaling is also evidenced to induced *UGT1A* induction (Xie *et al.,* 2003). Buckley and Klaassen, (2009) observed *Ugt1a1* and *Ugt1a9* induction mRNA expression was induced by CAR prototypical ligand, 1,4-bis[2-(3,5-dichloropyridyloxy) benzene (TCPOBOP). Guo *et al.,* (2003) exposed FXR-null and PXR-null mice models to TCPOBOP which were fed 1% cholic acid. Metabolic gene products including hepatic *CYP2B, CYP3A, MRP2* and most importantly *UGT1A*s were significantly elevated (Guo *et al.,* 2003). These findings represent CAR clinical significance in bile acid detoxification. CAR is also a member of the NR superfamily similar to VDR and PXR (Krasowski *et al.,* 2011). PXR is a key hepatic *UGT1A1* inducer, mainly responsible for bilirubin clearance (Sugatani *et al.,* 2012). Raynal *et al.,* (2010) observed that PXR-expressing LS174T, SW480 and SW620 cells induced *UGT1A1*, *UGT1A9* and *UGT1A10* mRNA expression. PXR-mediated *UGT1A1* transactivation was robustly enhanced compared to CAR and AhR (Sugatani *et al.,* 2012). Following the discovery of PXR in the 1990s, it has mostly been implicated with abrogating clinical consequences that include hyperbilirubinemia (Saini *et al.,* 2005). However, *UGT1A* enhanced induction, amongst other metabolic genes means that PXR is implicated with enhanced DDI, or reduced drug toxicity (Guo *et al.,* 2003). Lamotrigine metabolism by *UGT1A4* was enhanced by rifampicin exposure, which activated PXR. (Chai *et al.,* 2013). The oxysterol-activated NR, Liver X-Receptor alpha (LXRα) is also a known *UGT1A* gene inducer (Edwards *et al.,* 2002). *UGT1A3* enhanced induction was observed in hepatic cells and *Tg-UGT1A* mice (Chen *et al.,* 2012). The involved LXR response element (LXRE) was identified by ChIP assay and subsequent mutagenesis studies confirmed its functionality following *UGT1A3*

expression abrogation and reduced LCA glucuronidation (forming LCA-24G) (Chen *et al.,* 2012). Bedi *et al.,* (2017) identified that, following LXRα activation, RXR heterodimer formation and binding to the LXRE, the LXRα recruits the SRC-1α and NcoR co-regulatory proteins for direct *UGT1A3* transactivation. In addition, Farnesoid X receptor (FXR), predominantly expressed in the liver is implicated with bile acid metabolism (Sun-Gi *et al.,* 2016). FXR also forms a heterodimer with RXR prior to the complex binding to FXR response element (FXRE), recruiting co-activators and inducing gene expression (Sun-Gi *et al.,* 2016). Researchers including Erichsen *et al.,* (2010) also observed FXR-mediated *UGT1A3* induction, in addition to the identification of an FXR element within the gene's 5' upstream promoter region. This regulation was also confirmed by electrophoretic mobility shift assay (EMSA) following GW4064 exposure in colonic cells (Erichsen *et al.,* (2010). FXR mediated chenodeoxycholic acid (CDCA) glucuronidation further confirmed the biological relevance of FXR in the human bile acid detoxification (Chiang *et al.,* 2013). Peroxisome proliferator-activated receptor alpha and gamma (PPARα and PPARγ) are ligand-activated TFs also belonging to the NR superfamily (Barbier *et al.,* 2003). Barbier *et al.,* (2003) identified that these NRs both induced *UGT1A9* following prototypical ligand exposure using human hepatocytes, macrophages and murine adipocytes (Barbier *et al.,* 2003). PPARα mutagenesis abrogated *UGT1A9* expression and enzymatic activity. The direct mediation of this gene confirmed by a response element at the -719 to 706bp position of the *UGT1A9* gene (Barbier *et al.,* 2003). This induction suggest that PPAR is clinically relevant in the genotoxic catecholestrogen metabolism and the control of fibrates. The Nuclear factor erythroid 2-related factor 2/Kelch-like ECH-associated protein 1 (NRF2/KEAP1) signaling pathway described in Section 1.7 induces *UGT1A1* expression (Yueh and Tukey, 2007). In this case, HepG2 cell lines exposed to NRF2 ligands implicated *UGT1A1* with neutralization of oxidative and electrophilic stress. In addition to *UGT1A1*/NRF2 induction in Tg-*UGT1A* mice models, the ARE was identified at position -3328/-3323bp from the TSS (Yueh and Tukey, 2007). Both *UGT1A8* and *UGT1A10* were also induced by NRF2 in KYSE70 cell lines (Kalthof *et al.,* 2010). Likewise, in *Tg-UGT1A* mice exposure to coffee, which has been identified to activate NRF2 signaling, resulted in a 10-fold and 14-fold *UGT1A* induction in the liver and stomach respectively (Kalthof *et al.,* 2010). Diminished *UGT1A* activity is associated serious clinical conditions (discussed

in Section 1.6.3). As such, drugs, including Phenobarbital (PB) are widely used to restore *UGT1A1* activity (Sugatani *et al.,* 2001). In fact, the use of PB led to the more extensive research on 5' flanking region of *UGT1A1* promoter region. Termed the PB responsive enhancer module (gtPBREM), this 290bp fragment located at position -3499 to -3210, and was characterized to contained multiple NRs binding sites including that for PXR, CAR and AhR. Sugatani *et al.,* (2001) also identified that Glucocorticoid Receptor (GR) regulates *UGT1A1* and as such, GR responsive elements (GRE1 and GRE2) were also identified within the gtPBREM (Figure 1.10). Studies by Eeckhoute *et al.,* (2004) also identified that major liver-enriched TFs, Hepatocyte Nuclear Factor 1 alpha (HNF1α) and HNF4α induce *UGT1A* expression. Following concerns over the TFs' contribution in inter-individual variability, Aueviriyavit *et al.,* (2007) further characterized this induction. *UGT1A1, UGT1A3, UGT1A4, UGT1A6, UGT1A9* induction was altered in human liver samples by the two TFs.

On the other end of the spectrum *UGT1A* regulation can be suppressed through post-translational involvement of microRNAs such as miR-103b, miR-141–3p, miR-200a-3p, and miR-376b-3p. This also suppresses glucuronidation acitivity by approximately 30% (Papageorgiou and Court, 2010). Dluzen *et al.,* (2015) further confirmed *UGT1A* mediated miR-491-3p regulation in HepG2 cells. Nonetheless, controlled glucuronidation by the above-mentioned factors ensures homeostatic balance of endogenous compounds and elimination of toxic foreign substances. Compromised expression leads to devastating consequences discussed in Section 1.6.3

Figure 1.8: The phenobarbital responsive enhancer module nucleotide sequence. *Shown here is the 290bp sequence at position -3499/-3210 upstream of the UGT1A1 promoter region. The fragment contains multiple NR response elements including DR3-type and DR4-type motifs which are recognised by NR heterodimeric complex binding and lead to subsequent UGT1A1 transcription. Sugatani et al., (2005).*

1.6.3 *UGT1A* clinical relevance

Diminished UGT1A enzymatic activity has highlighted its biological relevance. Single nucleotide polymorphisms (SNPs), resulting from a nucleotide mutations often lead to variants that confer reduced or increased UGT1A enzymatic phenotypes (Cox *et al.,* 2013; Ehmer *et al.,* 2012). The wild-type *UGT1A1*1* allele normally includes six thymine-adenine (TA_6) repeats, referred to as the TATA box (Du *et al.,* 2019). However, the most commonly studied variant, *UGT1A1*28* is characterized by seven TA $(TA)_7$TAA7) repeats and presents with impaired proper transactivation, resulting in close to 30% decrease in glucuronidation activity (Du *et al.,* 2019). *UGT1A1* is the only enzyme associated with bilirubin metabolism. Diminished metabolism results in increase serum bilirubin (hyperbilirubinemia) (Wagner *et al.,* 2018). This clinical concern is usually a benign consequence of Gilbert's Syndrome (GS) were serum bilirubin levels are above 5mg/dL (Yueh *et al.,* 2017). GS symptoms are very mild and manifest at adolescence as jaundice due to stress or fasting. (Yueh *et al.,* 2017).

Other symptoms include tiredness, weakness, abdominal pains and nausea. The link between the latter symptoms and high serum bilirubin levels is still unclear (Sampietro and Iolascon, 1999 and Wagner *et al.,* 2018). GS diagnosis typically requires genotyping, liver function tests and measurement of serum bilirubin (Sampietro and Iolascon, 1999). There currently is no treatment for GS, mostly due to its benign nature (Sampietro and Iolascon, 1999). However, undesirable clinical consequences such as toxic effects from use of certain drugs such as irinotecan, metabolised by UGT1A1 may manifest (Singh and Jialal, 2019). With over 3% of the global population as carriers and 1 in 3 individuals unaware, it is increasingly important to be aware of potential GS management avenues, to prevent devastatine consequences such as drug toxicity (Wagner *et al.,* 2018).

On the other hand, Crigler Najjar Type 1 (CNS1) disease is a serious form of hyperbilirubinemia, where individuals are homozygous or heterozygous carries of a completely inactive *UGT1A1* allele (Viveksandeep and Savio, 2019). If left untreated, CNS I is fatal, due to irreversible fatal encelopathy (Fujiwara *et al.,* 2017). A milder phenotype, CNS II results from mild UGT1A1 enzymatic activity following mutations with the *UGT1A1* gene (Fujiwara *et al.,* 2017). Hyperbilirubinemia in this case is usually treated by PB, however if left untreated, kernicterus (bilirubin build up in brain tissue) may still develop due to trauma or sepsis may develop (Aggarwal *et al.,* 2001). CNS I usually requires phototherapy or even liver transplantation (Hammad *et al.,* 2017).

Additionally variants such as *UGT1A1*37* have eight TA repeats and its enzymatic activity is significantly lower than the *UGT1A1*28* variant, whereas *UGT1A1*36* has five TA repeats and results in increased enzymatic activity (Reira *et al.,* 2018). Moreover, in Asian and African populations the *UGT1A1*6* variant is the most common (Gao *et al.,* 2013). This variant results in approximately 30% lower enzymatic activity and so carriers present with GS and neonatal hyperbilirubinemia (Ullah *et al.,* 2016). Currently, there are more than 113 *UGT1A* isoform variants, which either diminish or increase glucuronidation activity (Barbarno *et al.,* 2014). Many of these variants have also been linked to malignancies (Barbarno *et al.,* 2014). For example, *UGT1A7*3* variant exhibited a highly significant association with colorectal cancer (Strassburg *et al.,* 2002). Benzo (α) pyrene-7, 8-dihydrodiol-9, 10-epoxide is a potent carcinogen and a *UGT1A1* substrate (Barbarino *et al.,* 2014).

Furthermore, Vukovic *et al.,* (2018) found that *UGT1A1*28* allele correlates with the development of colorectal and breast cancer risk in Asian and European populations. *UGT1A1*6* specifically increases the risk of colorectal cancer in Chinese populations (Tang *et al.,* 2005). In addition to this, Lucy-Driscoll syndrome, a rare metabolic disorder, increases UGT1A1 activity inhibitors, also resulting in familial neonatal hyperbilirubinemia (Singh and Jailal, 2019).

UGT1A7 is predominantly expressed in the oral cavity and as such, diminished expression is linked to oropharyngeal cancer development (Lacko *et al.,* 2009). Additionally estrogen is a *UGT1A10* substrate; therefore, cases of reduced glucuronidation have been associated with estrogen-related cancers (Lazarus *et al.,* 2009). Glucuronidation also plays a role in the elimination of over 50% of clinically administered drugs (Yang *et al.,* 2017). For example, Irinotecan (used to treat colon cancer) is activated by phase I hydrolysis reaction to 7-Ethyl-10-hydroxycamptothecin (SN-38) (Wang *et al.,* 2012). SN-38 is topoisomerase I inhibitor and thus prevents inhibition of both DNA replication and transcription (Wang *et al.,* 2012). SN-38 is a known *UGT1A1* substrate. The effects of reduced *UGT1A1* expression lead to undesireably high amounts of unconjugated SN-38, leading to adverse effects such as diarrhoea and immunosuppression (Wang *et al.,* 2012 and Ramchandani *et al.,* 2007).

Furthermore, *UGT1A8* and *UGT1A10* are known substrates of mycophenolic acid (MPA), an immunosuppressant usually prescribed to kidney transplant patients (Wang *et al.,* 2014). An increase in their expression enhances drug clearance. This has become a major problem within the pharmaceutical industry due to inter-individual variability, drug-drug interactions and reduced drug efficacy (Wang *et al.,* 2016).

On the other hand, Wang *et al.,* (2014)'s findings of 25(OH)D_3-3-glucuronides in human plasma suggest that UGT1A3 and UGT1A4 enzymes may contribute towards homeostatic control of 1,25D in humans, although these findings are still limited, this may suggest a link between *UGT1As* and the 1,25D/VDR signaling pathway which will be explored further in this study.

Table 1.3: Differential glucuronidation of endogenous and exogenous substrates.

***UGT1A* Sub-family**	**Endogenous Substrates**	**Exogenous Substrates**
UGT1A1	Bilirubin	Etoposide
	Cathecols	β-Estradiol
	Thyroid hormones	SN-38
	Bile Acids	Ezetimibe
UGT1A3	Cathechol	Ezetimine
	Thyroxine	Telmisartan
	Bile Acids	
	1,25D	
	Chenodeoxycholic acid	
UGT1A4	Pregnanediol	Lamotrigine
	1,25D	Trifluoperazine
	Androstanediol,	Amitriptyline
		1-OH midazolam
UGT1A5	Bile Acids	Scopoletin
		4-methylumbelliferone
		1-hydroxypyrene
UGT1A6	Serotonin	Paracetamol
	5-OH-tryptophol	Propofol
		Sorafenib
UGT1A7	Triiodothyronine (T3)	Benzo(α)pyrene
	Tetraiodothynine (T4)	Caffeine
	Glutaric Acid	
	Linoleic Acid	
UGT1A8	Estriol	Myophenolic acid
	Tetraiodothynine (T4)	Quercetin
	Triiodothyronine (T3)	Chrysin
		7-hydroxycoumarin
UGT1A9	Thyroid Hormones	Myophenolic acid
	Estrogens	Sorafenib
	5-hydroxyeicosatetraenoic acid	Entaceponoe
	Tetraiodothynine (T4)	Paracetamol
UGT1A10	Serotonin	Myphenolic Acid
	Estrogen	Nitrosamine
	Estrone	Warfarin

examples of susceptible substances commonly metabolised by the *UGT1A* gene family members (Franklin, 2007, Wang *et al*.,2014) Due to high sequence homology, there is evidence of substrate overlap; however the differential expression significantly contributes towards distinct clearance of these substances. *UGT1A5* is the least studied isoform; however, Finel *et al.*, (2005) did confirm its glucuronidation capabilities of bile acids and a number of drugs.

Table 1.4: Examples of *UGT1A* single nucleotide polymorphism (SNP) and their associated clinical concequences.

***UGT1A* SNP**	**Increased Risk**	**References**
*UGT1A1*27*	Irinotecan-induced toxicity	Fukuda *et al.,* 2018
*UGT1A1*28*	Hyperbilirubinemia, Irinotecan toxicity	Iyer *et al.,* 2002
*UGT1A1*6*	Gilbert's Syndrome	Iyer *et al.,* 2002
*UGT1A1*34*	Crigler Najjar Syndrome I	Marques *et al.,* 2010
*UGT1A1*35*	Crigler Najjar Syndrome II	Marques *et al.,* 2010
*UGT1A1*37*	Gilbert's Syndrome	Marques *et al.,* 2010
*UGT1A3*1/3/5*	Estrogen related cancers	Cailier *et al.,* 2007
*UGT1A4*3*	Haematological malignancies	Joeng *et al.,* 2018
*UGT1A6*1/2*	Lung Cancer	Kua *et al.,* 2012
*UGT1A7*2/3*	Orolaryngeal Cancer	Zheng *et al.,* 2001

1.7 NRF2: The master regulator of oxidative stress

Following oxidative stress (OS) insults, a number of signalling pathways, converging in the regulation of TFs, including NF-κβ, SP1, cAMP responsive element binding protein 1 (CREB-1) and Nuclear factor erythroid 2-related factor 2 (NRF2) are provoked (Belleza *et al.,* 2018; Morgan and Liu, 2011; Ryu *et al.,* 2003 and Ichiki *et al.,* 2003) . Their activation induces the expression of genes required for detoxification of intrinsic and external insults, cellular repair and homeostatic control

(Tonelli *et al.,* 2015). OS neutralization mediated by TFs can take place by protein synthesis or degradation, cytoplasm to nuclear trafficking or DNA binding and transcriptional activation (Sun *et al.,* 2015). In this study, NRF2, and its contributory role in the co-operative matrix with the VDR signalling pathway in OS protection, particularly *UGT1A* induction will be evaluated.

1.7.1 NRF2 Discovery and Function

Moi *et al.,* (1994) was the first to successfully clone and characterize NRF2 gene based on its ability to bind to the tandem nuclear factor erythroid 2/ activating protein 1 (NF-E2/AP1) repeats on β-globin promoter region. NRF2 is a member Cap 'n' collar (CNC) leucine b-zipper TFs. Other CNC members include NRF1 and NRF3, the former being involved in cholesterol homeostatic control (Chowdhury *et al.,* 2017). Proteomics identified 605 amino acid in human NRF2 protein, compared to 597 amino acids in rodents (Hayes and McMahon, 2009). Characterization of the NRF2 protein architecture revealed seven highly conserved domains referred to as NRF2-ECH homology (Neh) domains (Figure 1.9), each with a distinct role (Sun *et al.,* 2015). Neh1 is characterized by a DNA binding domain encompassing CNC-type basic-region leucine zipper (Canning *et al.,* 2015). Kelch-like ECH-associated protein 1 (Keap1), a known ubiquitin ligase substrate adaptor responsible to NRF2 suppression binds to the Neh2 domain of NRF2 (Canning *et al.,* 2015). Neh2 consists of two highly conserved sequences at the N-terminal, namely high affinity ETGE motif and the low affinity DLG motif to which Keap1 binds, subsequently allowing cullin -3 (Cul3) to facilitate NRF2 ubiquitination and subject it to proteosomal degradation (Tong *et al.,* 2006). Lysine residues between the two motifs make it susceptible for NRF2 to undergo ubiquitination (Villeneuve *et al.,* 2010). The carboxyl – terminal Neh2 domain is a transactivation domain that is able to interact with components of the transcriptional apparatus (Nioi *et al.,* 2005). This characterization was identified by Nioi *et al.,* (2005), who deleted 16 amino acids of Neh3, resulting in diminished ability to induce both gene and reporter-based activaty. Furthermore, these experiments did not alter DNA binding capabilities, confirming the independent Neh2 and Neh3 roles (Nioi *et al.,* 2005). The work of Hayes *et al.,* (2017) demonstrated that Neh4 and Neh5 domains mediate the recruitment of CBP/p300 to the proximal and distal regulatory regions of anti-oxidant containing

genes. Additionally, Katoh *et al.,* (2001) identified that both domains co-operatively bind to cyclin adenosine monophosphate (cAMP) response element-binding protein (CREB) thereby increasing transactivation through gene promoter interaction. Chowdhry *et al.,* (2013) identified, through boitinylated-peptide pull-down assays that Neh6 domain encompasses serine resides and two β-transducin repeat containing protein (β-Trcp), namely DSGIS and DSAPGS that function to negatively regulate NRF2. Gycogen synthase kinase-3 (GSK-3) phosphorylation to the DSGIs motif initiates this regulation (Beurel *et al.,* 2016). To date, Wu *et al.,* (2014) have advanced knowledge into Neh7 domain role. Experiments on A579 cell line demonstrated RXRα inhibited NRF2 transactivity through Neh7 domain, an effect that was independent of Keap1 (Wu *et al.,* 2014).

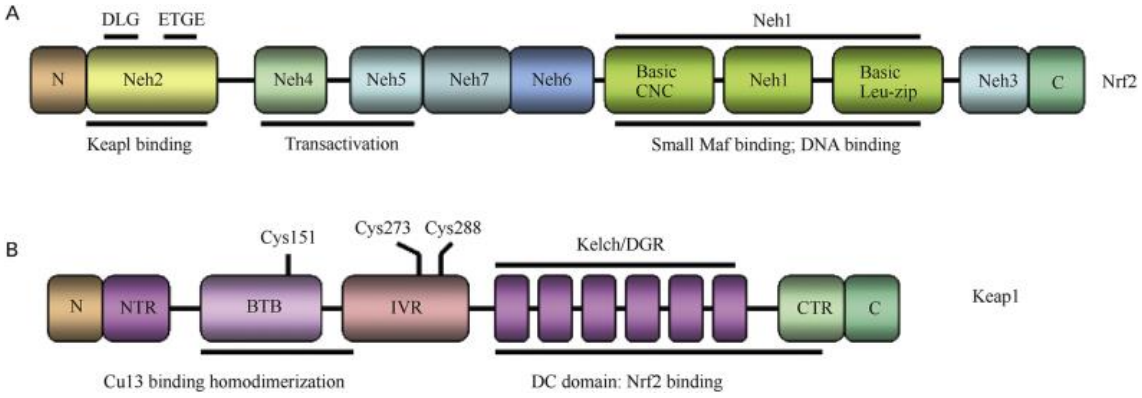

Figure 1.9: NRF2 structural domain. *NRF2 comprises an N-terminal hydrophobic domain, followed by a Keap1-binding domain, transcriptional activation domain, CNC domain and basic leucine zipper domain. NRF2, through its leucine zipper domain forms a heterodimer with its partner sMaf and the ARE binding motif (Sun et al., 2015).*

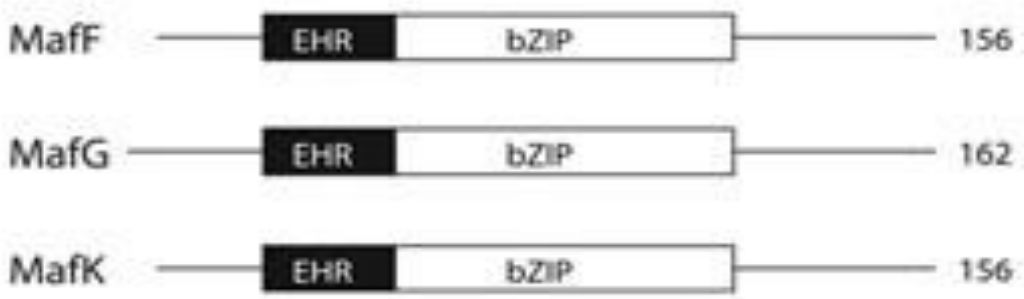

Figure 1.10 The domain structure of small Maf proteins. This comprises of a extended homology region (EHR) and a bZIP domain (Image edited from Hayes *et al.,* 2010).

1.7.2 NRF2 activation and repression

Keap1, using the Neh2 domain of the NRF2 protein is the principal negative regulator, by so doing, keeping its basal levels under control (Tonelli *et al.,* 2018). Keap1 first characterized by Itoh *et al.,* (1999) using yeast two-hybrid assay also identified 27 cysteine residues. Its dimeric module encompasses tram track and brica-brac (BTB) domain which facilitates the recruitment of Cul3, and intervening region (IVR), a cysteine-rich domain and a C-terminal Kelch-repeat domain consists of subdomains including Gly-Gly motifs, which form β-propeller with anti-parallel β-strands that form twisted β-sheet (Itoh *et al.,* 1999). These are required for Keap1/NRF2 interaction via the Neh2 domain (Itoh *et al.,* 1999). The human Keap1 comprises 624 amino acids has multiple OS sensitive cysteine based sensors (Wakabayashi *et al.,* 2004). Watai *et al.,* (2007) have since defined the localization of Keap1 in the cytoplasm contrary to NRF2 which is also found in the nucleus. Under basal conditions, NRF2 is bound to Keap1 and undergoes constant ubiquitylation by the Cul3 E3 ubiquitin ligase, and subsequently degraded by the proteasome (Villeneuve *et al.,* 2010). OS inducers such as Sulforaphane (SFN: a isothiocynate compound obtain from cruciferous vegetables e.g. broccoli), curcumin, *tert*-butylquione (*t*BHQ), environmental toxins, UV rays, and ROS prompt a Keap1 conformational change (Wu *et al.,* 2010; Kraft *et al.,* 2004; Osburn and Kensler, 2008). Cys-151 then prompts NRF2 activation pathway by allowing Keap1 to bind to Cul3 instead (Canning *et al.,* 2015). An important discovery was by Luo *et al.,* (2007) who conducted *in vitro* alkylation and *in vivo* site directed mutagenesis and identified that

Cysteine (Cys)-151, -226, -273,-434, -288 and -613 in Keap1 are key cysteine residues responsible for NRF2 activation.

NRF2 then translocates into the nucleus where it forms a heterodimer with small Maf proteins (sMafF, sMafG and sMafK), which are also members of the bZip family of TFs that recognize distal and proximal anti-oxidant response elements (ARE) within the genome (Nguyen *et al.,* 2009). However, ChiP-seq data revealed the absence of ARE binding, suggesting that NRF2 may also interact with other DNA binding protein (Hirotsu *et al.,* 2012). This leads to the recruitment of ATP-dependent nucleosome remodeling complexes including the SWI/SFN chromatin-remodeling complex (Kansanen *et al.,* 2013). Furthermore, the chromo-domain helicase DNA binding protein 6 (CHD6), receptor-associated co-activator 3 (RAC3) and Sirtuin 6 (SIRT6) are recruited, prompting chromatin remodeling and recruitment of RNA polymerase II, leading NRF2 target gene transactivation (Tonelli *et al.,* 2018).

1.7.3 NRF2 and Target genes

Several studies have implicated NRF2 activation with genes involved in protein transport, cell cycle, cell growth, and phosphorylation (Ma´rton *et al.,* 2018; Fan *et al.,* 2017). ChIP-seq data from mouse embryonic fibroblasts and human lymphoblastoid cell line models showed that amongst the common OS responsive genes, adipogenesis genes were also induced (Chorley *et al.,* 2012). Over 240 novel NRF2 genes were further characterized using qPCR and short interfering RNA (siRNA) following sulforaphane exposure (Chorley *et al.,* 2012). ARE motif sites were the most enriched following *de novo* motif analysis (Nioi *et al.,* 2003). Additionally activated NRF2 mediates *Notch1* mouse gene involved in osteoblast differentiation (Wakabayashi *et al.,* 2015) There is also enough reason to speculate NRF2 has a role in retinoid-mediated pathways following evidence of its ability to also regulate RXRα (Chorley *et al.,* 2012). Nevertheless, the most common element of the novel NRF2 genes is their role in preventing cellular damage, ROS detoxification, NADPH production and GSH synthesis (Tonelli et al., 2018. Examples of these are shown in the Figure 1.10.

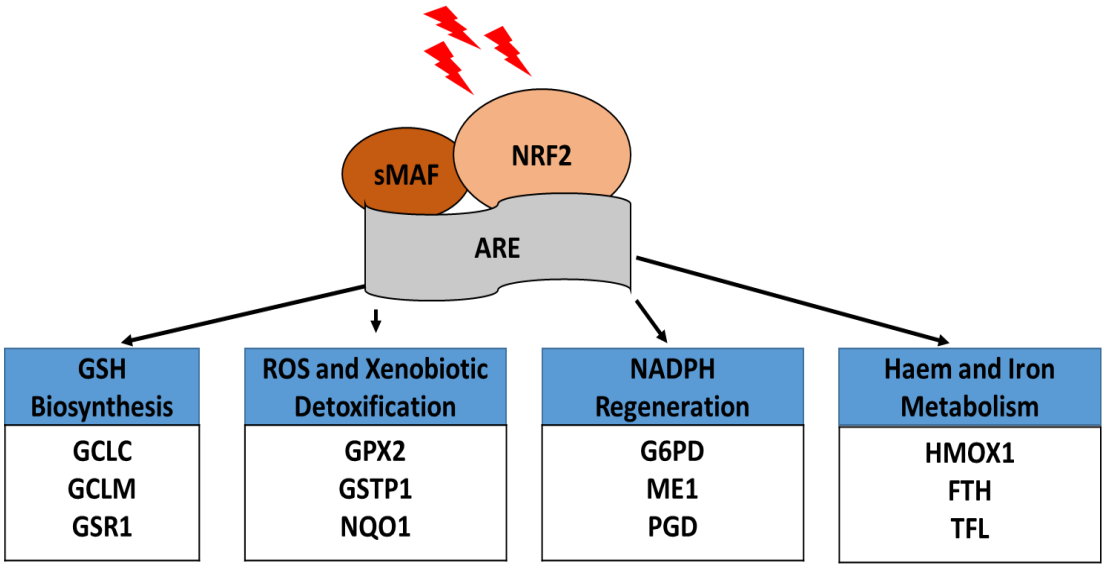

***Figure 1.11*: Examples of NRF2 target genes.** *Depicted are the co-ordinated effects of NRF2 signalling involving OS neutralization through GS production, in addition to ROS and xenobiotic detoxification, NADPH regeneration and lastly Haem and iron metabolism. NRF2 signalling pathway ensures cyto-protection through the enhancement of a network of genes regulating the processes as shown (Tonelli et al., 2018). Glutamate cysteine ligase (GCLM);Glutathione reductatse (GSR1);Glutathione peroxidase 2 (GPX2); Glutathione S-transferase P (GSTP1);NAD(P)H dehydrogenase (quinone) 1 (NQO1); Glucose-6-phosphate dehydrogenase (G6PD);Malic Enzyme 1(ME1); Phosphogluconate dehydrogenase (PGD); Heme Oxyhenease 1 (HMOX1);Ferritin (FTH) and Terminal Flower (TFL).*

1.7.4 NRF2 in Health and Disease

Research over the past two decades has established that NRF2 suppresses carcinogenesis, especially during the early stages (Ma *et al.*, 2015). The use of *Nrf2* -/- mice exposed to carcinogens has shown that activated NRF2 is chemo-preventative, through the induction of detoxification pathways and sequestering of ROS (Khor *et al.*, 2008). NRF2 activators such as sulphorafane (SFN) have been evidenced to inhibit carcinogenesis in the gastrointestinal tract, skin, lung, bladder and breast tissue (Melba *et al.*, 2013; Chen *et al.*,2014 and Lu *et al.*, 2017). Other cancer prevention studies implementing oleanane triterpenoids, a synthetic NRF2 ligand have showed a delay in tumorigenesis, through the suppression of oncogenes such as *Kras*, *Trp53* and

Her2 (Bishayee *et al.,* 2013). Furthermore, lung carcinogenesis was suppressed following oleanane triterpenoids exposure (To *et al.,* 2015). Contrariwise, somatic mutations in NRF2 that result in its overexpression positively correlate with tumorigenesis, indicating the selective advantage to cancer cells which are susceptible to proliferation induced OS (Kitamura and Motohashi, 2018). Additionally the NRF2 protective effects against OS that characterizes neurodegenerative diseases have been exemplified *in vitro* and mice models of Parkinson's disease (PD) (Lui *et al.,* 2017). Furthermore, SFN was evidenced to protect against mitochondrial complex I inhibitors 1-methyl- 4-phenyl-1,2,3,6-tetrahydropyridine (MPTP) induced death of nigral dopaminergic neurons and also decrease of astrogliosis and inflammatory cytokine release, which is associated with neurodegenerative disorders (Sita *et al.,* 2017).

1.8 Vitamin D – 'A custodian for phenotypic stability'

Emerging evidence has linked 1,25D to the regulation of vital signalling pathways that are important for cellular health (Nakai *et al*., 2014; Chen *et al.,* 2013 and Wang *et al.,* 2012). The cellular antioxidant defences maintain a highly reduced internal state (Birben *et al.,* 2012). An imbalance of this steady state is caused by reactive oxygen species (ROS) due to trauma, hypertoxia, infection or excessive exercise increases free radicals (e.g. superoxide, hydrogen peroxide and peroxynitrite) (Valko *et al.,* 2007). Furthermore, exposure to UV, environmental toxins, carcinogens and dietary compounds disrupts this steady state, causing oxidative stress, thus cells become susceptible to damage or cellular death (Dunning *et al.,* 2006). In addition, carcinogenesis, diabetes mellitus, age-related disease and neurodegenerative disease have been implicated with ROS (Berridge, 2015). The fundamental basis of ROS signalling is its reversibility. 1,25D in conjunction with Klotho and Nrf2 has been linked to the modulation of antioxidant systems that prevent OS by removing ROS (Berridge, 2015). In expanding upon the 'defensome' properties of 1,25D, Gaucion *et al.,* (1999) were the first to observe gamma-glutamyl transpeptidase (γ-GT) gene expression and enzymatic activity were augmented by 1,25D in primary cultures of newborn rat astrocytes, although Ito *et al.,* (2014), observed contradicting findings in LLC-PK1 porcine renal tubular epithelial cells. Additionally 1,25D abrogates NADPH oxidase-2 (NOX-2), NOX-4, and $p67^{phox}$ genes, all involved in ROS

generation, an effect observed in human renal arteries Dong *et al.,* (2012). Glucose-6-phosphate dehydrogenase (G6PD) glutamate cysteine ligase (GCLC) and glutathione reductase (GR) all increase GSH and their increased expression is linked to 1,25D exposure (Jain and Micinski, 2014). NRF2, the cellular modulator of over 300 genes involved in the neutralization of oxidative stress is also regulated by 1,25D (Chorley *et al.,* 2012). Moreover, bipolar disorder treatment such as valproate and lithium known to inhibit HDAC, also enhance NRF2 expression (Correa *et al.,* 2011). Epigenome regulation by 1,25D was also observed in the mediation of DNA methyltransferases such as Jumonji Domain Containing 3 (JMJD3) (Fetahu *et al.,* 2014). The 'defensome' properties of 1,25D and involvement in diabetic cardiomyopathy were investigated by Lee *et al.,* (2014) using diabetic induced rats. Upon 1,25D exposure, the diabetic effects on receptor advanced glycation end (RAGE) products, mediated by Angiotensin II receptor type 1 (AT1R), anti-inflammatory and anti-oxidative responses were decreased (Torino *et al.,* 2017). Higher than normal RAGE levels are also observed in Alzheimer's disease, osteoarthritis and malignancies, all of which have been linked to 1,25D deficiency (Torino *et al.,* 2017). 1,25D is also involved in the regulation of Klotho, a transmembrane bound anti-aging protein, crucial for homeostatic function of numerous organs Tsujikawa *et al.,* (2003). There is also enough evidence to speculate that insulin, tumour necrosis factor (TNF), Wnt signalling pathway and cytokines are amongst the different signalling pathways regulated by 1,25D (Larriba *et al.,* 2013). The above-mentioned classical, non-classical, cellular protective properties together with cell cycle properties, further highlight the need to maintain optimum 1,25D levels.

Additionally, its (1,25D) ability to modulate hepatic and extrahepatic properties, it is reasonable to speculate this beneficial function also in the blood brain barrier (BBB) and placenta (Shin *et al.,* 2010). The former was confirmed by Takahashi *et al.,* (2017) who observed that 1,25D decreased damage to the BBB in following treatment of the human brain microvascular endothelial cell line. Consequently, Berridge (2015) proposed a hypothesis, in which 1,25D was defined as a 'custodian for phenotypic stability'. This explains why numerous diseases are associated with 1,25D deficiency,

also, their manifestation correlates with dysregulation of calcium, redox signalling, including NRF2 and Klotho modulation.

Expanding upon Berridge's (2015) hypothesis, our study also focuses on examining the co-operative effects of enhanced detoxification responses, through *UGT1A* induction mediated by VDR and NRF2 (Figure 1.11). As already mentioned, NRF2 increases the expression of multiple *UGT1A* isoforms that include the *UGT1A7-UGT1A10* cluster (Kalthof *et al.*,2010; Sakakibata *et al.,* 2015 and Wu *et al.*, 2012). Interestingly, Wu *et al.*, (2012) identified that NRF2 increases the mRNA expression of UDP-glucose-6 dehydrogenase (UGDH) and solute carrier family 35 member D1 (SLC35D1). These enzymes are involved in the synthesis and transport of UDPGlcA into the ER respectively (Wu *et al.,* 2012). UDPGlcA is the co-factor that facilitates glucuronidation of *UGT1A* susceptible subtrates (Fujiwara *et al.,* 2010). These findings suggest that NRF2 is a key factor in the bioavailability of UDPGlcA and glucuronidation processes altogether. Since activation of VDR increases NRF2 mRNA expression, it is reasonable to speculate that the interplay between both TFs is likely to enhance *UGT1A* expression and activity (Nakai *et al.,* 2014). We and others have correlated VDR to the modulation of pivotal metabolic (e.g. CYPs) and transporter-related activities (e.g. *MDR1*) (Maguire *et al.*, 2012 and Chow *et al.*, 2011). Furthermore, our unpublished data has also confirmed *UGT1A* up-regulation by VDR ligands in colon cancer cells. Altogether, there is compelling evidence that suggests that *UGT1A* regulation may be further enhanced by VDR acting in concert with NRF2 to facilitate detoxification pathways, thus maintaining cellular intergrity.

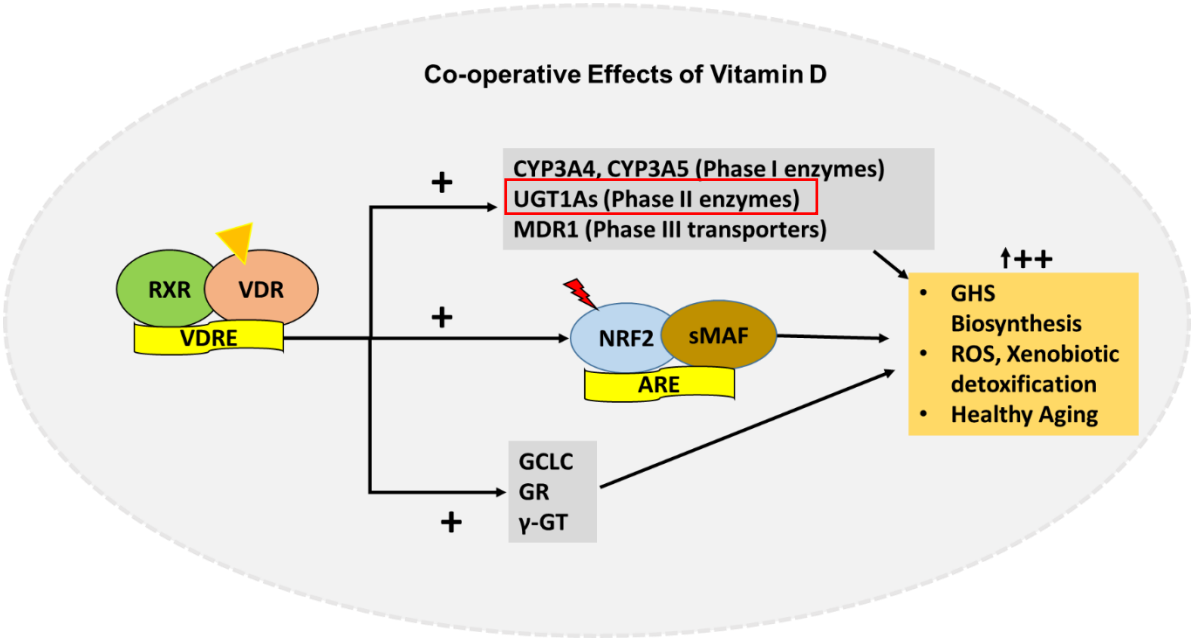

Figure 1.12: A proposed model of Vitamin D and NRF2 co-operative effects. *A concept based upon Berridge's phenotypic stability hypothesis, we propose that that modulation of metabolic gene products, and NRF2 it's self by VDR signalling enhances detoxification and tightly regulates cellular phenotypic stability.*

1.9 Research Aims and Objectives

Taking into consideration the above-mentioned evidence, it is reasonable to speculate that VDR may be a potent inducer of vital extrahepatic metabolism. This project aims to fully define the impact of VDR induced *UGT1A.* Our findings will be of biological significance particularly where UGT1A expression is compromised (e.g. neonatal jaundice). Additionally, our findings will re-inforce the implications of drug-drug interactions, whilst also at a functional level, this study will also re-inforce the co-operative effects of VDR in the redox-signaling pathway. Using LS180 cells as our main model system, we aim to:

1. **Investigate the regulation of extrahepatic *UGT1A* gene family members by VDR.**

Transcriptomic characterization through mRNA and protein expression profile and reporter-based activity under various conditions, in cells exposed to VDR ligands will be examined. For the latter, this will also involve the identification of VDREs within the *UGT1A* promoter regions, following which confirmation of its functionality by mutagenesis experiments will be implemented, where diminished activity will signify a functional VDRE. Functional read-out experiments measuring glucuronidation activity will examine the ability to translate our transcriptomic evidence into a clinical setting.

2. **Examine whether there is an interaction between VDR and NRF2 signalling pathways that encompasses *UGT1A* gene regulation.**

Here also transcriptomic characterization through mRNA levels, protein expression and reporter-based activity of cells exposed to VDR and NRF2 prototypical ligands will be examined. Inter-dependency of NRF2 signalling upon VDR signalling pathway will be determined through mutation of response elements, followed by measurement of promoter activity. Growth inhibitory assay as a functional study will fundamentally measure whether 1,25D enhances chemo-protective features where both pathways are activated. This will also be translated in a prostatic cancer cell context.

3. Characterize VDR/RXR binding motifs within the *UGT1A* locus

Due to the dramatic *UGT1A4* responsiveness by VDR ligands, this project also aims to conduct a more focused evaluation of the *UGT1A* locus to delineate the contribution of potential binding motifs that may contribute to this unique response. The cloning of *UGT1A* locus will allow further manipulation of the identified binding sites that will then be used for *UGT1A4* transcriptomic characterization. The use of Clustered Regularly Interspaced Short Palindromic Repeats Interference (CRISPRi) technique will allow simultaneous VDRE deactivation in a native context, thereby characterizing the effects of *UGT1A* transactivation through a series of gene expression and reporter-based assays.

2: Chapter 2
Materials and Methods

2.1 Reagents

Ethanol was purchased from Romil Pure Chemistry (E314), EB1089 was obtained from Enzo Scientific and Calcitriol (1,25D) was purchased from Tocris Biosciences, Bristol, UK. Methanol was purchased from Fisher Scientific (M/H056/17), Trypan Blue Stain 0.4% was purchased from GIBCO, UK (15250), GW474064A was purchased from Gaskosmithkline and Cas9-Dead-NLS, produced in *E.coli*, expressing a *Streptococcus pyogenes* Cas9 gene with two amino acid substitutions in the protein (D10A and H840A) was purchased from Eupheia Biotech, Germany. Rifampicin (R3501), 5β-Cholanic acid 3-one (3kLCA, C6271), Dimethyl sulfoxide (DMSO, D2650), Sulforaphane (574215), *tert*-butyhydroquione (*t*BHQ, 112941), phosphate buffered saline (PBS, P4417), Nuclease-free water (W4502) and TO901316 (T2320) were all purchased from Sigma-Aldrich, Dorset UK.

2.2 Cell Culture

2.2.1 LS180 Cells

LS180 cells are derived from a 58-year-old Caucasian female with Dukes type V adenocarcinoma of the colon (Public Health England, 2020). This cell line was evaluated as a suitable in vitro model for investigating VDR signaling as they mimic 1,25D extrahepatic, in addition to (Aiba *et al.*, 2005) who observed the suitability of LS180 cells in elucidating mechanisms that regulate intestinal metabolic gene products. Additional cell line models were used to evaluate VDR signaling in a different context. LS180 cells were obtained from the European Collection of Cell Cultures at passage 52 (ECACC, LOT06/C/039). Cells were maintained in complete media made up of Minimum Essential Medium (MEM) (Invitrogen, UK) supplemented with 10% fetal bovine serum (FBS) Invitrogen) 50 units/ml penicillin G, 50µg.ml streptomycin (P/S) (Invitrogen,UK), 1% MEM Non-Essential Amino Acid Solution (NEAA) (Invitrogen, UK) and 1% Sodium Pyruvate (Invitrogen, UK). For experiments using steroid depleted conditions, MEM was supplemented with 5% charcoal stripped serum (CSS) (GIBCO, Invitrogen).

2.2.2 Human Embryonic Kidney cells (HEK293 cells)

HEK293 cells were generated from normal human embryonic kidney cells exposed to sheared fragments of human adenovirus type 5 DNA (Ad5) in by Alex van der Eb *et al.*, (1973). Although direct comparison to kidney tissue may be questionable, this cell line model is standard and very efficient co- transfection. In this study, HEK293 cells were used to evaluate precise VDR effects. The cells were obtained from (ECACC, 8512062). For maintenance, High Glucose (4.5%) Dulbecco's Minimum Essential Medium (DMEM, supplemented with 10% FBS, 1% L-glutamine and 1% P/S.

2.2.3 LNCaP cells

LNCaP cell line was isolated from a needle aspiration biopsy of the left supraclavicular lymph node of a 50 year of Caucasian male (blood type B+) with metastatic prostate carcinoma. This cell line was use to evaluate VDR mediated metabolic gene product regulation and cross talk with NRF2 signaling in a prostatic context and how it compares to the gastrointestinal context. LNCaP cell line were obtained from (ECACC 89110211, LNCaP clone FGC). Cells were maintained in RPMI 1640 with 10% FBS, 1% P/S and 1% L-Glutamine (Invitrogen).

2.2.4 Sub-culture Routine

Cells were split to sub-confluent cultures between 70 to 80% (1:3 to 1:6), seeding at 4 x 10^6 cells/ T175 cells. LS180 cells were split by use of non-supplemented MEM and 0.5 EDTA. HEK293 and LNCaP cells were split but by 0.05% Trypsin (Invitrogen). Cells were incubated at 37^{o}C and 5% CO_2 atmosphere.

2.2.5 Cell Storage

For cell storage, cells were centrifuged at 1,500rpm for 5 minutes and the supernant was discarded and re-suspended in 1ml freezing solution/4 x 10^6 cells, comprising of 5% DMSO and 95% FBS. Cells were transferred to Nalgene 5100-0001 PC/HDPE Mr. Frosty 1 Degree C Cryogenic Freezing Container immediately frozen for 48 hours,

then transferred to a permanent storage box at -80°C or liquid nitrogen for long-term storage.

2.2.6 Thawing cells

Cells were removed from the -80°C freezer and immediately thawed in a 37°C waterbath. 5ml media was added to the cells drop-wise, followed by centrifugation at 1,500rpm for 5 minutes. Supernatant was discarded and the cell pellet was re-suspended in 5ml media. Cells were transferred to a T75 cell culture flask and maintained as described in Section 2.2.4.

2.2.7 Cell Density

Cell density and viability for seeding determined using a haemocytometer (See Table 2.1). Following detachment from culture flasks, cells were centrifuged at 1200prm for 5 minutes (RT). The supernatant was discarded and the pellet was re-suspended in 5ml media. 14µl cell suspension was mixed with 14µl Trypan Blue Stain 0.4% (Sigma-Aldrich, Dorset, UK) 12µl of the 1:1 suspension was pipetted on to a coverslip. Cell viability is determined by the absence of Trypan Blue staining. Unstained cells were visualized using the an automated cell counter which also determined the percentage cell viability and quantification of live cells. The total number of cells in suspension were calculated per ml were the total number of cells is multiplied by the dilution factor with Trypan Blue and multiplication factor obtained with the volume in 5ml.

Table 2.1: Common seeding densities

Cell Line	Plate	Volume of Media	Cell Density (Cells/ml)
LS180	100mm dish	10ml	$1.5x10^6$
LS180	6-well	2ml	$4x10^5$
LS180	24-well	500µl	$1x10^5$
LS180	96-well	100µl	$18x10^3$
HEK293	24-well	500µl	$1x10^5$
LNCaP	6-well	2ml	$4x10^5$
LNCaP	24-well	500µl	$1x10^5$
LNCaP	96-well	100µl	$4x10^3$

2.2.8 Dosage with Ligands

1,25D (10^{-8}M), the biologically active form of Vitamin D which activates VDR was used in the investigation of all VDR signalling experiments. 3-ketolithocholic acid (3KLCA), a major metabolite of the cytotoxic secondary bile acid (BA), lithocholic acid was also used in our experiments as it also a VDR ligand, although less potent. Our interest in using this ligand was to identify the role of VDR in controlling the bioavailability of BA as a chemo-preventative measure through the regulation of extrahepatic *UGT1A* gene family members. EB1089, a Vitamin D synthetic analogue was included in our experiments to also examine the effects of *UGT1A* regulation. EB1089 is a very potent VDR ligand and also has been synthetically modified such that, if VDR induced UGT1A is clinically relevant, EB1089 may be a safer alternative dude to the absence of side effects such as hypercalcemia, which are often observed upon administering Vitamin D. PXR is a well-known *UGT1A* regulator and is a close relative of VDR. PXR activation by rifampicin was included as a positive control, in addition to establishing the most potent extrahepatic *UGT1A* inducer. Also included in this study were well-known LXR and FXR ligands TO901317 and GW474066 respectively. Both NRs are known to enhance *UGT1A* gene expression. These were included in our experiments to confirm VDR specific activities in our chosen cell model systems. *Tert*-butylhydroquinone (*t*BHQ) and sulphorafane (SFN), both activate NRF2 signaling and were included in the examination of VDR and NRF2 interplay.

Ligand stock concentration was diluted in media in a 1:1000 dilution. All experiments were treated with ligands as stated in table 2.2.

Table 2.2: Ligands and common concentrations used in this study

Ligand	Solute	Stock concentration	Working Concentration	Action
Ethanol	-	100%	100%	Vehicle
DMSO	-	100%	100%	Vehicle
Methanol	-	100%	100%	Vehicle
1,25D	Ethanol	10^{5}M	10^{-8}M	Biological VDR ligand
EB1089	Ethanol	10^{-5}M	10^{-8}M	Synthetic VDR ligand
3kLCA	Ethanol	10^{-2}M	10^{-5}M	Secondary bile acid known to be a VDR ligand
*t*BHQ	Ethanol	40mM	40μM	NRF2 ligand
SFN	DMSO	6mM	6μM	NRF2 ligand
TO901317	DMSO	10^{-2}M	10^{-5}M	LXR ligand
GW474066	DMSO	10^{-2}M	10^{-5}M	FXR ligand
Rifampicin	Methanol	10^{-2}M	10^{-5}M	PXR ligand

2.3 Polymerase Chain Reaction (PCR)

2.3.1 RNA Extraction

Following ligand exposure at appropriate time points for each experiment, RNA extraction from cells was performed using the Qiagen RNAeasy® Plus Mini Prep Kit (Qiagen, Sussex, UK). The procedure was carried out using the manufacturer's instructions. Briefly, media with ligands was discarded and cells were dislodged by either scrapping or typsinisation. Cells were collected by centrifugation at 1,200 rpm

for 5mins. Cell pellet was lysed using 350µl Buffer RLT containing β-Mercaptoethanol (Sigma-Aldrich, Dorset, UK). Lysate homogenization was performed by passing through a 20-gauge needle with RNAase free syringe. DNA was removed by passing be lysate through a gDNA Eliminator column. For each sample, 350µl of 70% Ethanol was added, and the solution was passed through an RNAeasy mini column. Bound RNA was washed using RW1 buffer, then RPE buffer. Total RNA was eluted in 30µL RNase free H_2O. RNA concentration was determined by nanodrop using an ND-1000 Spectrophotometer (Labtech, Ringmer, UK). Approximately 1µl was loaded and the absorbance was measured at 260/280nm. RNA quantification was given in ng/µl. All samples were stored at -80^oC to avoid degradation.

2.3.2 Ethanol Precipitation

Ethanol precipitation was performed were RNA purity was significantly low. It concentrates RNA and de-salts nucleic acids in an aqueous solution. Briefly, 0.1 volume of 3M sodium acetate (NaOHC) pH 5.2 was pipetted into RNA sample, 2.5µl of ice cold 100% Ethanol was mixed thoroughly into the solution, which was then incubated at -20^oC for 1 hour. Centrifugation at 12,000 rpm for 15 minutes at 4°C was carried out and the supernatant was discarded. The pellet was washed by adding 300µl of 70% Ethanol, then briefly centrifuged for 10minutes at 12,000rpm at 4^oC. The supernatant was discarded and the pellet was left to air dry prior to dissolving in RNAase free H_2O (30µl).

2.3.3 cDNA Synthesis

For each cDNA conversion, 2000ng of RNA was diluted with 1µl Oligo dT primers, 1µl 10mM dNTP mix (Invitrogen, UK) and distilled H_2O (ddH2O), made up to a 12µl volume. The mixture was heated on the Multi-Block System (MBS) for 5 minutes at 65^oC to ensure Oligo dT primer annealing to RNA, then cooled for 2 minutes at 4^oC. Subsequently, a 7.5µl mixture containing 4µl 5Xfirst Strand Buffer (Invitrogen), 2µl of 0.1M DTT and 1.5µl of ddH_2O. This was heated at 42°C for 2 minutes to optimize the temperature for the reverse transcriptase to work. To each sample, 0.5µl Superscript II Reverse Transcriptase (Invitrogen, Paisley, UK) was added. Reverse

transcription was carried out at 42°C for 50 minutes, then then halted by heating to 70°C for 15 minutes. cDNA is was then diluted to 1:10 using ddH_2O to a total concentration of 200ng. cDNA is more stable than RNA and was stored at -20^{o}C.

2.3.4 Primer Design and preparation

Custom primers that only code for specific upstream or downstream sites of gene sequences being amplified were designed using Primer3 version 4.1.0. Software available online (Untergasser *et al.,* 2012). The sequence for each designed primer is listed in table 2.4. The gene mRNA sequence was retrieved from the NCBI database which was then inputted to the Primer3 software. The criteria for each primer pair included the following optimum parameters:

Table 2.3: Optimum parameters for endpoint PCR primer design

Primer length	20 nucleotides
Primer melting temperature (Tm)	60°C
Primer GC% content	60%
Product Size	150-250bp

Each primer pair was designed to span to exons, with one of the primers spanning across two exons itself. This minimized the chances of DNA contamination and the inclusion of intronic sequences.

Table 2.4: Endpoint primer oligonucleotide sequences

Gene	Oligonucleotide sequences 5' to 3'

β-Actin	Forward AAACTGGAACGGTGAAGGTG
	Reverse TCAAGTTGGGGACAAAAG
CYP24A1	Forward CAGCGAACTGAAAATGGTCG
	Reverse TCTTCTCATACAACACGAGGCAG
CYP3A4	Forward FCGTGGCCCAATCAATTATCT
	Reverse GCTGAATCTTTCAGGGAGGA
CYP3A5	Forward GGAGATGTTCCCCATCATTG Reverse CGTTGAGGCGACTTTTCTTC
UGT1A1	Commercially available at Thermo Fischer Scientific, UK
UGT1A3	Commercially available at Thermo Fischer Scientific, UK
UGT1A4	Commercially available at Thermo Fischer Scientific, UK
UGT1A5	Commercially available at Thermo Fischer Scientific, UK
UGT1A7	Commercially available at Thermo Fischer Scientific, UK
UGT1A8	Commercially available at Thermo Fischer Scientific, UK
UGT1A10	Commercially available at Thermo Fischer Scientific, UK
VDR	Forward CCAGTTCGTGTGAATGATGG
	Reverse GTCGTCCATGGTGAAGGACT
PXR	Forward TGTCAACGCAGATGAGGAAG
	Reverse TCCCTGTCCGTTCACTTTTC
FXR	Forward GTCAGCAGGGAGGATCAAAG
	Reverse CTGCATGCTGCTTCACATTT
LXRα	Commercially available at Thermo Fischer Scientific, UK
LXRβ	Commercially available at Thermo Fischer Scientific, UK
G6PD	Forward TTGCCAACAGGATCTTCGGC
	Reverse GGTCGTCCAGGTACCCTTTG
NQO1	Forward GAAAGGATGGGAGGTGGTGGTGG
	Reverse CGTGGATCCCTTGCAGAGAG
GCLC	Forward ACCCAAACCATCCTACCCTT Reverse GGCTTGGAATGTCACCTGGA
SOD1	Forward GCAGAAGGAAAGTAATGGACCA
	Reverse GTCACATTGCCCAATGGACCA

GSR	Forward	TGCGTGAATGTTGGATGTGT
	Reverse	TATTCCTAAGCTGGCACCGG
GPX2	Forward	TGAATGGGCAGAACGAGCAT
	Reverse	CCAGCAGTGTCTCCTGAAGG

2.3.5. Endpoint PCR

Endpoint PCR was performed prior to initial gene expression analysis to detect house-keeping gene, *β-actin* as a quality control in addition to detection of genes of interest listed in Table 2.4 All primers were supplied by Invitrogen, UK and all for the PCR recipe (Table 2.5), reagents were supplied by Promega (Madison, USA). The dNTP mixture was from Invitrogen (Paisley, UK).

Table 2.5: Endpoint PCR reaction mixture

Reagent	**Volume (µl)**
5X PCR Buffer	5
25mM $MgCl_2$	1.5
10mM dNTP mix	0.5
10µM Forward Primer	0.5
10µM Reverse Primer	0.5
Taq Polymerase	0.1
ddH_2O	Up to 20µl

20µl of the reaction was added to each 0.5ml Eppendorf and 5µl of 200ng cDNA template or ddH_2O for negative control were added to each mixture. The samples were placed in the thermocycler with the following thermo-cycler conditions:

Table 2.6: Endpoint PCR conditions

Step	Conditions	
Initial Denaturation	94°C for 2 minutes	
Denaturation	94°C for 30 seconds	**30 to 35 cycles**
Annealing Tm	60°C for 30 seconds	
Extension	72°C for 3 minutes	
Final Extension	72°C for 10 minutes	
Hold	Hold	

2.3.6 Gel Electrophoresis

1.5% agarose gel was prepared with 1.5g of agarose electrophoresis grade powder (BIA1176 Apollo Scientific, UK) was added to 100ml of 1X Tris Acetate Buffer (TAE). The powder was completely dissolved by heating the mixture. Once the mixture cooled down to approximately 60°C prior to adding 3µl of the fluorescent nucleic acid Gel Red dye (Sigma-Aldrich, UK). The solution was poured on to a casting tray and allowed to solidify. The cell was transferred into an electrophoresis tank immersed in 1X TAE buffer. 8µl pf PCR product was added to each well of the gel and run alongside 100bp or 1Kb DNA ladder (Invitrogen, Paisley, UK) depending on the expected product size. Electric current was run at 100V for approximately 15 minutes. PCR product was visualized using a UV transluminator and images captured using the Sygene G BOX Chemi system.

2.3.7. Real Time PCR

For this study, real time PCR using using Taqman® mono colour hydrolysis probes (Applied Biosystems) was the method of choice for gene expression analysis.

This allowed direct comparison of relative mRNA expression changes induced by the above-mentioned ligands the chosen cell model systems. Each hydrolysis probes reaction comprised of component.

Table 2.7: Light Cycler 480 Individual Hydrolysis Probes Recipe

Reagent	Volume (μl)
2 PCR H_2O	2
Probe	0.5
1 2X Probes Master	5

For each reaction, 2.5µl of cDNA was added to the PCR master mix, then, loaded to each well on a white 96 LightCycler® 480 Multi-well plate. Each PCR sample was performed in triplicates. Negative controls consisted of RNAase free H_2O. An Optical adhesive cover (Applied Biosystems) was used to cover the well to avoid evaporation. The plate was plus centrifuged to 800rpm for approximately 10 seconds using Hettich Rotanta 460R centrifuge. The plact was placed in the Light Cycler 480 system set according to the manufacturer's User Manual. Relative gene expression in samples was calculated relative to vehicle control treated samples using the equation below:

$$\Delta\Delta Ct = 2\text{^-}(\Delta Ct_{TARGET} - \Delta Ct_{CONTROL})$$

The Ct value is the raw output from the LightCycler 480 system. The ΔCt is the difference in Ct values between the target gene and house-keeping gene (*HPRT*). Fold Induction was determined relative to each vehicle control.

Table 2.8: Light Cycler Probes used in this study (Roche Diagnostics Germany).

Hydrolysis Probe	**Catalogue 1D**
CYP24A1	112269
CYP3A4	135760
UGT1A1	138404
UGT1A3	140686
UGT1A4	140612
UGT1A5	145870
UGT1A7	145839
UGT1A8	145843
UGT1A10	145837
VDR	111894
PXR	137125
NRF2	113587
ARK1C1	117462
CDH1	103920
BIRC5	101365
HMOX1	110977
NQO1	147227
G6PD	147654
GCLC	147654

2.4 DNA Extraction

To collect the pellet 5 x 10^6 LS180 cells were obtained by washing with ice cold PBS and scrapping from a T175 flask. Cells were then recovered by centrifugation at 1500g for 10 minutes at 4°C. The supernatant was discarded and re-suspended in 500µl of ice cold PBS. Added to the cell suspension also was 500µl of ice-cold C1 lysis buffer (Qiagen, UK) and 500µl ddH_2O. Cell lysates were centrifuged at 1300g for 15 minutes at 4°C. The supernatant was discarded and 250µl of C1 lysis buffer (Qiagen, UK) and 750µl of ice-cold ddH_2O. The pellet was re-suspended by vortexing and again centrifugation at 4°C for 15 minutes at 1300g following which the supernatant was discarded. DNA extraction was carried out using the Blood and Cell

Culture Mini Kit (Qiagen: 13323) using the manufacturer's protocol. DNA concentration was determined by nanodrop using an ND-1000 Spectrophotometer (Labtech, Ringmer, UK). Approximately 1µl was loaded and the absorbance was measured at 260/280nm DNA quantification was given in ng/µl, thereafter stored at -80ºC.

2.4.1 DNA amplification

ChIP-seq data by Meyer *et al.,* (2012) evidenced multiple 1,25D dependent VDR/RXR binding motifs within the *UGT1A* loci in LS180 cells. In this study, we evaluated one of these enhancer regions. The sequence was obtained from the National Centre of Biotechnology Information (NCBI) website and was used to design primers for the *UGT1A* loci region of interest as described in Section 2.13.

Table 2.9: *UGT1A* enhancer region primer sequencers amplify a 1532bp product.

Primer	**Oligonucleotide sequence 5'-3'**
UGT1A enhancer region	Forward GGAGTTGGCCGTGATGACA Reverse ACCTCTAGACACTGCCGGT

Endpoint PCR technique was used to generate copies of the targeted sequences. The extracted DNA was used as a template for PCR to amplify the *UGT1A* promoter region using Q5 High Fidelity DNA Polymerase (See Table 2.9) (PCR reagents supplied by NEBLabs, UK (M0491). The PCR reaction was run under the conditions described in Table 2.9. The PCR product was visualized in 0.9% agarose gel as described in Section 2.3.6.

Table 2.10: DNA amplification PCR reaction recipe.

Component	Volume (µl)
5 x Q5 Reaction Buffer	5
10mM dNTPs	0.5
10µM Forward Primer	1.25
10µM Reverse Primer	1.25
DNA Template	200ng
Q5 High Fidelity DNA Polymerase	0.25
Nuclease Free Water	to 25

Table 2.11: DNA amplification thermocycler conditions.

Step	Condition	
Initial Denaturation	98°C for 1 minute seconds	
Denaturation	98°C for 1 minute	30 cycles
Annealing	60°C for 30 seconds	
Extension	72° for 90 seconds	
Final Extension	4°C	

2.4.2 Gel Excision and DNA purification

The agarose gel was placed on an open Ultra Violet (UV) box and was set at 70nm wavelength. This visualized the desired DNA fragment, which was sliced and placed in a clean 1.5 Eppendorf. DNA purification, which removes chaotropic salts and non-specific fragments was carried out using an alcohol-based wash using the Wizard® SV Gel and PCR Clean-Up System, following the manufacturer's instructions. DNA was eluted in TE buffer and concentration determined using the nanodrop using an ND-1000 Spectrophotometer (Labtech, Ringmer, UK) as previously described.

2.5 Western Blot Analysis

Western Blot analysis was used to determined UGT1A protein induction following ligand exposure to LS180 cells. The effects of VDR prototypical ligands was compared to various ligands in their ability to induce this protein.

2.5.1 Extraction of Protein from Whole Cell Lysates

To collect whole cell lysates, LS180 cells were scrapped using non-supplemented MEM and 0.5M EDTA. The pellet was collected by centrifugation at 1,200rpm for 5 minutes. The supernatant was discarded and re-suspended in ice cold PBS, followed by centrifugation at 1000g for 5 minutes at 4^{o}C. The supernatant was removed at 250µl of Radio-immunoprecipitation assay (RIPA) buffer consisting of 1M Tris-HCl (pH 7.5) , 5M NaCl, 10% Igepal CA630, 10% sodium deoxycholate, 10% SDS, 0.5M EDTA (pH 8.0), 0.1M DTT, 80% Glycerol, 1% Protease inhibitor cocktail and ddH_2O. Each sample was sonicated at 4 amplitude microns for 3 cycles at 10 seconds. Centrifugation at 15,000g for 15 minutes at 4^{o}C to remove cellular debris. The supernatant was transferred to a new pre-chilled 1.5ml Eppendorf. For long-term storage, protein samples were stored at -80^{o}C.

2.5.2 Extraction of Protein from Microsomal fractions

The microsome Isolation Kit (ab206995: Abcam) was used to isolate microsomal fractions from LS180 cells for UGT1A protein profiling and enzymatic activity. Briefly, the cells were seeded in 100mm dishes as described previously and treated for a further 24 hours. The next day, cells were washed in 1ml ice cold PBS, then centrifugation at 700xg for 5 minutes at 4°C. Supernatant was discarded and the pellet was re-suspended in 500µl ice-cold homogenization buffer followed by homogenization using a chilled Dounce homogenizer. The homogenate was transferred to a microcentrifuge tube and vortexed for 30 seconds prior to chilling on ice for 1 minute, followed by centrifugation at 10,000xg for 15 minutes at 4°C. A thin, floating lipid layer was aspirated using a Pasteur pipette. The supernatant was transferred to a new pre-chilled microcetrifuge tube and centrifuged at maximum speed >20,000xg for 20 minutes at 4°C. Supernatant was discarded and pellet was gently washed with homogenization buffer, then re-suspended in pre-chilled storage buffer. Protein quantification was determined as described in Section 2.5.3.

2.5.3. Quantification of protein

Protein concentration was determined using the Bio-Rad DC protein assay (Bio-Rad,UK) following the manufacturer's protocol. Each LS180 whole cell lysate sample was diluted in 1:10 dilution with ddH_2O. The assay was performed in a 96 well plate where absorbance at 750nm was measured using FLUO star Omega microplate reader (BMG Labtech). A standard curve was calculated using the serial dilutions on the standard Bovine Serum Albumin (BSA;Bio-Rad;0206). BSA stock (2mg/ml) was diluted 1:2 in PBS. DC™ Protein Assay Reagent S was added to DC™ Protein Assay Reagent A in a 1:50 dilution, followed by 200µl of DC™ Protein Assay Reagent S (all reagents from Bio-Rad 500113-115). Then added to both BSA and LS180 protein samples. This was incubated for 15 minutes at room temperature prior to an absorbance reading at 750nm using the UV spectrophotometer. LS180 protein was quantified from the standard curve using the formula Y=mX+C.

2.5.4 Blotting

Western blot reaction mixtures was prepared as shown in Table 2.13. Protein was denatured in a 95^oC heat block for appoximately 5minutes. The denatured samples were transferred in a 4-12% NuPage® Bis-Tris Mini Gel (IM-8042: Thermo Scientific) along with 7.5µl of Spectra of Spectra^{TM} Multicolour Broad Range Protein Ladder (Fermentas, 26628). For electrophoresis the X-cell sure Lock ^{TM} novex mini cell kit (Invitrogen), using 1X NuPage SDS MOPS running buffer (NP001: Invitrogen) at 200Volts constant for 47 minutes with an expected current of 100-125mA/gel start; 60-80mA/gel end was utilized. After protein distribution on the gel, the protein fragments were placed on a Nitrocellulose blotting membrane (Amersham Biosciences; 10600018) using semi dry transfer methodology. The transfer buffer comprised of 100% Methanol, 10X Tris-Glycine buffer and ddH_2O. This was run in a Trans-Blot SD Semi-Dry Transfer cell (Bio Rad) for 60 minutes at 20Volts. Subsequent transfer of protein was distinguished via Ponceau S Solution (Sigma-Aldrich; P71701L). The stain was carefully removed by washing the membrane with 1X TBS-T (Tris-buffered Saline pH 7.4 and 1% Tween-20). Blocking was carried out using 0.5% dried

semi-skimmed milk (Marvel, UK) dissolved in 1X TBS-T for one hour at room temperature, then washed with 1XTBS-T prior to incubation with antibody.

2.5.5 Probing with antibody

The membrane was incubated with primary antibody as depicted in table 2.12 for 14 - 16 hours at 4^{o}C, then washed with 1XTBS-T three times for approximately 10 minutes, followed by secondary antibody incubation at room temperature for 1 hour. The secondary antibody was subsequently detached using 1X TBS-T. For protein development, the membrane was incubated in Immunbilon® Western Chemiluminescent HRP Substrate (Millipore; WBKLS0050) for approximately 5 minutes. The membrane was placed on a black screen inside the G-Box Chemi XRQ system where the GeneSys software and Kodak X Omat camera captured images of the protein.

Table 2.12: Western Blot sample preparation recipe

Reagent	**Volume (µl)**
Protein Lysate (30µg)	
NuPage LDS Loading buffer (4X)	7
NuPage Reducing Agent (10x)	3
RIPA buffer	Up to 30µl

Table 2.13: List of primary antibodies used in this study

Antibody	**Source**	**Catalogue ID**	**Dilution**

Mouse Anti-UGT1A	**Santa Cruz**	**Sc-271268**	**1:5000**
Rat Anti-VDR 9A7	**Thermo Fisher**	**MA1-710**	**1:5000**
Mouse Anti-β-Actin	**Sigma**	**A2228**	**1:20000**
Rabbit Anti-HPRT	**Santa Cruz**	**Sc-20975**	**1:2000**

Table 2.14: List of secondary antibodies used in this study

Antibody	Source	Catalogue ID	Dilution
Goat anti-Mouse IgG HRP	**Abcam**	**Ab205719**	**1:5000**
Goat anti-Rat IgG HRP	**Santa Cruz**	**Sc-2006**	**1:10000**
Mouse anti-Rabbit 1gG HRP	**Santa Cruz**	**Sc-2357**	**1:3000**

In order to re-probe the membrane with another antibody, either mild or harsh stripping (See Table 2.14) to remove the previously detected antibodies. For the harsh stripping, the membrane was incubated at 60°C for 30 minutes with bouts of agitation. The protein was blocked using 0.5% semi-skimmed milk (Marvel) dissolved in 1X TBS-T for one hour at room temperature, then washed with 1xTBS-T and probed with primary, then secondary antibody as described in above.

Table 2.15: Recipe for antibody stripping.

Mild Antibody Stripping	Harsh Antibody Stripping
O.1M Glycine-HCl pH 2.5	50mM Tris-HCl pH6.8
1% SDS	50mM DTT
	2% SDS

2.6 Glucuronidation Activity Assay

Glucuronidation activity investigated in LS180 cells following the methodology outline by Dellinger *et al.,* (2012), briefly described below.

2.6.1 Preparation of cell homogenates

Cells were seeded in 100mm (See Table 2.1) for 24 hours prior to dosage with VDR prototypical ligands. Media from cells was discarded and cells were collected by scrapping after adding 5ml of ice cold PBS. Once detached, LS180 cells collected and centrifuged for 1,200rpm for 5 minutes. The supernatant was discarded and the pellet re-suspended in 200µl Tris Buffered Saline (TBS) homogenate buffer consisting of 25mM Tris base, 138mM NaCl, 2.7mM KCl pH 7.4 and 5% protease inhibitor cocktail (P8340; Sigma Aldrich, UK). The cell lysates subdued a series of freeze thaw cycles using dry ice with ethanol for freezing and a 37^{o}C water bath to thaw the samples. Each homogenate was transferred into a 2ml glass Dounce homogenizer and forcefully disrupted using a homogenizing plunger. Each homogenate was transferred into a pre-chilled 1.5 Eppendorf and was subject to protein quantification was per section 2.5.3 or stored at -80^{o}C.

2.6.2 Glucuronidation Assay using UGT-glo

1µl of alamethicin (BML-A150-0005, Enzo) was added to each well in an opaque 96-well plate, then incubated at 37°C for 1 hour to evaporate the ethanol. 50µg of each homogenate was added to each well containing alamethicin in triplicate. (Although 6 wells per sample in order to compare basal levels were UDPGA, the co-factor of glucuronic acid transfer is absent). UGT multi-enzyme was prepared as depicted in table 2.15 and added to each well. The reaction was incubated for 10 minutes on ice.

Table 2.16: Multi-Enzyme Substrate reaction mixture

Reagent	**Volume (µl)**
5X UGT-Glo Buffer	8
UGT multi-enzyme substrate (0.16mM)	5
ddH_2O	7

Following incubation, 10µl of UDPGA (16mM) was added to half of the wells and ddH_2O in all – UDPGA samples. The plate was incubated for 90 minutes at 37°C.

2.6.3 UGT Activity Detection

Luciferin detection solution was prepared by mixing both reconstitution buffer and Luciferin detection agent. 1X D-Cysteine was added to the detection solution. After 1-hour incubation, 40µl of Luciferin Detection reagent was added to each well followed by stabilization of luminescent signal by incubating plate for 20 minutes at room temperature. Luminescence signal was detected using FLUO star Omega micro plate reader (BMG Lab tech). The values were reported in percentage (%) relative light units increase.

2.7 Reporter Activity Assay

2.7.1 Plasmids

To investigate *UGT1A1* promoter activity induction by VDR ligands, the firefly luciferase based pGL3-UGT1A1-2K which contains 2kbp (-5193/-3092) and the pGL3-UGT1A1-290 (-3483/-3194) which contains 290bp distal enhancer sequence were kindly gifted by Professor Masahiko Negishi (Research Triangle Park, North Carolina). The pGL3-UGT1A1-290 mutant was produced previously in the laboratory by site directed mutagenesis (Agilent,UK) (See section 2.8). This contained a 2bp mutation of the DR3 putative VDRE within the 290bp fragment. *CYP3A4* is significantly induced by VDR and so in this study, the firefly luciferase based pGL3-CYP3A4 reporter which contains 10kbp of the *CYP3A4* promoter region (-10466/+53) (Bertilsson *et al.,* 2001) was kindly gifted by Dr Patrik Blomquist (Karolinska Institute, Sweden). pSG5-hVDR, pSG5-hPXR, pSG5-hRXRα and pSG5-LXRα were gifted by Professor Mark Haussler, University of Arizona, from which V5 based constructs were then generated using the gateway cloning system (Thermo Fisher Scientific, UK). In addition, V5-hFXR was also previously generated by *LR clonase* reaction using an existing pDONER entry clone for hFXR. The VDRE minimal promoter was previously constructed through VDRE oligonucleotide insertion in to the pGL3-promoter vector (Promega, UK). The vector was cut with Nhel and Xhol restriction enzymes that created complimentary overhangs into which the VDRE

oligonucleotides were inserted. The ARE minimal promoter (pGL4.37[luc2P/ARE/Hygro]) (See Figure 2.1) which contains four copies of the ARE was purchased from Promega E364A (Madison, USA).

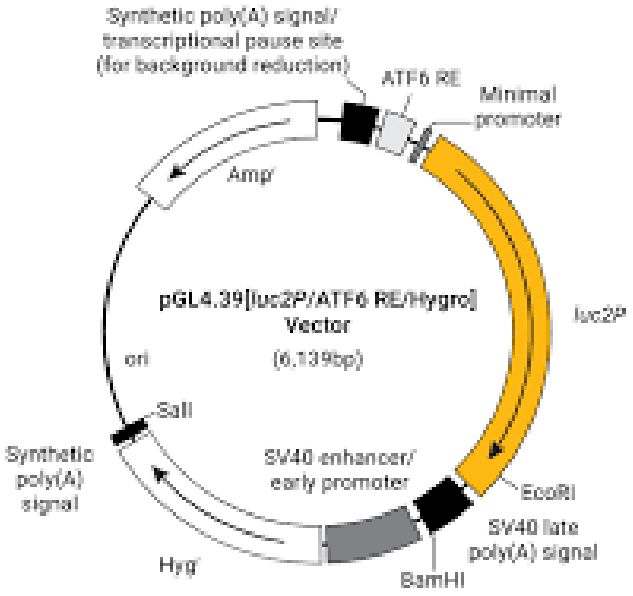

Figure 2.1: The pGL4.37[luc2P/ARE/Hygro] Vector *depicted contains multiple AREs derived from that induce Photinus pyralis luciferase gene transcription. The vector backbone comprises an ampicillin resistance gene that allows E.coli selection to allow stably transfected mammalian cell limes (Promega, 2020).*

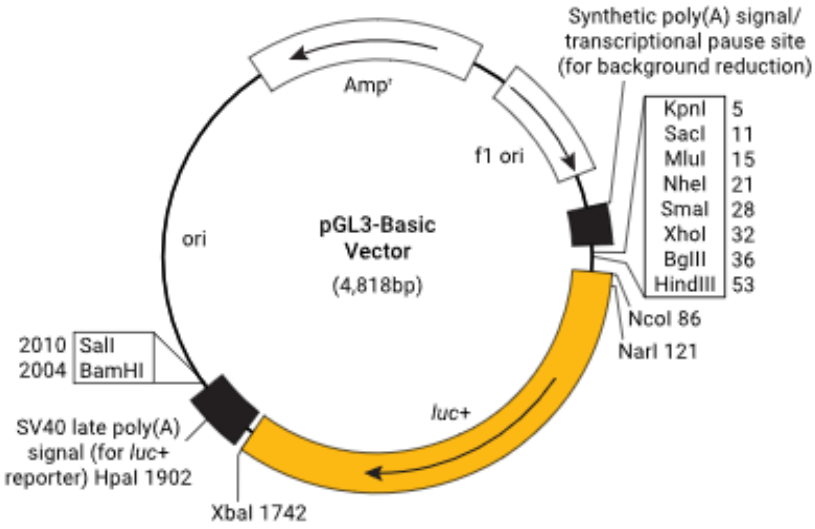

Figure 2.2: The pGL3- Luciferase Reporter Vector *contains Photinus pyralis firefly luciferase gene used to measure transcriptional activity in successfully transfected cells. The basic vector also contains restriction enzyme sites utilized to clone a promoter sequence of interest. (Promega, 2020)*

2.7.2 Transformation of plasmids into Library Efficiency® DH5α E.coli (Invitrogen)

40µl Library Efficiency® DH5α E.coli (Invitrogen Cat: 18263-012) were added to 1µl of plasmid. The mixture was incubated on ice for 35minutes prior to heat-shock at 42°C water bath for 45 seconds, followed by 2 minutes chill on ice. 600µl of SOC media (Invitrogen Cat: 15544-034) was added to the culture which was then incubated at 37°C in a 200rpm shaker for 1 hour. The culture was centrifuged at 13,000rpm for 1 minute at room temperature, following which 400µl of the supernatant was discarded. The pellet was then re-suspended in the remaining 200µl and plated onto LB Amp plate and streaked using beads. The plates were incubated at 37°C overnight for 8 to 10 hours. Individual colonies were then observed on the plate were inoculated into LB Amp broth which was grow overnight. PureLink™ HiPure Plasmid Filter Maxi-prep Kit (Invitrogen: K210016) was then used to extract plasmid DNA.

2.7.3 Transfection Methodology

2.7.3.1 Lipofectamine Transfection

For Lipofectamine transfection, LS180 and LNCaP cell lines were seeded in 24 well plate or 100mm (See Table 2.1 for seeding density) for 24 hours to reach approximately 70% confluency. This was followed by DNA transfection using Lipofectamine 2000 Invitrogen, 11668-019) in a 1:3 ratio (See Table 2.16 for DNA concentrations). The DNA-Opti-MEM® was added to the Lipofectamine- Opti-MEM® mixture and incubated for 45 minutes at room temperature. The DNA-Lipofectamine mixture was added to cells and incubated for 5 hours at 37°C, following which fresh media containing ligands. The cells were treated for 24 hours unless stated for individual experiments.

Table 2.17: Concentration of transfected DNA

Plasmid DNA	Concentration per well (ng)
pGL3-UGT1A1-2K	650
pGL3-UGT1A1-290 WT and MUT	650
pGL3-CYP3A4	500
ARE-Luc	650
pGL3-VDRE	650
hVDR	100
hPXR	100
hLXRα	100
hFXR	100
pRL-TK	30
pcDNA.3.1	Promoter vector control

2.7.3.2 Calcium Phosphate transfection

Calcium phosphate transfection, developed by Graham and van der Eb (1973) is less expensive and easy to master. However, the cytotoxic effects meant it was unsuitable for LS180 and LNCaP cell line models used in this study. However, HEK293 cells can endure the harsh effects also achieve high transfection efficiency.

HEK293 cells were seeded in 24-well plate for 24 hours to reach approximately 70% confluency (See Table 2.1 for seeding density). The required plasmid DNA was added to 2M $CaCl_2$ (Sigma, C8106) (See Table X). The mixture was added drop-wise to 2X HBS (50mM HEPES, 280mM NaCl, 1.5mM Na_2HPO_4) in a 1:1 ratio (See Table 2.17). The mixture was incubated for 30 minutes at room temperature. Cells were exposed to the mixture for 16 hours at 37°C. Cells were washed with PBS prior to treatment with designated ligands after 24 hours.

Table 2.18: Calcium Phosphate transfection volumes

Plate Size	**Surface Area**	**2X HBS (µl)**	**2M $CaCl_2$ (µl)**	**Maximum Amount of DNA (µg)**	**Culture Media (ml)**
24-well plate	.25X	35	4.3	1	0.5

2.7.4 Reporter Assay Reading

Following treatment at specified time points for each experiment, media was removed and the cells were washed with PBS. 150µl of 1X passive lysis buffer (Promega, E941) and plate was placed on a shaker for 15 minutes. After which, 80µl of cell lysates were transferred into 96-well opaque plate. 50µl of Dual-Glo® Luciferase reagent (Promega, E195A) was added to each well and left to equilibrate at room temperature for 5minutes. Luminescence was measured FLUO star Omega micro plate reader (BMG Lab tech). 50µl of Dual Glo®- STOP &GLO® reagent (Promega, E641A) which detects pRL-TK vector, signifying transfection efficiency was then added to each well and left to equilibrate for 5 minutes prior to detecting luminescence. Furthermore, this reading was used to normalize the former luciferase readings.

2.8 Site-directed Mutagenesis

Yueh and Tukey (2006) previously identified three AREs within the *UGT1A1* promoter, which when mutated reduced NRF2 mediated induction. Upon *in silico* analysis, the ARE sequence was identified within the pGL3-UGT1A1-290 used in this

study (Sequence in Figure 2.3). Mutagenesis primers introducing a 2bp mutation on the ARE were designed using the Agilent Quik-change primer tool (Table 2.18). The mutagenesis mixture was depicted in table 2.20 was then subjected to PCR reaction with the thermocycler conditions depicted in (Table 2.21). The reagents were from the QuikChange II-XL Site-Directed Mutagenesis Kit (Agilent, 200521).

Figure 2.3: UGT1A1 promoter sequence (Tukey and Yueh, 2010)

Table 2.19: UGT1A1-290 primers designed for site-directed mutagenesis.

Primer	Oligo sequence 5' to 3'
UGT1A1 290bp Forward	gttacataacctgaaacccggactaagcacttggtaagcac
UGT1A1 290bp Reverse	gtgcttaccaagtgcttagtccgggtttcaggttatgtaac

Table 2.20: Site-directed mutagenesis PCR reaction recipe

Reagent	Amount
10X reaction buffer	5µl
Forward Primer	200ng
Reverse Primer	200ng
pGL3-UGT1A1-290 reporter plasmid (Wild-type, WT)	
dNTPs	1µl
Pfu Polymerase	1µl
Nuclease free H_2O	Up to 50µl

Table 2.21: Site Directed Mutagenesis PCR conditions

Step	Conditions	
Initial Denaturation	95°C for 30 seconds	
Denaturation	95°C for 30 seconds	18 Cycles
Annealing	60°C for 1 minute	
Extension	68°C for 10 minutes	
Hold	4°C	

1µl of *Dpnl* restriction enzyme (Agilent, UK) was added to the PCR product, then, incubated at 37°C for 90 minutes. 1µl of the sample was transformed into 40µl of XL1-Blue super competent cells (Agilent, 200249). The reaction was left on ice for 30 minutes, then subjected to heat shock (42°C temperature). NZY^{+}Broth with NZ amine (casein hydrolysate (Sigma C0626), 0.5g of yeast extract (Sigma, Y1625), 0.5g of NaCl (Sigma, S7653) dissolved in 100ml deionised water and pH adjusted to 7.5. To this 12.5 µl of 1 M MgCl2, 12.5 µl of 1M MgSO4, 20µl of 20% (w/v) glucose was added to 1 ml of the NZY broth, freshly prior to transformation and incubated in a waterbath. The reaction was streaked on LB agar plates with 50µg/ml ampicillin and incubated at 37°C overnight. Plasmid DNA was extracted using Pure-Link^{TM} Quick plasmid mini-prep kit, then sequenced as described in Section 2.9, prior to a maxi prep extraction as describe previously.

2.9 Sequencing

Plasmid DNA sequencing was performed using the Applied Biosystem 3100 Genetic Analyser with Bing Dye Terminator version 3.1 Cycle Sequencing Kit (Applied Biosystems Cat: 4337-457). To confirm the presence of ARE mutation, UGT1A primers as were sequenced under the conditions described below.

Table 2.22: Sequencing mixture

Reagent	Volume (µl)
Big Dye Ready Reaction Mix	2
5X sequencing buffer	3.5
UGT1A Sequencing Primer Forward (3.2pmol/µl)	1
UGT1A Sequencing Primer Reverse (3.2pmol/µl)	1
Plasmid DNA Template	300ng
Nuclease free water	Up to 20µl

The sequencing mixture was run under the following cycling conditions

Table 2.23: Thermocycler conditions for sequencing mixture

Step	Conditions	
Initial Denaturation	96°C for 1 minute	
Denaturation	96°C for 30 seconds	30 cycles
Annealing	55°C for 30 seconds	
Extension	60°C for 4 minutes	
Hold	4°C	

The PCR product was subjected to ethanol precipitation by the addition of 16µl nuclease free ddH_2O and 64µl of ethanol (95%). The reaction was incubated overnight at -20°C, followed by centrifugation at 14,000rpm for 20 minutes. The supernatant was discarded the pellet re-suspended in 250µl of ethanol (70%), then centrifugation for a further 10 minutes and supernatant discarded. The sample was placed on a 95°C heat blot for 2 minutes to ensure ethanol evaporates, prior to chilling on ice for a further 2 minutes. Formamide (20µl) was added to the sample following 5 minutes of

heat shock (95°C) and chilling for 3 minutes. The sequencing reaction (Table 2.21) was loaded to the DNA sequencing 96 well plate, which was then loaded on to the Applied Biosystem 3100 Genetic Analyser, which works on a capillary electrophoresis basis. Bound DNA fragments migrate through a polymer and the fluorescence emissions are measured. Each fluorescence signal is represented by a different colour which correlates which one of the nucleotides.

2.10 Cell Viability Assay

Cell Viability was conducted using CellTiter-Glo® Luminescent Cell Viability Assay (Promega: G7570) using the manufacturer's protocol. Briefly, LS180 cells were seeded in 96 well plates (See Table **2.1** for seeding density) for 24 hours prior to dosage with ligands for another 24 hours. Control wells containing only media were also incubated to obtain a value for background luminescence. The plate was equilibrated at room temperature for approximately 30 minutes, following which 100µl of the CellTiter-Glo® Reagent was added to the opaque 96 well plate. The content were placed on an orbit shaker for 2 minutes to induce cell lysis then a further 10 minutes incubation at room temperature to stabilize luminescent signal. Luminescence was recorded using the FLUO star Omega micro plate reader (BMG Lab tech).

2.11 Growth Inhibition Assay

LNCaP cells were seeded in 96 well plate as described in table X for 24 hours prior to dosage with ligand for 144 hours. In addition to control wells containing media only for background luminescence, un-treated cells were included as a negative control. Growth inhibition was determined by CellTiter-Glo® Luminescent Cell Viability Assay (Promega: G7570) as described in section 2.10.

2.12 In Silico Analysis

2.12.1 In Silico Screening for putative response elements

The *UGT1A* loci sequence obtained from NCBI was screened for putative VDRE and ARE using the Regulatory Sequence Analysis Tool (RSAT). The loci was inputted into the bioinformatics analysis tool and either the VDRE or the ARE consensus

sequence were inputted. For VDRE, the search generated DR3, ER6 and IR6-type motifs. The ARE identified by Yueh and Tukey (2007) was applied.

2.13 CloneJet PCR cloning

2.13.1 Ligation formula

Purified and quantified 1632bp long DNA product was ligated with the PJET1.2/blunt end-cloning vector Thermo Scientific (Cat: K1232) using the ligation formula adapted from NEBcalculator™ v1.10.0 as described below at either 1:1, 1:3 or 1:5 insert/vector molar ratios.

Required mass insert (g) = desired insert/vector molar ratio x mass of vector (g) x ratio of insert to vector lengths

Q5 High Fidelity DNA polymerase (NEBlabs, UK) with 3' to 5' exonuclease activity was used to amplify the *UGT1A* enhancer region and so produced blunt-end DNA fragments therefore the blunt end cloning protocol was implemented as described by the manufacturer. In other instances, Taq DNA polymerase was used. This produced PCR products with 3'dA overhangs.

Table 2.24: Ligation mixture for cloning

Component	Volume (µl)
2X Reaction Buffer	10
Purified blunt end DNA fragment	1
pJET1.2/blunt Cloning Vector (50ng/µl)	1
T4 DNA ligase	1
Nuclease free Water	Up to 20µl

The ligation mixture was vortexed briefly and centrifuged for 3 – 5 seconds, then incubated for either 5 minutes, 30 minutes or overnight at room temperature, at 4°C or on ice. The ligation mixture was used for transformation as described in Section 2.72. Identified colonies were inoculated and subjected to colony PCR as described below.

2.13.2 Analysis of recombinant clones

Analysis of recombinant clones was carried out by colony PCR (See Table 2.24 and 2.25 below) followed by analysis on an agarose gel for the presence of the PCR product. The expected product size was the addition of the *UGT1A* insert and pJET1.2/blunt vector.

Table 2.25: Colony PCR reaction mixture.

Component	**Volume (µl)**
10X Taq buffer	2
dNTPs (2mM)	2
pJET1.2 Forward Sequencing Primer (10µM)	0.4
pJET1.2 Reverse Sequencing Primer (10µM)	0.4
Taq DNA polymerase	0.1
25mM $MgCl_2$	1.2
Bacterial Broth (Colony)	1

Table 2.26: Colony PCR conditions.

Step	**Conditions**	
Initial denaturation	95°C for 3 minutes	
Denaturation	94°C for 30 seconds	25 cycles
Annealing	60°C for 30 seconds	
Extension	72°C for 1minute/kb	
Hold	4°C	

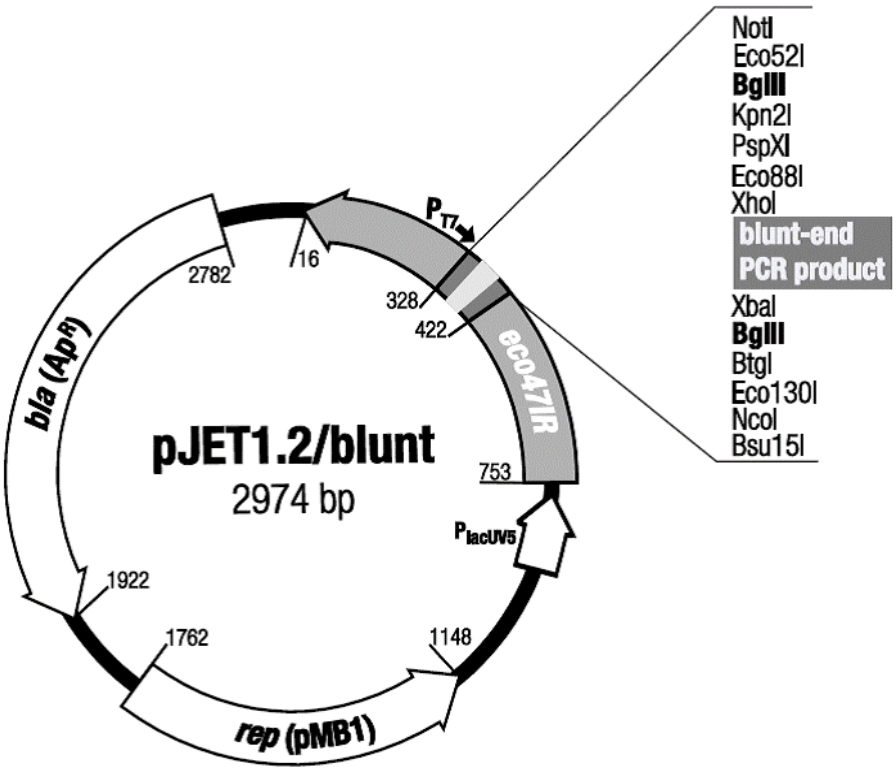

Figure 2.4:PJET1.2/blunt is a blunt- end-cloning vector *that is 2934bp long. It includes a lethal restriction enzyme gene, eco471R that is disrupted by ligation of a DNA insert into the cloning site. For this reason, only the bacterial cells with recombinant plasmids are able to form colonies. If the vector re-circularizes without an insert the expression of the lethal restriction enzyme kills the transformed E.coli cell. The vector also carries a T7 promoter for transcription initiation. (Image from Thermo Fisher Scientific, 2020).*

2.14 Clustered Regulatory Interspaced short palindromic repeats interference (CRISPRi) engineering

2.14.1 Single guide RNA design

Single guide RNA (sgRNA) that target the *UGT1A* enhancer region containing the DR3-type VDRE were designed using CRISPR.MIT.EDU, Zhang lab, (2019) previously available online. The generated output is listed in table 2.26. The *UGT1A* loci sequence was retrieved from the human genome browser (Kent *et al.,* 2002). Output sgRNA were chosen based on specificity to target DNA sequence. Target guides with a scoring of <70, which predict on-target activity were chosen.

2.14.2 Ribonucleoprotein (RNP) complex formation and lipofection

For cell suspension preparation, LS180 cells were washed in PBS and detached from the flask by scrapping and the cell density was determined as described in section 2.1. $1x10^5$ cells or $4x10^5$ cells (for 24 well plates and 6 well plates respectively) were transferred into a 1.5ml microcentrifuge tube and the cells were collected by centrifugation at 200xg for 5 minutes. The supernatant was discarded and the supernatant and cells were re-suspended in 500µl of supplemented MEM. RNP complex was formed using the Synthego, USA guidelines as depicted in table 2.29. The transfection solution was formed as depicted in table **2.27** and was incubated at room temperature for 5 minutes. The RNP complex was then added to the transfection solution, mixed by pipetting and left to incubate for no more than 10 minutes. For lipofection, the RNP-transfection solution was added to each well, followed by each cell suspension previously prepared, by pipetting. 500µl or 2ml of supplemented MEM with each ligands (EtOH or 1,25D) was then added to each well. Plates were incubated at 37°C/5% CO_2 for 48 hours prior to analysis. Samples seeded in 24-well plate were subjected luciferase activity assay as described in section 2.74, whereas samples prepared in 6-well plate were subjected to RNA extraction and gene expression analysis as described in section 2.31 and section 2.37.

Table 2.27: sgRNA sequences for CRISPRi-based approach

Target	On target locus	sgRNA sequence	Specificity score	Off target for [0:1:2:3] + next to PAM
UGT1A guide 1	chr2:+234665495	AACGGTTCATAAAGGGTATT	79	[0:0:0:9:56]+ 0:0:0:3:3
UGT1A guide 2	chr2:+234665495	AACATTCTAACGGTTCATAA	78	[0:0:3:6:76] 0:0:0:0
UGT1A guide 3	chr2:+234665495	TGAACCGTTAGAAGAATGTTCTT	73	[0:0:0:12:62]+ 0:0:0:2:5
UGT1A (Non-targeting)	chr2:234665763-234665833	AGGAATGAGCTTGGACAGGTGGG	46	[0:0:3:71:704] +0:0:0:2:3

Table 2.28: RNP formation reaction

Reagent	6-well plate/well	24-well plate/well
Opti-MEM I reduced Serum Medium	100µl	25µl
Cas9-Dead-NLS	600pmol	100pmol
UGT1A sg RNA guide	780pmol	130pmol
Lipofectamine CRISPRMAX Cas9 Plus Reagent	4µl	1µl
pGL3-UGT1A-290		500ng
pRL-TK		30ng

Table 2.29: CRISPRi transfection mixture

Reagent	Volume (µl) (6-well plate)	Volume (µl) (24-well plate)
Opti-MEM I Reduced Serum Medium	100	25
Lipofectamine CRISPRMAX Transfection Reagent	6	1.5

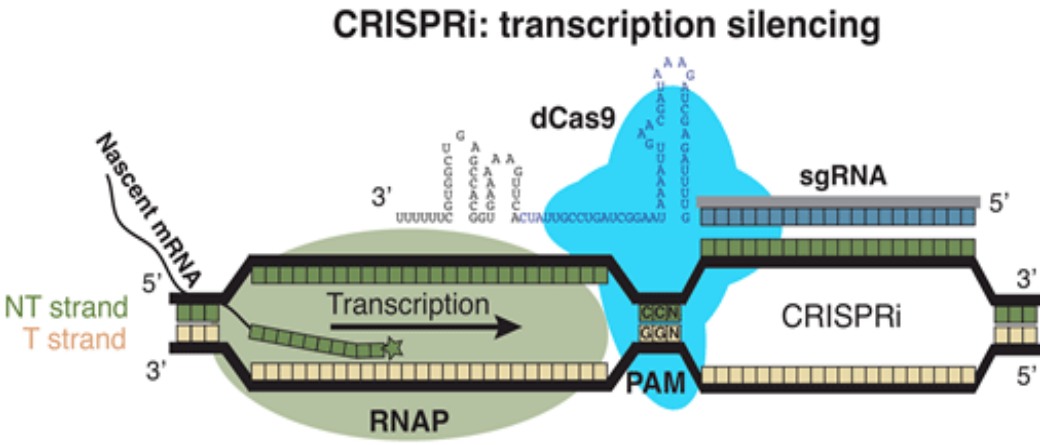

Figure 2.5: CRISPRi transcriptional silencing model. *This technique employs a 20bp sequence that is complementary to the targetted DNA (sgRNA). SgRNA is fused with dCas9, catalytically inactive enzymes that blocks the targeted DNA sequence. Altogether, this simaltenously silences the activity of the targeted sequence (e.g VDRE), which silences trascriptional activity without genetic modification. (Image edited from www.addgene.com, 2020).*

3: Chapter 3

Induction of *UGT1A* gene family members by Vitamin D Receptor

3.1 Introduction

Following the discovery that PXR is a pharmacologically distinct *CYP3A* inducer, the concept of PXR mediated drug metabolizing enzymes has been under scrutiny in recent years, prompting potential implications in drug-drug interactions in humans (Lehmann *et al.*, 1998; Pascussi *et al.,* 2000 and Luo *et al.,* 2002). Predominantly investigated in a hepatic context, PXR is highly homologous to VDR both in its mechanistic action and in sequence (Sueyoshi and Negishi, 2001). Consequently, scientists have taken an interest in translating these findings to an extrahepatic context, where VDR is predominantly expressed (Lee *et al.,* 2018). In addition to phase I metabolic genes, *UGT1A1, UGT1A6* and *UGT1A9* are regulated by liganded PXR (Chen *et al.,* 2012; Hanioka *et al.,* 2012). Multi-drug resistant 1 (MDR1), Multi-drug resistance-associated protein 2 (MRP2) and organic anion transporting polypeptide 2 (OATP2) enzymes that facilitate in the basolateral efflux of metabolites are also induced by PXR (Wagner *et al.,* 2005).

Schmeidlin-ren *et al.,* (1997) were the first to identify an increase in *CYP3A4* mRNA and protein level in Caco-2 cells by 1,25D/VDR signaling. To date, this focus is still rudimentary, but what we know so far is that Thompson *et al.,* (2002) identified a distal DR3-type (-7719/-7733) and a proximal ER6 (-169/-152) VDRE within the *CYP3A* promoter. Expanding upon this concept, Maguire *et al.,* (2012) identified that *CYP3A4* and *CYP3A5* are modulated by VDR in LNCaP prostate cell line model. Disrupted VDR examined in mice models ($Vdr^{\Delta IEpC}$) generated by Cheng *et al.,* (2014) consequently exacerbated LCA-induced hepatotoxicity. Evidently, liganded VDR is important in regulating *CYP3A4*, and in this context, the detoxification of bile acid induced toxicity in the gastrointestinal tract.

Phase II metabolic enzymes have attracted less attention than CYPs, mainly because drug interactions involving these enzymes are relatively rare. Conversely, emerging evidence raises clinical concern. For example, in 2004, Echchgadda *et al.,* observed an increase in phase II metabolic gene *SULT2A1* expression by VDR. This finding was supported by the identification of a VDRE at the -191 to -168 position of rat and mouse *Sult2A1* promoter, supporting its direct inducibility by VDR activation (Echchgadda *et al.,* 2004). Expanding upon this concept, Rondini *et al.,* (2014) later

investigated the regulation of phase II enzymes *SULT1* gene family members by multiple NR signaling pathways in LS180 cells, amongst these was an observation that 1,25D/VDR signaling induced *SULT1C2* mRNA, protein and reporter activity, the latter by a 5.5-fold increase. More evidence of this effect by Seo *et al,* (2013) implicated liganded VDR to *SULT2B1* induction in mice and prostatic cancer cell line models. *SULT2B1* is known to convert dehydroepiandosterone (DHEA) to 3β-sulfates, thus interfering with intra-prostate androgen synthesis (Seo *et al.,* 2013). These findings highlight VDR's therapeutic role in controlling prostate cancer growth.

The interest of VDR mediated phase II metabolic products has since broadened to investigate *UGT1A* family members as glucuronidation has been identified as an important cause of drug-drug interactions (DDI), and as such, a growing clinical problem and potential economic loss for the pharmaceutical industry (Ciotti *et al.,* 1999). The liver is the primary glucuronidation site; however, extrahepatic glucuronidation, mediated by VDR has been shown to hold clinical significance (Strassburg *et al.,* 2002). Evidenced by Kaeding *et al.,* (2008), liganded VDR was identified as a negative regulator of *UGT2B15* and *UGT2B17* in LNCaP and 22Rv1 cell lines, an effect thought to reduce androgen glucuronidation. This suggests that VDR ligands may have profound consequences for androgen homeostasis and activity in androgen-sensitive prostate cancer cells, but most importantly corroborates UGT regulation by VDR.

Interestingly Kasai *et al.,* (2005), observed a link between UGTs and Vitamin D metabolism. Their laboratory demonstrated that the hexafluorinated analog of the active form of 1,25D, 26,26,26,27,27,27-Hexafluoro-1α,25-dihydroxyvitamin D3 [F6-1α,25(OH)2D3], used as a clinical drug in the treatment of hyperparathyroidism, was subjected to CYP24A1 catabolism, but also UGT1A3 mediated glucuronidation, forming a F6-1α, 23S,25(OH)3D3 metabolite in the liver. This was followed by the discovery that recombinant UGT1A3/UGT1A4 isozyme generated three 25OHD3 monoglucuronides (25OHD3-25-glucuronide, 25OHD3-3-glucuronide, and 5,6-trans-25OHD3-25-glucuronide) in the human liver microsomes and human hepatocytes (Wang *et al.,* 2013). From these findings, it is reasonable to speculate that *UGT1A*

gene products are a critical part in Vitamin D homeostasis, an effect we see in the phase I *CYP24A1*, a potent VDR target gene.

Wang *et al.,* (2014) later emphasized the growing concern in *UGT1A* isoform mediated induction by VDR. Mycophenolic acid (MPA) was found to be a susceptible intestinal *UGT1A8* and *UGT1A10* glucuronidation substrate; an effect that influences the drug's pharmacokinetics in kidney transplant recipients. Further supporting *UGT1A* induction by VDR was the identification of VDREs following a genome-wide study. Multiple VDRE were identified, including those within the *UGT1A* locus, upon 1,25D exposure in LS180 cells (Meyer *et al.,* 2012). Additionally, antiretroviral (ARVs) drugs such as Raltegravir and Efavirenz are metabolized by UGTs (Belanger *et al.,* 2009 and Cattaneo *et al.,* 2010). This topic is a major concern where there is high prevalence of *UGT1A1*28 and UGT1A1*6* polymorphisms and Human Immunodeficiency Virus (HIV) cases. Contrariwise, Atazanavir inhibits *UGT1A1* activity. Kanestri *et al.,* (2014) found that homozygous *UGT1A1*28* carriers, whose *UGT1A1* mediated glucuronidation is already decreased (e.g. bilirubin), upon administration of this drug were at even higher risk of severe hyperbilirubinemia. Additionally, over 50% of known drugs are metabolized by different *UGT1A* isoforms (e.g. Irinotecan- *UGT1A1*, Tamoxifen- *UGT1A4*), the need to investigate the characteristics of each isoform regulation is of great importance. From the nine biologically active isoforms within the *UGT1A* locus, (Chapter 1; See Figure 1.6) there is limited evidence of its intestinal regulation by VDR, however the above-mentioned findings highlight the need for its investigation, as it could be as important as hepatic glucuronidation and even phase I metabolism. Although an increase in *UGT1A* expression raises concerns concerning drug metabolism its upregulation is much appreciated in diseases were *UGT1A* expression is compromised. Hyperbilirubinemia is one such case where *UGT1A1* up-regulation would be appreciated.

Clinical relevance of *UGT1As* extend beyond DDI. Cancer researchers are increasingly taking an interest in *UGT1A* regulation following the discovery of its differential expression in normal versus malignant tissue (Strassburg *et al.,* 1997; Izumi *et al.,* 2012; Yilmas *et al.,* 2015; Zhou *et al.,* 2015 and Hanioka *et al.,* (2012). Sumida *et al.,* (2013) were the first to characterize *UGT1A1* expression HaCat skin

cells and humanized mice models treated with UVB exposed tryptophan. This came after concerns of inadequate *UGT1A1* expression in human neonates, who then present with hyperbilirubinemia, or kernicterus if left untreated. This finding was crucial in that, Vitamin D through sunlight exposure can induce *UGT1A1,* increasing bilirubin metabolism, treating neonatal jaundice, while allowing breast-feeding. As per Arias *et al.,* (1964) and more recently Gourley (2002), it is reasonable to speculate that breast-fed neonates have high total serum bilirubin due to pregnane−3α,20β-diol which is evidenced to inhibit bilirubin glucuronidation *in vitro*. Contrary to these findings, Murphy *et al.,* (1981) barely detected pregnane-3α, 20β-diol in breast milk. However, non-esterified fatty acid, β-glucuronidase in the milk were also thought to cause high serum bilirubin (Yigit *et al.,* 2001). Zanardo *et al.,* (2007) hypothesized that inflammatory signaling caused by an abundance of cytokines in breast milk inhibited intestinal UGT1A1 activity. However, this phenomenon is still underdeveloped. Sumida *et al.,* (2013) findings could be a start in eliminating the risk of breast-feeding, complications of phototherapy, invasive blood transfusion and mother-infant separation.

The identification of *UGT1A1* induction by VDR could be a key finding in restoration of UGT1A1 activity where *UGT1A1* expression is compromised. To date over 50 mutations are associated with hyperbilirubinemia (Canu *et al.,* 2013). The most common hereditary hyperbilirubinemia conditions are caused by single nucleotide polymorphisms (SNPs) *UGT1A1*28, UGT1A1*6, UGT1A1*34* and *UGT1A1*35*. *UGT1A1*6* being prevalent amongst the Japanese population (Akiyama *et al.,* 2008). These conditions include Gilbert's Syndrome (GS), Crigler –Najjar Syndrome I (CNS I) and CNS II which presents with reduced *UGT1A1*-mediated glucuronidation capacity, and the latter complete loss, which is life threatening (Jansen *et al.,* 1969). VDR mediated *UGT1A1* induction could possibly aid in managing and reducing these devastating consequences. Our findings will be of clinical importance since GS prevalence is as high as 9% globally and 1 in 3 patients are unaware of their status until they present with drug toxicity due to reduced glucuronidation ability (Fretzayas *et al.,* 2012). Whilst the rest of the symptoms including jaundice (yellowing of the skin) are benign, drug toxicity remains a critical clinical concern and as such raising awareness for genotyping prior to drug administration.

Comprehensive examination of *UGT1A1* regulation by VDR could potentially lead to Vitamin D analogues as treatment for the abovementioned conditions. Nevertheless, advancement in this direction are still limited, also because of the lack of animal models presenting hyperbilirubinemia. Progress in this route was conducted by Chen *et al.,* (2005) who cross-bred *Ugt1*+/- with transgenic (Tg)*UGT1* mice to generate a fully humanized model system (hUGT). Chen *et al.,* 2012 went on to examine h*UGT* with PXR deficiency. Surprisingly, hyperbilirubinemia was not observed, but rather a gradual decline in serum bilirubin, which shortly recovered; an effect implying intestinal UGT1A1 bilirubin metabolism. It was speculated that other signaling pathways could be involved, such as nuclear factor kappa-light-chain-enhancer of activated B cells (NF-κB). NF-κB plays an important role in *UGT1A1* regulation. This was proven by Fujiwara *et al.,* (2012) who compared the effects of breast milk to formula milk in h*UGT1* mice models. Breast milk suppresses intestinal IκB kinase α and β. These enzymes are part of the NF- κB signal transduction cascade.

As shown, VDR plays an important role in the metabolism circuit. In addition to phase I and II metabolic gene products, others and we intimate 1,25D also to up-regulate phase III transporters, including MDR1 from which EMSA identified multiple DR3 and DR4-type VDREs within between -7.9/-7.8kp upstream of the TSS (Saeki *et al.,* 2008). Knowing that hyperbilirubinemia is also caused by a decrease in phase III transporters, perhaps VDR activation could reverse these effects (Keppler, 2014). This evidence sees Vitamin D and its cognate VDR as a necessity in phenotypic stability, disease protection and efficacy of exogenous compounds, again highlighting the importance of understanding this regulation further. Whilst the above mentioned studies have characterized VDR in the involvement of metabolic pathways, data linking VDR and *UGT1A* gene family members has been limited. In this study we aim to fully characterize the entire *UGT1A* gene family's responsiveness to activated VDR and transcriptional and functional level, in addition to defining the molecular mechanisms involved, including the manipulation of possible binding motifs which may be contribute towards the direct regulation of the gene.

3.2 Results

3.2.1 Vitamin D regulates the expression of *UGT1A* gene family members

Preliminary endpoint PCR analysis confirmed the expression of *UGT1A* genes and known VDR targets *CYP24A1 and CYP3A4* in LS180 cells (Figure 3.1) however, through implementing real-time Q-PCR analysis using TaqMan gene expression assay, a quantitative measure of gene expression was obtained. Previous studies have investigated individual *UGT1A* isoform expression, whereas here the entire expression profile across this gene family are analyzed, relative to their transcriptional responses from exposure to VDR or PXR prototypical ligand exposure for 24 hours.

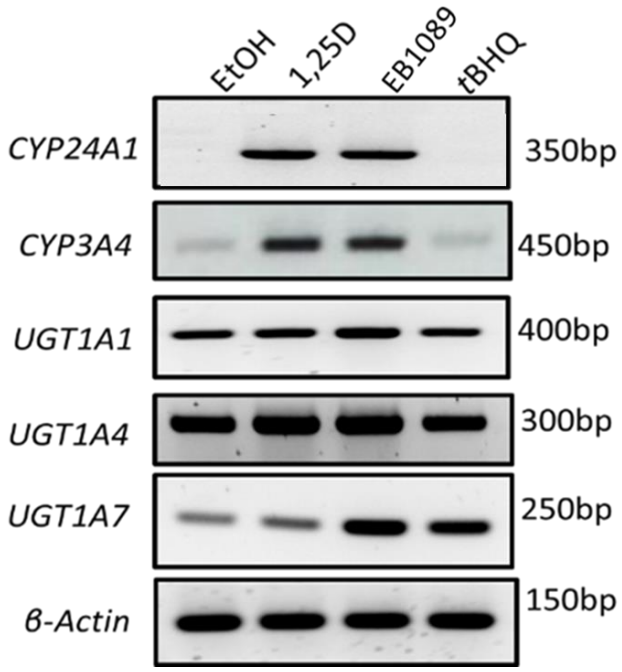

Figure 3.1: Gene expression in LS180 cells. To detect NR expression, RNA was extracted in LS180 cells exposed to EtOH, 1,25D, EB1089 and *t*BHQ for 24 hours. RT-PCR was carried followed using 1.5% agarose gel electropherosis. The PCR product was visualized using a UV transluminator and images captured using the Sygene G BOX Chemi system.

Figure 3.2 shows differential fold induction (**a**) and relative mRNA expression levels (**b**) across all *UGT1A* isoforms in LS180 colonic cancer cells. *UGT1A1* is significantly enhanced by 1,25D (2.1-fold) and its synthetic analogue EB1089 (3.5-fold), but no significant effects are noted for 3kLCA and rifampicin (RIF). 3kLCA is a less potent VDR agonist we included in our investigation. Its ability to induce *UGT1A* gene family members would suggest that VDR is also involved in the bioavailability of secondaty bile acids which in excess cause colorectal cancer (Ishizawa *et al.*, 2018). Enhanced *UGT1A* gene expression by 3kLCA would confirm VDR to be a crucial in chemoprevention. RIF on the other hand is a PXR agonist. As already mentioned, PXR is a close relative of VDR and has also been identified to enhance *UGT1A* gene family members, we included this ligand in our experiments to compare these known effects to that of activated VDR. *UGT1A1* and *UGT1A3* show a similar profile in the overall levels of mRNA expression in LS180 (colon adenocarcinoma) cells, although here in addition to 1,25D- (2.1-fold) and EB1089- (1.96-fold) mediated, the expression of *UGT1A3* is increased 1.3-fold by 3kLCA, an effect that is statistically significant. *UGT1A3* and *UGT1A4* share 93% identity in primary amino acid sequences, yet Figure 3.1 depicts a different expression profile (Jiang *et al.,* 2015). While *UGT1A4* exhibits a relatively low basal level of mRNA expression (compared to *UGT1A1*), this isoform exhibits the highest sensitivity to treatment with VDR ligand. Our experiments found that 1,25D, EB1089 and 3kLCA significantly enhance the levels of *UGT1A4* mRNA expression by 9.9-, 14- and 4.8-fold increase respectively with rifampicin having no effect. A similar profile of expression is noted for *UGT1A5*, with 1,25D, EB1089 and 3KLCA increasing its expression by 5.7-, 8.5- and 2.8-fold, respectively. More modest, albeit still significant effects on *UGT1A7* are also noted with 1,25D and EB1089. Contrary to previous findings Wang *et al.,* (2014), we find no significant change in *UGT1A8* and *UGT1A10* gene expression to be elicited through our selected treatments. Our findings highlight EB1089 to have the most potent *UGT1A* regulatory effects. Similarly Hansen *et al.,* (2000) who identified that the synthetic analogue is 50 to 200 times more potent than 1,25D in inducing genes with antiproliferative effects in U937 lymphoma cells, MCF-7 breast cancer cells and HaCaT cell. Furthermore, although PXR is a known *UGT1A* inducer, we observed a trend in that its actions are less potent that VDR ligands (Xie *et al.,* 2003).

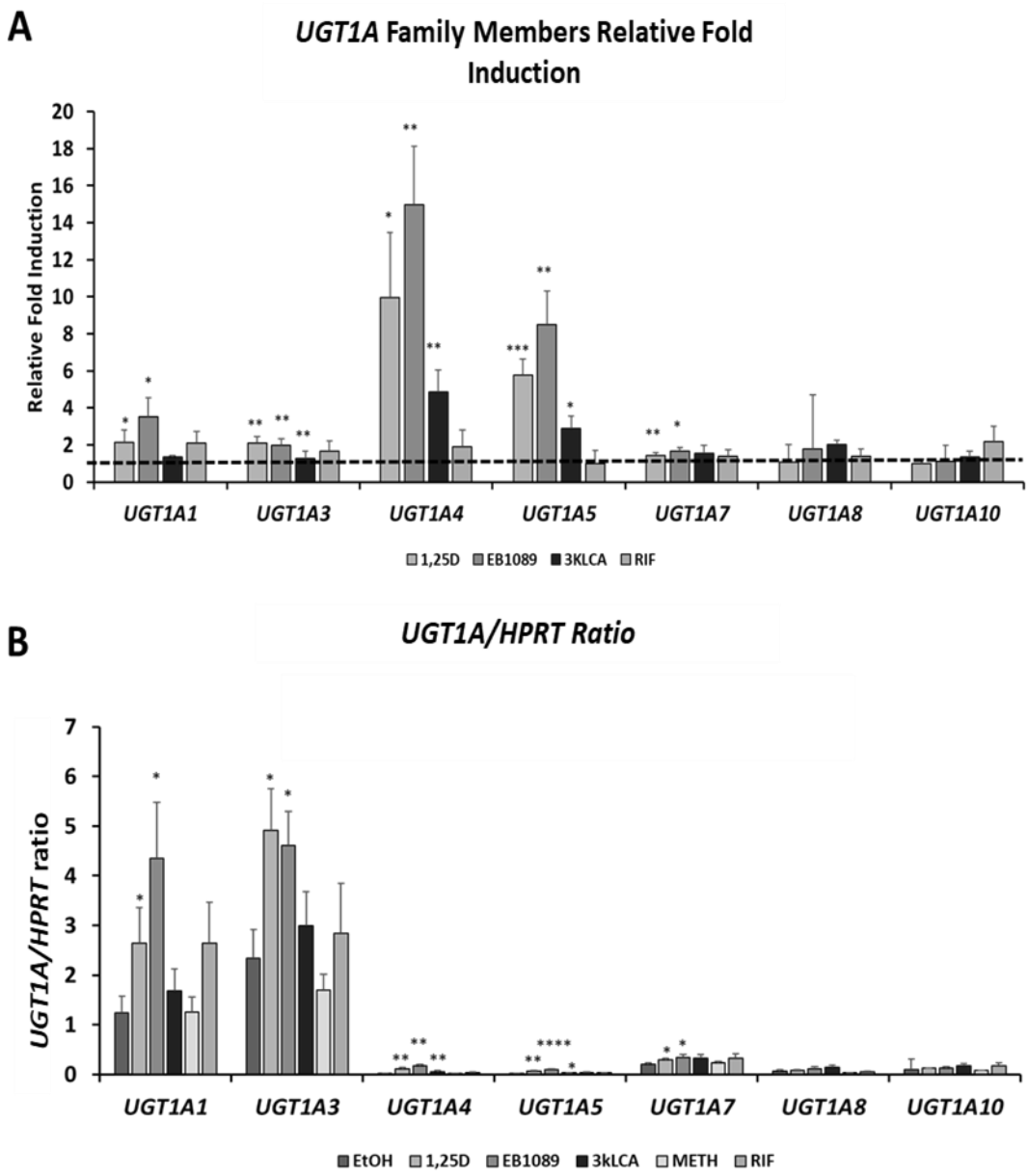

Figure 3.2: UGT1A expression profile in LS180 cells. *RNA was extracted from LS180 cells treated with 1,25D (10^{-8}M), EB1089 (10^{-8}M), 3kLCA (10^{-5}M), RIF(10^{-5}M) or vehicle control for 24-hours. ETOH was the vehicle control for 1,25D, EB1089 and 3kLCA. Methanol (METH) was the vehicle control for RIF. Represented here are fold inductions (ΔΔCT) obtained relative to the vehicle* ***(A)*** *and ΔCT was calculated relative to HPRT as a housekeeping gene* ***(B).*** *Data presented in an average of three independent experiments were n=3. Statistical analysis was obtained from Student's two-tailed t.test were *P<0.05, **P<0.01 and ***P<0.001.*

In order to confirm the validity of our findings, we investigated the mRNA expression levels of known VDR target genes. Figure 3.3 shows *CYP24A1* is significantly induced by all VDR ligands whereas PXR ligand did not induce this gene. Our findings for *CYP3A4* modulation by activated PXR are comparable to that of Hustert *et al.,* (2001), as a 2.5-fold increase was observed in LS174T cells, although this was still minimal compared to a 155-,222- and 86-fold increase modulated by 1,25D, EB1089 and 3kLCA respectively. Finally, treatment of LS180 cells with 10^{-8}M 1,25D and EB1089 resulted in a drastic increase in *TRPV6* expression. 3kLCA also enhanced *TRVP6* expression by 26.7-fold. Our previous unpublished data depicted in Figure 3.4 shows that *UGT1A1* and *UGT1A4* are induced in a time-dependent manner. Both 1,25D and EB1089 significantly increased *UGT1A1* expression after 12 hours by 2- and 3-fold respectively. After 24 hours, EB1089 increased *UGT1A1* expression by approximately 5-fold, peaks at 8-fold after 48 hrs. 1,25D increased *UGT1A1* by 2.5-fold after 24-hours also peaks after 48-hours at 2.6-fold. 3kLCA induced *UGT1A1* gene expression by a significant 1.7-fold, 1.9-fold and 2.1-fold increase following 12-, 24- and 48-hours treatment. 1,25D induced *UGT1A4* by 8-fold, 15-fold and 9-fold after 12-, 24- and 48-hour treatment respectively, while EB1089 induced the same gene significantly, by 15-, 38- and 35-fold after the same time points. Additionally, 3kLCA was also inducible in a time dependent manner (2-, 5- and 7-fold). Rifampicin significantly alters *UGT1A1* and *UGT1A4* expression after 12- and 24-hours respectively (1.3-fold and 3-fold). Time-dependent effects similar to VDR ligands were not observed in this case. Our data show a significant difference in the expression profile of *UGT1A1* and *UGT1A4* induced by 1,25D and EB1089. Clearly, both ligands influence these genes in a time-dependent manner, although EB1089 is more potent than 1,25D.

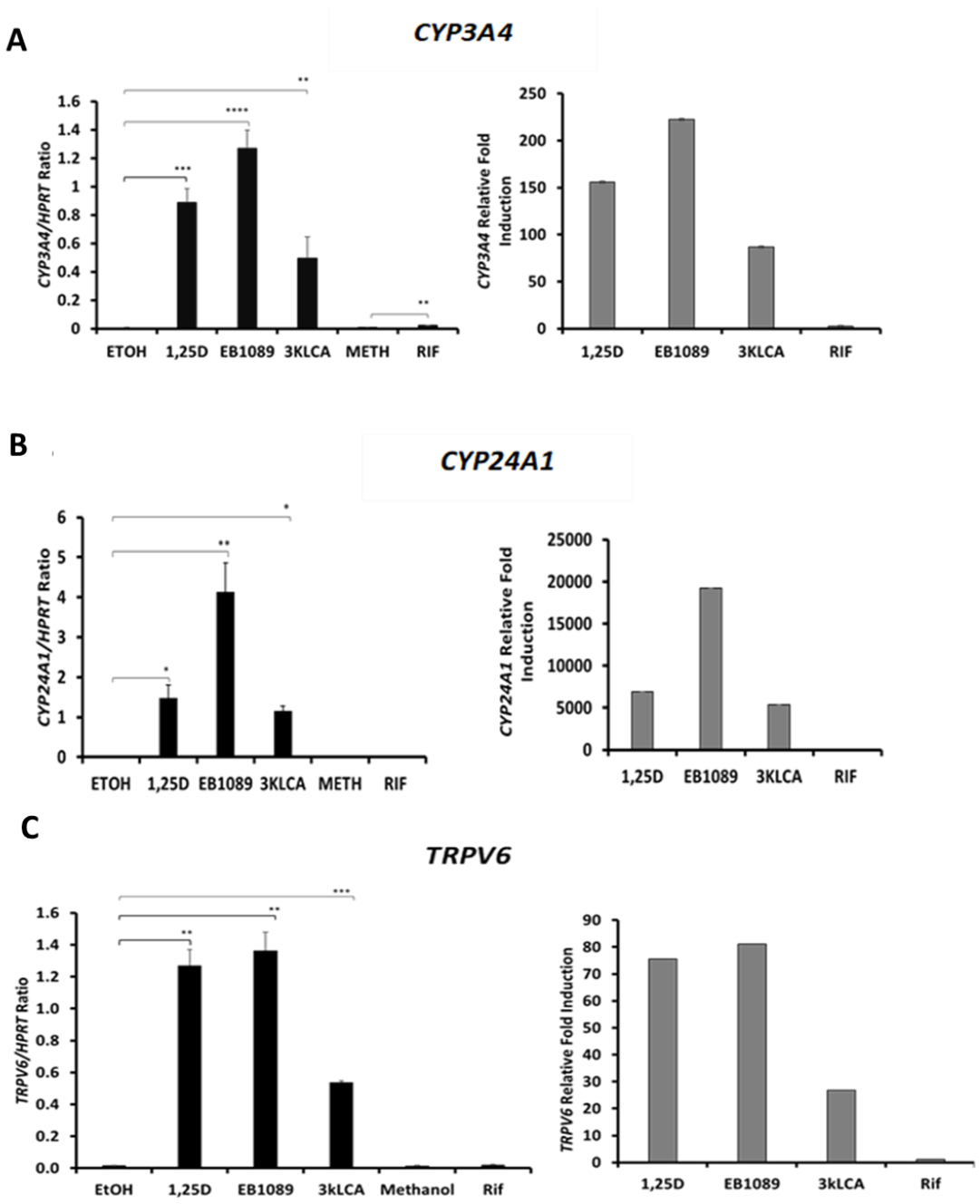

***Figure 3.3*: mRNA expression of VDR target genes in LS180 cells.** *RNA was extracted from LS180 cells treated with 1,25D (10^{-8}M), EB1089 (10^{-8}M), 3kLCA (10^{-5}M), Rif (10^{-5}M) or vehicle control for 24 hours. ΔCT was calculated relative to HPRT as a housekeeping gene. Fold inductions (ΔΔCT) obtained relative to the vehicle. Data shown is an average of three independent experiments were n=3. Statistical analysis was obtained from Student's two-tailed t.test were *P<0.05, **P<0.01 and ***P<0.001.*

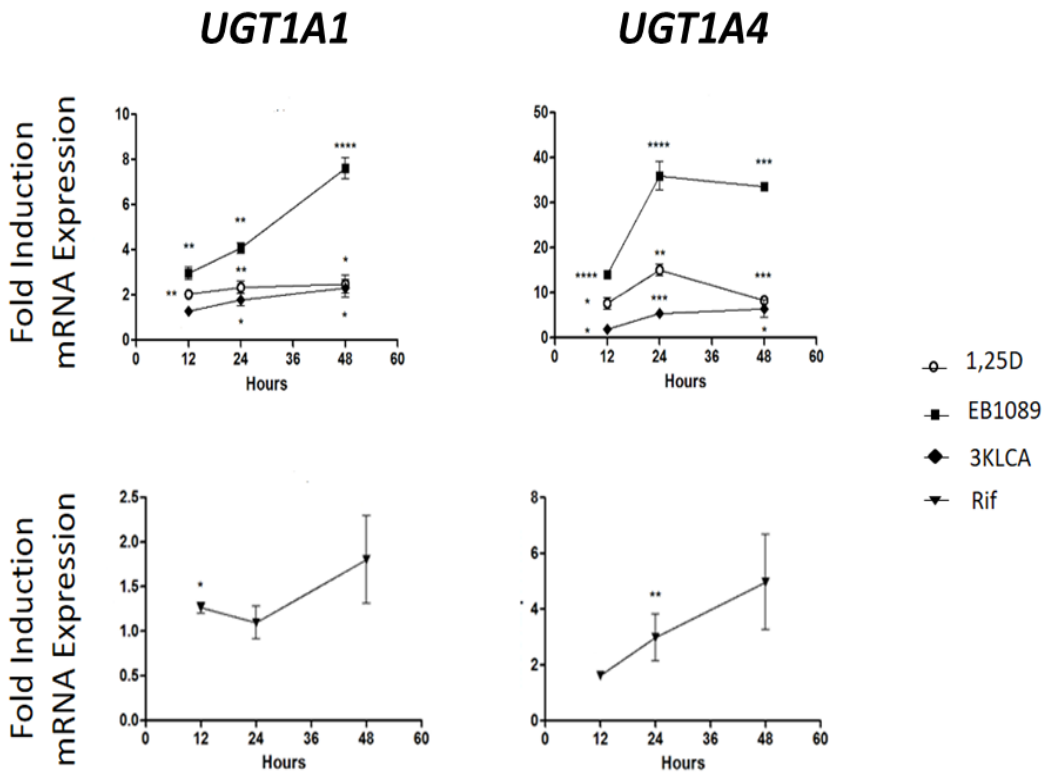

Figure 3.4: Time-dependent mRNA expression of UGT1A genes by VDR and PXR ligands.*RNA was extracted from LS180 cells treated with 1,25D (10^{-8}M), EB1089 (10^{-8}M), 3kLCA (10^{-5}M), Rif (10^{-5}M) or vehicle control for 24 hours. ΔCT was calculated relative to HPRT as a housekeeping gene. Represented here are fold inductions (ΔΔCT obtained with ligand relative to the vehicle). Represented are fold induction of the average of three independent experiments were n=3. Statistical analysis was obtained from Student's two-tailed t.test were *P<0.05, **P<0.01 and ***P<0.001. (**Unpublished data from our laboratory**).*

3.3 VDR is an autonomous regulator of the *UGT1A1* gene

The significant induction of *UGT1A1*, *UGT1A3*, *UGT1A4*, *UGT1A5* and *UGT1A7* (Figure 3.2) gene transcripts following 1,25D, EB1089 and 3kLCA would suggest that these genes are directly regulated by VDR. Seeing that *UGT1A1* is the most abundantly expressed isoform in our chosen cell model system, we investigated the *UGT1A1* promoter region more closely using reporter-based luciferase assays as described in section 2.7. For this, we obtained pGL3-UGT1A1-2K, which contains 2kbp (-5193/-3092) and the pGL3-UGT1A1-290 (-3483/-3194) which contains 290bp

distal enhancer sequence. These were kindly gifted by Professor Masahiko Negishi (Research Triangle Park, North Carolina) (Figure 3.5). LS180 cells were transiently transfected with the pGL3-UGT1A1-2K (U2K) or pGL3-UGT1A1-290 (U290) and also either a VDR expression vector or an empty parent vector, followed by 24-hour treatment with 10^{-8}M 1,25D, 10^{-8}M EB1089 or 3kLCA. Data was obtain from dual luciferase glo assay (Promega, UK). As shown in Figure 3.6 *UGT1A1* promoter activity effects activated by endogenous VDR were observed following transient transfection of LS180 with either the U2K or the U290 reporter vectors. This data suggests that, within both the 2kbp and 290bp fragments, there are putative VDREs that are potentially accountable for inducing *UGT1A1* promoter activity. 1,25D increased *UGT1A1* promoter activity by 3.8- and 2.9-fold, EB1089 by 4.8- and 2.8-fold, and lastly 3kLCA by 3.6 and 9.5-fold for the U2K and U290 reporter plasmids respectively. Our findings suggest that U290 is the most responsive reporter construct. However, for 3kLCA U2K was the most responsive. After overexpression of VDR in LS180 cells, the activities of both the U2K and U290 reporter plasmids became further augmented. Exogenous VDR increased U2K and U290 reporter plasmid activity following 1,25D exposure by 13-fold and 10-fold respectively. For EB1089 treatment, a 7.7-fold and a dramatic 21.2-fold increase was observed. These findings suggest a direct correlation between VDR expression and *UGT1A1* promoter activity. It is noteworthy that in this instance, VDR protein expression was not analysed. However it is important to support our data measurement of VDR levels upon overexpression in order to fuller determine a positive correlation between VDR and *UGT1A* expression.

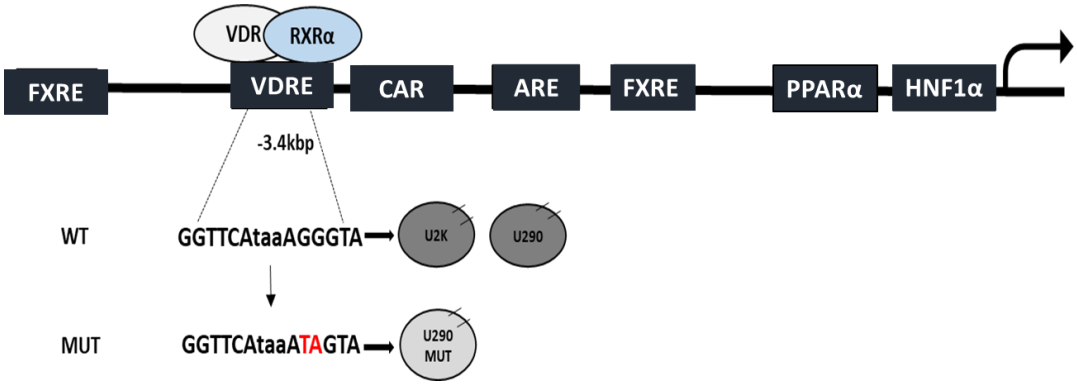

Figure 3.5: The UGT1A1 phenobarbital responsive enhancer module. *Binding sites for multiple NRs were previously identified to be clustered within the human UGT1A1 promoter region (-3.5 to 3.2kbp) termed the phenobarbital responsive enhancer module (gtPBREM). Our laboratory obatined a 2kbp fragment (U2K) and a 290bp fragment of this region, both containing a putative DR3-type motif VDRE.A promoter vector containing 2bp mutation of the VDRE was generated and subsequently used to characterization and involvement UGT1A regulation. (Edited from Sugatani et al., 2005)*

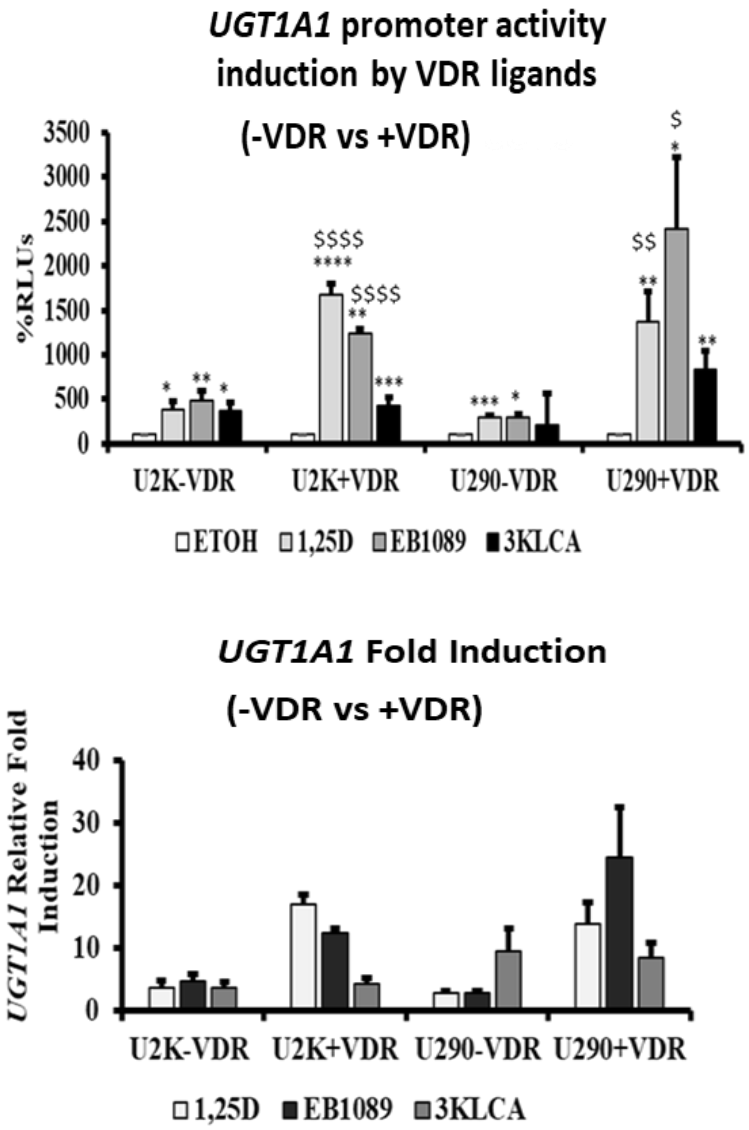

Figure 3.6: VDR regulates UGT1A1 promoter activity. *LS180 cells were co-transfected with either the pGL3-UGT1A1-290 (U290) or pGL3-UGT1A1-2K (U2K) reporter plasmid and either VDR expression construct or parent vector control using Invitrogen™ Lipofectamine™ 2000 Transfection Reagent, followed by 24-hour treatment with VDR ligands. Reporter activity was measured after 24 hours with Dual-Luciferase® Reporter Assay System (Promega, UK). Figures represent an average percentage (%) relative light units (RLUs) relative to vehicle control from three independent experiments where n=3 for each data point. Statistical analysis was obtained from Student's two-tailed t.test were *P<0.05, **P<0.001, ***P<0.0001, ****P<0.00001. $ represents exogenous VDR statistical significance relative to endogenous VDR ($ P<0.05, $$P<0.001 and $$$$ P<0.00001).*

3.4 Direct repeat 3 (DR3) motif within the *UGT1A1* proximal gene promoter is a functional Vitamin D response element (VDRE)

The 290bp *UGT1A1* promoter sequence was screened for putative VDREs using the RSAT tool (Figure 3.7). A DR3-type putative was identified. This led to the construction of a pGL3-UGT1A1-290 mutant (U290 MUT) by site directed mutagenesis. Sequencing confirmed the engineered 2bp change within the 3' half-site of the VDRE, where the VDR component of the heterodimer is expected to bind. To confirm the functionality of the identified VDRE, transcriptional effects of the pGL3-UGT1A1-290 mutant (U290 MUT) were compared to those generated by the wild-type reporter in LS180 cells, following exposure to 1,25D (10^{-8}M) , 3kLCA (10^{-5}M) and vehicle control for 24-hours. *Renilla* luciferase construct was also co-transfected and used as a reference for normalisation of transfection efficiency in all our luciferase based assays. As depicted in Figure 3.8, our findings confirm the DR3-type motif within the U290 reporter vector is conceivably a functional VDRE. As expected, when compared to the activities elicited by the intact reporter vector, the transcriptional responses to 1,25D and 3kLCA for the mutant version of the reporter become, significantly diminished by 75% and 41% respectively. Based upon these observations, this DR3-type motif is suggestive to be responsible for direct VDR modulated *UGT1A1* expression, although it is noted the VDRE mutation does not completely abolish the responses to 1,25D and 3kLCA. This suggests that other motifs within the promoter region may also contribute to VDR-mediated effects, or that the 2bp mutation did not completely abrogate binding of the heterodimer to this element.

We also aimed to characterize the putative DR3-type element in terms of its specificity for mediating response to VDR ligands, compared to other nuclear receptors. This was achieved through transfecting LS180 cells with either the wild type or mutant versions of the 290bp promoter vector. Upon co-tranfection with VDR or PXR expression vectors, LS180 cells were exposed to 1,25D (10^{-8}M) or Rifampicin for 24-hours, then luciferase activity was measured by dual luciferase glo assay (Promega, UK). Similar to previous findings, exogenous VDR significantly increased *UGT1A1* promoter activity. Our findings also confirm PXR as a regulator of the phase II metabolic gene (Figure 3.9**)**. U290 MUT exhibited reductions in luciferase reporter

activity (compared to the wild type construct) by 69% and 33.4% respectively, following 24-hour 1,25D and Rifampicin exposure.

To characterize further the potential exclusivity of this DR3 element for VDR-mediated effects, we compared *UGT1A1* luciferase activity in LS180 cells co-transfected with expression vectors for either LXRα or FXR (both expressed as N-terminal 'tagged' with the V5 epitope).

LXRα has been shown to transcriptionally activate *UGT1A* both *in vitro* and *in vivo* studies (Verreault *et al.*, 2006). Here a similar effect is shown where reporter activity is increased by approximately 3.5-fold after 24 hour treatment with TO901317, a potent LXR agonist. We further investigated the consequence of exposing LS180 cells to FXR agonist GW474066 prior to transfection with either DR3-type motif wild type or mutant. Similar to the above-mentioned outcome, FXR activation increased *UGT1A1* promoter activity by approximately 8-fold (Figure 3.10). Our data here show that both FXR and LXR are unaffected by the putative VDRE mutation. This confirms that specificity of the DR3-type motif and its functionality, in addition to the fact that VDR is the most potent *UGT1A1* mediator in an extrahepatic setting.

***UGT1A* promoter region sequence**

TGGCGTGTCTTTGGTGTGTCTGAAGGAAAAGAGATAGTGGAACAACATTGGGAGAAAAGGAATGAAACTCA
AGAATTCCAAGATGTTCCTCCCCTGCCAGGGTAAGATAGCAGTGGTTCACAGACAATCGCAATGCTGGGTCTG
AGAAAAATAACTAAACAGAAGATTAGTGAGGACCAAGGCTTCGAGATGGCCAGGAGAGGAAAGCTTGGGAG
CAGGGAAGGTTGAGATATATGTGGGTTACTGGGAATGCGTGATGGTGAAGTCACAGATGACCCACATGGTGT
CTAAGTGCTAAAGAAGAATTCTGGGAAAATGAAATGCATTTGGGAAGGGAAAATCTAATTAAAAGCCTAAAC
TAAAAATACAAAATTCTTGGTAAAGTTTAGGAGTTATGTTAAATGTCTCATTTTGGCTGGTGAAGTCTCATCAG
AACAGGGAAATTCTCTCATTCAGGGGCATCTCATCTTTTCTTTGAAGGGAATCAATGGTGGGGGATTGGAGTG
TTATTTTCAGTTAATATGTTGCTTCACTCTTTGGTCATTCCGGTAACTGTGAAGTCAGGGTGAAGTTTAAGGGA
AGCTTTGCCAAGTAGGGGATGGACTTCACCTTTATTGAGCCTCATAGTAGCTGGCTCAGGTAGGAGTTGGCCG
TGATGACAACTTCTCTGCAGTTTGCCCTGCGTGAATCTCCAGATGAACTTTTGTGCCATTTAAACTTTCGTGATC
TCCTGCTATTTAACTTCGAATGTTTATGGACCTGTGGGTTCAATTTTGTGTGAATCACATCCTGCTGATTGCTGA
GTGGGCGTGTGGGAGGGTGTGCCTGGAGGAGAACTTAGACTCGGCCTTTTCCAGATGAGCTTCAGTGTAAGA
GTGGGTTTCATGAAGAGCAAAGGTCCTAGGAAATTTAAGTAAGCCATTTACCAACGCTCAGAAGAAAGAACT
TGAAGAGCACTTGGAAATGAGCTGTGTCTCCCCAAGAAAGAGGGAGAGAAAGAGGGGAGAGATGTGGTGC
AGACCCTAGGGAGGAAGGAGTTCAGAAAAACCATCCTCAGGGTGTTCTTGCTACAAACCAAAAAATGCAGCA
TGGTGGTGGGGAGGATGACTCTGTCCTCCCTGACTTTTAGATGAGCCCAAGGGAAAAGGCAAAGACAAAGCC
CTTAAGAGCCAGAGGACTCACGAGGGCCTGGGGCTGGTGAGAGTGGCGGGGAGAGAGGGCTCACCTTGGG
AGAAGGATGGTCAGTGTCTGGGGCTTTCCTGGTCATGTTCCAAATCAGGCTTGGCAGGAGTCCTGCTGTGCAA
ATTGCGTTTGCTGAGCCCTGTCAGAGGTCTCCTGTGTCTCACATCTAGGGTGACCAGCATCCTGGCTTCCTCAG
GACTGTTCAGGTTTTAGCACTGAACATCACATGTCCTAGGGAACCCCTCAGTTTGGGCAAGCCCTGCCACATC
ACACAATCATATTAGTGCCCTCAGTATTCTTTGCAAACATAAAACCATAGACTCAGTAATCCCATTACTGGGTA
TATACCCAAAGAAATATAAATTATTCTACTATAAAGACACATGCACATATTTGTTTATTGCAGCACTATTCACAA
TAACAAAGTCATGGAACCAACCCAGATGCC

Figure 3.7: UGT1A sequence. *Grey represents TF rich sites identified from the genome browser database and the multi-colours represent putative VDREs. (Kent et al., 2002).*

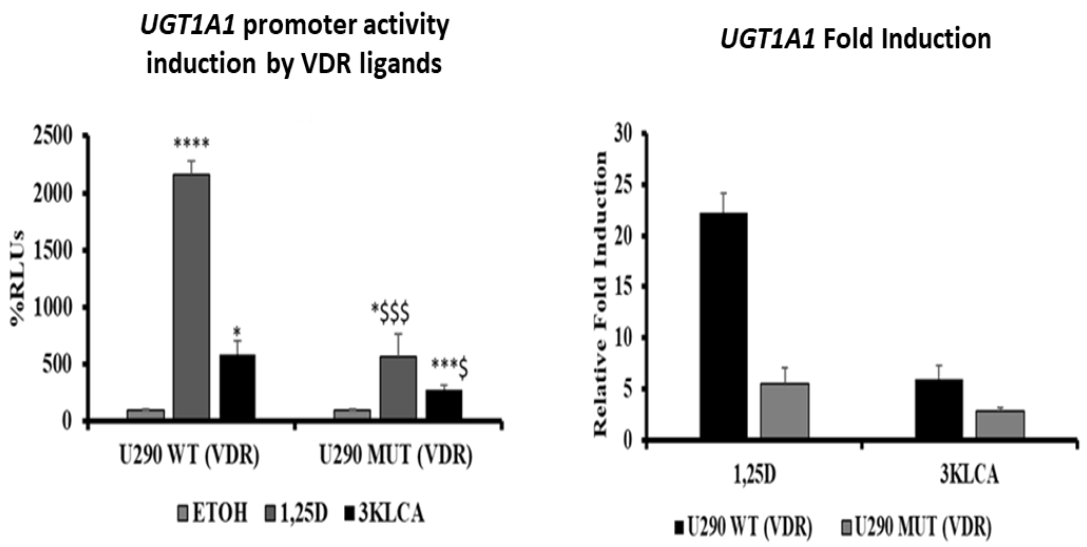

Figure 3.8: Identification of a functional VDRE within the UGT1A1 promoter region. *LS180 cells were co-transfected with either the wild-type U290 (U290 WT) or (U290 MUT) reporter VDR expression vector using Invitrogen™ Lipofectamine™ 2000 Transfection Reagent, followed by 24 hour treatment with VDR ligands. Reporter activity was measured after 24 hours with Dual-Luciferase® Reporter Assay System (Promega, UK). Figures represent an average percentage (%) relative light units (RLUs) relative to vehicle control from three independent experiments where n=3 for each data point. Statistical analysis was obtained from Student's two-tailed t.test were *P<0.05, **P<0.001, ***P<0.0001, ****P<0.00001. $ represent U290 MUT statistically significance relative to U290 WT. ($ P<0.05, $$P<0.001 and $$$ P<0.0001*

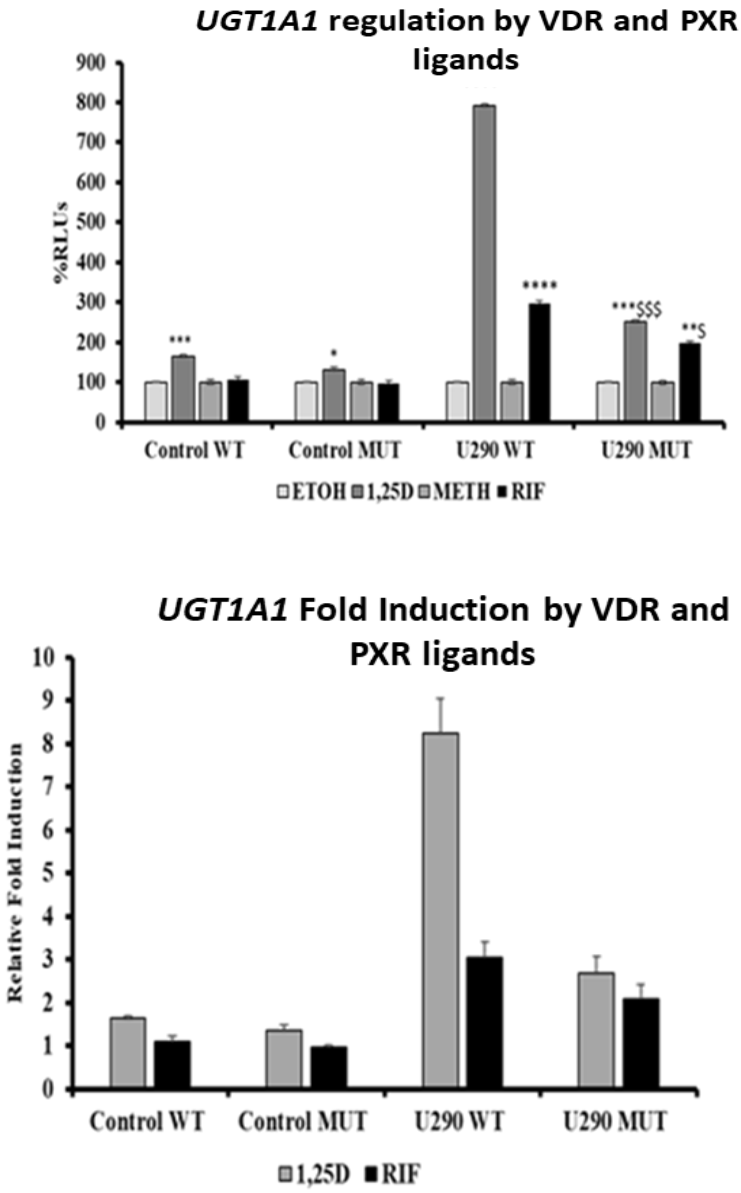

Figure 3.9: VDR and PXR share the same DR3-type binding motif within the UGT1A1 promoter region. *LS180 cells were co-transfected with either the wild-type U290 (U290 WT) or (U290 MUT) reporter VDR, PXR or control expression vector using Invitrogen™ Lipofectamine™ 2000 Transfection Reagent, followed by 24 hour treatment with VDR or PXR prototypical ligands. Reporter activity was measured after 24 hours with Dual-Luciferase® Reporter Assay System (Promega, UK). Figures represent an average percentage (%) relative light units (RLUs) relative to vehicle control. Fold induction was calculated relative to vehicle control from three independent experiments where n=3 for each data point. Statistical analysis was obtained from Student's two-tailed t.test were *P<0.05, **P<0.001, ***P<0.0001,*

*****P<0.00001. $ represent U290 MUT statistically significance decrease relative to U290 WT. ($ P<0.05, $$P<0.001 and $$$ P<0.0001*

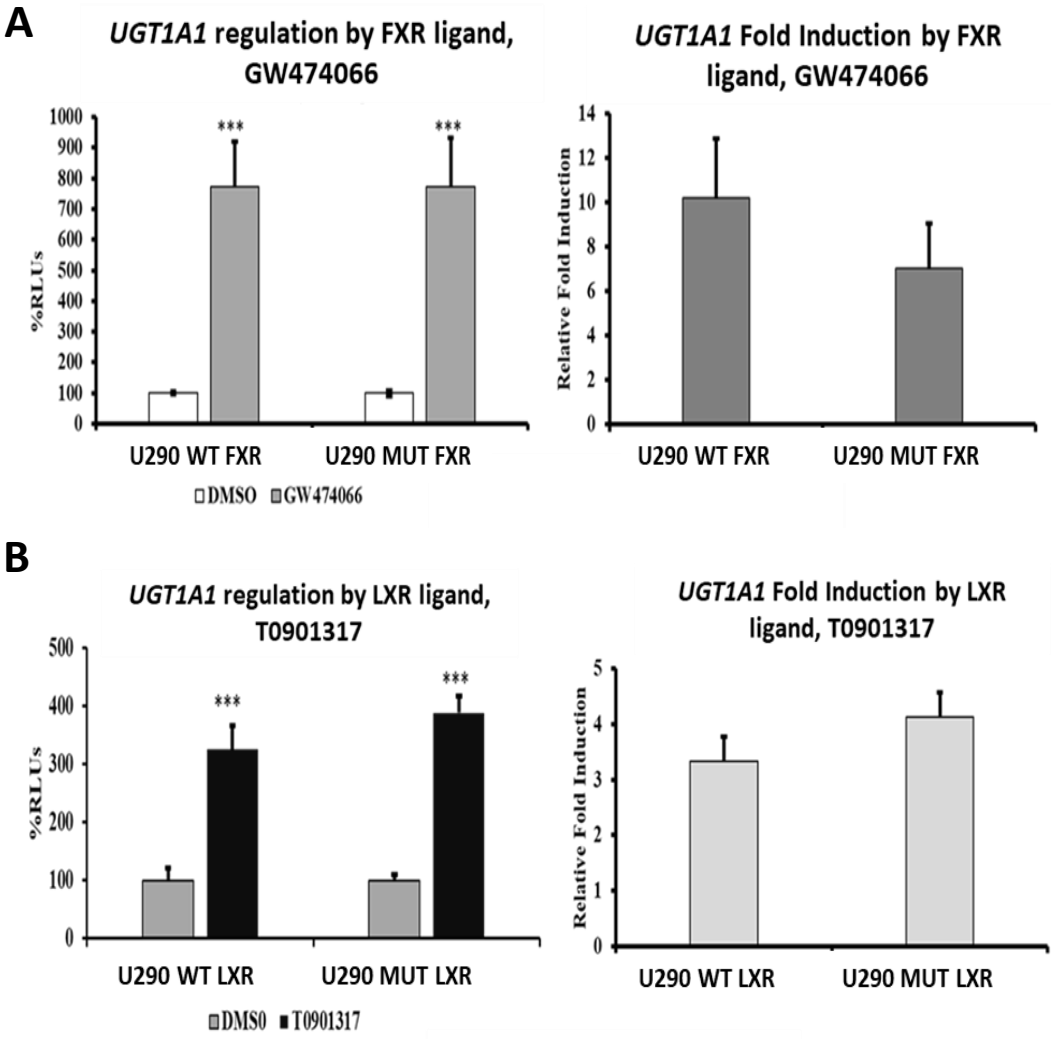

Figure 3.10: Defining the DR3-type motif specificity within the UGT1A1 promoter region *LS180 cells were co-transfected with either the wild-type U290 (U290 WT) or (U290 MUT) reporter LXR (A) or FXR (B) expression vector using Invitrogen™ Lipofectamine™ 2000 Transfection Reagent, followed by 24 hour treatment with LXR or FXR prototypical ligands. Reporter activity was measured after 24 hours with Dual-Luciferase® Reporter Assay System (Promega, UK). Figures represent an average percentage (%) relative light units (RLUs) relative to vehicle control. Fold induction was calculated relative to vehicle control from three independent experiments where n=3 for each data point. Statistical analysis was obtained from Student's two-tailed t.test were *P<0.05, **P<0.001, ***P<0.0001, ****P<0.00001.*

3.5 Vitamin D enhances UGT1A protein expression in LS180 cells

Since mRNA expressions of *UGT1A1, UGT1A3, UGT1A4, UGT1A5, UGT1A7* all appear as modulated through VDR signaling, we then wished to determine if these changes were also manifest at a protein level in the same colonic cell line. However, the *UGT1A* gene family members share a very high level of sequence identity (70-95%); obtaining isoform specific antibodies has been a challenge (Ikushiro *et al.*, 2006). The work of Ikoshiro *et al.*, (2006) successfully used a peptide specific antibody strategy against each *UGT1A* gene, whose findings demonstrated the independence of each isoform in its induction by various substances.

We then wished to examine the effects of nuclear receptor ligands upon the detectable levels of UGT1A protein expression in LS180 cells. Initially we compared the effects after 24 hours exposure to ligands for VDR, (1,25D, 3kLCA), FXR (GW474066) or LXR (TO901317) at concentrations defined in Table 2.2. Whole cell lysates were derived from treated cells and then probed through western blot analysis as described in section 2.5.3. Commercially, antibodies for the individual isoforms are still unobtainable, and so this study incorporated an anti-UGT1A antibody (that likely recognizes all 10 functional isoforms. This antibody is raised against amino acids 234-533 located at the C-terminus of the human UGT1A (Santa Cruz Biotechnology, 2020).

Analysis of the protein expression data shows that 1,25D and 3kLCA enhanced the detectable levels of UGT1A protein, the former, more robustly (Figure 3.11). There was a slight Rifampicin effect relative to methanol. Interestingly DMSO, known for its ability to stabilize protein even at as low concentrations as 4% (v/v) (Yedavalli and Rao, 2013), also slightly raises the detection of UGT1A protein in relation to the ethanol vehicle control. Both LXR and FXR agonists (TO901317 and GW474066, respectively) also cause a modest increase in UGT1A protein. Interestingly, 1,25D remains the strongest inducer (Figure 3.11). Our data also confirms that EB1089, similar to 1,25D increases UGT1A protein expression. (Figure 3.12).

We then examined the effects of exogenous VDR and PXR expression on UGT1A protein levels in LS180 whole cell lysates following 24-hour treatment with VDR or

PXR agonists (1,25D 10^{-8}M and Rifampicin 10^{-5}M). Our findings conclude that, while over expressing PXR did not affect UGT1A protein expression, exogenous VDR on the other hand further enhanced UGT1A protein levels as demonstrated by the significantly intensified band (See Figure 3.1). Our protein expression data also show that VDR expression modestly increases UGT1A expression in the absence of ligand (1,25D). Our findings are consistent with our gene expression and reporter based data. A possible reason for VDR as the most relevant UGT1A regulator due to the NR's expression levels relative to the PXR, FXR and LXR in LS180 cells. Our endpoint PCR data show negligible FXR expression in colonic cancer cell lines LS180, Caco-2 and LNCaP prostatic cancer cell line (Figure 3.13). Other NRs were expressed in the investigated cell lines.

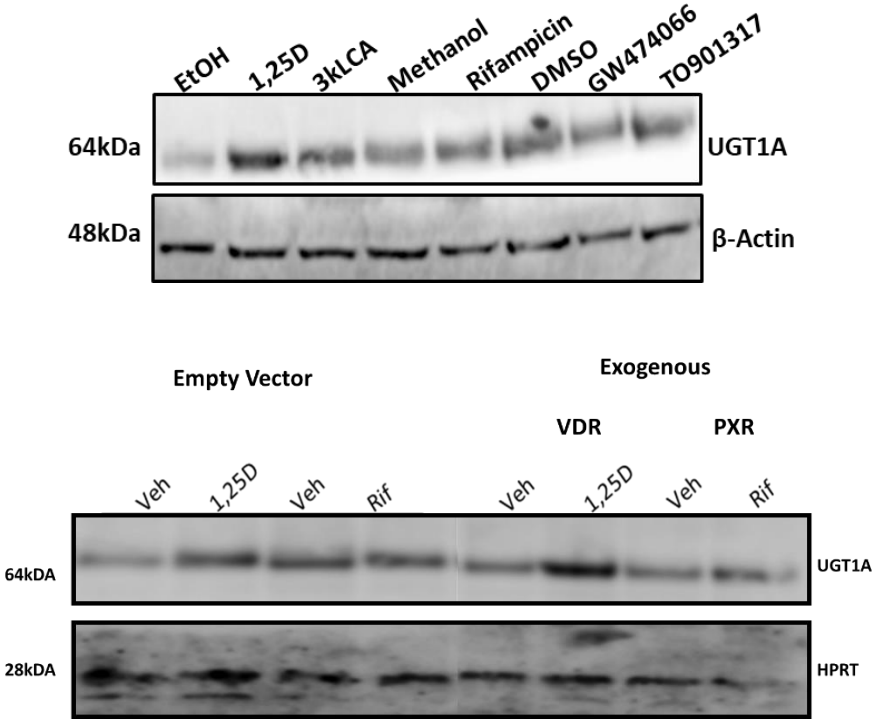

Figure 3.11: Western Blot analysis showing UGT1A protein expression in LS180 cells. *LS180 cells were exposed to VDR (1,25D and 3kLCA), PXR (RIF), LXR (TO901317) or FXR (GW474066) prototypical ligands (A) followed by protein extraction (endogenous NR expression). B represents LS180 co-transfected with either PXR, VDR (exogenous) or control empty vector (endogenous) followed by 1,25D or Rifampicin treatment for 24 hours. UGT1A protein was then detected. β-actin and HPRT were used as loading controls respectively. Figures show a representation of three independent experiments.*

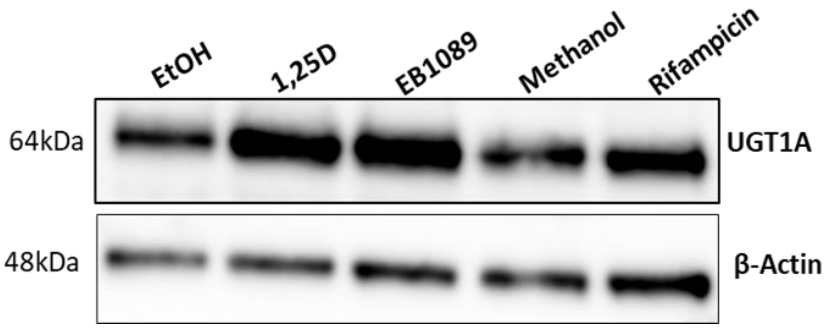

Figure 3.12: UGT1A protein expression in LS180 cells by VDR and PXR ligands. *LS180 cells were exposed to VDR and PXR ligands for 24-hours followed by protein extraction. UGT1A protein was then detected. β-Actin was utilized as a loading contr ol. Figure shows a representation of three independent experiments.*

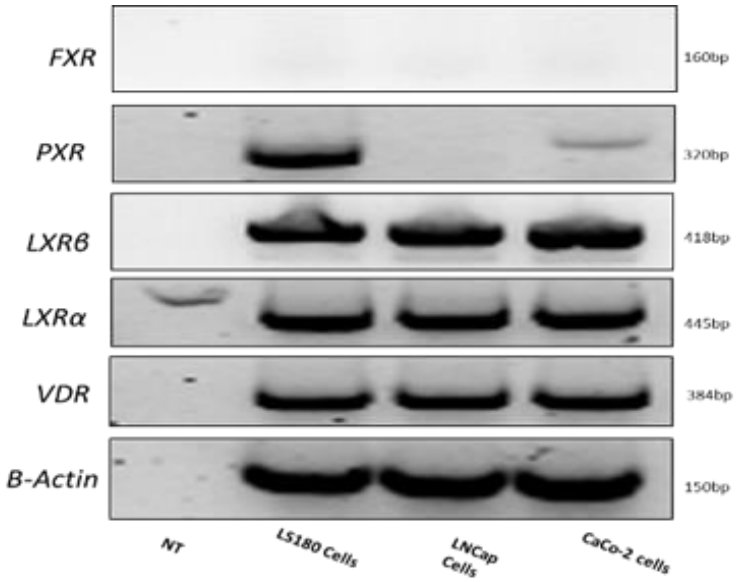

Figure 3.13: Nuclear receptor expression in various cancer cell lines. *To detect NR expression, RNA was extracted in LS180, LNCaP and CaCo-2 cells exposed to ethanol for 24 hours. RT-PCR was carried followed using 1.5% agarose gel electropherosis. The PCR product was visualized using a UV transluminator and images captured using the Sygene G BOX Chemi system.*

3.6 Vitamin D increases glucuronidation activity in LS180 cells

After demonstrating, the regulation of UGT1A isoform expression by 1,25D at both mRNA and protein level, with identification of a DR3-type motif within the *UGT1A* promoter region as a functional VDRE, we next addressed the question as to whether this regulation had relevance for detectable changes in functional enzymatic activity. For this purpose, we examined glucuronidation activity through the UGT-Glo assay within microsomal fractions extracted from cells treated with 1,25D, EB1089 or vehicle control for 24 hours. The treated microsomal fractions were exposed to a multi-enzyme substrate susceptible for glucuronidation. The addition of Luciferin and D-cysteine converted the substrate to luciferin which in turn emitted light. Glucuronidation reduces the amount of substrate available for luciferin conversion and therefore this enzyme activity is noted as a reduction in the level of emitted light Therefore the glucuronidation activity measured was inversely proportional to the luciferin/emitted light. Using this approach, we note UGT1A enzyme activity to be significantly increased in response to 1,25D by a modest 1.5-fold. In addition, EB1089 also enhanced this activity by 1.62-fold although we could not obtain statistical significance for this experiment (Figure 3.14). Upon investigating glucuronidation in human liver microsomes (HLM) which were used as a positive control due to high UGT1A concentrations, our findings showed drastically high endogenous levels of glucuronidation activity, compared to effects obtained in LS180 extracts perhaps leading to questioning the sensitivity of using cell culture based system in our chosen assay system.

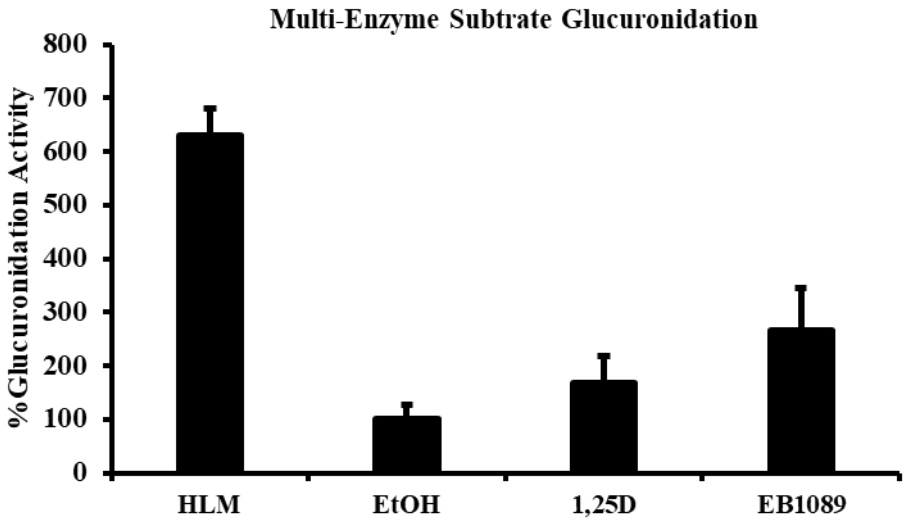

Figure 3.14: VDR ligands enhance glucuronidation activity in LS180 cells

Glucuronidation activity was analysed using the UGT-glo Assay using 50ug of LS180 microsomal fractions treated with 1,25D, EB1089 and EtOH as the vehicle control for 24 hours. Human Liver Microsomes (50µg) were used as a positive control. Figure represents % increase of glucuronidation activity relative to vehicle control from one independent experiments.

3.7 Discussion

The generation of a humanized mouse model, that expresses the entire *UGT1A* loci with a *Ugt1*-null background has contributed towards advancing knowledge in *UGT1A* regulatory mechanisms, particularly with emerging evidence of its clinical significance ranging from disease prevention to drug clearance (Cai *et al.,* 2010). Scientists have to date demonstrated that *UGT1As* are highly regulated in response to various compounds that act as NRs agonists including dietary substances, environmental toxins clinical drugs and endogenous substances (Walle *et al.,* 2000; Malfatti *et al.,* 2005; Wang *et al.,* 2014 and Duguay *et al.,* 2004). Most *in vivo UGT1A* regulatory investigations have been limited to a hepatic context. Although all *UGT1A* family members are highly homologous, they exhibit differential expression, and are modulated by different NR agonists (Ikushiro *et al.,* 2006; Sugatani *et al.,* 2005).

VDR on the other hand has emerged as a crucial TF in regulating a number of genes related to metabolism. By probing a Chip-seq data set derived from Pike's Laboratory (University of Wisconsin-Madison), multiple peaks representing enrichment of VDR/RXR binding within the *UGT1A* locus were identified. In expanding upon this knowledge, this study demonstrates for the first time a profile of *UGT1A* expression modulated by VDR in an extrahepatic context. LS180 cells were primarily used due to their ability to recapitulate transcriptional regulatory mechanisms of 1,25D in the intestine and colon (Yamaura *et al.,* 2016). Wang *et al.,* (2014) were the first to investigate VDR mediated *UGT1A8* and *UGT1A10* VDR mediated transactivation in LS180, HCT-116 and CaCo-2 cells. However, we, examine the entire *UGT1A* family in this regulation. Interestingly, in this study, VDR agonists did not modulate *UGT1A8* and *UGT1A10* possibly due to the low mRNA expression levels observed in this cell line. Notably *UGT1A1* was significantly induced by 1,25D and more strongly by EB1089 (See Figure 3.2). As depicted in Figure 3.4, we observe a time-dependant and dose-dependent induction of *UGT1A1* and *UGT1A4* gene family members. These findings imply VDR is directly involved in the transcription of these genes. PXR agonist rifampicin also increases *UGT1A1* and *UGT1A4* but significantly less so when compared to VDR ligands. This may be caused by low levels of PXR expression compared to VDR in our cell line model. Since both PXR and VDR share the same response element, the differences in gene transcription noted between the two sets of

ligands suggest that VDR regulation of *UGT1A* genes is the most physiologically relevant in an extrahepatic setting, whereas PXR, predominantly regulates hepatic metabolism.

In consideration of the overlap in substrate glucuronidation, *UGT1A1* is the sole enzyme responsible for bilirubin conjugation, with no other alternative pathway existing for its clearance (Kadakol *et al.,* 2000). Conditions such as Gilbert's Syndrome (GS), characterized by intermittent unconjugated bilirubin is a result of reduced *UGT1A1* activity by up to 30% (Fretzayas *et al.,* 2011). GS is benign and as such, symptoms manifest as intermittent mild jaundice in adolescence (Singh and Jialal, 2019). However, combination of Glucose 6-phosphate dehydrogenase (G6PD) deficiency, spherocytosis, thalassemia and GS cause severe hyperbilirubinemia (Fretzayas *et al.,* 2011). GS is a pharmacogenetic risk factor for drug toxicity including irinotecan. Its active metabolite (irinotecan), 7-ethyl-10-hydroxycamptothecin (SN-38) is metabolized by *UGT1A1*; therefore reduced clearance capacity results in irinotecan toxicity in GS patients (Lankisch *et al.,* 2008). Since the condition can only be managed and not cured, GS genotyping should be carried out prior to drug administration and much attention should be drawn to homozygous *UGT1A1*28* polymophism carriers. Other hereditary hyperbilirubinemia conditions that result from *UGT1A1* gene mutations are Crigler-Najjar Syndrome Type (CNS) type I and CNS II. The former is a much more serious condition characterized by complete loss of *UGT1A1* activity (Liaqat *et al.,* 2018). Serum bilirubin levels reach 20-50mg/dL and patients usual develop fatal encephalopathy (Liaqat *et al.,* 2018).

Efforts into restoring *UGT1A1* expression to combat this condition have been carried out by numerous scientists including Fujiwara *et al.,* (2014) who previously identified that glucose increased extrahepatic *UGT1A1* expression in Caco-2 cells. In the same study, glucose enhanced intestinal *UGT1A1* in *hUGT1* mice, and upon measurement, serum bilirubin was significantly reduced. In addition, Medley *et al.,* (1995) transplanted small intestinal tissue from Wistar rats to homozygous Gunn rats deficient in *UGT1A* expression and this allayed hyperbilirubinemia. Their work and findings regarding VDR mediated *UGT1A1* expression are strong evidence for the

potential for enhanced intestinal *UGT1A1* as an alternative treatment where *UGT1A1* expression is reduced. It is also noteworthy that vitamin D administration could revive *UGT1A1* expression in neonates for better and less invasive management of neonatal jaundice, to counteract the effects of breast-feeding, and most importantly to prevent kernicterus. Moreover, since *UGT1A* play a role in the metabolism of endogenous and exogenous carcinogenic compounds, numerous case studies as discussed by Hu *et al.,* (2016) have characterized *UGT1A* polymorphisms as a genetic risk factor for a wide range of cancers including, colorectal, prostate, oesophageal and breast cancer. Our findings on *UGT1A* regulation intimate vitamin D as a chemo-preventative or chemotherapeutic measure.

UGT1A3 together with *UGT1A4* are expressed both in a hepatic and extrahepatic context and possess very similar sequence homology (Jiang *et al.,* 2015). However, our findings reveal higher *UGT1A3* mRNA expression levels in LS180 cells compared to *UGT1A4*, but *UGT1A4* as the most sensitive isoform to VDR ligands. (Figure 3.2). *UGT1A3* plays a role in bile acids, catechol oestrogens, androgen glucuronide formation, in addition to drug clearance including, anti-retroviral (ARVs) drugs (e.g. *Dolutegravir*, *Raltegravir*), L-Thyroxine (T_4) (thyroid cancer drug) Cyproheptadine and Clozapine glucuronidation (Ramsey *et al.,* 2014; Santoro *et al.,* 2014; Mallayasamy and Penzak, 2019). *UGT1A4* on the other hand conjugates pregnanediol, steroids, dietary carcinogen and numerous drugs including antihistamines, antipsychotics (e.g. clozapine), antidepressants such as imipramine and tamoxifen (Sutiman *et al.,* 2016; Suzuki *et al.,* 2019 and Benoit-Bianamano *et al.,* 2009). Our results could imply that a VDR agonist could alter the glucuronidation rate of the above-mentioned substances. 1,25D or its analogues could contribute towards the prevention or treatment of diseases where high oestrogen (U*GT1A3*) or perhaps dietary carcinogens (*UGT1A4*) for example, lead to ovarian cancer, breast cancer, blood clots or colon cancer. Conversely, VDR mediated *UGT1A3* and *UGT1A4* implicate drug clearance, especially with emerging evidence of intestinal tissue as a major glucuronidation site (Wang *et al.,* 2014 and Mizuma *et al.,* 2009). Therefore, our findings imply that VDR agonists or vitamin D status may be a consideration when administering susceptible drugs.

Interestingly, *UGT1A3* conjugates the 23-hydroxylated metabolite of the analogue 26,27-F_6-1α,25-$(OH)_2D_3$ Kasai *et al.,* (2005) and Hashizume *et al.,* (2008) found that *UGT1A4* metabolizes glucuronidation of 1,25D itself. Research on 1,25D glucuronidation is in itself rudimentary, however closely related is the use of recombinant UGT1A3/UGT1A4 isozyme by Wang *et al.,* (2014) who detected 25-$(OH)D_3$ monoglucuronides (25-$(OH)D_3$-25-glucuronide, 25-$(OH)D_3$-3-glucuronide, and 5,6-trans-25$(OH)D_3$-25-glucuronide) in the human liver microsomes and human hepatocytes. Also in the same study, 25OHD_3-3-glucuronides were identified in the plasma and bile. These findings point to an alternative catabolic pathway of 25-$(OH)D_3$ elimination, affecting the regulation of 1,25D regulation. Additionally, 25OHD_3-3-glucuronides in the bile may indicate an initial step in the paracrine signaling loop, which regulates intestinal VDR target genes such as *TRPV6* and *CYP3A4* (Wang *et al.,* 2014). At physiological level, the induction of *UGT1A3* and *UGT1A4* could contribute calcium absorption and influence metabolism. These findings point to a possibility that UGT1A3 and UGT1A4 may play a role in vitamin D homeostasis.

Upon characterization, *UGT1A7* transcripts were identified in the stomach esophagus and orolaryngeal tissue (Zheng *et al.,* 2001). Our findings reveal a modest elevation in their expression through 1,25D and EB1089 but not 3kLCA (Figure 3.2). Interestingly, Fang *et al.,* (2013), characterized azidothymidine and estradiol glucuronidation in primary hepatocytes from C57BL/6NCr mice following the addition of taurolithocholic acid (TLCA; a taurine conjugated form of lithocholic acid) and recombinant *UGT1A* isoforms. Findings differed for each *UGT1A* isoform; however, TLCA (100μM) inhibited *UGT1A7* activity by 90%. Lithocholic acid derivatives (e.g. LCA acetate) can act as VDR agonists (Adachi *et al.,* 2006). In this study, we include 3kLCA, another LCA as one of the VDR agonists to examine. Taking into account Fang *et al.,* (2013) and this study, 3kLCA could also be inhibiting *UGT1A7* modulation, although the molecular mechanisms at this stage were not explored further. *UGT1A3, UGT1A4, UGT1A5* expression was significantly enhanced by 3kLCA, implicating VDR activation with extrahepatic circulation of bile acids as well as enhancing its glucuronidation as a preventative measure against colonic cancer. On the other hand, enhanced *UGT1A7* by 1,25D and its analogues could also

increase the clearance of tobacco carcinogens associated with orolaryngeal cancer (Zheng *et al.*, 2001).

UGT1A5 is the least studied isoform amongst the phase II metabolic genes. Recent work by Finel *et al.*, (2005) detected its low basal levels in human hepatocytes and protein detection in human liver is limited unless exposed to rifampicin. This suggests that *UGT1A5* is expressed only in response to its transcription factor agonist. Contrariwise, our findings reveal that rifampicin did not enhance *UGT1A5* mRNA expression and similarly to *UGT1A4*, mRNA expression levels were substantially low compared to *UGT1A1* and *UGT1A3*. So far, its clinical relevance has been linked to 1-hydroxypyrene, 4-methylumbelliferone and scopletin glucuronidation (Finel *et al.*, 2015). Although this study identified a similar expression profile to *UGT1A4*, its catalytic activity differs, for example, *UGT1A5* glucuronidation of 4-aminobiphenyl was absent. This is a good *UGT1A4* substrate (Al-Zhoughool and Takaska, 2006).

Both *UGT1A4* followed by *UGT1A5* were markedly the most sensitive of the tested isoforms to all VDR agonists tested, EB1089 being the most potent (Figure 3.2). Our findings implicate this finding to the possible involvement of multiple VDRE binding sites within the promoter region. ChIP-seq data from the Pike laboratory reveal multiple binding sites at potential 1,25D dependant major cis-regulatory module upstream of *UGT1A1*, which could affect *UGT1A* isoform expression near this loci, including *UGT1A4* and *UGT1A5*. Furthermore, using the GeneHancer database, which reveals clustered interactions of specific gene enhancers, mapped the *UGT1A4* enhancers clustered within the identified cis-regulatory module (Kent *et al.*, 2002). With this evidence, there is more reason to speculate that the involvement of multiple enhancer modules synergistically enhance gene transactivation. The DR3-type motif identified as a functional VDRE was mutated and although significantly reduced promoter activity was recorded after both VDR and PXR agonist exposure, it was not completely abolished; implying the involvement of other response elements in the promoter vector (Figure 3.8). Moreover, this study along with those previously mentioned demonstrate cell-type specific and complex *UGT1A* gene regulation. Subsequent chapters attempt to investigate this phenomenon more closely.

As previously established, numerous exogenous and endogenous substrates for UGT1A are biologically active molecules that activate specific NRs. As such, their glucuronidation forms part of a feedforward or feedback mechanism by which the substrates mediate their own NR-mediated metabolism.

Up to now, studies such as those by Fisher *et al.,* (2000) have correlated *UGT1A1* and *UGT1A6* expression to estradiol-3- and acetaminophen-O-glucuronidation respectively. NR mediated glucuronidation was reported by Chen *et al.,* (2005) whose findings showed an enhanced SN-38 glucuronidation correlated with *UGT1A1, UGT1A9* and *UGT1A10* mRNA induction in PXR-expressing cells. Closely related to our study was Wang and colleagues' work (2014) who reported altered mycophenolic acid (MPA) drug pharmacokinetics following inter-individual variability in kidney transplant patients who often co-administer Vitamin D supplements. Our study did not examine specific substrate glucuronidation (e.g. measurement of bilirubin glucuronides upon 1,25D exposure by LC-MS/MS), but for the first time, we report UGT1A protein expression dramatically enhanced by 1,25D, and this also correlates with exogenous VDR expression (Figure 3.11). We investigated this expression with PXR, FXR and LXR prototypical agonist whose effects were modest (Figure 3.11) Finally, the multi-enzyme glucuronidation assay reveals 1,25D significantly increases enzymatic activity. The limitation to this assay was very low sensitivity relative to HLM, which have concentrated amounts of UGTs (Figure 3.14).

The study highlights yet another important role of VDR and possibly how extensively it is involved in maintaining overall cellular health. The ability for VDR-mediated intestinal *UGT1A* induction means that Vitamin D supplementation could be used as treatment where the *UGT1A* gene expression is compromised (e.g. GS and CNS). Similar to Aoshima's *et al.,* (2014) work Vitamin D can be used to combat neonatal jaundice. Since GS prevalence is as high as 16% in other populations, genotyping and Vitamin D co-administration could revive UGT1A1 enzymatic activity. 1,25D could be classed as a chemo-preventative measure due to enhanced carcinogen glucuronidation. Breast-feeding could be continued along with vitamin D supplementation to maintain the otherwise suppressed *UGT1A* expression. On the

other hand, since enhanced *UGT1A* expression and activity increase drug clearance, it is important to avoid co-administration for optimum drug efficacy. Further *in vivo* functionality experiments are needed to confirm these clinically significant effects. The use of UGT1A transgenic mice models with a *Ugt1*-null background will be ideal to investigate the physiological relevance as well as functionality of *UGT1A* regulation. Upon Vitamin D administration, examination of metabolites such as that of total serum bilirubin can then be measured in order to determine whether extrahepatic UGT1A regulation by VDR is relevant in hyperbilirubinemia treatment. Additionally, a limitation to this study was the use of one intestinal cell line model. As previously mentioned, the chosen cell line (LS180 cells) imitates the biology of vitamin D in an intestinal context (Meyer *et al.,* 2012), however the investigation of UGT1A regulation in other VDR expressing cell lines (e.g. kidney, skin, breast and other colon cell lines) will further strengthen our findings. Optimization of the functionality assay or use of LC-MS/MS to measure substrate metabolites upon exposure to VDR ligands will also strengthen evidence of VDR activity's relevance in *UGT1A* biology. It is also noteworthy that VDR protein levels should be analysed upon over-expression to further streghthen our findings on VDR mediated UGT1A regulation.

Altogether, findings also highlight the need to fully understand the molecular pathways involved in *UGT1A* regulation and the role of 1,25D as a 'guardian for phenotypic stability' (Berridge, 2015).

3.8 Summary of key findings

- *UGT1A1, UGT1A3, UGT1A4, UGT1A5* and *UGT1A7* are significantly enhanced by activated VDR
- *UGT1A4* is the most sensitive isoform to VDR activation
- *UGT1A1 is the most abundantly expressed isoform in LS180 cells.*
- UGT1A protein is enhanced by VDR ligands (1,25D, 3kLCA and EB1089).
- VDR expression positively correlates with UGT1A protein expression and promoter activity.
- VDR is more potent at enhancing *UGT1A* expression compared to PXR in LS180 cells.
- The DR3-type motif within the *UGT1A1* promoter region is a functional VDRE and is only specific to VDR and not other nuclear receptors (e.g. LXR and FXR).

4: Chapter 4

Examining the cross-talk between Vitamin D Receptor and Nuclear Factor Erythroid 2-Related Factor 2 signalling pathways

4.1 Introduction

Upon activation, Vitamin D Receptor (VDR) forms a heterodimer with retinoid X receptor (RXR) and the complex binds to vitamin D response elements (VDRE). This transcriptional activity initiates the expression of numerous genes, that in turn lead to several functional processes including mineral homeostasis, cell growth, anti-aging and detoxification processes. Many of these processes depend on the ability of VDR to increase the expression of *UGT1A* gene family members and Nuclear factor erythroid 2-related factor 2 (NRF2), a key transcriptional factor involved in the neutralization of a plethora of cellular oxidative stress inducers (Ahmed *et al.*, 2017). NRF2 in-turn enhances a number of its target genes (Discussed in chapter 1) including Glutamate-Cysteine Ligase Catalytic Subunit (*GCLC),* NAD (P) H dehydrogenase quione 1 *(NQO1),* Glutamate-Cysteine Ligase Modifier Subunit (*GCLM*) and *UGT1A* genes itself (Tonelli *et al.*, 2018). Berridge *et al.,* (2015) identified that a dysregulation VDR signalling resulted in the elevation of oxidative stress, augmented cellular aging and increased neural calcium levels in Alzheimer's disease transgenic mice. This dysregulation was reversed by the administration of Vitamin D which also led to increased NRF2 expression. This evidence raises questions as to whether VDR signalling is a major component particularly in the neutralization of oxidative stress. Knowing that NRF2 also enhances *UGT1A* gene family members (Tonelli et al., 2018), and linking that to our findings of VDR mediated UGT1A gene expression, we sort to investigate whether VDR ultimately plays a key role in enhances NRF2 mediated responses and more importantly, whether there is an interplay between VDR and NRF2 in further enhancing *UGT1A* gene expression.

Under normal conditions, NRF2 is bound to Keap1 that presents it to the E3 ligase complex by Cullin-3 (Cul3), leading to constant degradation by the ubiquitin proteasome system (Zhang *et al.,* 2004). Upon insults, NRF2 translocates into the nucleus, where it forms a heterodimer with small Maf (sMaf) proteins (Zhang *et al.,* 2004). The complex binds to anti-oxidant response element (ARE) motifs within the promoter region of target genes; co-regulatory complexes are then recruited, leading to gene transcription (Nguyen *et al.,* 2009).

NRF2 activation interplays with other molecular pathways including innate immune responses (Thimmulappa *et al.,* 2006). Scratch injury to culture primary astrocytes elevates tumour necrosis factor-alpha (TNF-α), interleukin -1β (IL-1β), IL-6 and matrix metallopeptidase 9 (MMP9) more prominently in NRF2 knockout (KO) than wild-type counterparts (Pan *et al.,* (2012). The elevation of pro-inflammatory cytokines suggests that NRF2 controls inflammation responses through the control of nuclear factor kappa-light-chain enhancer of activated B cells (NF- *κ*B) and its downstream targets (Wardyn *et al.,* 2015). NF-κB modulates immune, inflammatory responses, cellular development and differentiation (Liu *et al.,* 2008). The NF-κB p65 subunit also antagonizes NRF2 signaling through the recruitment of co-repressors and histone deacetylases (HDACs) (Liu *et al.,* 2008). Heme Oxygenase 1 (*HMOX1*) is a key NRF2 target gene involved in haem metabolism, ultimately producing serum bilirubin (Loboda *et al.,* 2016). Seldon *et al.,* (2007) observed that in endothelial cells, *HMOX1* inhibited E-Selectin and vascular cell adhesion molecule 1 (VCAM-1), both mediated by NF-κB.

Furthermore, NRF2 interplay evidenced through extrahepatic *UGT1A8* and *UGT1A10* induction was co-ordinated by cross-talk with Aryl hydrocarbon Receptor (AhR) (Kalthof *et al.,* (2010). NRF2 also directly enhances heat shock factor 1 (*HSF1*) gene expression in MCF7 breast cancer cells exposed to OS (Paul *et al.,* 2018). Furthermore, NRF2 signalling is a well-characterized pathway in various pathologies including diabetes, cardiovascular diseases, and neurodegenerative disorders (Berridge, 2015).

Based on the abovementioned evidence and that activated VDR enhances NRF2 expression, we speculate its potential interplay with VDR to further enhance antioxidant responses. Evidence by Nakai *et al.,* (2013) observed that systemic and intra-renal OS was diminished by 1,25D treatment in Type 2 diabetes rats that presented with nephropathy. Additionally, NRF2 expression was restored in the rats exposed to 1,25D (Nakai *et al.,* 2013). This evidence is enough to speculate that 1,25D could enhance cyto-protection through NRF2 crosstalk, thereby enhancing detoxification and expression of OS neutralizing enzymes. Lee *et al.,* (2015) observed a synergistic regulation of *Wnt*-pathway target genes (*AXIN, Cyclin D1 and C-MYC*)

where Caco-2 cells were exposed to both VDR and NRF2 ligands (1,25D and Sulphorafane (SFN) respectively). The *Wnt*-pathway controls cell growth, differentiation and survival; however, alteration in genes involved in this pathway also lead to malignancies such as colorectal cancer where ~ 90% of cases present with aberrant *Wnt*-pathway signalling (Duchatre *et al.,* 2016). Moreover, numerous studies have demonstrated that NRF2 itself increases *UGT1A* expression, both in *in vitro* and transgenic mice models (Yueh and Tukey, 2007). Kalthoff *et al.,* (2010) later identified that coffee, a known NRF2 ligand enhances *UGT1A* isoforms by up to 6.1-fold. From these findings, we speculate that NRF2 pathway is altered by 1,25D/VDR signalling, thus leading to a greater *UGT1A* response, contributing towards its role as a 'custodian for phenotypic stability, as Berridge's (2015) hypothesised.

We hypothesize that VDR signalling, together with NRF2 signalling, enhance the expression of *UGT1A* responses to further amplify the scavenging of toxic insults and the neutralization of OS. Moreover, their interplay results in enhanced chemo protection and control of tumorigenesis through anti-proliferative and apoptotic properties. We hypothesize that diminished functionality of either transcription factor leads to impaired signalling of the other. To test this hypothesis, we exposed LS180 cells to SFN (synthesized from glucoraphanin through hydrolysis by myrosinase enzyme were cruciferous vegetables, including broccoli are mechanically damaged or digested) and *tert*-butylhydroquione *(t*BHQ) (common food additive), the most common NRF2 activators. LS180 cells were also exposed to 1,25D and 3kLCA as vitamin D receptor (VDR) prototypical ligands derived from endocrine and bile acid pathways, respectively (Abbaoui *et al.,* 2018 and Zargorski *et al.,* 2013). Comparative analysis was also performed on androgen-sensitive LNCaP human prostate adenocarcinoma cells derived from the left supraclavicular lymph node metastasis due to the evidence of functional NRF2 activity and correlation between OS to the initiation and progression of prostate cancer (PCa) (Bellezza *et al.,* 2017). In addition, since SFN increases the efficacy of anti-androgens, its interplay with 1,25D was examined (Khurana *et al.,* 2016).

4.2 Results

4.2.1 Cell Viability Assay

In this study, we sought to address whether NRF2 and VDR signalling pathways interact to neutralize oxidative stress by enhancing *UGT1A* gene expression. As a model system, we used LS180 and HEK293 cell lines to compare this interaction. Firstly, to determine ideal concentrations for the chosen NRF2 ligands SFN and *t*BHQ, LS180 cells were treated with different concentrations of SFN (0, 5, 10, 30, 40, 50 and 100µM) and *t*BHQ (20, 40, 60, 80, 100, and 500µM) for 24 hours (Figure 4.1). Afterwards, cell viability, which quantifies ATP presence, correlating to metabolically active cells was, assessed (Kumar *et al.*, 2018). Of note, both SFN and *t*BHQ inhibited viability in a dose dependant manner, although not to the level that would determine an IC50. SFN significantly reduced cell viability at 20µM up to 100µM, suggesting that lower concentrations are ideal for investigating NRF2 responses in LS180 cells. In comparison, LS180 cells were less sensitive to the synthetic aromatic organic NRF2 inducer, *t*BHQ. Concentrations up to 80µM were not toxic to cells, but an approximate 30% and 50% decrease in cell viability was observed following exposure to100µM and 500µM of *t*BHQ, respectively.

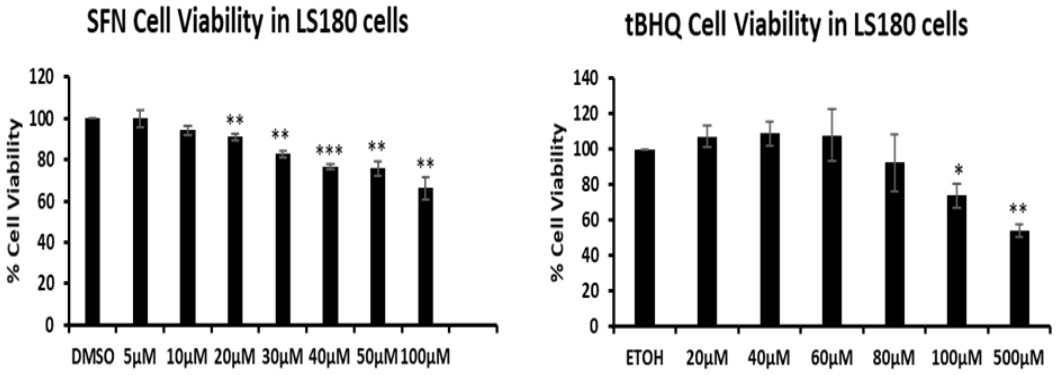

Figure 4.1: Cell Viability of NRF2 ligands in LS180 cells. *LS180 cells were seeded in 96-well plate for 24-hours, followed by dosage with increasing concentrations of SFN (0-, 5-, 10-,20-, 30-, 40-, 50- and 100µM) or tBHQ (20-, 40-, 60-, 80-, 100-, 500µM) for another 24 hours. Cell Viability was obtain using the Cell-titre-glo assay (Promega, UK). Data represents 3 independent experiments where n=3, shown in percentage (%) viability. Statistical analysis was obtained from Student's two-tailed t.test were * P<0.05, **P<0.005, ***P<0.0005.*

4.2.2 NRF2 and VDR ligands alter ARE signalling in LS180 cells

Both SFN and *t*BHQ are known to promote NRF2/ARE association (Kubo *et al*., 2017 and Kalthof *et al.*, 2010). We therefore examined ARE minimal promoter driven functionality by transiently transfecting pGL4.37[luc2P/ARE/Hygro] which contains four copies of the ARE. LS180 cells were treated with varied concentrations of each NRF2 agonist (SFN: 5-, 10-, 20-, 30-, 40-, 50- and 100μM and *t*BHQ: 20-, 40-,60-, 80-, 100-, 500μM) for 24-hours. Luciferase activity, testing the responsiveness of the endogenous NRF2 system was also measured by Dual Luciferase Reporter Assay system (Promega, UK). Reporter activity showed a gradual concentration-dependent response to *t*BHQ (7.3-, 9.9-, 51.9-, 68.5- and 70-fold, relative to the above mentioned concentrations) with a diminished response at 500μM (Figure 4.2 A and B) correlating with a decline on cell viability (Figure 4.1). Of note SFN also significantly enhanced ARE promoter activity by 38.4-, 78.3-, 45.9-, 21.8-, 3.1-, 4.3 and 9.1-fold increase relative to the concentrations mention previously. SFN was the most effective NRF2 agonist with the maximum response at 10μM (78.3-fold increase). It is also noteworthy that the SFN and *t*BHQ profile are different. SFN induced ARE activity peaks at 10μM, a much lower concentration compared to *t*BHQ (100μM). This may be attributed by the fact that SFN is a natural compound that requires low physiological concentrations to exert an intact ARE response. *T*BHQ on the other hand is synthetic food preservative, which, at low concentrations initiates cyto-protection, and only at higher concentrations, cytotoxic properties are triggered.

The ARE activity profile observed is similar to our cell viability assay in Figure 4.1.This data confirms functionality of ARE and the responsiveness of the two NRF2 prototypical ligands. For future experiments, we chose 40μM for *t*BHQ, 6μM for SFN as these do not elicit significant reductions in cell viability, and produce significant transcriptional responses.

In view of the fact that NRF2 signalling is mediated via ARE promoter activity, and 1,25D has been reported to upregulate NRF2 mRNA expression (Chen *et al.*, 2019), we examined whether co-operative ARE reporter activation could be observed in response to increasing doses of 1,25D (10^{-7}M, 10^{-8}M and 10^{-9}M) and how this may be

impacted through addition of exogenous VDR to the cell system (Figure 4.2 C and D). In LS180 cells expressing endogenous VDR, 24-hour treatment with 1,25D

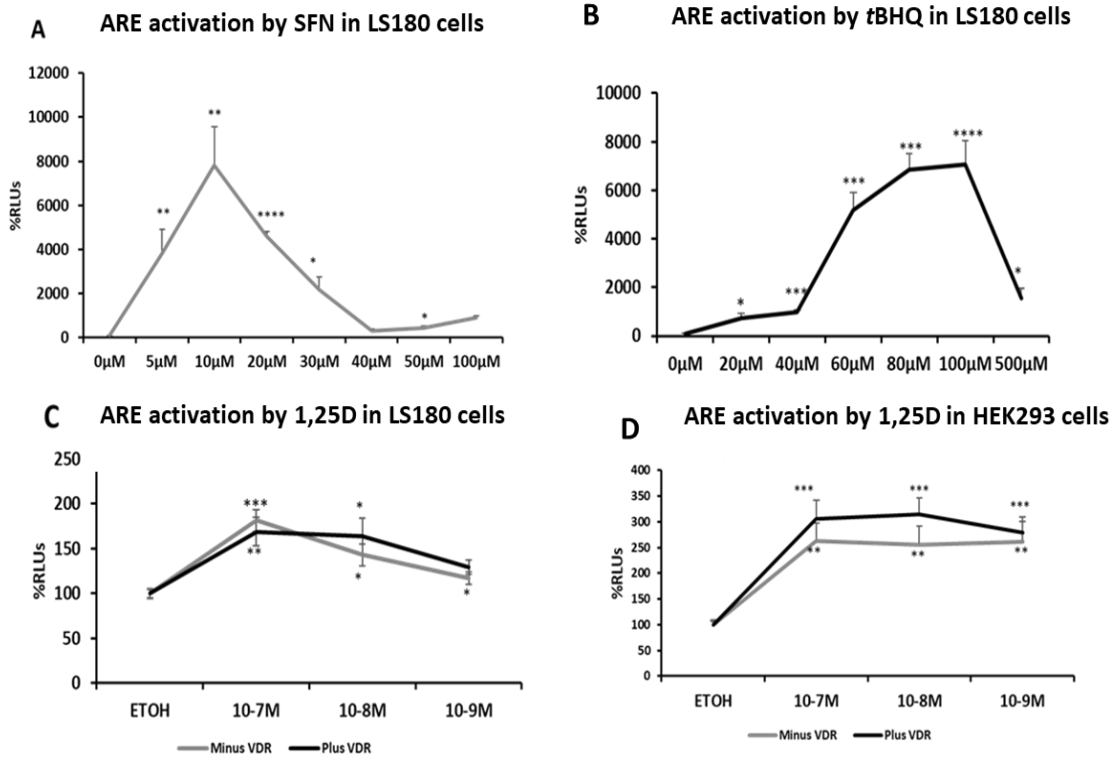

significantly enhanced ARE activity by 1.81-, 1.42- and 1.17- fold respectively. Exogenous VDR altered this activity as a 1.6-, 1.6- and 1.29-fold increase was observed respectively, however our statistical analysis did not show any significance. We conducted the same experiment in HEK293 cells, where endogenous VDR expression is negligible. We found that 1,25D enhanced ARE activity by 2.62-, 2.55- and 2.61-fold at the concentrations applied, respectively. VDR over-expression further increased ARE activity by 1.03-, 0.59- and 0.18-fold. Similar to LS180 cells, the effects of over-expressing VDR were not statistically significant. This data show that 1,25D augments ARE activity, although this response is not concentration dependent. Compared to endogenous VDR, ARE activity following overexpression of VDR was notably greater, particularly in HEK293 cells. Our data also show that 1,25D has significantly less influence on ARE activation compared to SFN and *t*BHQ.

Figure 4.2: Titration curve of ARE activation in LS180 and HEK293 cells. *The titration curve shown was obtained from the titration of SFN (A), tBHQ (B) and 1,25D (C) in LS180 cells and 1,25D in HEK293 cells (D). C and D also depicts ARE activation in both cell lines were endogenous or overexpressed VDR (100ng) are also*

*activated. Luciferase activity was measured using the Dual-Glo Assay (Promega, UK). Data represents 3 independent experiments were n=3 shown as % Relative Light Units (RLUs). Statistical analysis was obtained from Student's two-tailed t.test were * P<0.05, **P<0.005, ***P<0.0005).*

4.2.3. ARE-signalling in Vitamin D pre-treated LS180 cells

Given that there is considerable evidence to suggest that NRF2/ARE signalling alterations may contribute to numerous diseases linked to Vitamin D deficiency, and that 1,25D treatment resulted in a modest increase in ARE basal activity (Figure 4.2), we sought to investigate whether prolonged 1,25D exposure has an impact on further augmenting ARE activation when NRF2 is activated. Furthermore, since 1,25D slightly increases ARE activity, it is worth investigating an additive effect of this kind.

Cells were exposed to either EtOH or 1,25D for 24-hours, before then dosed with SFN (3, 6 or 9μM) or *t*BHQ (30, 50 or 70μM) for further 24-hours, followed by measurement of reporter activity. ARE reporter activity was significantly increased by both NRF2 prototypical ligands, as expected. SFN evidently altered ARE activation in a dose-dependent manner where a gradual increase in ARE activation is observed by approximately 5-fold, 15-fold and 30-fold respectively (Figure 4.3A). On the other hand, *t*BHQ dose-dependent response while less impressive, nonetheless, significantly increased ARE activity by approximately 17-fold to 25-fold (Figure 4.3B). 1,25D has no apparent effect on 'priming' any further enhancement of ARE activity. Although there is a trend in that 1,25D pre-treated cells result in greater reporter activity, the effects are not significant compared to EtOH pre-treated cells.

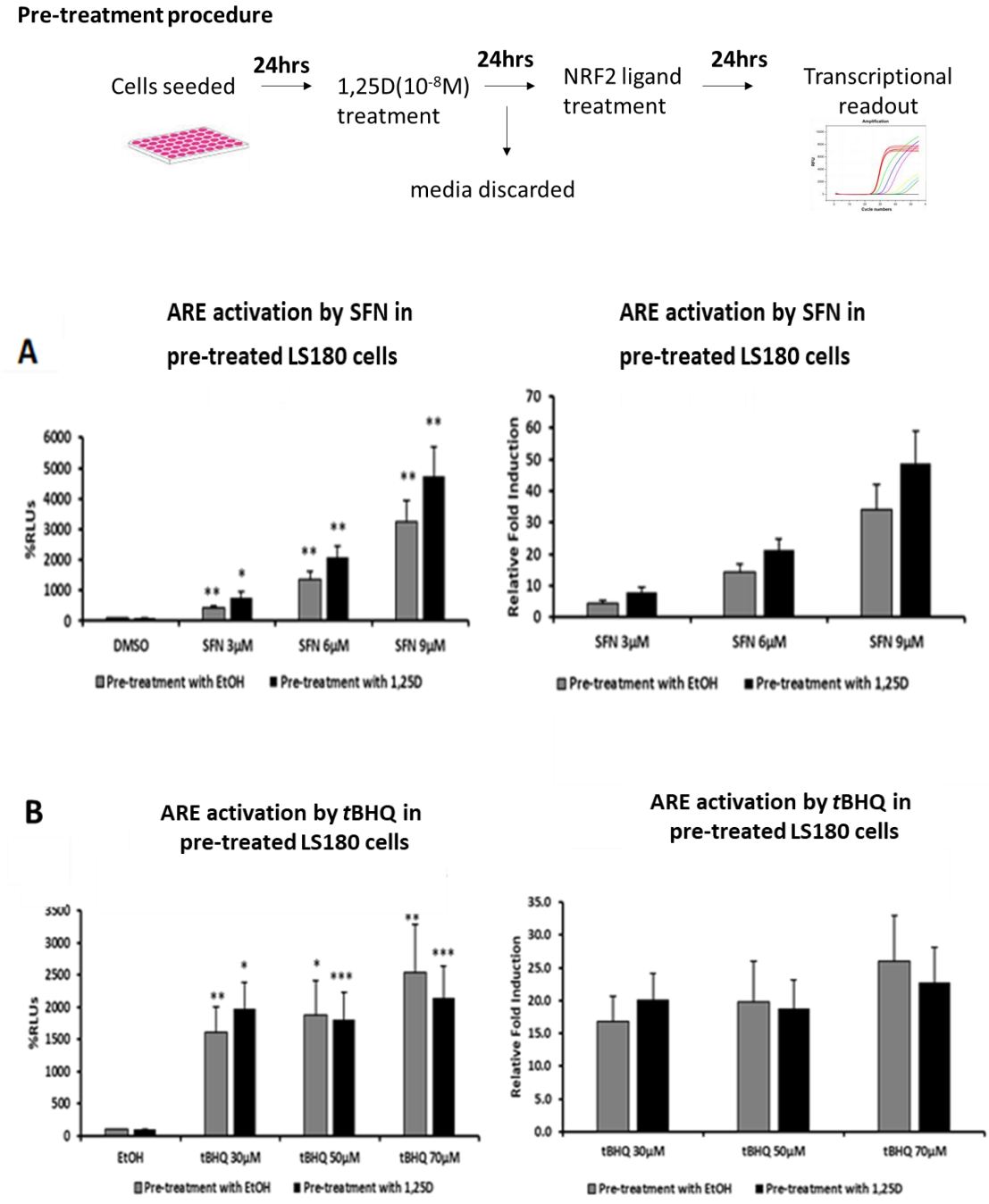

Figure 4.3: ARE activation by NRF2 ligands following pre-treatment in LS180 cells.

ARE activation by NRF2 and VDR ligands. LS180 cells were transfected with ARE-luc reporter construct (650ng/well). The cells were subsequently pre-treated with ETOH or 1,25D for 24 hours, followed by SFN (3-, 6-, and 9µM) (A) and tBHQ (30-, 50-and 40µM) (B) for 24 hours. Relative Light units were then measured by Dual Glo Luciferase Assay (Promega, UK). Data represented as Light Units relative to

vehicle control were n=3. Statistical analysis was obtained from Student's two-tailed t.test were p<0.05= , p<0.005=***

4.2.4 ARE minimal promoter activity is modulated by NRF2 and VDR ligands

We then examined whether ARE activity could be influenced by another VDR ligand, 3kLCA in comparison to 1,25D. LS180 cells were transiently transfected with pGL4.37[luc2P/ARE/Hygro] then subsequently treated with VDR ligands (1,25D or 3kLCA) (Figure 4.4.A) or NRF2 ligands (SFN and tBHQ) (Figure 4.4 B) for 24 hours. Similar to preliminary findings of 1,25D inducing ARE activation, there was a notable 1.35-fold increase in transcriptional activity by 1,25D (Figure 4.4C). Surprisingly, the 3kLCA had a more significant effect and increased ARE activity by a 4.03-fold. This result is indicative of the fact that ARE/NRF2 signalling may be the first line of defence against secondary bile acid toxicity in the intestine. It is therefore reasonable to speculate that ARE promoter activity increase suggests a more rapid and efficient clearance of 3kLCA through neutralization of oxidative stress, leaving the intestinal tract less susceptible to injury that they might be. 3kLCA responses were observed with endogenous VDR in our chosen cell line, however to test whether this is a VDR dependant response, silencing the VDR silencing using Small interfering RNA (SiRNA) can be used to confirm this mechanism in the future.

SFN and *t*BHQ induce nuclear accumulation of NRF2 and NRF2-dependant regulation of ARE mediated gene expression, therefore it was not surprising that in LS180 cells, our data shown a significant 17.4- and 16.22-fold increase respectively.

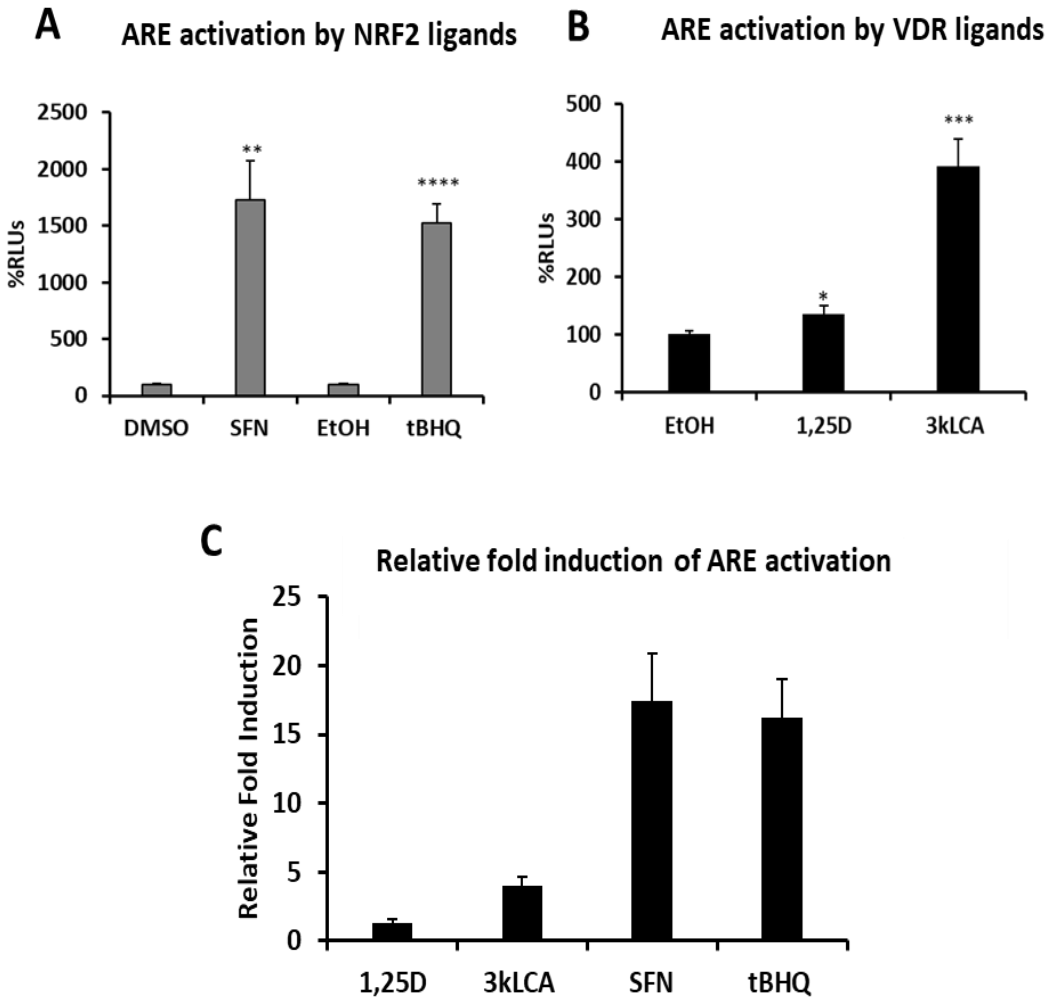

Figure 4.4: ARE minimal promoter activity is mediated by NRF2 and VDR ligands.

*LS180 cells were transfected with ARE-luc reporter construct (650ng/well). The cells were subsequently treated with SFN (6μM), tBHQ (40μM) (A), 1,25D (10^{-8}M) or 3kLCA (10^{-4}M) (B) for 24 hours. Luciferase activity was obtained using Dual-Glo Luciferase Assay (Promega, UK). Data represents 3 independent experiments were n=3. %RLU are relative to vehicle control. Statistical analysis was obtained from Student's two-tailed t.test were *P<0.05, **P<0.005, ***P<0.0005, ****P<0.0001*

4.2.5 The effects of NRF2 and VDR ligands co-treatment in LS180 cells

Next, we wanted to verify whether co-treating LS180 cells with both VDR and NRF2 ligands (simultaneously, rather than pre-treatments) would enhance ARE activity. The previous sets of experiments indicate that each of our tested ligands has some noted effect on ARE activity. Both VDR and NRF2 ligands significantly increased ARE

activity. This was confirmed in the above experiments, where individually we see a significant modulations of ARE promoter activity (SFN 43-, *t*BHQ 32- 1,25D 5.5- and EB1089 13-fold increase). We questioned whether simultenously treating cells with a combination of VDR and NRF2 ligands would additively increase ARE activity, particularly because two signalling pathways are involved.

Surprisingly, co-treatment of 1,25D and SFN reduced ARE activity by 20.5% compared to SFN alone. 1,25D and *t*BHQ combinatorial treatment also reduced ARE activity by a dramatic 63.7% compared to *t*BHQ treatment alone. Also shown in Figure 4.5B, co-treatment of LS180 cells with the EB1089 (the synthetic 1,25D analogue) and SFN reduced ARE activity by 50% compared to SFN treatment alone. Additionally, *t*BHQ and EB1089 co-treatment suppressed ARE activation by 57.8% compared to *t*BHQ treatment alone.

Overall, co-treatment with either 1,25D or EB1089 did not cause any synergistic or additive effects when applied in combination with NRF2 ligands, but instead elicited a profound repression of the NRF2 mediated effect. Taking into consideration the above-mentioned results, this may suggest the presence of inhibitory interaction between the receptors, although unclear, it will be worth investigating further by competitive binding assay in which NRF2 ligands may compete for radiolabelled VDR ligands or their binding motifs.

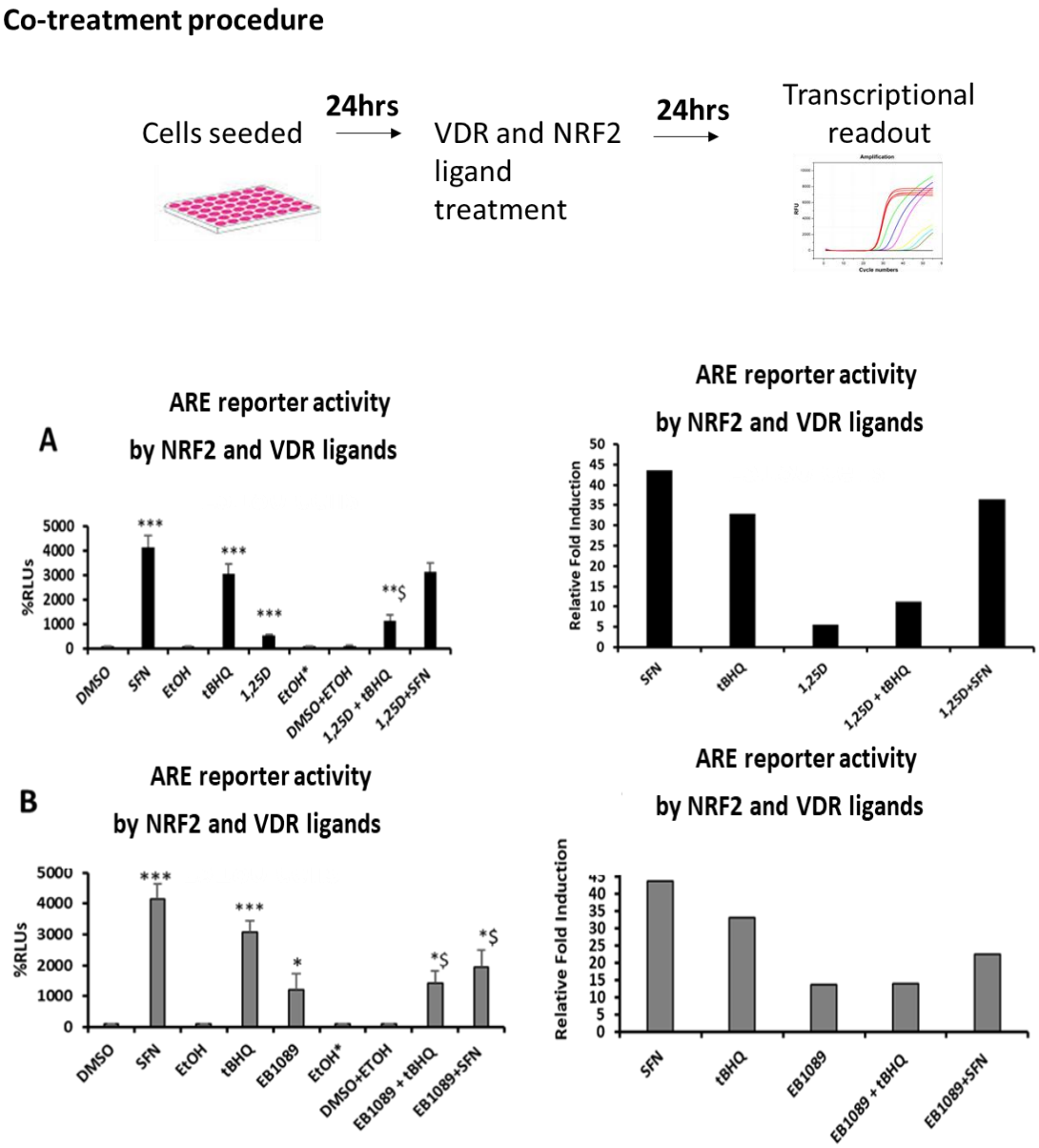

Figure 4.5: VDR and NRF2 ligands co-treatment in LS180 cells. *LS180 cells were transfected with ARE-luc reporter construct (650ng/well). The cells were subsequently treated with SFN (6μM), tBHQ (40μM), 1,25D (10^{-8}M) (A), EB1089 (B) or combination (1,25D+SFN/tBHQ or EB1089+SFN/tBHQ) for 24 hours. Luciferase activity was obtained using Dual-Glo Luciferase Assay (Promega, UK). Data represents 3 independent experiments were n=3. % RLU are relative to vehicle control. Statistical analysis was obtained from Student's two-tailed t.test were *P<0.05, ***P<0.0005, ****P<0.000. $ represents significant relative to SFN or tBHQ treatment alone.*

4.2.6 Establishing interactions between VDR and NRF2 in regulation of UGT1A expression.

290bp of *UGT1A1* promoter plasmid containing the mutagenized VDRE or ARE was transfected into LS180 cells that were subsequently treated with either 1,25D, 3kLCA, SFN or *t*BHQ for 24 hours. The use of the alternate mutant reporter vector was intended to further examine possible interactions between the VDR and NRF2 mediated pathways in regulation of *UGT1A* genes. Mutagenesis of the respective response element is expected to diminish responses to VDR and NRF2 ligands, but a question to peruse was if these effects of mutated response element on ligand responses were mutually exclusive or exhibited co-dependency?

As expected, both VDR ligands enhanced significant *UGT1A1* promoter activity. 1,25D by 6-fold and 3kLCA by a less prominent 2.5-fold increase. The introduction of the VDRE mutation significantly lessened these effects by 45% and 62.9% respectively. The 2bp mutation of an identified and well-established ARE within the *UGT1A1*-290bp promoter resulted in simultaneous decrease of the responsiveness of the *UGT1A1* reporter to VDR ligands. The mutation resulted in a 42% and 58% fold decreased responsiveness to 1,25D and 3kLCA respectively (Figure 4.6.A). On the other hand, SFN (~3-fold) and *t*BHQ (~3-fold) also increased *UGT1A1* promoter activity, confirming that NRF2 signaling trans-activates *UGT1A* isoforms, which are key in the detoxification of endogenous and exogenous toxins (Figure 4.6B) (Kalthof *et al.,* 2010). VDRE mutagenesis did not affect NRF2 mediated *UGT1A1* mediated activity whereas, ARE mutagenesis dramatically diminished *UGT1A1* promoter activity by 61% (SFN) and 50% (*t*BHQ). Our data show that while mutagenesis had effect on the respective signals, *UGT1A1* promoter activity was not completely abrogated, suggesting that there are other response elements involved in this regulation. Our laboratory and others have identified multiple putative VDREs within the *UGT1A* promoter region, which may further contribute to the VDR effects in *UGT1A* regulation (Wang *et al.,* 2016 and Meyer *et al.,* 2012). Additionally, Yueh and Tukey (2007) identified three AREs within a 60-nucleotide sequence spanning -3712/-2068 of the *UGT1A1* promoter region that contributed towards *t*BHQ mediated *UGT1A1* promoter activity. Similar to the VDR effects, NRF2 responses were not completely abrogated due to the other binding motifs that contribute towards ARE activity.

Surprisingly, our findings also suggest a degree of dependency of VDR signaling upon an intact NRF2 pathway, at least for *UGT1A1* promoter activity.

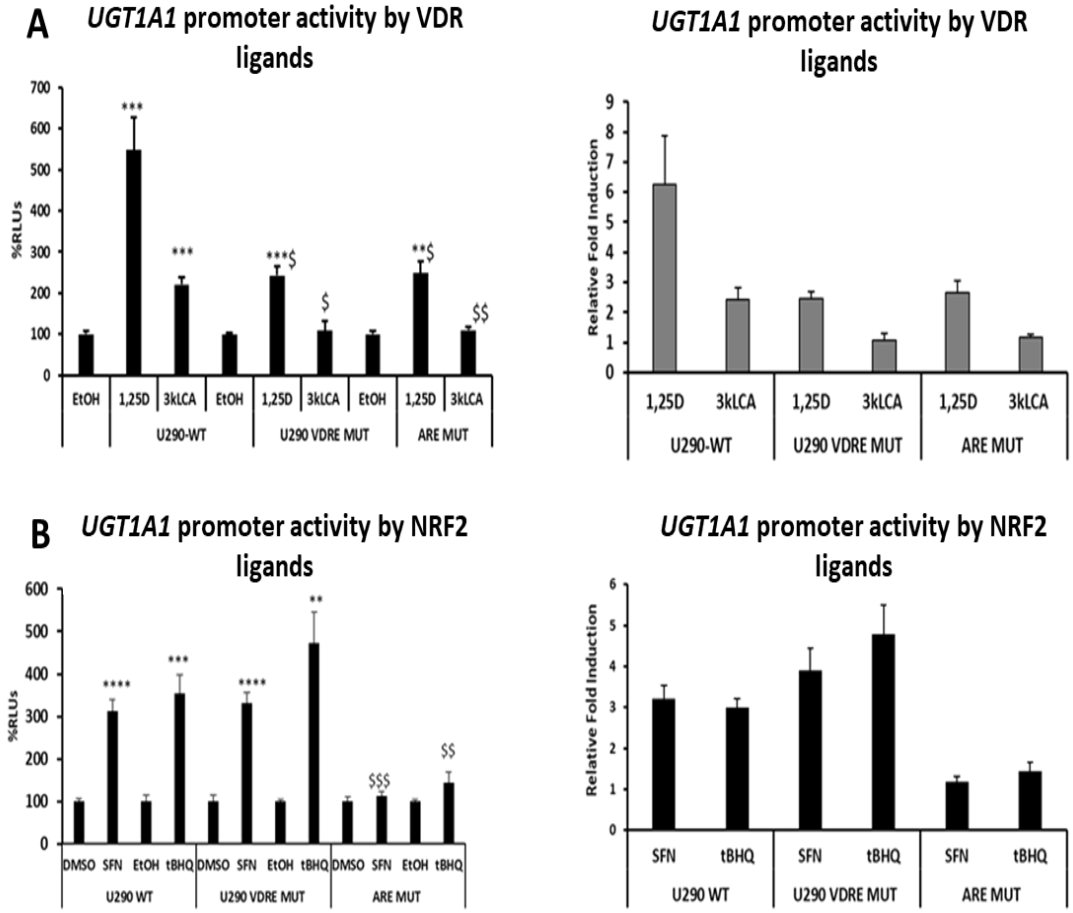

Figure 4.6. VDR and NRF2 co-dependency in UGT1A1 induction. *LS180 cells were transfected with U290 WT promoter vector (U290 WT), U290bp promoter vector containing VDRE mutation (U290 VDRE MUT) or U290 promoter vector containing an ARE mutation (ARE MUT). Cells were treated 1,25D (10^{-8}M), 3kLCA (10^{-4}M) (A), SFN (6μM) or tBHQ (40μM) for 24 hours followed by luciferase activity measurement by Dual Glo Luciferase Assay (Promega, UK). Data represented as Light Units relative to vehicle control were n=3. Statistical analysis was obtained from Student's two-tailed t.test were **P<0.005, p<0.05=*, ***P<0.005, ****P<0.0001. $ represents significance relative to U290-WT.*

4.2.7. Effects of VDR and NRF2 ligands in combinatorial treatments

Since the previous experiments intimate an element of co-dependency/interaction between the VDR and NRF2 signaling pathways, at least in the amplification of *UGT1A1* promoter activity, the next experiments investigated whether combinatorial treatments would impact upon the expression on endogenous target genes. Figure 4.7A and B show qRT-PCR analysis of the expressions of the vitamin D target genes *CYP3A4* and *CYP24A1* (relative to *HPRT* housekeeping gene). Both genes show a significant 650- and ~500-fold induction respectively where LS180 cells were treated with 1,25D alone. SFN exposure to LS180 cells had no effect on the expression of these genes. However, combinatorial treatment of 1,25D with the more prominent NRF2 ligand, SFN, there was a dramatic decline in gene expression to approximately 85% and 90% respectively, relative to 1,25D treatment alone.

A similar approach was used to examine *UGT1A1* and the VDR sensitive *UGT1A4* gene expression levels. 1,25D alone enhanced gene expression by 4.5-fold and 25-fold respectively. Treatment with SFN for 24 hours increased *UGT1A1* expression by significant 2-fold and *UGT1A4* by 2.5-fold. However, upon combination of 1,25D with SFN, *UGT1A1* expression increased by a further 2.5-fold, whereas *UGT1A4* expression dramatically decreased by 51% (Figure 4.7 C and D). This was expected as previously established that both the VDRE and ARE motifs are present within the *UGT1A1* promoter region. Our findings suggest that SFN had no significant effect on *UGT1A4* gene, similar to *CYP24A1* and *CYP3A4* suggesting that it is not regulated through NRF2/ARE signaling.

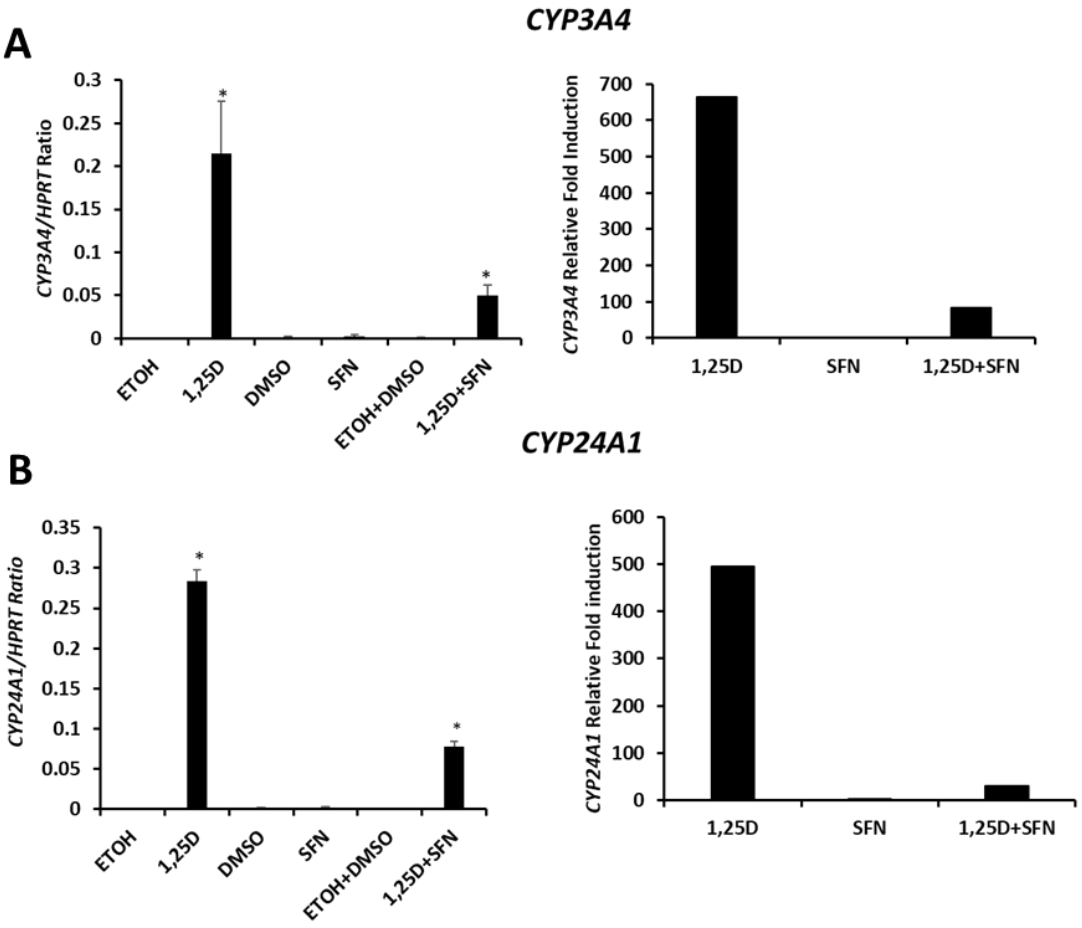
A
CYP3A4
CYP3A4/HPRT Ratio
0.3
0.25
0.2
0.15
0.1
0.05
0
ETOH
1,25D
DMSO
SFN
ETOH+DMSO
1,25D+SFN
CYP3A4 Relative Fold Induction
700
600
500
400
300
200
100
0
1,25D
SFN
1,25D+SFN
B
CYP24A1
CYP24A1/HPRT Ratio
0.35
0.3
0.25
0.2
0.15
0.1
0.05
0
ETOH
1,25D
DMSO
SFN
ETOH+DMSO
1,25D+SFN
CYP24A1 Relative Fold induction
600
500
400
300
200
100
0
1,25D
SFN
1,25D+SFN

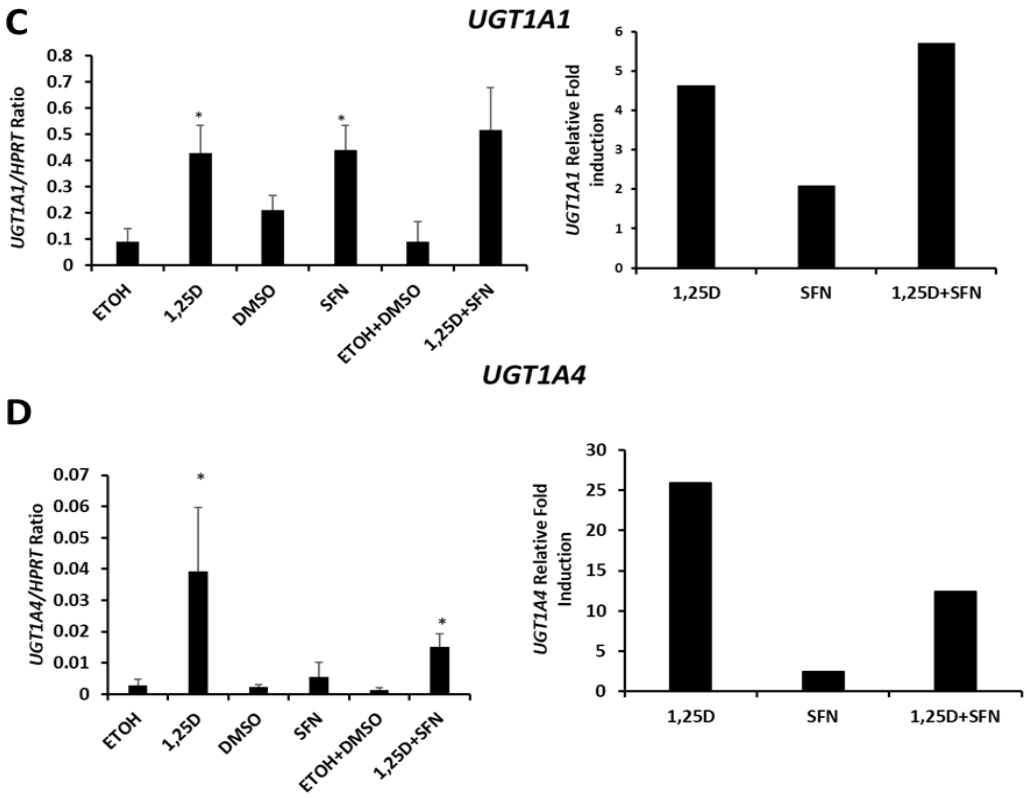

Figure 4.7: Effects of VDR and NRF2 target genes in combinatorial treatments. *For gene expression analysis, cells, RNA was extracted in LS180 cells treated with 1,25D (10^{-8}M), SFN (6μM) or a combination of both for 24 hours, followed by Real Time Q-PCR. ΔCT was calculated with HPRT as a house-keeping gene. Fold induction represented are relative to each vehicle control. Statistical analysis was obtained from Student's two-tailed t.test where is *P<0.05.*

In addition, protein was extracted from LS180 whole cell lysates previously exposed to 1,25D (10^{-8}M), SFN (6μM) or combined treatment of the two ligands for 24-hour treatment. Western blot analysis was perform using the UGT1A antibody. As shown, lane 2 and lane 4 confirm that both 1,25D and SFN increase the levels of detection on the 64kDa UGT1A protein. When given in combination, the intensity of the band corresponding to the UGT1A protein is enhanced (lane 6). (See Figure 4.8A). Furthermore, VDR protein (approximately 48kDa) was detected as present across all treatments. There was a slight increase in VDR protein upon exposure to 1,25D, relative to EtOH (See Figure 4.8B). DMSO surprisingly caused a greater VDR protein signal than SFN treatment, possibly attributed to its ability to stabilize protein. From this data, the effects of VDR protein suppression are not obvious, considering Schwab

et al., (2008) observed that SFN amplified VDR expression, although this was in Caco-2 cell line. What this data implies is that SFN decreases the expression of VDR protein. Nonetheless, combinatorial treatment did abrogate VDR protein expression.

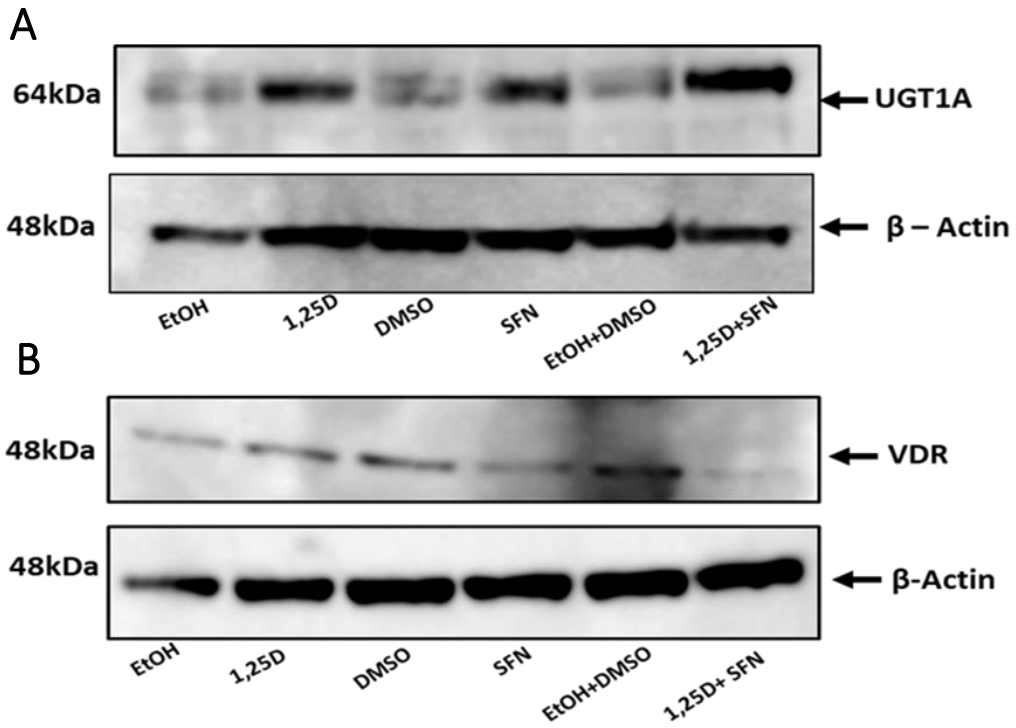

Figure 4.8: Effects of VDR and NRF2 target genes in combinatorial treatments. *For western blot analysis, LS180 whole cell lysates were obtained following 24-hour treatment with 1 25D (10^{-8}M), SFN (6μM) or a combination of both for 24 hours. This was followed by signal detection of UGT1A (A) and VDR (B) protein were β-actin was used as loading control.*

4.2.8 VDRE minimal promoter activity is suppressed by sulphorafane (SFN)

Following the investigation of ARE responses to VDR and NRF2 ligands, the activity of VDRE was investigated in the same manner. The use of a VDRE minimal promoter-driven firefly luciferase vector system, which consists of three copies of VDRE, facilitated in the examination of specific and defined protein interactions to achieve accurate transactivation, was implemented. In view of the fact that PXR and VDR share similar DR3 based binding motifs, and interesting findings by Zhou *et al.,*

(2006), identified that SFN inhibits PXR-mediated responses, it was of interest to examine the comparative effects for how NRF2 ligands upon PXR and VDR responses driven off a VDRE (DR3)-based reporter. As highlighted in Figure 4.8A, SFN causes a dose-dependent reduction in the luciferase signal elicited from the VDRE-reporter by rifampicin (PXR ligand) over a concentration range 6-, 10- and 20μM in LS180 cells. SFN was able to significantly inhibit the responses elicited by rifampicin by 45%, 60% and 74% respectively. VDRE activity remained significantly enhanced in LS180 cells treated with rifampicin in combination with 6μM and 10μM of SFN. However, a similar effect was not observed after 24-hours exposure with rifampicin and 20μM SFN treatment. (See Figure 4.9A). These results were not different from experiments in which LS180 cells were also transfected with the VDRE minimal promoter and subsequently exposed to VDR ligands 1,25D or 3kLCA, also in combination with increasing doses of SFN (6μM, 10μM and 20μM) (See Figure 4.9B). As expected, 1,25D treatment significantly enhances VDRE signalling. The addition of SFN does not affect this significance, although inhibition of 22% and 43.75% of the 1,25D signal generated by VDRE reporter is observed, following co-treatment with SFN (10μM and 20μM respectively). 3kLCA on the other hand, appears to be even more sensitive to inhibited by SFN also in a dose-dependent manner. LS180 exposure to 10^{-4}M of 3kLCA significantly enhances VDRE signalling by 31-fold. The addition of SFN increments (6μM, 10μM and 20μM) dramatically abrogated this effect by 62%, 93.75% and 92.2% respectively (relative to 3kLCA treatment alone). Lastly, SFN alone as a single agent evidently enhances VDRE reporter activity by 1.6-, 1.4- and 1.2-fold increase respectively. However compared to 1,25D (32-fold increase), rifampicin (4.5-fold increase) and 3kLCA (31-fold increase), the changes are minor.

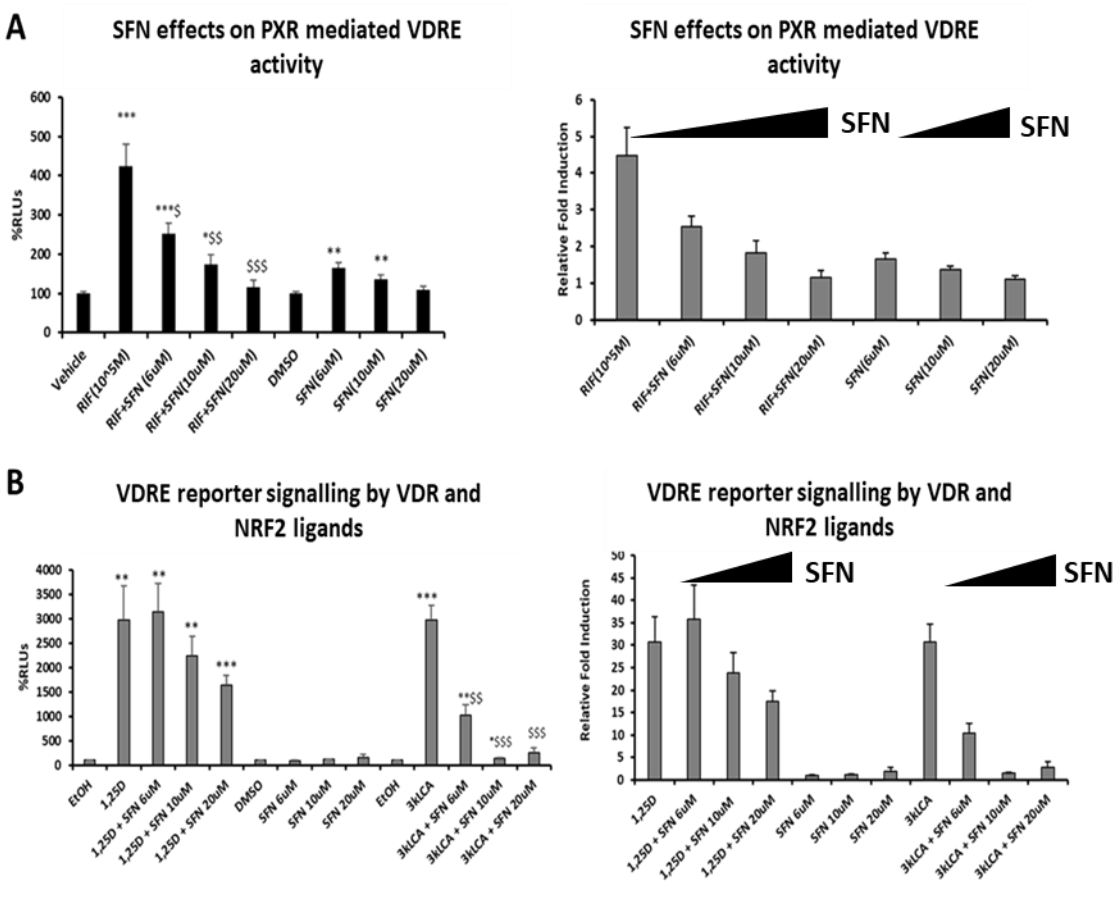

Figure 4.9: *VDRE signalling in LS180 cells.* *LS180 cells seeded in 24-well plates were transfected with VDRE minimal promoter vector (650ng) and subsequently treated with rifampicin (RIF; 10^{-5}M) only or RIF combined with SFN (6-,10- or 20μM) (A). B represents LS180 cells exposed to 1,25D (10^{-5}M) only, 3kLCA only or combined with SFN (6-,10- or 20μM). Luciferase activity was measured using Dual-glo Luciferase Assay (Promega, UK). Data presented as %RLU relative to vehicle control. Data represents 3 independent experiments where n=3. Statistical analysis was obtained from Student's two-tailed t.test where *P<0.05, **P<0.005, ***P<0.0005. $ represents significance relative to RIF, 1,25D or 3kLCA alone.*

4.2.9 Vitamin D pre-treatment enhances NRF2-mediated *UGT1A1* activity

So far, our data does show that VDR and NRF2 ligands modulate ARE-driven activity to varying degrees, however VDRE signalling, based on a DR3 motif, is specific to VDR (and PXR) prototypical ligands. The addition of SFN appears to antagonize PXR and VDR function, an effect that we speculate may be attributed by inhibition of

ligand binding, inhibition of co-activator recruitment, or diminished expression of VDR (and PXR) protein (Figure 4.8B). Gene expression analysis is in agreement with the antagonistic effects of SFN, as VDR-specific target genes are repressed following combinatorial treatment. However, for *UGT1A1*, which contains both the ARE and VDRE binding motifs, the response to 1,25D and other VDR ligands is relatively unaffected.

For this reason, we decided to further investigate the interplay between these two pathways by use of the 290bp long *UGT1A1* promoter vector (-3499/-3210) (Sugatani *et al.,* 2005). At least one functional VDRE and ARE are known to be present within this region (Sugatani *et al.,* 2005). LS180 cells were transiently transfected with this promoter vector prior to pre-treatment with either EtOH or 1,25D to evaluate the ability of VDR activation in priming the activity of NRF2. Cells were subsequently treated with increments of either SFN (3μM, 6μM, 9μM) or *t*BHQ (30μM, 50μM, 70μM). Here we show that SFN as a single agent, modestly but significantly increases the activity of the *UGT1A1* based reporter by 1.5- to 2-fold. (Figure 4.10A) The addition of 1,25D pre-treatment further enhances this effect with a dose-dependent response to SFN becoming more obvious (4-, 5- and 6-fold increases respectively). Furthermore, *t*BHQ doses of 30μM, 50μM and 70μM also increase luciferase activity albeit more modestly than those achieved with SFN (1.76-, 2.45- and 2.51-fold increase). 1,25D pre-exposed cells caused an even greater response (3.1-, 3.7 and 4.2-fold increase respectively) (Figure 4.10B). These results confirmed that 1,25D primes NRF2 responses in *UGT1A1* induction, or perhaps the involvement of both VDRE and ARE binding.

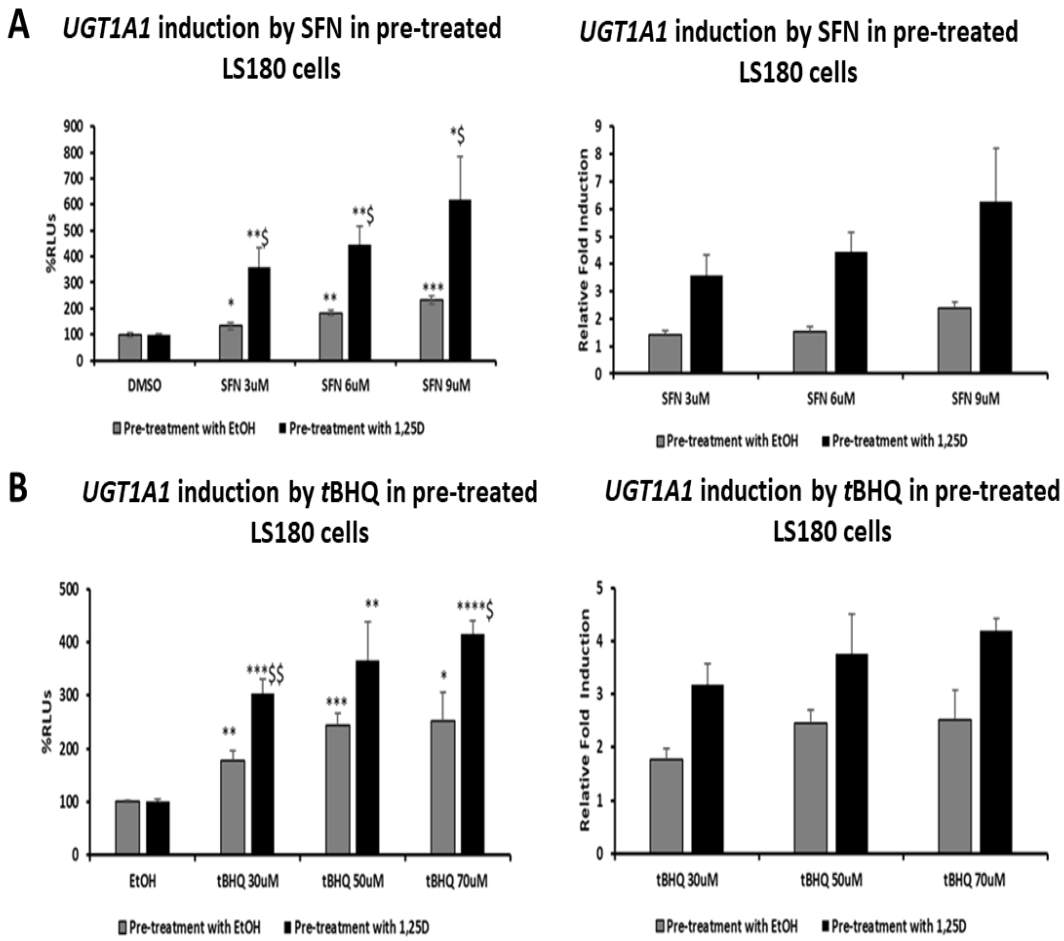

Figure 4.10: UGT1A1 induction in LS180 cells pre-treated with 1,25D. *LS180 cells seeded in 24-well plates were transfected with UGT1A1-290bp promoter vector containing a VDRE and an ARE, following which, cells were subjected to 1,25D or EtOH pre-treatment for 24-hours, then SFN (3-, 6-, or 9μM) or tBHQ (30-, 50- or 70μM) for another 24-hours. Luciferase activity was measured using Dual-glo Luciferase Assay (Promega, UK). Data presented as %RLU relative to vehicle control. Data represents 3 independent experiments where n=3. Statistical analysis was obtained from Student's two-tailed t.test where *P<0.05, **P<0.005, ***P<0.0005. $ represents 1,25D pre-treated induction relative to corresponding EtOH pre-treatment.*

4.2.10 Modulation of detoxification products in pre-treated LS180 cells

In order to test whether 1,25D enhances the regulation of other NRF2 target genes concerned with control of oxidative stress, LS180 cells were again pre-treated with 1,25D or EtOH for 24-hours. Since we hypothesized that VDR does enhance NRF2 responses, our pre-treatment experiments investigate whether prolonged exposure does contribute towards a more prominent NRF2 responses. Clinically, this could mean that individuals should maintain optimum levels of Vitamin D in order to heighten detoxification responses. The cells were then further exposed to increasing amounts of SFN (3μM, 6μM and 9μM) for another 24-hours, followed by analysis through real-time qPCR. In EtOH pre-treated cells, SFN significantly reduced *CYP3A4* expression by 30%, 36% and 38% respectively (relative to DMSO treatment). However, pre-exposure to 1,25D augmented *CYP3A4* expression by a 58.7-, 53.03- and 81.4-fold, relative to its EtOH pre-treated cells in cells exposed to 3μM, 6μM and 9μM of SFN (Figure 4.11A).

In EtOH pre-treated cells, SFN did not alter *CYP24A1* expression; however, the prolonged exposure to 1,25D induced a dramatic 2278.1-, 1465.56- and 1289.9-fold increase relative to EtOH pre-treated cells after a further 24-hour exposure to 3μM, 6μM and 9μM of SFN (Figure 4.11B). Our *CYP3A4* and *CYP24A1* data suggests of inhibitory interactions caused by SFN, which we previously observed in Figure 4.7A and B. The increased *CYP3A4* and *CYP24A1* gene expression were attributed to 1,25D exposure.

Surprisingly SFN significantly down-regulated *UGT1A4* expression by 7%, 50% and 59.3%, (relative to DMSO) upon EtOH pre-treated cells and 24-hour SFN exposure (3μM, 6μM and 9μM). The effects of 1,25D pre-treatment altered gene expression by a 2.6-, 4.3- and 5.2-fold increase regardless of 24-hour treatment with SFN treatment (See Figure 4.11C).

SFN alone, in EtOH pre-exposed cells slightly but not significantly inhibits VDR gene expression by 2%, 3% and a modest 1.12-fold increase upon 3µM, 6µM and 9µM of SFN treatment respectively (relative to DMSO). 1,25D pre-treatment further reduced VDR expression by 28%, 14% and 18% (relative to EtOH pre-treatment) upon 3µM, 6µM and 9µM SFN treatment.

VDR specific genes

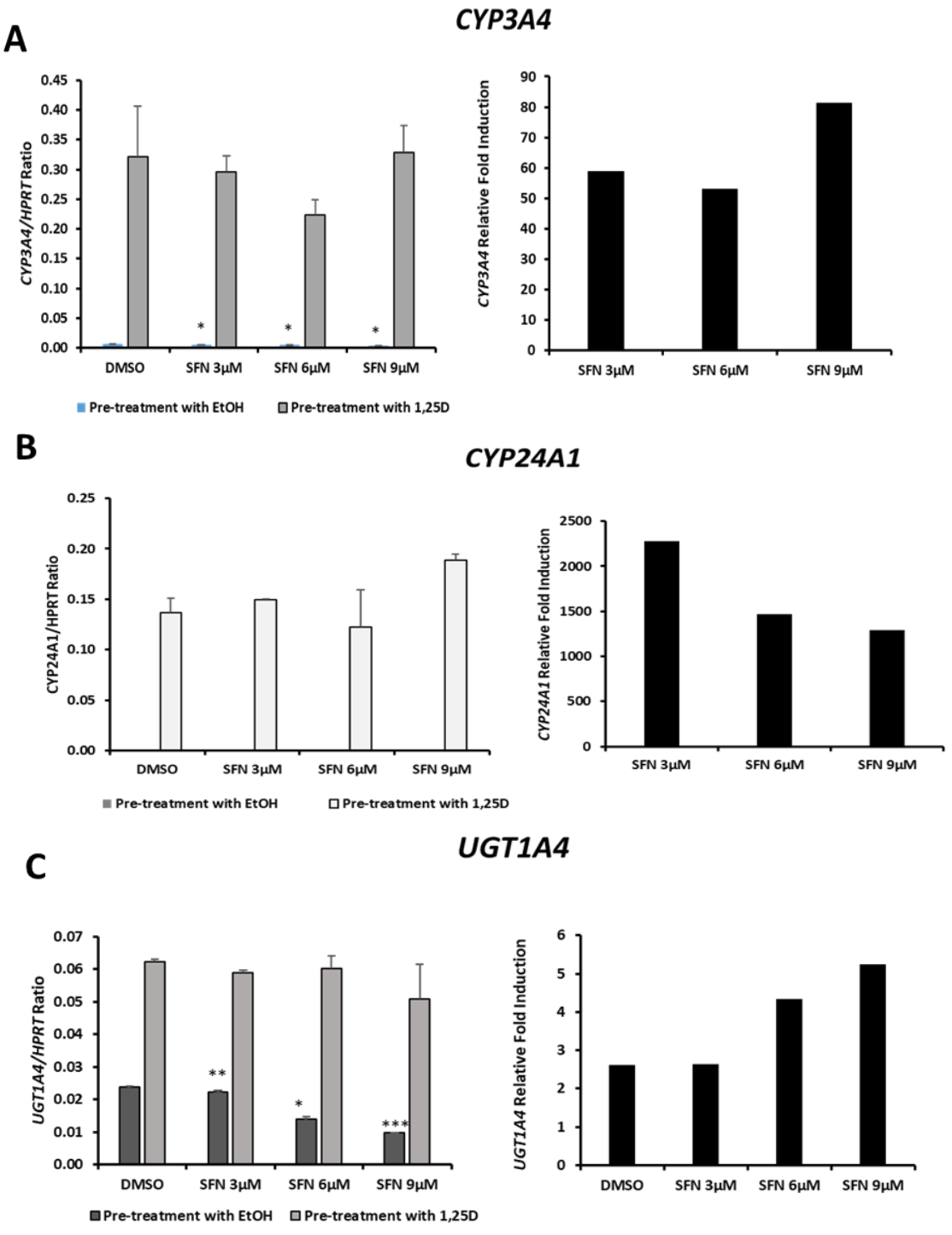

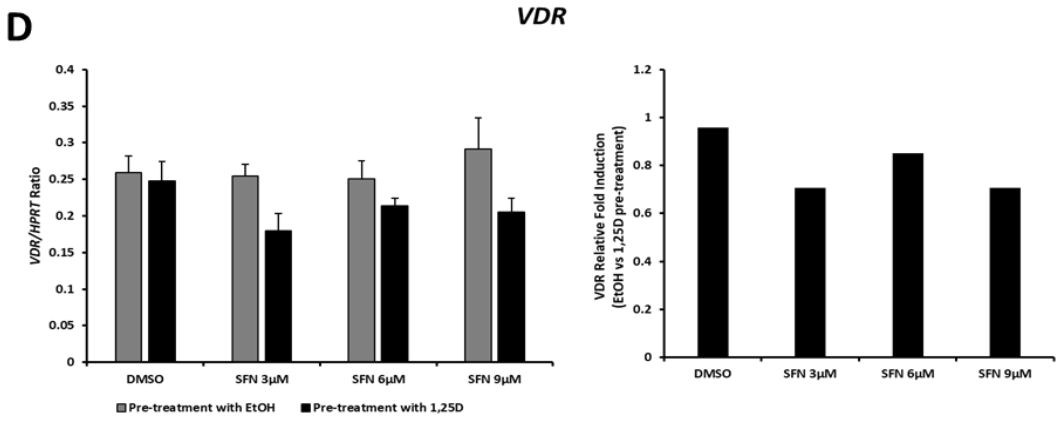

NRF2 specific genes

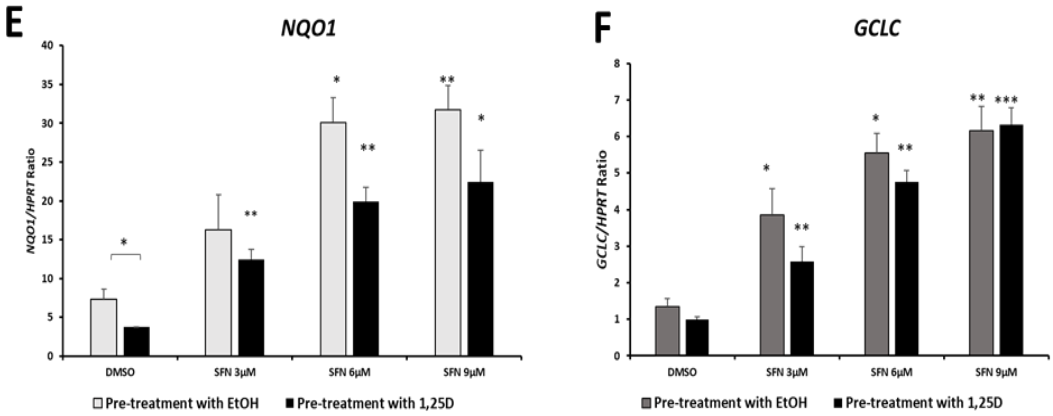

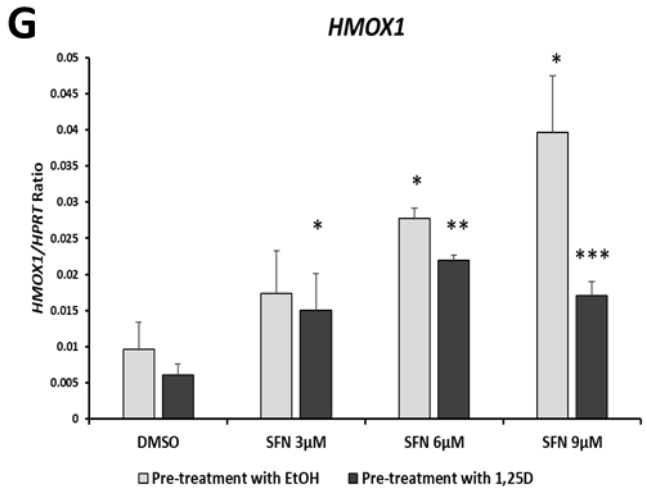

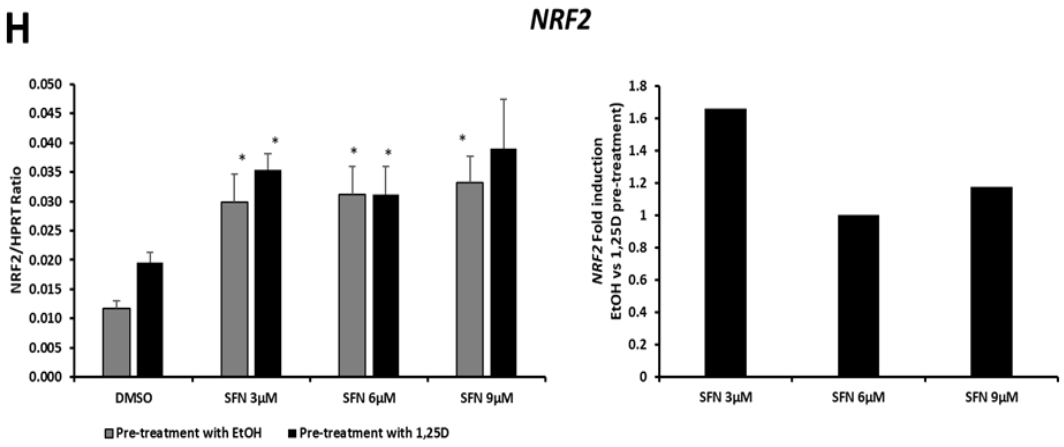

VDR and NRF2 specific genes

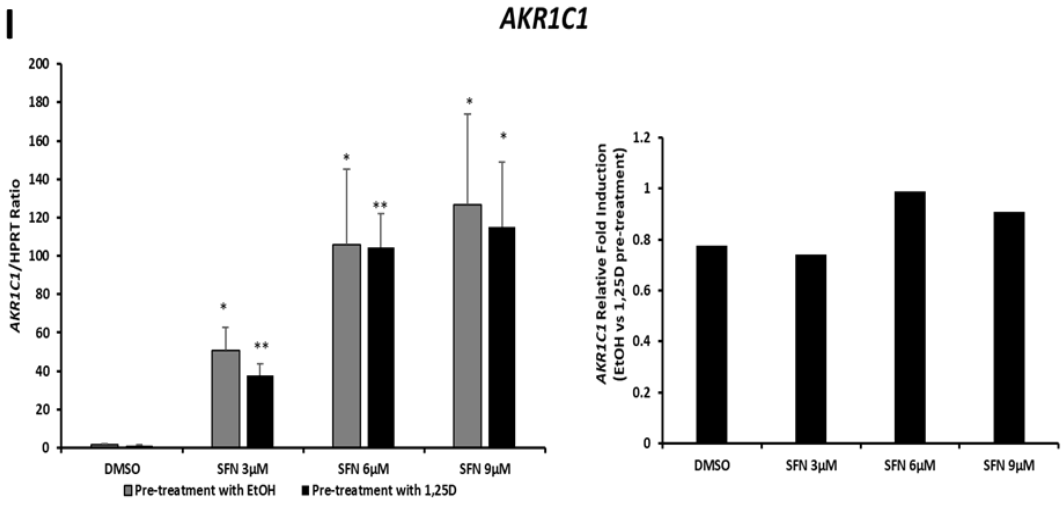

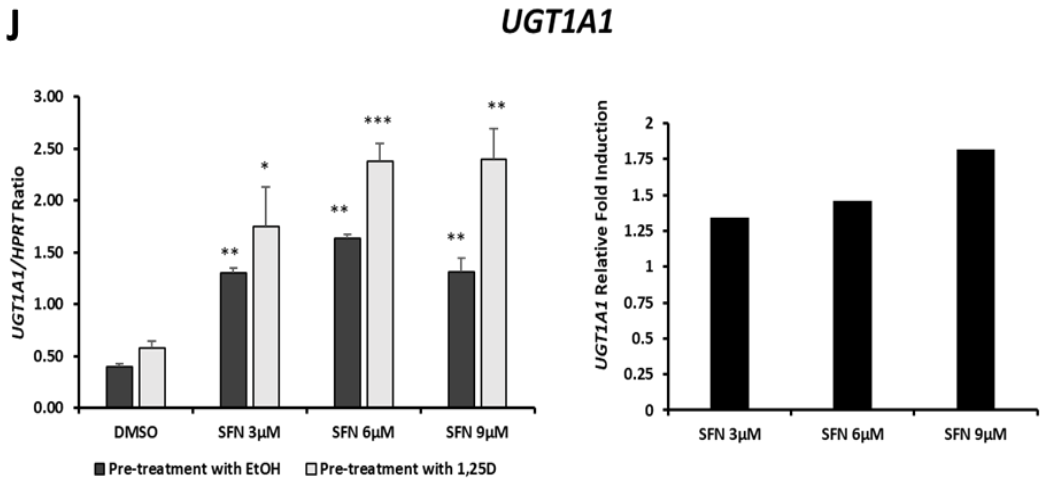

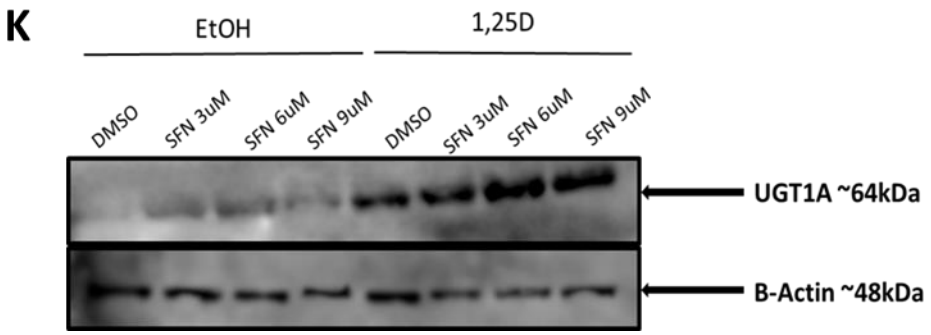

Figure 4.11: Effects of VDR and NRF2 target genes in 1,25D pre-treated LS180 cells. *For gene expression analysis, cells, RNA was extracted in LS180 cells pre-treated with 1,25D or EtOH as vehicle control for 24 hours, followed by SFN (3-, 6- or 9μM) dosage for another 24-hours. Real Time Q-PCR was performed and ΔCT was calculated with HPRT as a house-keeping gene. Fold induction represented are relative to each vehicle control. For western blot analysis, LS180 whole cell lysates were obtained following 24-hour pre- treatment with 1 25D (10^{-8}M) or EtOH followed by SFN (3-,6- and 9μM) for 24 hours. This was followed by signal detection of protein were β-actin was used as house-keeping gene. Statistical analysis was obtained from Student's two-tailed t.test where is *<P 0.05, **P<0.005, ***P<0.0005*

Considering our abovementioned luciferase assay findings (Figure 4.9) and VDR protein expression analysis (See Figure 4.8B) this data points to the fact that SFN itself may interact with VDR ligands or VDR itself, thus suppressing its activities (VDR), the expression itself or VDR specific genes (See Figure 4.11D*).*

Next, expression of NRF2-specific genes was assessed in 1,25D pre-treated cells. *NQO1* gene is involved in the removal of quinines as a detoxification measure against ROS and as such, it is a common NRF2 target gene (Shen *et al.*, 2017). As expected *NQO1* expression is altered by SFN in a dose-dependent manner (4.5-, 3.2- and 3.1-fold increase respectively). 1,25D pre-treatment down-regulates this expression, though not significantly. Surprisingly the effects of 1,25D alone were noted to decrease the basal expression of *NQO1* by 49% (Figure 4.11E). *GCLC* expression was significantly enhanced by SFN alone, by a 3.8-fold increase (EtOH pre-treated cells) and this effect was not significantly altered by 1,25D pre-treatment (3-fold increase) suggesting that 1,25D does not affect *GCLC* expression (Figure 4.11F). *HMOX1* gene, which mediates haem catabolism to form biliverdin, is also an NRF2 target gene (Jiraskova *et al.*, 2017). Expectedly, *HMOX1* induction was influenced in an SFN dose-dependent manner (1.8-, 2.8- and 4.1-fold increase respectively). However, there was no significance observed cells we also exposed to 1,25D (Figure 4.11G). The NRF2 gene itself was also significantly responsive to SFN, (2.5-, 2.64- and 2.8-fold increase) however, 1,25D does not influence this expression as previously identified (Nakai *et al.*, 2010), and this is possibly due to low level of expression of NRF2 in LS180 cells (Figure 4.11H).

To further understand the interplay between VDR and NRF2, we evaluated genes that have been previously reported to be influenced by both signalling pathways. Campos *et al.,* (2013) observed that aldo-keto reductase family 1 member C1 (*AKR1C1*), an NAD (P) H-dependent oxidoreductase that catalyzes aldehydes and ketones for easy excretion from the body was enhanced by 1,25D treated breast carcinoma associated fibroblasts following microarray analysis. Furthermore, functional ARE motifs were localized within the distal promoter of *AKR1C1* confirming that it is also influenced by NRF2 signalling (Lou *et al.*, 2006). Firstly, *AKR1C1* is highly expressed in LS180 cells and the gene is significantly increased by SFN in a dose-dependent manner (28.6-, 59.7- and 71.5-fold increase respectively) (Figure 4.11I). This data however suggests that 1,25D has no influence on *AKR1C1* gene expression as it remained enhanced (27-, 76- and 84-fold increase), although not significantly different compared to SFN treatment alone. Examination of SFN altered *UGT1A1* expression also in a dose-dependent manner, suggestive of its direct regulation through the ARE/NRF2 signaling (3.2-, 4.0- and 3.2-fold increase respectively). As we previously observed, pre-treatment with 1,25D further increased these expressions in SFN treated cells (3-, 4.08- and 4.11-fold increase) also suggesting that the involvement of multiple motifs further enhanced *UGT1A1* expression (Figure 4.11J). Figure 4.11K depicts that our *UGT1A1* gene expression data correlates with protein expression analysis. Although the antibody detects the entire *UGT1A* family members, there is a clear distinction of LS180 whole cell lysates pre-treated with EtOH and those pre-exposed to 1,25D. The bands intensify as SFN dosage increases, similar to the above-mentioned *UGT1A1* expression (Figure 4.7D).

4.2.11 Anti-tumoural actions of VDR and NRF2 signalling pathways

Given that our results indicate that the nature of VDR and NRF2 signaling cross-talk appears to be gene specific, it was of interest to evaluate impact in another cellular signaling pathway, which is the *Wnt*-signalling pathway involved in cellular fate determination, for which 1,25D has been reported to alter its expression. We evaluated Survivin (*BIRC5*) that identifies as an apoptosis inhibitor; known to be inhibited by 1,25D (Li *et al.,* 2005). We evaluated the effects of our pre-treatment experimental condition on these genes. As shown in Figure 4.11 the levels of *BIRC5* expression became reduced when exposed to SFN treatments at 3μM, 6μM and 9μM (23%, 13%

and 17% reduction respectively, relative to DMSO treatment). The addition of 1,25D had no overall effect on the levels of SFN mediated repression, with 1,25D applied as a single agent also achieving a 16% reduction in the expression of this gene (See Figure 4.12A).

We then investigated whether the NRF2 and VDR have overlapping properties in enhancing E-cadherin (*CDH1*) gene expression. *CDH1* is an epithelial cellular adhesion gene implicated with cancer progression and metastasis. It is a strictly modulated gene, known to be transcriptionally activated by VDR (Pena *et al.*, 2005). LS180 cells were exposed to SFN 3μM, 6μM and 9μM for a 24-hour prior to real-time qPCR. An insignificant 1.5-, 1.2- and 1.4 fold increase was observed (relative to DMSO). This data shows that, although ARE/NRF2 signaling is involved in cancer prevention activities, it is not implicated with *CDH1* gene transcription. Our data however, confirm a significant increase in *CDH1* expression following 1,25D exposure alone (2-fold increase). This is in agreement with previous findings by Lopes *et al.,* (2012) who also observed an increase in *CDH1* expression in 1,25D exposed MDA-MB-231 breast cancer cell line (See Figure 4.12C).

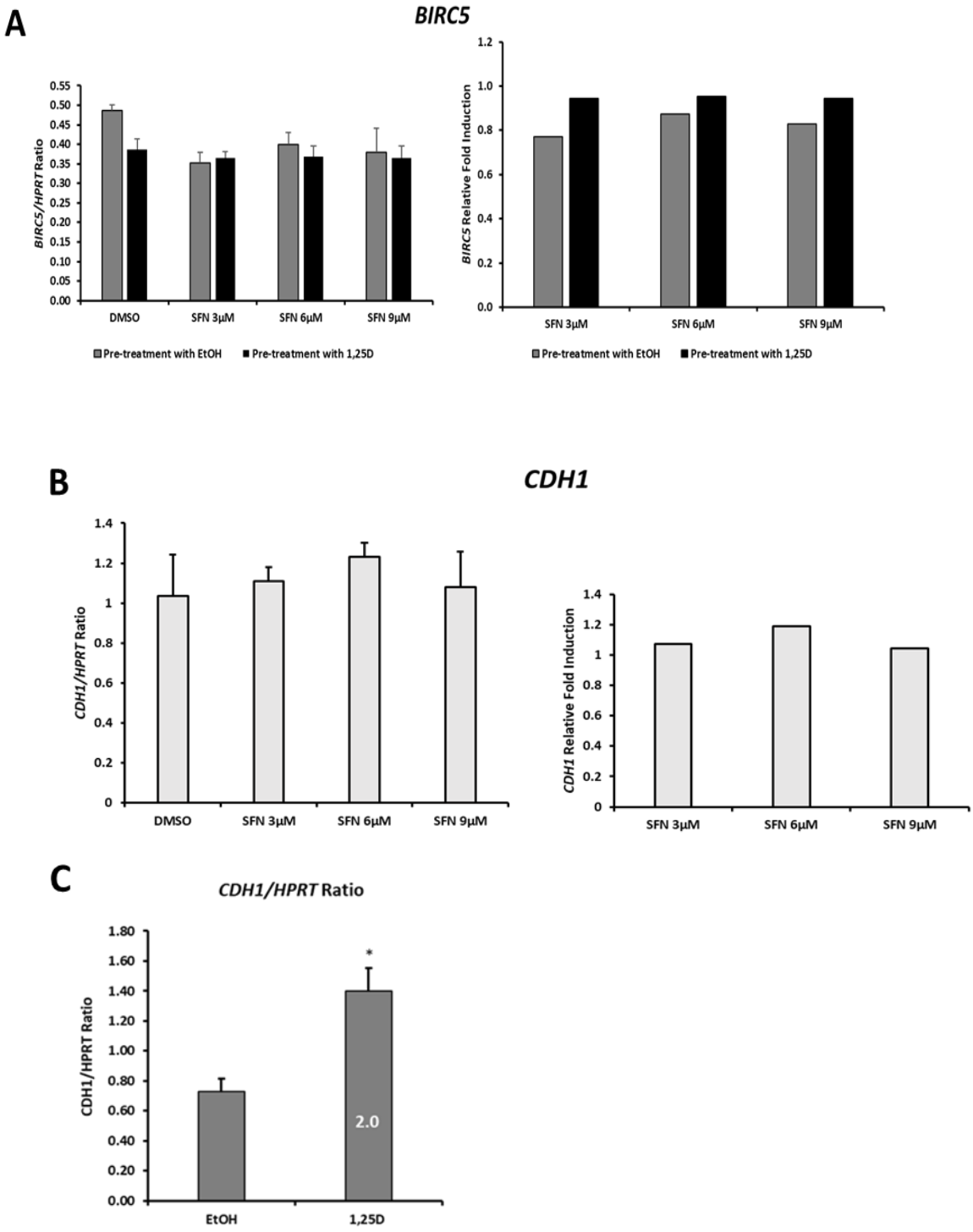

Figure 4.12: Effects of VDR and NRF2 ligands on anti-tumoural genes. *For gene expression analysis, cells, RNA was extracted in LS180 cells pre-treated with 1,25D or ETOH for 24 hours, then subsequently exposed to SFN (3-, 6- and 9µM) (A) or B, cells exposed to SFN (3-, 6- or 9µM) dosage for 24-hours and C, cells treated with 1,25D (10^{-8}M) for 24 hours. Real Time qPCR was performed and ΔCT was calculated with HPRT as a house-keeping gene. Fold induction represented are relative to each*

*vehicle control. Statistical analysis was obtained from Student's two-tailed t.test where is *P<0.05.*

4.3.1 NRF2 and VDR interplay in LNCaP cells

Next, we tested our hypothesis within a prostatic cellular context, using LNCaP cells. OS is linked to initiation and progression of PCa and NRF2 activation appears to inhibits prostate cancer (PCa) cell growth through various mechanisms, such as ferroportin (a protein involved in iron metabolism) (Xue *et al.,* 2016). SFN also suppresses PCa cells by causing apoptosis and in a different context increasing the efficacy of anti-androgens (Xue *et al.,* 2016, Singh *et al.,* 2005). Taking this into consideration and our knowledge on 1,25D/VDR in LNCaP cells, a targeted combinatorial approach could be applied to combat PCa.

Depicted in Figure 4.13 we first examined the presence of functional ARE signalling responses in LNCaP cells by transfecting cells with the pGL4.37[luc2P/ARE/Hygro] (ARE minimal promoter subsequently followed by SFN (6μM), 1,25D (10^{-8}M) and their respective controls for 24 hours. Luciferase activity represented in % RLUs shows a significant 5.5-fold increase in response to SFN. Similar to LS180 cells, 1,25D significantly, activated ARE signalling by approximately 2-fold (See Figure 4.13A).

Next, we evaluated whether prolonged 1,25D exposure primes LNCaP cells to further enhance NRF2 target gene expression. Cells were exposed to either EtOH or 1,25D for 24-hours, followed by a SFN (6μM) treatment for another 24-hour period followed by gene expression analysis by real time q-PCR. As shown in Figure 4.14, our gene expression data show that SFN significantly increased *GCLC* by ~ 2.5-fold increase (A) with 1,25D pre-treatment having no further effect on this regulation. *NQO1* expression was significantly altered by 1,25D pre-treatment alone with a 1.69-fold increase (B). As expected SFN significantly altered *NQO1* gene expression by 9.8-fold increase. Unpredictably there was an 8% decreased where both SFN and 1,25D pre-treatment was present. *HMOX1* gene expression was similar to that of *GCLC*, in that 1,25D pre-treatment alone did not alter its expression, yet the effects of SFN

exposure show a 2.6-fold increase (C). Again, *HMOX1* gene induction is slightly reduced but not significantly, where LNCaP cells were exposed to both ligands.

We further investigated the levels of NRF2 under the same experimental conditions. Although NRF2 expression levels were modest in LNCaP cells, we observed a significant 1.2-fold and 1.59-fold increase by 1,25D and SFN alone respectively. Pre-treatment with 1,25D and further SFN exposure did not significantly affect NRF2 expression. A 1.21-fold increase was observed (relative to SFN treatment alone); an effect likely attributed by SFN. (See Figure 4.13B).

We evaluated similar effects with the *AKR1C1* gene, which we found to be highly expressed in LNCaP cells. Our data show that 1,25D on its own does not alter its expression, however SFN significantly increases it by 23-fold. There was no significant difference in *AKR1C1* gene expression in EtOH (SFN alone) versus 1,25D pre-treated cells and although *AKR1C1* expression was still significantly increased for the latter (13-fold), it is an effect likely attributed to SFN exposure (See Figure 4.13A). We found that *UGT1A1* was surprisingly not responsive to 1,25D in LNCaP cells, whereas dosage with SFN increased its expression (12-fold) (Figure 4.14B). Interestingly, pre-treatment with 1,25D appeared to reduce this effect by 20.7%.

UGT1A4, the most sensitive isoform to 1,25D was not responsive in LNCaP cells (See Figure 4.14C). The *UGT1A* gene expression patterns in this cell line suggest that the genes may not be highly expressed and hold less clinical relevance in this context compared to the colonic tissue. Finally, Figure 4.14E confirms the regulatory effects of 1,25D upon *CYP3A4* gene in LNCaP cells following 24-hour exposure (4.6-fold increase). The addition of SFN did not alter the regulatory effects of 1,25D. Similar to LS180 cells, SFN does not influence the *CYP3A4* gene. Collectively, these results show that cross-talk between VDR and NRF2 signalling is gene and cellular specific. Additionally, the inhibitory trends observed upon co-administration suggest much more complex molecular mechanisms that cannot be explained by gene expression analysis alone.

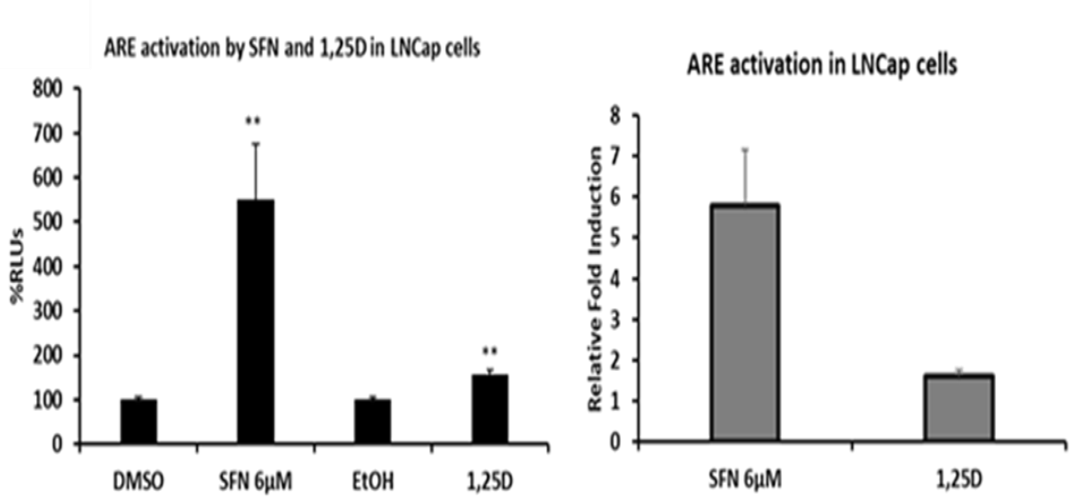

Figure 4.13: ARE signalling in LNCaP cells. *LNCaP cells seeded in 24-well plates were transfected with ARE-luc promoter vector following which, cells were subjected to 1,25D or SFN (6μM) for another 24-hours. Luciferase activity was measured using Dual-glo Luciferase Assay (Promega, UK). Data presented as %RLU relative to vehicle control. Data represents 3 independent experiments where n=3. Statistical analysis was obtained from Student's two-tailed t.test where is *P<0.05, **P<0.005*

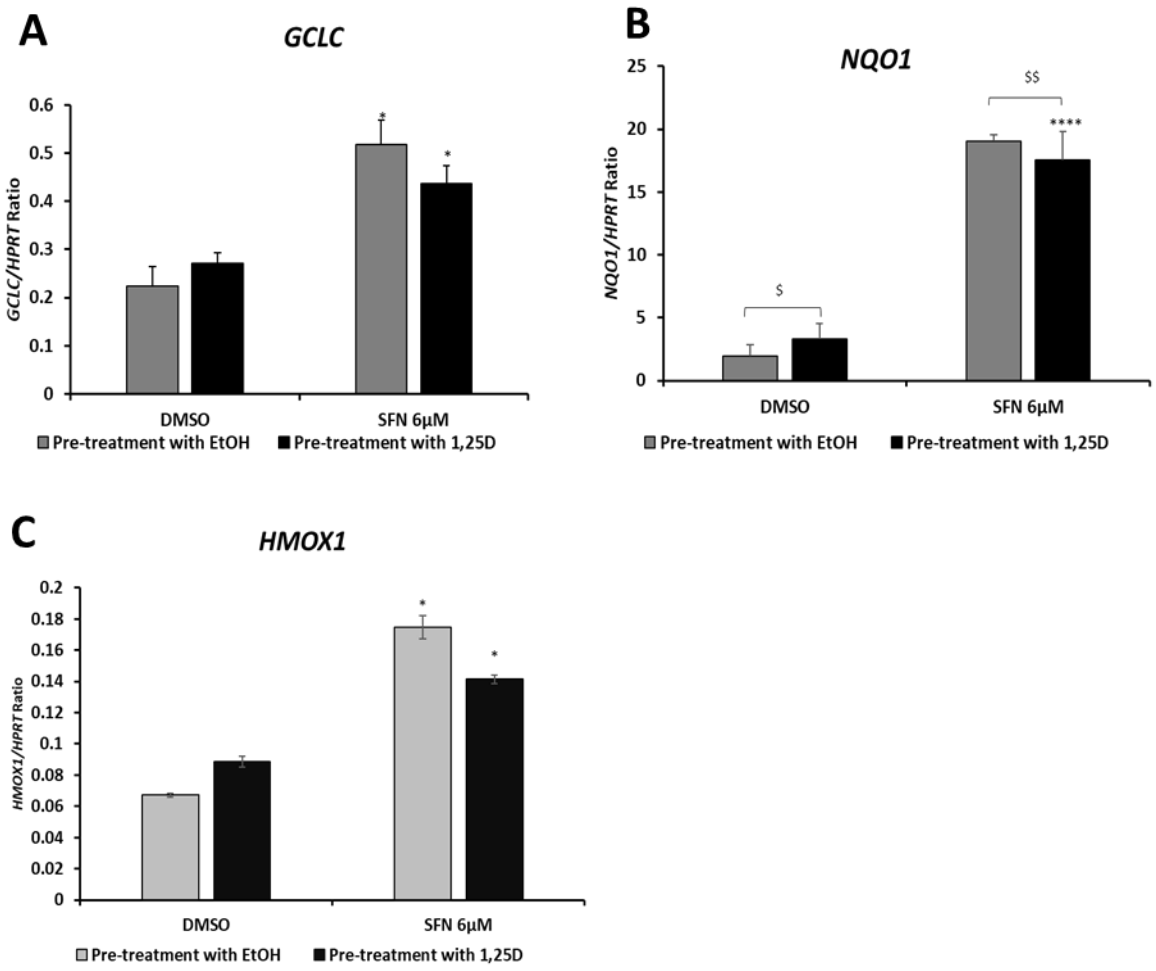

Figure 4.14: NRF2 target gene regulation in LNCaP cells pre-treated with 1,25D.

*For gene expression analysis, cells, RNA was extracted in LNCaP cells pre-treated with 1,25D or EtOH as vehicle control for 24 hours, followed by SFN (6µM) dosage for other 24-hours. Real Time Q-PCR was performed and ΔCT was calculated with HPRT as a house-keeping gene. Fold induction represented are relative to each vehicle control. Statistical analysis was obtained from Student's two-tailed t.test where is *P<0.05, ****P<0.00001. $ represents 1,25D pre-treatment significance relative to EtOH.*

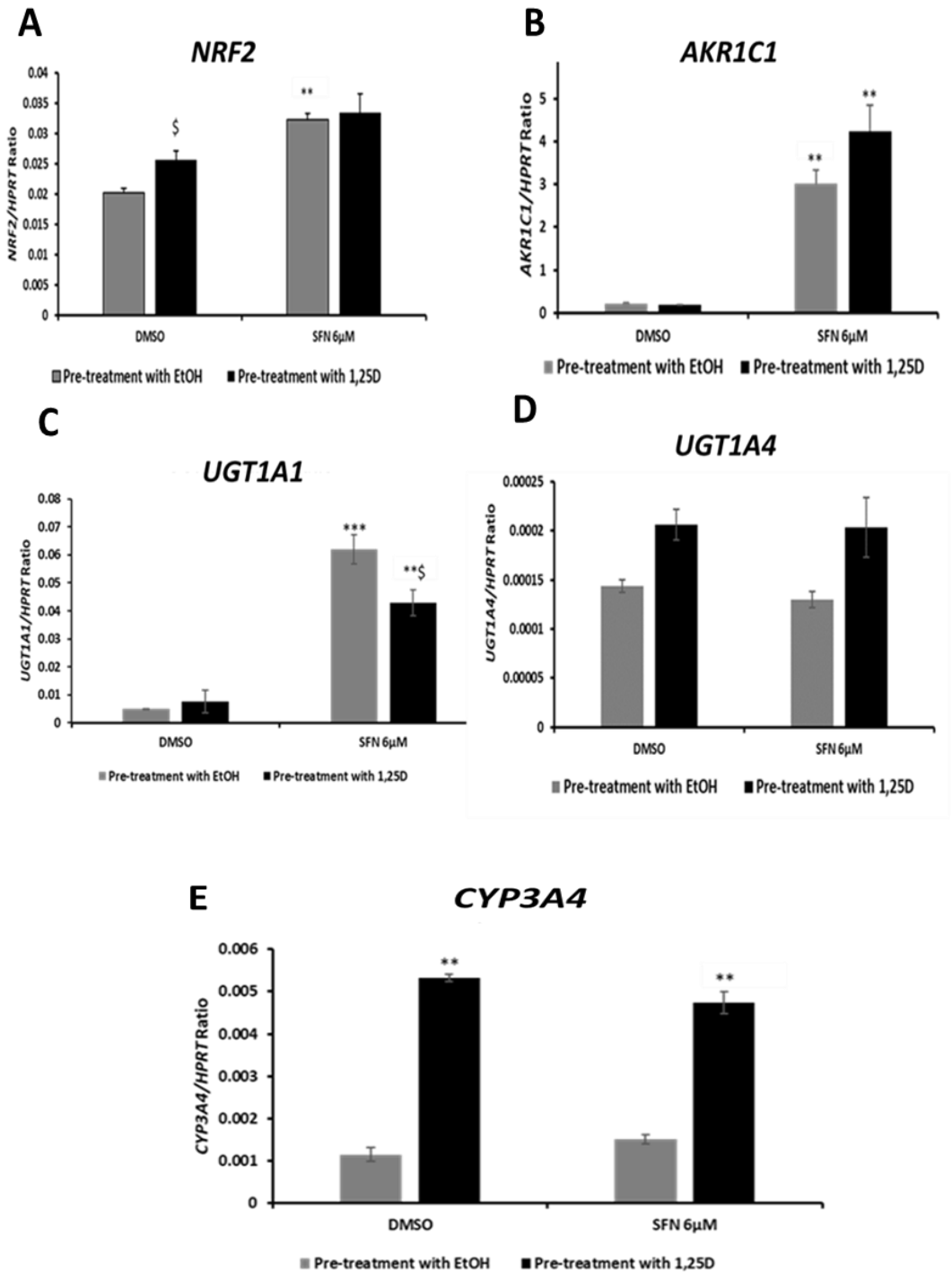

Figure 4.15: VDR target gene regulation in LNCaP cells pre-treated with 1,25D.

For gene expression analysis, cells, RNA was extracted in LNCaP cells pre-treated with 1,25D or EtOH as vehicle control for 24 hours, followed by SFN (6µM) dosage for another 24-hours. Real Time Q-PCR was performed and ΔCT was calculated with HPRT as a house-keeping gene. Fold induction represented are relative to each vehicle control. Statistical analysis was obtained from Student's two-tailed t.test

*where is *P<0.05, ****P<0.00001. $ represents 1,25D pre-treatment significance relative to EtOH.*

4.3.2 VDR and NRF2 ligands inhibit LNCaP and LS180 cell growth

Data from growth inhibition assay of LNCaP cells exposed to 1,25D (10^{-8}M), SFN (6μM) or combination of the two ligands for 144-hours is shown in Figure 4.15A. For cells exposed to 1,25D, there was a significant 40% growth inhibition relative to vehicle control. In LNCaP cells exposed to SFN growth was inhibited by 80%, relative to DMSO. Co-treatment of LNCaP with 1,25D and SFN for 144-hours inhibited growth by 66.8%, although significant collaborative effects were not observed. In LS180 cells, 1,25D significantly inhibited growth by 26%, whereas SFN inhibited growth by 50%. Co-treatment with both ligands inhibited LS180 cell growth by a significant 66.7%. In the previously conducted cell viability assay (Figure 4.1), 6μM did not cause growth inhibition as observed in this experiment. The differences is results are likely due to differences in SFN incubation time. For our cell viability experiments, cells were exposed to SFN for 24-hours. Similar to our LNCaP findings, there were no distinct antiproliferative effects between both VDR and NRF2 ligands. Our data strongly suggest that VDR and NRF2 signalling pathways work independently in the control of colon and prostate cancer (See Figure 4.16).

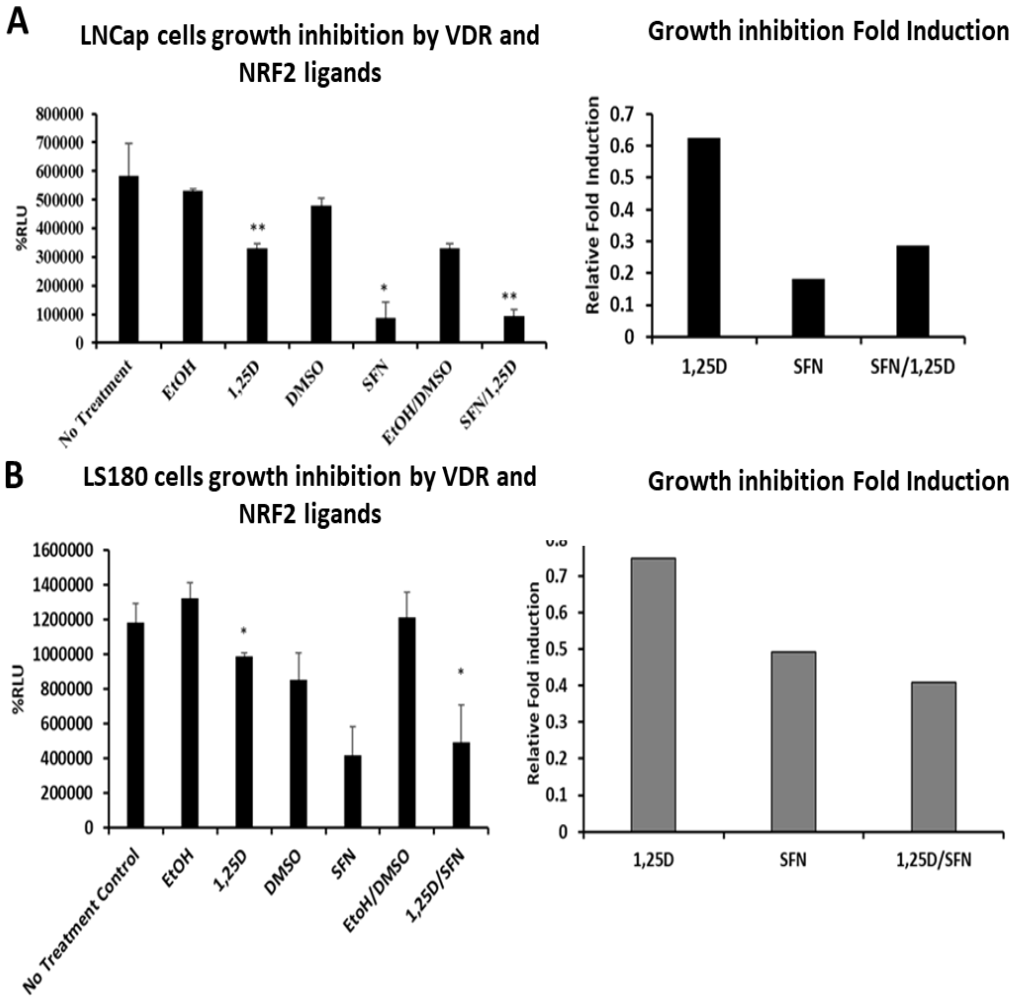

Figure 4.16: Growth inhibition assay in LNCaP and LS180 cells. *SFN (6μM) and 1,25D (10^{-8}M) responses to growth in LNCaP (A) and LS180 cells (B) are shown. Cells were treated for 6 days followed by measurement of Light Units using Cell-titre glo assay (Promega, UK). Data represents 3 independent experiments were n=3. Figures are presented as %RLU relative to vehicle control. Statistical analysis was obtained from Student's two-tailed t.test where is *P<0.05, **<P.0.005.*

4.4 Discussion

NRF2 signalling pathway represents a critical cyto-protective system that neutralizes intracellular imbalance between oxidant production and antioxidant mechanisms (Ahmed *et al.*, 2017). Prolonged or severe exposure to OS influences cellular health and numerous clinical consequences (Berridge, 2015). Induction of OS-related genes through NRF2 activation is the key to cellular redox homeostatic control (Tebay *et al.*, 2015). A number of *UGT1A* isoforms, such as *UGT1A1, UGT1A7, UGT1A8* and *UGT1A10* function as detoxification enzymes in response to NRF2 regulation through *cis-acting* AREs within their 5'-flanking promoter regions (Kalthof *et al.*, 2010, Yueh and Tukey, 2007). NRF2 knock out mice that posses a deficiency in this protective genetic profile acquired severe OS damage (Iizuka *et al.*, 2005).

In this study VDR and NRF2, signalling interplay was characterized through evaluating their respective and combined effects on the *UGT1A* regulation, expression of NRF2 target genes and interactions through VDRE and ARE reporter constructs. These data show that this cross-talk appears to be gene specific, owing to the presence of distinct ARE and VDRE motifs within the promoter region (*UGT1A1*). In VDR (e.g. *CYP24A1, CYP3A4*) or NRF2 (*NQO1, HMOX1* and *GCLC*) specific targets, our studies of combinatorial effects intimate inhibitory effects suggestive of indirect regulatory mechanisms. Our reporter based and growth inhibitory assays suggest that VDR does not enhance NRF2 mediated signalling responses, other than *UGT1A1*.

Both the cell viability assay and titration curve (See Figure 4.1 and 4.2) establish the non-cytotoxic concentrations of NRF2 ligand whilst also confirming ARE functionality in LS180 cells. Our data show that 10μM SFN was an optimal ARE activating, yet non-toxic concentration, however, to fully explore the potential ARE responses without reaching 'plateau' of activation, NRF2 responses were mainly investigated using 6μM. Although SFN concentrations >5μM is not likely to be realistically derived through dietary doses, examination of *in vitro* NRF2 responses was still possible. For instance, the study by Schwab *et al* (2008) using Caco-2 cells revealed a significant 1.6-fold increased expression of *β-defensin 2* (also an NRF2 target) using the same concentration. *T*BHQ (40μM) was previously observed to activate NRF2 in KYSE70 colon cells (Kalthof *et al.*, 2010). Our data also confirmed

this as a non-cytotoxic and NRF2/ARE activating concentration ideal for subsequent experiments.

Interestingly 1,25D had modest, although significant effects on ARE activity, although the effects plateaued at 10^{-7}M. (See Figure 4.2). Ectopic VDR expression in HEK293 cells which otherwise express negligible amounts of VDR did not alter ARE activity. Our data suggests that ARE activation may involve a multi-factorial process, that is, 1,25D may initiate non-genomic actions that converge on the NRF2/ARE signalling complex. Since indirect NRF2/ARE activation was observed via the c-JUN-N-terminal kinase (JKN) pathways and 1,25D is known to activate other signalling pathways such as MAP kinases and c-JUN-N-terminal kinase (JKN) pathways, this could be a plausible explanation for our findings (Morelli *et al.*,2001 and Keum *et al.*, 2009). The involvement of the two signalling pathways (VDR and NRF2) in this context could mean enhanced inflammatory responses, cell proliferation, differentiation and apoptosis.

The participation of 1,25D in inducing ARE activity led us to analyse the effects of 1,25D pre-treatment in NRF2 induced LS180 cells. 1,25D through the activation of VDR initiates the expression of NRF2, which in turn increases the expression of genes involved in redox and detoxification pathways (Nakai *et al.*, 2014 and Berridge, 2016). Therefore, we proposed that, priming cells with 1,25D would further enhance NRF2 and its signalling in our cell model system.

Pre-treatment with 1,25D resulted in a non-significant trend towards enhanced ARE reporter activity (See Figure 4.3). These findings suggest that maintenance of optimum 1,25D levels in colon cells does not in itself improve antioxidant responses. 1,25D may increase cytosolic NRF2 expression, but not affect its translocation as Teixeria *et al.*, (2017) would suggest.

It was previously shown that NRF2 genes are induced by bile acids (Weerachayaphorn *et al.*, 2012). Here we identified that the secondary bile acid, 3kLCA significantly alters ARE activity more potently that 1,25D (See Figure 4.4). Our findings imply that since 3kLCA is highly toxic with genotoxic and mutagenic properties, its potential

to initiate colon carcinogenesis may be counteracted by NRF2/ARE signalling (Tan *et al.,* 2007). Since bile acids activate several cell signalling pathways including FXR, PXR and VDR, NRF2 signalling could also converge to regulate a complex colonic bile acid metabolism network (Zhao *et al.,* 2014; Wagner *et al.,* 2005 and Makishima *et al.,* 2002).

Next, we tested whether (simultaneous) co-treatment of NRF2 and VDR ligands augment ARE signalling in LS180 cells (See Figure 4.5). Contrary to Lee *et al.,* (2015) who observed a synergistic mediation of the *Wnt*-pathway, we observed that combinatorial treatment significantly diminished ARE reporter activity. Co-treatment may induce an adaptive mechanism to suppress an overwhelming NRF2 response in LS180 cells. Our results were similar to Furue *et al.,* (2018) who verified that dioxin and cinnamaldehyde co-treatment (AhR and NRF2 ligands respectively) inhibited AhR-*CYP1A1* OS neutralization axis, in this case, to control dioxin activity on NRF2 activation, which is difficult to degrade. Furthermore our findings indicate that SFN or *t*BHQ treatment alone is more effective than VDR ligands in inducing ARE activity. We predict that our inconsistencies with the work of Lee *et al.,* (2015), who utilized Caco-2 cells exposed to 1-2.5μM SFN, are a result of our use of supraphysiological SFN concentrations. The dietary SFN concentration is approximately 2.5μM (Yagishita *et al.,* 2019). However, Chiang *et al.,* (2019) co-treated melanoma cells with 5μM SFN and 5-aza-2'-deoxycytidine (DAC) and yielded a combinatorial effect, suggestive of a cell specific issue rather than concentration. The fact that *t*BHQ (40μM) in combination with VDR ligands produced a similar effect to SFN further implies that there is cross-talk between VDR and NRF2 at least within a colonic context. Whether this happens through direct ligand interaction or recruitment of co-repressors is still in question. Our findings do not support the proposed hypothesis that VDR enhances NRF2 responses.

The mutagenesis experiments in our study indicate that the presence of both ARE and VDRE is essential for a VDR mediated *UGT1A1* induction, however VDRE is not required for *UGT1A1* regulation by activated NRF2 (See Figure 4.6). However, from our data, VDR signalling is surprisingly dependant on an intact ARE. For future validation, implementing short interfering RNA (siRNA) experiments or

electrophoretic mobility shift assay (EMSA) will confirm the nature of VDR interdependency.

Given that, VDR and NRF2 ligands individually activate ARE to differing degrees, co-treatment reduced this activity, and interdependency between the two signalling pathways was observed, we evaluated if these effects could be noted for the expression of endogenous metabolic genes in LS180 cells. Our results reveal a conspicuous trend in gene expression, in which combinatorial treatment inhibits the expression of VDR specific genes (*CYP3A4, CYP24A1, UGT1A4 and VDR* itself), but further enhanced *UGT1A1* where both VDRE and ARE are present, suggesting that there is collaborative control of its expression. Combinatorial also treatment enhanced UGT1A protein expression, although given the unavailability of specific UGT1A isoform antibodies, we cannot absolutely verify that this is solely due to effects on UGT1A1. Our *in vitro* model demonstrates inhibition of VDR protein after SFN exposure, contradicting Schwab *et al.,* (2008) data who identified increased VDR expression leading to enhanced β-defensin 2 expression (See Figure 4.7). Collectively our findings on SFN inhibitory effects suggest that SFN may interact with VDR itself, limiting its transcriptional activity and expression.

SFN exhibits histone deacetylase inhibitor (HDACI) activity by facilitating the formation of histone acetyltransferase/co-activator (HAT/CoA) complexes which induce hyper acetylation. This was evidenced to regulate TF binding, gene transactivation, proliferation, differentiation and apoptosis in HCT-116 and PC-3 prostate cancer cells, the latter which also corresponds to the non-classical properties of vitamin D (Myzak *et al.*, 2004; Myzak et al., 2006; Dashwood and Ho, 2007). The unexpected SFN inhibitory properties in our data suggest that our chosen model systems may not be the best to investigate collaborative properties with vitamin D, and examining the response *in vivo* may yield the expected evidence.

What could be driving the enhanced *UGT1A1* response in the combinatorial experiments is the involvement of the multiple AREs within *UGT1A1* promoter region, previously characterized by Yueh and Tukey (2007). In expanding upon the inhibitory effects of co-treatments in ARE signalling, we evaluated similar effects

using a VDRE minimal promoter. Zhou *et al.,* (2007) previously characterized antagonistic effects of SFN on PXR mediated *CYP3A4* expression. We replicated this experiment in our LS180 cells in addition to characterization of VDR and NRF2 mediated effects upon VDRE-mediated signalling (Figure 4.9). Our results are analogous to that of Zhou *et al.,* (2007). SFN significantly inhibited PXR mediated signalling in a concentration dependant manner. Additionally, SFN slightly suppressed VDRE signalling in 1,25D treated LS180 cells, although this was not significant, contrary to the dramatic effect noted on 3kLCA. Our findings suggest that SFN may compete with rifampicin and 3kLCA for binding to the LBD of PXR and VDR, respectively, but is a less effective inhibitor of 1,25D association with VDR. Interestingly, Kahlon *et al.,* (2005) identified cruciferous *in vitro* vegetable binding of bile acids. Since SFN, as already mentioned is a sulphur-rich compound derived from vegetables, findings on its inhibitory effects on 3kLCA suggest that SFN may possibly bind to 3kLCA, preventing re-circulation, which results in reduced re-absorption, facilitate in its excretion, as another chemo-preventative measure (Kahlon *et al.,* 2005).

We also showed that pre-treatment with 1,25D significantly achieved higher levels of *UGT1A1* promoter activation from subsequent treatment with NRF2 ligand (Figure 4.10). This is most likely due to collaborative effects of both binding motifs as opposed to effects of 1,25D priming SFN and *t*BHQ mediated *UGT1A1* induction. Our gene expression analysis under pre-treatment experimental conditions suggests that SFN has no effect on VDR-specific genes (*CYP3A4, CYP24A1 and UGT1A4*) (Figure 4.11). Interestingly SFN significantly inhibited *CYP3A4* and *UGT1A4 1,25D* mediated effects. *CYP24A1* mRNA expression was not altered by dosage with SFN. On the other hand, the expressions of NRF2-specific genes (*NQO1, HMOX1* and *GCLC*) were significantly increased by SFN in a dose-related manner. 1,25D pre-treatment did not alter mRNA expression levels; contradictory to our proposed hypothesis (Figure 4.11). Our data did not reproduce the findings of Chen *et al.,* (2019) who demonstrated that 1,25D transcriptionally up-regulated NRF2. This discrepant result may be a consequence of the fact that Chen *et al.,* (2007), and Nakai *et al.,* (2010) used mouse models for this analysis. Species-specific regulation may be an explanation, and although NRF2 is expressed in LS180 cells, levels are low (See Figure 4.11H). The

results of this study suggest that any interaction between VDR and NRF2 is likely complex and difficult to assess through mRNA expression.

Aldo-keto reductases (AKRs) are phase 1 metabolic NAD (P) H-dependent oxidoreductases that convert aldehydes and ketones to primary and secondary alcohols for subsequent phase II metabolic reactions (Penning *et al.,* 2017). AKRs are consistently the most overexpressed in response to NRF2 activation (Penning *et al.,* 2017). Tian *et al.,* (2016) previously described their presence in breast and prostatic context. Our data show that *AKR1C1* is highly abundant in LS180 cells (Figure 4.11C). 1,25D pre-treatment unexpectedly does not enhance *AKR1C1* mRNA expression levels although previous knowledge shows that *AKR1C1, AKR1C2* and *AKR1C3* were enhanced by 1,25D in breast carcinoma fibroblasts (Campos *et al.,* 2013). *AKR1C1* was regulated by NRF2 activation in a dose-dependent manner (See Figure 4.11C). Our data correspond to that of Agyeman *et al.,* (2012) who conducted transcriptomic gene expression by microarray in MCF10A cells treated with SFN or Keap1 siRNA who observed a dramatic 15-fold increase and 37.4-fold increase respectively. Our data show a 29.6-, 59.7- and 71.54-fold increase following SFN (3-,6-, and 9μM) exposure alone in LS180 cells. *In silico* analysis by Tebay *et al.,* (2015) identified distal consensus ARE within AKR promoters. On the other hand, no functional VDRE have yet been reported within *AKR1C1*, suggestive that any 1,25D effects may be mediated through indirect regulatory mechanisms, which are overwhelmed by direct SFN mediated regulation. 1,25D pre-treatment enhanced NRF2 mediated *UGT1A1* mRNA and UGT1A protein expression, certainly through binding motifs collaborative effects (See Figure 4.11D). Our data uncovers that *UGT1A1* up-regulation is likely a result of multiple binding motifs present for each pathway. Our correlative findings motivate the functional evaluation of response elements to determine if and how they work together to regulate gene expression.

Whilst it is common, that NRF2 protects cells from carcinogens by upregulating cytoprotective genes, and a substational body of research supports an inverse relationship between VDR activation and malignancy, our study aimed to evaluate collaborative effects of *BIRC5* expression, an anti-apoptotic gene known to promote cancer cell survival (Chen *et al.,* 2016). Chen *et al.,* (2017) previously demonstrated

that *BIRC5* is a Wnt/β-catenin dependent target gene in malignant cell types. This conserved regulatory pathway governs numerous normal cell fate processes. Lee *et al.,* (2015) demonstrated that 1,25D and SFN dosage of Caco-2 cells repressed *Wnt*-pathway-related genes. We used our pre-treatment conditions in LS180 cells to investigate this synergistic effect. Our data showed a decrease in *BIRC5* mRNA expression both SFN and 1,25D treatment alone, although a dose-related response was not observed (Figure 4.12). Furthermore, pre-treatment had little further impact, with the synergistic effects observed by Lee *et al.,* (2005) absent in our study.

The Wnt/β-catenin pathway is down regulated by 1,25D through VDR/β-catenin binding, thus reducing β-catenin binding to T-cell factor (TCF) (Larriba *et al.,* 2013). 1,25D also controls *Wnt* inhibitor, Dickkopf WNT Signalling Pathway Inhibitor 1 (*DKK-1*) and of Transcription Factor 4 (*TCF4*) gene expression (Larriba *et al.,* 2011, Larriba *et al.,* 2013). The effects of 1,25D upon the *CDH1* gene that encodes the E-cadherin protein, which sequesters β-catenin at the plasma membrane adherens junction regulation is already well-characterized in cancer cell lines. Increasing doses of SFN did not affect *CDH1* increase suggesting that NRF2 signaling does not affect *Wnt*/β-catenin pathway (Figure 4.12B and C).

Although the anticipated consequence, that VDR activation enhances NRF2 signaling in detoxification responses was marginal in most cases, much of the fold changes were not statistically significant thus, it was difficult to accept the proposed hypothesis based on these findings alone. VDR alone was more effective in inducing VDR specific genes and NRF2 activators were more effective alone in inducing NRF2-specific genes. The absence of synergism or additive effects of both signaling pathways may be ligand concentration dependent. Overall, in LS180 cells, our findings reveal an indirect interplay, contradictory to the phenotypic stability hypothesis (Berridge, 2015).

To eliminate cell specific limitations of our study, we tested our hypothesis in a prostatic cellular context were OS is one of the several hallmarks of aggressive phenotype due to progression and negative response to therapy (Khandrika *et al.,* (2009). Our initial experiments identified a functional ARE signaling system in

LNCaP cells, which were confirmed by significantly enhanced reporter activity by both SFN (6.5-fold), and 1,25D (2-fold) (See Figure 4.13A).

While 1,25D is able to stimulate NRF2 and g-glutamylcysteine synthetase (gGCSh) for GSH synthesis, our data confirm its ability to significantly enhance ARE signalling, although, similar to LS180 cells indirect mechanisms may be responsible, although not fully elucidated (Yang *et al.*,2005). On the other hand, SFN downregulated acetyl-CoA carboxylase 1 (ACC1), fatty acid synthase (FASN) and carnitine palmitoyltransferase 1A (CPT1A), which facilitates fatty acid uptake by mitochondria for β-oxidation, were also decreased, indication chemoprevention in LNCaP and 22Rv1 PCa cells Singh *et al.*, (2018).

Whilst OS is a hallmark of aggressive PCa phenotype, NRF2/ARE is a promising strategy for cancer prevention, although other findings link it to the survival of cancer cells (Yang *et al.*, 2005). We investigated NRF2 downstream gene expression in LNCaP cells pre-treated with 1,25D exposed to 6μM SFN for another 24 hours (See Figure 4.14). In agreement with Nakai *et al.*, (2010), Chen *et al.*, (2019) and Berridge's (2015) hypothesis, NRF2 was responsive to 1,25D alone. However, priming cells with 1,25D did not further enhance SFN mediated NRF2 expression. It was expected that *GCLC* mRNA expression would be altered by 1,25D pre-treatment, since Jain and Micinski (2013) previously identified that it was induced in U937 monocytes. Contrary to Teixeria *et al.*, (2017) who observed a significant *HMOX1* and *NQO1* induction in 1,25D pre-treatment in human umbilical vein endothelial cells (HUVECs) (4- and 2-fold respectively), there was no effect in our LNCaP cells, in fact, and significant downregulation of *NQO1* was observed. Our findings suggest that, although the two ligands poses chemo-preventative effects, VDR and NRF2 signalling acts independently in mediating antioxidant activity. 1,25D pre-treatment altered NRF2 expression, implying that 1,25D may initiate the activity of NRF2 in inhibition androgen receptor (AR) signalling which is responsible for PCa initiation and progression (Zhou *et al*., 2015; Khurana and Sikka, 2018). *UGT1A1* and *UGT1A4* are highly sensitive to 1,25D in LS180 cells but in LNCaP were not responsive compared to *CYP3A4*, owing to the low basal levels for the former. Our findings imply that NRF2 may be dominant in combating OS through its target genes (Figure

4.15). As shown in Figure 4.15**,** both in LNCaP and LS180 cells, 1,25D and SFN both significantly enhanced growth inhibition, although the effects of SFN was more dramatic. Combination of both ligands did not produce a synergistic effect although inhibition was still significant. These findings suggest that VDR and NRF2 activation may be useful for cancer therapy but 1,25D does not enhance the functional response of NRF2 activity as previously proposed. It is also noteworthy that our experiments using LS180 cells were conducted in minimum essential media (MEM) also supplemented with 10% foetal bovine serum (FBS), whereas our LNCaP cells were treated in a steroid-depleted charcoal stripped FBS (CSS). The functionality of the androgen receptor (AR) in LNCaP cells has a broad steroid binding specificity which may influence gene transcription. Therefore, conducting our experiments in a steroid depleted environment allowed independent analysis without the influence of steroids (Lee *et al.*, 2007). This may have contributed towards variable experimental outcomes between our chosen cell model systems and data reproducibility with the work of others. Furthermore, exogenous VDR and NRF2 protein expression levels were not analysed in this study and should be considered in the future to in order to verify the relevance VDR and NRF2 cross-talk or the absence thereof.

In summary, this study characterized VDR and NRF2 interplay in mediating detoxification pathways, mainly through *UGT1A1* regulation and involvement in enhancing other anti-oxidant and chemo-preventative pathways. Mutagenesis of functional ARE and VDRE motifs responsible for *UGT1A1* induction revealed the dependency of VDR to NRF2 signalling, which was unexpected. The inhibitory trend observed in combinatorial and other gene specific responses provides insight into possible interactions between ligands or indirect molecular mechanisms that also contribute to cellular defence systems. Although in this case our findings do not fully agree with the proposed hypothesis, these findings alone are not enough to elucidate this interplay. Further experiments to streghthen our findings include use of mammalian cell lines that express both a high level of NRF2 and VDR such as KYSE70 human oesophageal squamous cell carcinoma cell line (Kalthoff *et al.*, 2010). NRF2 gene expression levels are neglible in our chosen LS180 cell lines, and also NRF2 protein expression levels were not measured, it is difficult to conclude on absolute NRF2 and VDR interplay. Additionally, we identified inhibitory effects upon

combinatorial treatments and VDR protein expression was suppressed by NRF2 ligands. It is worth employing a competitive binding assay which will identify whether NRF2 agonists bind to VDR protein to cause this effect. The affinity of NRF2 ligands for VDR can be determined by measuring the their ability to compete with radioactivaley labelled VDR agonists for VDR.

4.5 Summary of key findings

- Both VDR (1,25D and 3kLCA) and NRF2 (SFN and *t*BHQ) ligands activate ARE driven activity.
- VDR does not enhance NRF2 mediated signalling other than *UGT1A1* gene and UGT1A protein expression (in both combinatorial or pre-treatment experiments)
- Co-treatment with VDR and NRF2 ligands inhibits ARE signalling.
- VDR signalling is dependent upon an intact ARE.
- SFN inhibits VDR specific genes (*CYP3A4, CYP24A1, UGT1A4* and *VDR*), VDR protein and VDRE/PXRE signalling.
- NRF2 and VDR signalling independently enhance anti-tumoural activities (*BIRC5* suppression and *CDH1* expression).
- 1,25D does not enhance redox/detoxification pathway genes mediated by NRF2 in LNCap cells.
- 1,25D and SFN inhibit LNCap and LS180 growth, but there are no collaborative effects.

5: Chapter 5

Characterization of *UGT1A* loci

5.1 Introduction

As already established, glucuronidation represents a major pathway through which the body detoxifies a range of hydrophobic compounds such as dietary chemicals, drugs, environmental toxins, steroids, bilirubin and bile acids (Kutsuno *et al.,* 2014). Modifications of such structurally diverse chemicals are mediated through the differentially expressed UGT1A isoenzymes (Levesque *et al.,* 2007). The differences in their alternative first exon, in addition to specific tissue expression contributes towards their differential glucuronidation capacity (Rouleau *et al.,* 2013 and Levesque *et al.,* 2007). Additionally, the presence of a TATA-box approximately 30bp upstream of each first exon sequence further indicates individual transcriptional regulation of each *UGT1A* gene (Kiran *et al.,* 2006).

In light of their clinical significance, *UGT1A* gene family members have been well characterized in a hepatic context (Strassburg *et al.,* 1998). Evidence suggests that the 5'-flanking region of each *UGT1A* alternative first exon contains response elements capable of regulating their own expression. (Tan *et al.*, 2006). Earlier work by Gregory *et al.,* (2003) also identified differential *UGT1A8, UGT1A9* and *UGT1A10* promoter activity. The *UGT1A8* and *UGT1A10* contained Sp1/initiator-like sites involved in gene induction. This was absent within the *UGT1A9* promoter region, thus affecting its inducibility. Promoter activity for Rat *UGT1A6* and *UGT1A7* has been demonstrated to mediate their transcription in liver cells (Gregory *et al.,* 2003). Bellemare *et al.,* (2010) further described alternative spliced isoforms (UGT1A_i2s) that utilized an alternative exon 5b. Although devoid of glucuronidation activity, detail for their clinical relevance and regulatory mechanisms are still rudimentary. Altogether, these findings further suggests complex differential regulation of each *UGT1A* isoform.

On-going research in our laboratory and others have examined the gtPBREM cluster within *UGT1A1* 290bp distal enhancer sequence (-3483/-3194) containing binding sites for a number of ligand activated transcription factors (TFs), that we demonstrate to include VDR (Sugatani *et al.,* 2005). From our data, within the *UGT1A7-UGT1A10* cluster, *UGT1A7* was the only isoform induced by activated VDR. This finding is contrary to Wang *et al.,* (2016) who identified that *UGT1A8* and *UGT1A10* also to be

enhanced by activated VDR in LS180 cells. Additionally, our data show that *UGT1A4* was the most sensitively induced isoform compared to *UGT1A3*, despite low expression in LS180 cells (Figure 3.1). Surprisingly, *UGT1A3* and *UGT1A4* share 95% sequence similarities and for *UGT1A7-UGT1A10* cluster, a 90% shared sequence similarity was observed (Oda *et al.,* 2017). What has not been well characterized is fine detail for how transcriptional expression of the different members of the *UGT1A* family are modulated through vitamin D/VDR.

VDR mediates its activity through recognition of specific DNA sequences within the promoter region of its target genes (Pike *et al.,* 2017). The DNA sequences, known as VDRE (See Section 1.4.2) are commonly composed of two hexameric core binding nucleotide half-sites 5′-AGGTCA-3′ separated by three nucleotides (DR3-type) (Peng *et al.,* 2004 and Carlberg and Campbell, 2013). Upon VDR/RXR heterodimer formation, the RXR binds to the 5' side of the VDRE DBD while the VDR binds to the 3' side of the VDRE DBD (Stees *et al.,* 2012). This binding leads to the recruitment of co-regulatory proteins that facilitate gene transcription (See Section 1.4.2) (Campbell, 2015). There are other less common VDREs such as the ER6-type motif that are characterized by everted repeats of the nucleotide half-sites separated by six nucleotides. Nonetheless, characterization of VDR target genes has been possible through the identification of functional VDREs (Nurminen *et al.,* 2019; Thompson *et al.,* 2002 and Pike *et al.,* 2016).

Efforts by Kim *et al.,* (2006), using DNA micro-array across the entire *Rankl* gene locus identified this gene involves up to five distal VDRE enhancers, one containing a specific element capable of direct transactivation. For *LRP5*, potent VDRE enhancers were located 30kb downstream of an intronic region (Zella *et al.,* (2006). As already mentioned, VDR binding to these enhancers increases hitstone acetylation and recruitment of RNA polymerase II, thus these enhancers facilitate direct gene transcriptional control, through chromatin-looping (Zella *et al.,* 2010).

More specific to our study are findings by Meyer *et al.,* (2012) who conducted a genome-wide study using LS180 cells, which identified 1674 VDR/RXR binding sites. The binding of VDR/RXR was enhanced depended upon 1,25D exposure in

established target genes such as *CYP24A1, TRPV6* and *CYP3A4* (Meyer *et al.*, 2012). Upon further *in silico* analysis, Meyer *et al.*, (2012) identified that the predominant VDR/RXR binding motif is the DR3-type motif. Interestingly, these binding sites overlapped with those of genes involved in cell proliferation (e.g. *c-FOS, c-MYC and SOX9*), giving sight to the role of vitamin D in cellular health in an intestinal context (Prevostel *et al.*, 2016; Ohri *et al.*, 2002).

While Meyer *et al.*, (2012) (Pike laboratory) did not show *UGT1A* binding sites from their genome wide data, upon our request; they kindly examined VDR/RXR binding sites within the *UGT1A* locus. LS180 ChIP-seq profile obtained from the Pike laboratory based on their LS180 data set revealed a number of elements within the *UGT1A* gene locus that bind to VDR/RXR in a 1,25D dependant manner, evidently with a potential major cis-regulatory module noted up-stream to *UGT1A1*. However, their involvement with respect to regulation of the different *UGT1A* family members is not clear, although it all suggests a complex mode of regulation. Thus, a significant remaining challenge in this study is to connect the identified binding sites and determine their individual contributions to regulation of the different *UGT1A* genes.

Additionally, to examine the VDR binding elements in their native cellular context, we explored the utility of a Clustered Regularly Interspaced Short Palindromic Repeats interference (CRISPRi) based approach. CRISPRi involves the use of an endonucleotic activity-deficient dead-Cas9 (dCas9) that contains two point mutations within the RuvC-like (D10A) and HNH nuclease (H840A) domains (Riberio *et al.*, 2018). DCas9 will not cleave but rather block the targeted DNA sequence after fusing with single guide RNA (sgRNA), which consists of crispr RNA (crRNA), a 20 nucleotide sequence complementary to the target DNA, in this case VDRE, and a tracr RNA which binds dCas9 (Riberio *et al.*, 2018) (See Figure 5.1). This approach does not alter the DNA sequence while functionally interrogating the regulatory region *in situ* (Carleton *et al.*, 2017). Theoretically, multiple VDR binding sites become simultaneously targeted. If the targeted DNA represents a regulatory motif important to *UGT1A4* response to vitamin D, CRISPRi will repress its transcription.

Our chosen approach intended to expand upon our knowledge of the regulation of *UGT1A4*, since it was the most sensitively induced by VDR ligands and previous studies suggest that this isoform may be involved in the autoregulation of vitamin D (Wang et al., 2014). We were interested in the identification and characterization of functional binding motifs within the identified *UGT1A* CRM that contributed to this induction in a 1,25D-dependant manner.

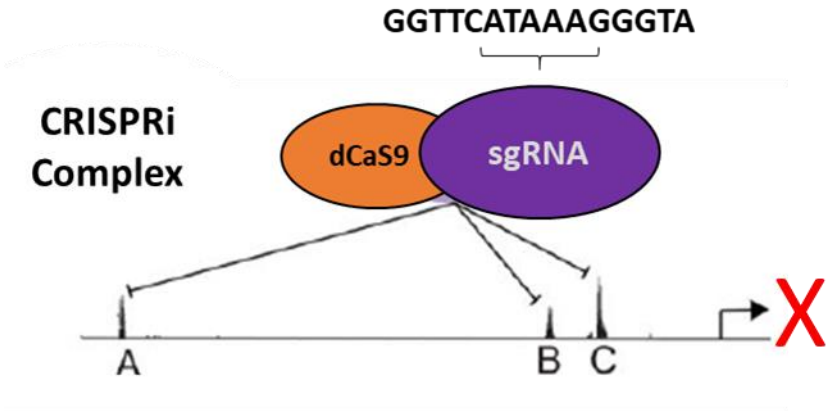

Figure 5.1: ***<u>CRISPRi –based approach model.</u>*** *The simplified CRISPRi model depicted here describes the fusion of the nuclease defiant form of Cas9 (dCas9) to the DNA targeting sgRNA (VDRE ; peak A, B and C). Co-expression of dCas9 and sgRNA efficiently disrupts gene transcription by blocking VDR/RXR binding on the VDRE. The blockage is determined by sgRNA which is juxtaposed to the VDRE, while the dCas9, in its catalytically inactive form blocks this binding site.*

5.2 Results

5.2.1 The *UGT1A* locus is regulated by novel VDR/RXR binding

We used the Regulatory Sequence Analysis Tool (RSAT) bioinformatics tool to scan potential VDREs within the target *UGT1A* fragment and identified 10 putative hexameric half-site VDRE sequences, as depicted in Figure 5.2. This further confirmed our speculation that multiple VDREs may act as distal enhancers for a number of isoforms, particularly *UGT1A4* that is the most responsive to vitamin D/VDR (Figure 5.2)

Consensus VDRE sequence

Putative VDREs within the UGT1A4 promoter region

PatID	Strand	Pattern	SeqID	Start	End	matching_seq	Score
START_END	DR	-	tmp_sequence_2017-06-14.130620_NfumDH.raw	-4001	-1	-	0.00
[AG]GGTCA	D	[AG]GGTCA	tmp_sequence_2017-06-14.130620_NfumDH.raw	-2025	-2020	actcAGGTCAggct	1.00
[AG]GGTCA	D	[AG]GGTCA	tmp_sequence_2017-06-14.130620_NfumDH.raw	-203	-198	cacaGGGTCAgatg	1.00
[AG]GGTCA	R	[AG]GGTCA	tmp_sequence_2017-06-14.130620_NfumDH.raw	-1977	-1972	agtgAGGTCAcccc	1.00
[AG]GTTCA	D	[AG]GTTCA	tmp_sequence_2017-06-14.130620_NfumDH.raw	-3822	-3817	cccaGGTTCAactg	1.00
[AG]GTTCA	R	[AG]GTTCA	tmp_sequence_2017-06-14.130620_NfumDH.raw	-744	-739	ggtgGGTTCAggga	1.00
[AG]GTTCA	R	[AG]GTTCA	tmp_sequence_2017-06-14.130620_NfumDH.raw	-233	-228	tccaAGTTCAagct	1.00
[AG]GGG[TC]A	D	[AG]GGG[TC]A	tmp_sequence_2017-06-14.130620_NfumDH.raw	-357	-352	gactAGGGCAatgg	1.00
[AG]GGG[TC]A	D	[AG]GGG[TC]A	tmp_sequence_2017-06-14.130620_NfumDH.raw	-102	-97	gaggAGGGCActtt	1.00
[AG]GGG[TC]A	R	[AG]GGG[TC]A	tmp_sequence_2017-06-14.130620_NfumDH.raw	-2144	-2139	ccttAGGGTAcaaa	1.00
[AG]GGG[TC]A	R	[AG]GGG[TC]A	tmp_sequence_2017-06-14.130620_NfumDH.raw	-2124	-2119	tcttGGGGTAaaca	1.00
[AG]GGG[TC]A	R	[AG]GGG[TC]A	tmp_sequence_2017-06-14.130620_NfumDH.raw	-1413	-1408	agagAGGGCAggtc	1.00
[AG]GGG[TC]A	R	[AG]GGG[TC]A	tmp_sequence_2017-06-14.130620_NfumDH.raw	-997	-992	tgtgGGGGCActac	1.00

Figure 5.2*: RSAT output of putative VDREs within UGT1A4 promoter region*

As previously stated, LS180 cells are an ideal model for examining transcriptional mechanisms pertaining to 1,25D/VDR signalling (Meyer *et al.*, 2012). In the previous chapters, we have described the induction of several *UGT1A* genes by 1,25D. As shown below, our *in-silico* analysis reveals that the potential functional VDRE for *UGT1A1* assessed through reporter assays as detailed in chapter 3 is within 'peak 1', as depicted below (Figure 5.3). Meyer *et al.,* (2012) also quantified the number of DNA binding sites for VDR and its heterodimer partner RXR across the LS180 genome using ChIP-seq analysis. The Pike laboratory shared with us data 'tracks' obtained for the *UGT1A* locus. As shown in Figure 5.3a, a total of 5 binding sites were identified across the *UGT1A1* and *UGT1A3* genomic regionsOur study aimed to

characterize the relevance of the additional peaks noted within the *UGT1A* loci, with particular attention to the regulation of *UGT1A4*, through cloning a 1532bp fragment which includes the ‘peak 4’ binding site (See Figure 5.3a.)

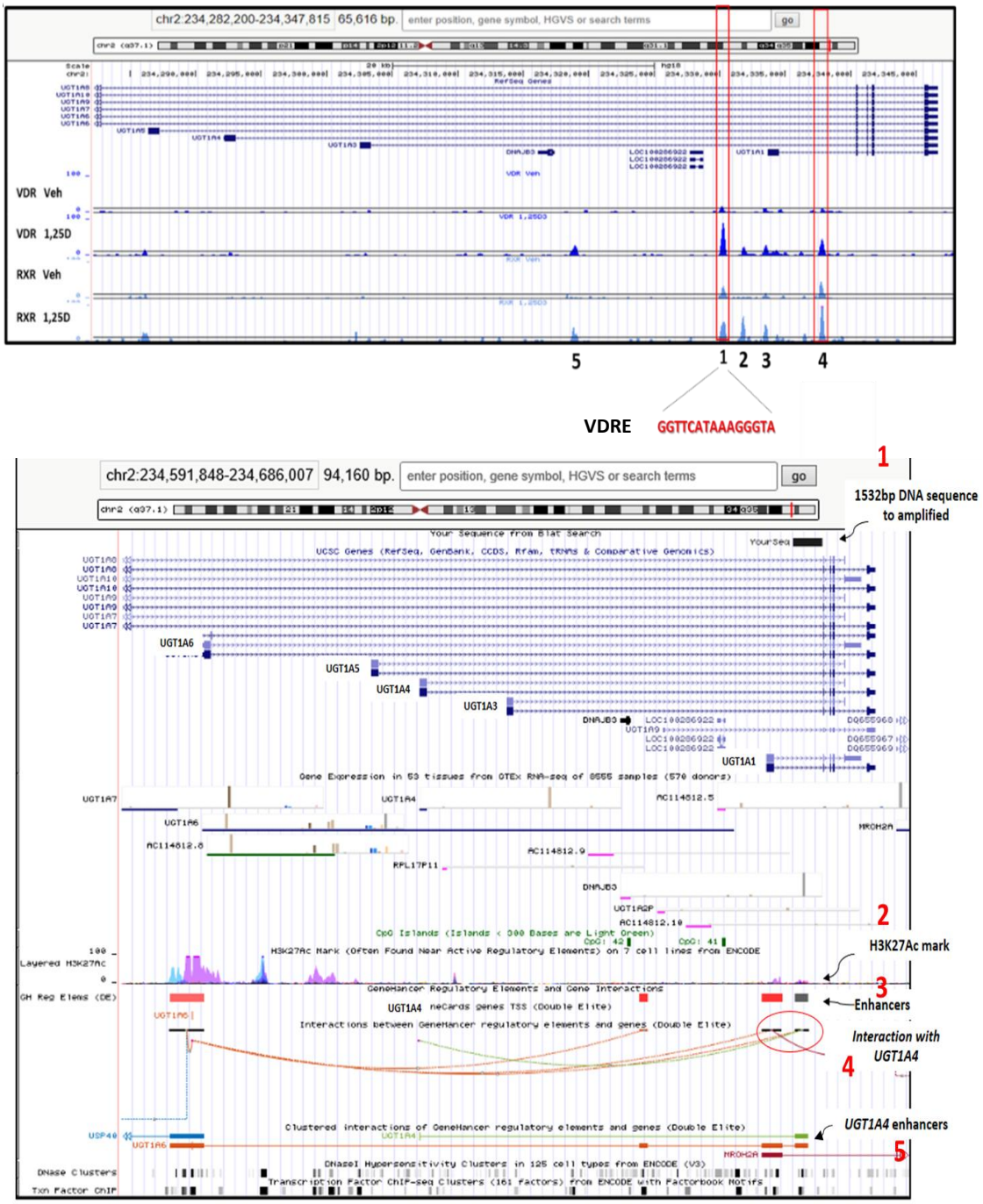

Figure 5.3: UGT1A loci is regulated by VDR/RXR binding motifs. ***A*** *represents ChiP-seq data kindly provided by Pike's laboratory. The data shows a number of 1,25D-dependant VDR/RXR binding elements within the UGT1A locus (labelled 1-5) with a potential major cis-regulatory module observed upstream to UGT1A1 gene.* ***B*** *represents an output from the Santa Cruz human genome browser database that corresponds to the UGT1A locus. We aimed to investigate the involvement of peak '4' in UGT1A4 regulation.* ***1*** *represents the our target DNA sequence that overlaps peak*

'4' which was used for cloning and characterization of this regulation. ***2*** *represents the occupancy of histone 3 lysine 27 acetylation (H3k27Ac) marks that signify active promoters and distal enhancers.* ***3*** *shows enhancers that also overlap the H3k27Ac mark.* ***4*** *and* ***5*** *show evidence of regulatory elements/enhancers from the GeneHancer database that specifically interact with UGT1A4. This data overlaps our target DNA sequence, providing evidence for potential binding sites involved in the significant UGT1A4 increase in expression by 1,25D*

UGT1A primers were designed using Primer3 Software, to amplify this region and (See Table 2.9) devoid of restriction enzyme overhangs. The LS180 genomic DNA was amplified with *Taq* DNA polymerase, which generated 3'-dA overhangs. The amplified PCR product was purified then was subjected to the DNA blunting enzyme prior to ligation with the vector. The blunt ends generated were universally compatible with the donor vector (pJET1.2/blunt vector) used in this study (Dallmeier and Neyts, 2013). The 5' ends of the pJET1.2/blunt vector contain phosphoryl groups; therefore, phosphorylation of PCR primers was not required. We sought to ligate the PCR product to the vector to generate a UGT1A_pJET vector (See Figure 5.4).

We attempted ligation reactions based upon 3:1, 3:3 and 1:1 molar ratios of purified DNA fragment and pJET1.2/blunt vector, respectively however, upon verification using a control PCR product efficient blunting and/or ligation was not achieved. The transformation of the ligation mixtures using Library Efficiency® DH5α *E.coli* did not produce recombinant clones.

If successful, the presence and orientation of isolated recombinant clones would have been analysed through DNA sequencing (See Section 2.9) using pJET1.2/blunt specific primers and validated using the NCBI blast tool. Successful recombinant clones would have led to the construction of a luciferase gene-reporter assay vector through further sub-cloning as detailed below (See Figure 5.4).

Briefly, our planned scheme was to involve ligation of the DNA insert to the pJET blunt vector. Restriction enzyme digestion is performed to excise the DNA insert from the recombinant pJET vector. The insert is purified using gel isolation then amplified

using PCR to increase the number of copies of the DNA fragment. Restriction enzyme digestion is performed on both the insert and recipient pGL3-Basic vector, creating a set of complementary restriction sites for cloning. Following gel purification of the digested pGL3-Basic vector, the insert and the recipient vector are ligated using the desired molar ratio. Confirmation of successful ligation and orientation is performed by PCR amplification using specific primers (e.g. *UGT1A* primers in this case: Table 2.9). The observation of the expected DNA insert product size after colony screening would confirm the presence of the insert and verifies orientation in the recipient plasmid (See Figure 5.4).

Since the Pike laboratory's ChiP-seq data identified VDR/RXR bindings sites driven by 1,25D, our successful cloning would have led to characterization of VDR induction on the *UGT1A* DNA fragment in *in vitro* experiments. Furthermore, the identification and characterization of functional VDREs and verification through mutagenesis may support the involvement of multiple binding sites in the expression of *UGT1A4*, mediated by VDR agonists. Based on the Pike Laboratory ChIP-seq data and evidence of *UGT1A4* distal interaction (See Figure 5.3), it is reasonable to assume that multiple regulatory sites potentially regulate a single gene. However, to evaluate the relationship between these binding sites, use of CRISPRi, in combination with reporter gene experiments based on the UGT1A_pGL3-Basic Vector could potentially shed light upon the involved mechanisms this complexity that underpin the sensitive responsiveness of *UGT1A4* to 1,25D. Co-transfection of cells with our library of expression constructs encoding NRs (VDR, PXR, FXR or LXR) will directly examine whether this region is exclusively VDR-driven. Additionally, since our data suggest that the 1532bp *UGT1A* fragment predominantly overlaps *UGT1A4* interaction, a comparison with responses obtained for the UGT1A1_2K or 290-promoter vector (Figure 3.4) may highlight differences in the regulated expression of these genes through VDR ligands. Whether such VDR-mediated expression of *UGT1A4* is cell specific could be evaluated in other cellular contexts. Apart from the liver, *UGT1A4*, is predominantly expressed in the gastro-intestinal tract (Benoit-Biancomano *et al.*, 2018). Co-transfection of the UGT1A-pGL3_Basic vector in other intestinal cell line models such as CaCo-2 and HCT-116 would distinguish this specificity. Since

UGT1A4 expression is also abundant in the kidneys, the use of kidney derived cell lines could be analysed to better understand this regulation (Jiang *et al.*, 2015).

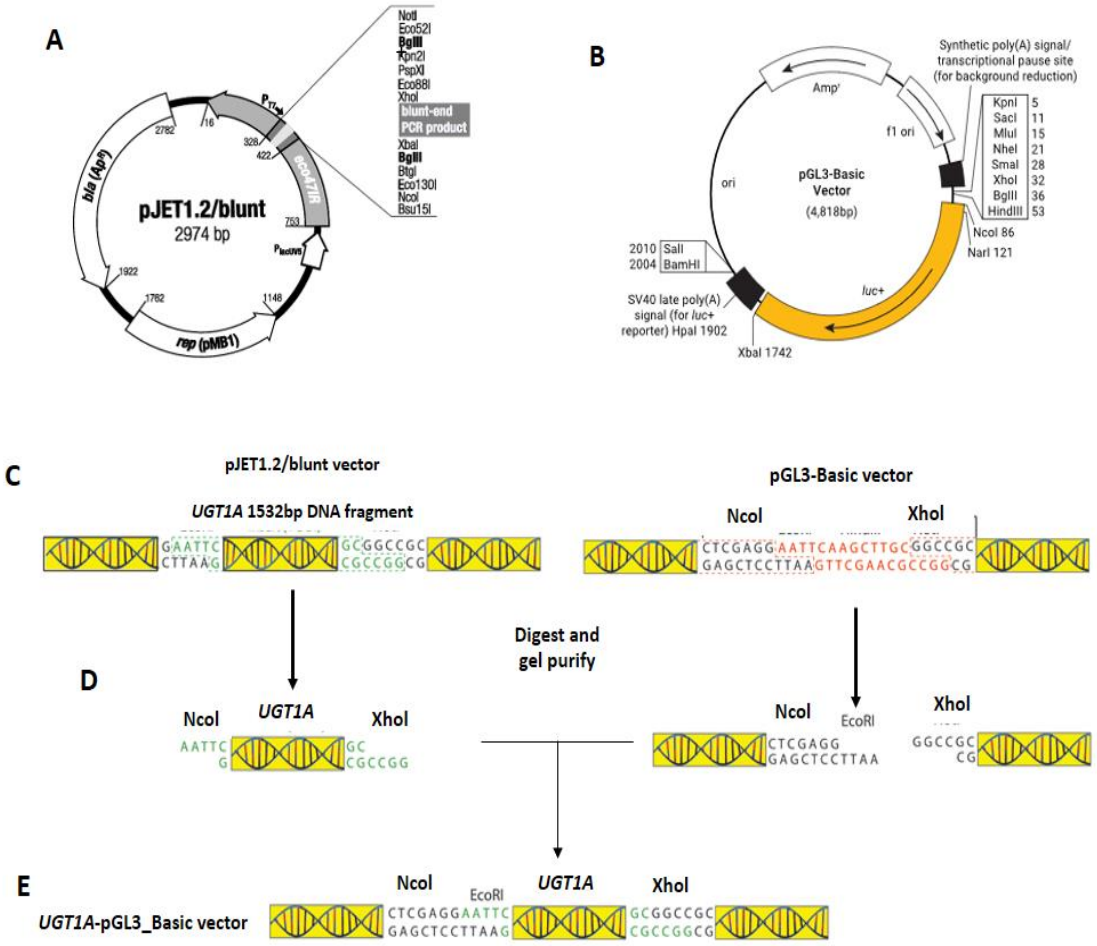

Figure 5.4: UGT1A plasmid construction by sub-cloning ***(A)*** *shows the pJET1.2/blunt cloning vector which acts as a donor plasmid. It comprises of an eco47IR lethal restriction enzyme, which is disrupted by ligation of DNA fragment to the cloning site.* ***(B)*** *The recipient plasmid, pGL3-Basic vector includes coding region for firefly luciferase for measurement of luciferase activity in transfected cells. The Basic vector also includes restriction enzyme sites to clone the promoter of interest. Sub-cloning steps include (**C**) Digestion of DNA into the pJET1.2/blunt cloning vector, (**D**) Isolating the UGT1A insert and vector by gel purification and (**E**) Ligation of the UGT1A insert to the recipient vector (pGL3-Basic vector**).**

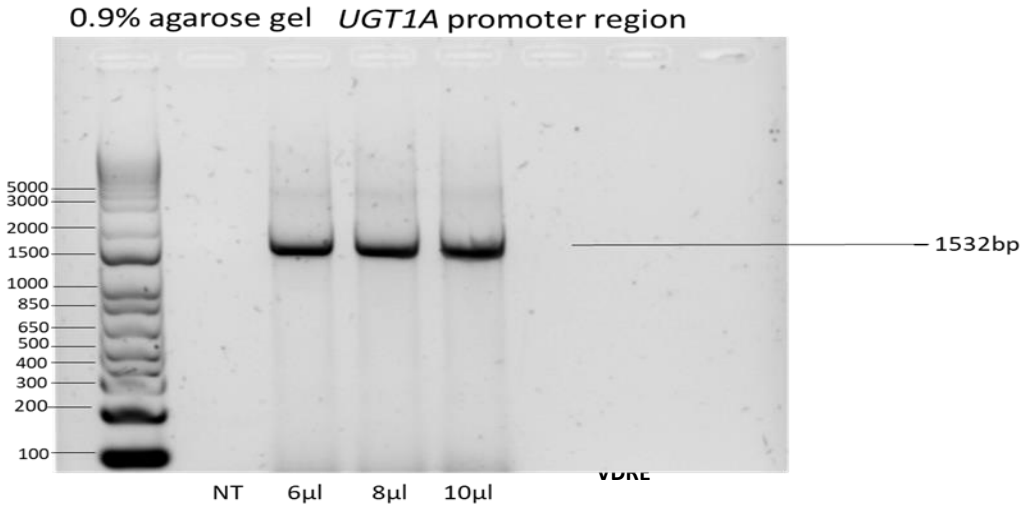

Figure 5.5: RT-PCR product of amplified of the 1532bp DNA fragment of the UGT1A locus.

Multiple ligation conditions were attempted, however limited to time in the scope of this study, we were only successful in amplifying the 1532bp DNA fragment as shown in Figure 5.5. In the future, it is worth considering the addition of a 5'-phosphorylated termini. This was absent in the PCR primers designed. It is suggested that the addition of 5'phosphate groups promotes successful ligation. The designed UGT1A PCR primers amplified DNA fragments that lack overhangs, and although Q5 high fidelity DNA polymerase with proofreading acitivity was used for DNA amplification, this may have caused lower ligation efficiencies upon insertion to the pJet1.2/ blunt vector. In the future, the incubation of DNA fragment with Taq DNA polymerase and dATP (3'dA tailing) for 30 minutes 72°C followed by purification will improve ligation efficiency (Thermo Fischer Scientific, 2020).

5.2.2 Characterization of the UGT1A gene using CRISPRi

With the intention to characterize *UGT1A4* regulation by VDR-1,25D, we incorporated CRISPRi-based technique, which enables the simultaneous deactivation of multiple elements that may serve as functional VDRE-based *UGT1A4* enhancers (See Figure 5.1) (Carleton *et al.*, 2017). SgRNA guides that target the classic functional DR3-type motif (GGTTCATAAAGGGTA; sgRNA guide 1) were designed. Our findings show that this VDRE is directly involved in *UGT1A1* promoter

activity in response to VDR ligands (Figure 3.5). We questioned whether the same motif is involved in *UGT1A4* regulation. Additionally, a sgRNA guide (AAAGGGTA; guide 2) targeting the 3' hexameric half-site was used in this study. This enabled us to examine the effects of inhibiting only binding of the VDR component of the heterodimeric complex and how that would affect overall gene transcription. Lastly, a non-targeting sgRNA with a sequence not found in our region of interest (1532bp DNA fragment) was included as a negative control. We designed sgRNA guides using the using CRISPR.MIT.EDU software by Zhang lab (2019). sgRNA guides scoring <70 'on target' in addition to a 'low off-target' score were screened, from which suitable guides that were followed by a PAM sequence (NGG) targeted by dCas9, were selected. A high 'off-target' score indicates that the sgRNA could potentially target sequences outside of our gene of interest (*UGT1A1*) and therefore not suitable for this experiment.

The CRISPRi technique simultaneously targets multiple VDREs of similar sequence without altering genomic sequences, allowing critical examination of the extent to which the entire VDRE (or its half-site) is involved in *UGT1A4* induction.
For our luciferase-based activity assay, LS180 cells were co-transfected with the RNP complex (sgRNA/dCas9) and the UGT1A1-290 promoter vector (U290) (See Figure 5.7). The U290 promoter vector (previously mention in Chapter 3) contains the targeted DR3-type motif VDRE. Transfected cells were either exposed to 1,25D (10^{-8}M) or vehicle (EtOH) for 24 hours prior to obtaining luciferase activity.

The gene reporter activity within LS180 cells that expressed the sgRNA guides 1 and 2, was significantly altered by 70% and 40% respectively relative to LS180 cells transfected with the non-targeting sgRNA (guide 3). The non-targeting sgRNA was associated with UGT1A1 promoter activity that was enhanced by 5-fold following 1,25D treatment. This data shows that *UGT1A1* induction achieved through 1,25D treatment is dependent upon an intact VDRE (See Figure 5.7).

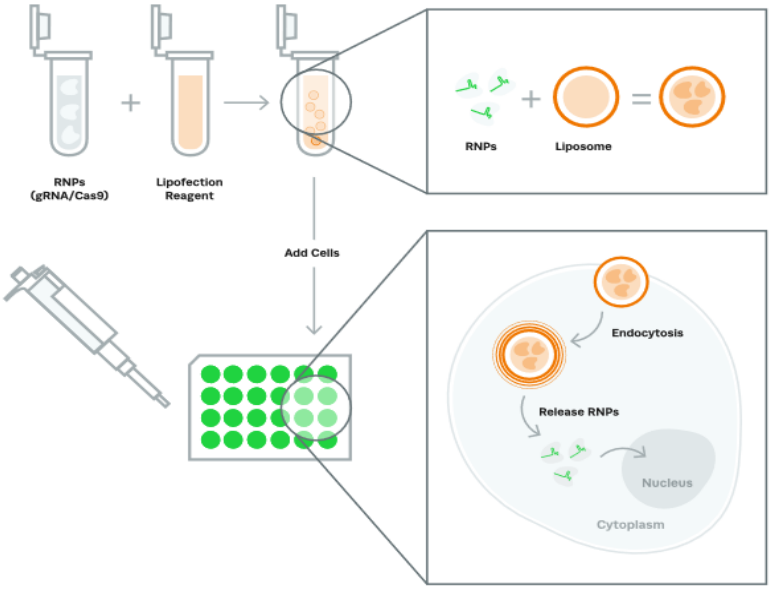

Figure 5.6: Lipofection procedure for CRISPRi technique. *A ribonucleoprotein (RNP) complex combining sgRNA and dCas9 is formed, and then mixed with lipofectamine reagent to form liposomes. Upon delivery to the LS180 cells, the RNPs diffuse through the cytoplasm to the cell's nucleus, where the sgRNA guide the RNP to the complementary DNA sequence to which dCas9 binds.*

To assess the effects of this approach upon the expression of the corresponding VDR responsive endogenous genes, LS180 cells were transfected with the RNP CRISPRi complex, then exposed to 1,25D (10^{-8}M) or EtOH and subsequently analysed through RNA extraction and real-time Q-PCR. We chose to examine *UGT1A1* gene expression, as the targeted VDRE is directly involved in its regulation (See Chapter 3). More importantly, we sought to investigate whether the CRISPRi interrogated VDRE identified within the *UGT1A1* promoter region is responsible for distal regulation of *UGT1A4*. Lastly, *CYP3A4* gene expression was also examined as a well-known VDR responsive gene.

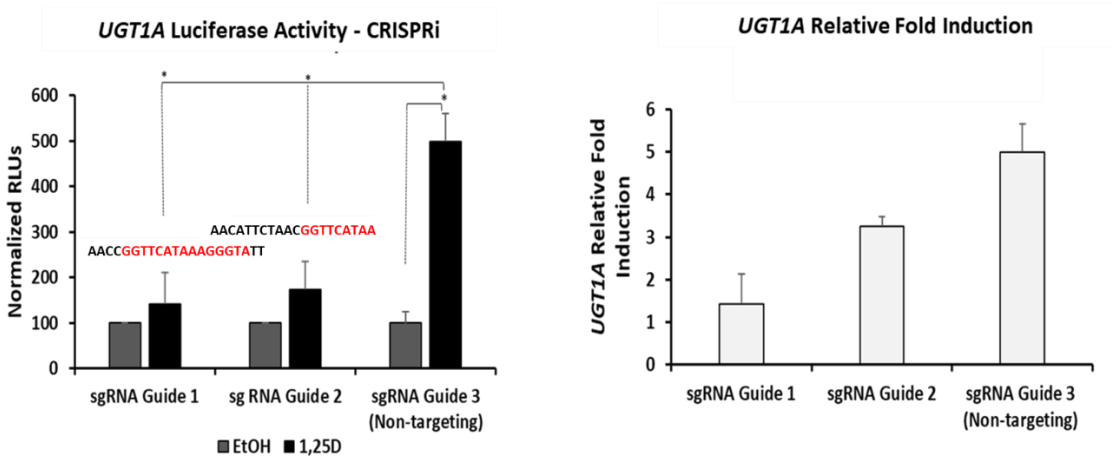

Figure 5.7: Deactivation of the VDRE using CRISPRi. *LS180 cells were transfected with dCas9/sgRNA complex, then subsequently treated with 1,25D (10^{-8}M) or vehicle control for 24 hours. UGT1A1 promoter luciferase activity was obtained using Dual-Glo Luciferase Assay (Promega, UK). Data represents 1 independent experiments were n=3. %RLU are relative to vehicle control. Statistical analysis was obtained from Student's two-tailed t.test where is *P<0.05, **P<0.005, ***P<0.0005, ****P<0.0001.*

The response of *CYP3A4* to 1,25D treatment was not significantly impacted, irrespective of the targeting or non-targeting sgRNA applied (160- and 180-fold increase respectively) (See Figure 5.8). *UGT1A1* was also significantly responsive to 1,25D, both in CRISPRi deactivated VDRE and the non-targeting guide by 3-fold and 4 fold respectively.. Similarly, *UGT1A4* whose regulation is suspected to involve multiple VDREs, a 19% reduction in expression in CRISPRi interrogated VDRE was noted relative to the non-targeting sgRNA.

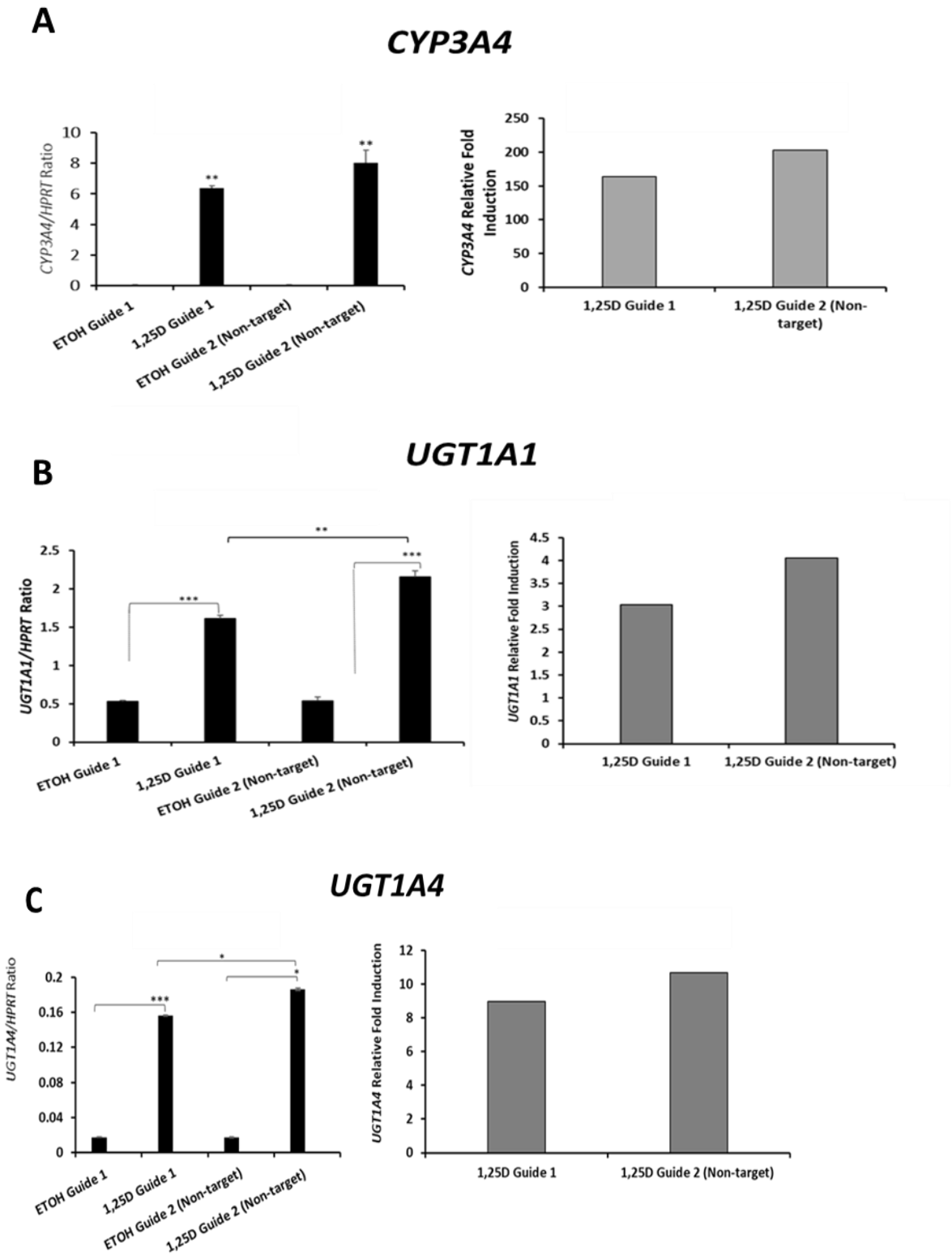

Figure 5.8: CRISPRi and gene expression analysis in LS180 cells. *For gene expression analysis, cells, RNA was extracted in LS180 cells transfected with dCas9/sgRNA complex and subsequently treated with treated with 1,25D (10^{-8}M) or vehicle control for 24 hours, followed by Real Time Q-PCR. ΔCT was calculated with*

*HPRT as a house-keeping gene. Fold induction represented are relative to each vehicle control. Statistical analysis was obtained from Student's two-tailed t.test were *P<0.05, **P<0.01 and ***P<0.001.*

5.3 Discussion

Among the examined nuclear receptors (NRs), we find VDR to be the most potent modulator of *UGT1A* expression. Although the regulatory mechanisms are not well established, Chip-Seq data obtained from the Pike laboratory indicate multiple VDR/RXR binding sites, the relevance of which remain to be fully characterized. In this study, we aimed to examine these binding sites as isolated enhancer fragments through; a) cloning of the *UGT1A* locus and b) its manipulation in its native context using the CRISPRi-based approach. This data aimed to reveal the complexity in control of *UGT1A* expression by extrahepatic VDR. In an attempt to analyse the regulatory elements through which VDR modulates *UGT1A4* expression, we amplified a 1532bp DNA fragment that contains one of the regulatory enhancers (peak 4) for VDR and its heterodimer partner RXR (See Figure 5.4).

Of the 1532bp fragment of the *UGT1A* regulatory sequence, *in silico* analysis revealed putative VDREs, which we thought may be contributory to *UGT1A* regulation (Figure 5.2). Additionally *UGT1A4* enhancer elements also correlated well within this region (See Figure 5.3B). The targeted region was successfully amplified (Figure 5.5); however, our attempts to ligate and clone the amplified PCR product to the pJET1.2/blunt were unsuccessful; therefore it was not possible to proceed with this type of analysis. The cloned *UGT1A* locus would have served as a template for manipulating the enhancer modules within cell based reporter assay analysis. Application of mutagenesis on putative VDREs, thereby measuring transactivity would have expanded our knowledge of collaborative actions of binding sites in *UGT1A* regulation. Our question for the robust *UGT1A4* induction remain unanswered, although, our findings and the GeneHancer database does speculate that multiple binding sites are involved. Important detail from these findings demonstrates a unique and complex mechanism that involves an element located within the *UGT1A1* promoter could possibly modulate the expression of a distant gene (*UGT1A4*).

These correlative findings motivated the functional evaluation for how potential VDRE motifs in their native context, may function in combination to determine overall *UGT1A* gene regulation. CRISPRi enables simultaneous interruption of distal regulatory regions (Carleton *et al.*, 2017). This method incorporates blocking the

already identified functional DR3-type VDRE across the *UGT1A* locus (Figure 5.2). We found that CRISPRi reporter based activity was significantly specific in targeting, when assessed through plasmid-based reporter analysis, but had little effect on the endogenous gene when assessed through Q-PCR. Our data suggests that transfection efficiency was relatively low to achieve any effects on an endogenous gene. In reporter-based assays, the read-out was specifically from successfully transfected cells that presumably contain reporter and the RNP complexes, whereas endogenous gene expression levels were obtained from all viable cells regardless of transfection. Our data may also point to the fact that other VDREs are involved and contribute towards gene expression. With multiple elements within the *UGT1A* locus as evidenced from Pike's laboratory, this explanation may be plausible. Fusion of the RNP complex with Krüppel-associated box (KRAB) domain could in the future successfully repressed gene expression more efficiently that dCas9 alone. KRAB facilitates in the recruitment of co-repressor complexes as if often implemented in CRISPRi technques for gene repression (Ying *et al.,* 2015).

The less dramatic differences between non-targeting versus targeting sgRNA in gene expression make it difficult to draw a conclusion. Although CRISPRi is very informative, in that, there are no DNA alterations, allowing for examination in native context, this approach requires extensive optimization in LS180 cells. The cost and time constraint, considering the scope of the study limited us from pursuing this approach further. This system does show potential for characterizing 1,25D regulated *UGT1A* expression. However, there are other regulatory factors involved in this gene expression beyond VDR/RXR binding. CRISPRi can be used to effectively screen putative VDREs and interrogate their functions in *UGT1A* induction without abrogating gene functions.

What is worth reinforcing from our limited data is that *UGT1A* luciferase activity was not abolished by CRISPRi, although the reduction was significant. Our findings reinforce that other elements that do not conform to classical VDRE arrangements may also be involved in this regulation. Interrogating multiple other putative VDREs within the *UGT1A* locus in combination, will enable full dissection of functional relationships between the binding sites. Implementing site-directed mutagenesis on

putative VDREs within the *UGT1A* locus followed by measurement of *UGT1A* luciferase activity or endogenous gene expression will characterize these binding sites as functional VDREs, if indeed there is diminished promoter activity/gene expression.

The simultaneous deactivation of multiple VDREs within the entire UGT1A locus and evaluating the gene expression will define which binding motifs contribute towards the direct increase in *UGT1A* gene expression. Furthermore, a question as to whether multiple VDREs are involved in UGT1A gene regulation and also whether multiple binding sites contribute towards synergistic or additive effects will be answered by designing and co-transfecting multiple sgRNAs at a time, followed by q-PCR analysis of the *UGT1A* gene family members. This, together with implementing co-repressors KRAB and SID in the CRISPRi approach will further strenghthen the findings of this study. While the physical mechanisms underlying the observed genetic interactions between VDREs remain unclear, our data suggest functional VDREs are directly involved in *UGT1A* regulation and this pathway may be utilized implemented in clinical cases were *UGT1A* is compromised.

Finally, as already mentioned, to successfully clone the targeted 1532bp DNA fragment, which overlaps one of the 1,25D dependent binding sites identified by Pike's laboratory, the addition of 5'phosphate groups to the designed PCR primers should promote successful ligation. Additionally, adjusting PCR conditions such as incubation of DNA fragments with Taq DNA polymerase and 3'dA tailing will improve ligation efficacy (Thermo Fischer Scientific, 2020).

5.4 Summary of key findings

- Multiple 1,25D dependent VDR/RXR binding sites identified within the *UGT1A* locus.
- *UGT1A* locus is rich in transcriptional activity and distal enhancers
- *UGT1A4* distal enhancers and interaction sites are potentially responsible for robust response to VDR activity
- CRISPRi deactivated VDRE significantly diminished *UGT1A1* promoter activity but not endogenous gene expression.

6: Chapter 6

General Discussion

The established and classical endocrine effects of 1,25D govern bone mineral health (Ryan *et al.*, 2013). However, over the past twenty years, a host of population and laboratory-based data have highlighted relatively uncharacterized but potential important activities with respect to xenobiotic detoxification, neutralization of oxidative stress (OS) immuno-regulatory and cardiovascular control. (Wang *et al.*, 2012; Berridge, 2016; Grishkan *et al.*, 2013; Wang *et al.*, 2020). Additionally, the Cancer Genome Atlas (TCGA) datasets also insinuate the impact of vitamin D receptor (VDR) in cancer prevention (Narvaez *et al.*, 2014). The modulation of many of the genes regulated by 1,25D/VDR have been assessed, however, the potential molecular pathways modulated in this manner have been attempted but not fully understood (Carlberg *et al.*, 2017).

Previously, our laboratory and others have identified VDR activation to enhance the expression of a number of phase I metabolic enzymes, principally members of the CYP3A family (Thompson *et al.*, 2002, Maguire *et al.*, 2012 and Doherty *et al.*, 2014). Maguire *et al.*, (2012) found that VDR can direct these phase I metabolic enzymes in a prostatic context, to limit the bioavailability of growth promoting androgens within the tumour environment. This further confirmed the direct involvement of DR3 and ER6 motifs found 10kb upstream of the *CYP3A4* promoter region (Thompson *et al.*, 2002). Additionally, Matsubara *et al.*, (2008) identified an enhanced expression of rat intestinal *Cyp3a1* and *Cyp3a2* mRNA following VDR activation. Roizin *et al.*, (2018) later observed an increase in *Cyp3a11* intestinal mRNA expression in mice by both VDR and PXR ligands. Phase I metabolites require further metabolism to allow easy excretion from the body. Hence, the phase II metabolic enzymes facilitate in conjugation reactions catalysed by a large group of transferases including Uridine 5'-diphosphoglucuronosyltransferase 1A (*UGT1A*), *UGT2* sulfotransferases (SULTs) and glutathione-S-transferases (GST) (Hirschmann *et al.*, 2014; Wang *et al.*, 2014; Agusa *et al.*, 2010). Upon conjugation of the polar functional groups of the susceptible substances, hydrophilic metabolites are produced that can undergo bilary or urinary excretion (Iyanagi, 2007).

This study critically examines the capacity of activated VDR to regulate expression of the *UGT1A* family of genes, in LS180 cells. *UGT1A1, UGT1A3, UGT1A4, UGT1A5* and *UGT1A7* were significantly affected by VDR ligands (1,25D, 3kLCA and more potently by EB1089), *UGT1A4* exhibiting the highest fold increased expression in response to VDR activation. Since *UGT1A4* is responsible for the homeostatic control of endogenous androstanediol, progesterone as well as exogenous drugs including Lamotrigine (anti-epileptic drug), functionally, our findings highlight a key role for VDR in maintaining homeostatic control of these hormones and facilitating in drug metabolism (Finel *et al.,* 2015 and Franklin *et al.,* 2007).

Considering our study was predominantly in LS180 colon cells and *UGT1A4* is abundant in the gastro-intestinal tract, it is reasonable to assume our may have some relevance in a physiological context. However, functional experiments to determine whether VDR, through its ability to modulate *UGT1A* expression, does result in glucuronidation will need investigated further. Human *ex-vivo* experiments on normal GI biopsies will determine the clinical relevance of our findings. So far we know that Wang *et al.,* (2016) showed that 1,25D (10^{-8}M) facilitated the *UGT1A8* and *UGT1A10* mediated glucuronidation of myophenolic acid (MPA) in human colorectal mucosa tissue samples.

Although the expressions of *UGT1A8* and *UGT1A10* were not modulated by VDR ligands in our study, Wang *et al.,* (2016) previously reported 13 putative VDREs within the *UGT1A8-UGT1A10* cluster promoter region in addition to increased mRNA expression in LS180, CaCo-2 and HCT-116 cell lines. There were no identified differences in technical approaches, since in both cases real-time q-PCR was performed in LS180 cells exposed to 1,25D (10^{-8}M) for 24 hours. However, the experimental set-up including seeding cell density was not specified and could have contributed to the differences in our findings (Wang *et al.,* 2016).

Our data show that *UGT1A7* is also responsive to VDR ligands however, in contrast the work of Kutuzova and Deluca (2006), who employed microarray technology to investigate detoxification genes mediated by 1,25D, identified that *UGT1A7* was decreased by 2-fold after a 3-hour treatment period. Wang *et al.,* (2014) found that

UGT1A3 and UGT1A4 enzymes were the primary isoforms responsible for modification of 25-OHD_3, resulting in 25-OHD_3-25-glucronide, 25OHD_3-3-glucuronide, and 5,6-*trans*-25OHD_3-25-glucuronide metabolites detected in the bile. Together with our gene expression data, these finding suggest that *UGT1A3* and *UGT1A4* may contribute towards an important 25OHD_3 clearance pathway. 25OHD_3-3-glucuronide has high affinity binding towards vitamin D binding protein (VDBP) which extends 25OHD_3 half-life and promotes hepatic re-uptake (Wang *et al.,* 2013). 25OHD_3-3-glucuronide in the bile could induce the paracrine signaling loop which up-regulates classical VDR target genes and perhaps intestinal metabolic genes including, *CYPs* and other *UGT1As* (Wang *et al.,* 2014).

ChIP-Seq data from various cell lines performed in the presence and absence of 1,25D have revealed much on the VDR cistrome (Meyer *et al.,* 2012 and Singh *et al.,* 2017). Interrogation of the LS180 ChIP-seq data set obtained from the Pike study revealed to us multiple VDR/RXR binding sites within the *UGT1A* locus. These findings prompted our characterization of *UGT1A4* regulation further as it was the most sensitive to regulation by VDR ligands. We adapted the Clustered Regularly Interspaced Short Palindromic Repeats Interference (CRISPRi) approach, which enabled simultaneous interruption of the functional DR3-type VDRE (GGTTCATAAAGGGTA) and the 5' hexameric half-site (GGTTCATAA) without modifying the gene. CRISPRi in-cooperates fusion of (1) the catalytically inactive deadCas9 (dCas9) which blocks binding of the targeted sequence and (2) short guide RNA (sgRNA) that directs dCas9 by binding to the complementary target sequence (Larson *et al.,* 2013). We found that CRISPRi significantly diminished the ligand responsiveness of the *UGT1A* promoter based luciferase reporter however; when applied in context of endogenous gene the mRNA expression levels were unaffected. These findings suggest that other non-targeted VDREs are involved in *UGT1A* regulation and that dCas9 on its own may be insufficient in repressing transcriptional activity. In support of the former, according to *in silico* analysis by Wang *et al.,* (2016) there are 83 other DR3-type VDREs within the entire *UGT1A* locus. Their ChIP-seq findings further predicted non-DR3-type VDREs, suggesting that ER6-type (everted repeat of 2 hexameric half-sites with a spacer of 6 nucleotides) maybe involved in *UGT1A* regulation. (Wang *et al.,* 2016).

In the future, fusing sgRNA/dCas9 with repressive domains such as SID, which promotes H3K27ac and enhancer deactivation together with Krüppel associated box (KRAB) repressor, which forms heterochromatin, could successfully repress *UGT1A* transcription as employed by Carleton *et al.,* (2017) who successfully to targeted multiple estrogen receptor alpha binding motifs in Ishikawa cells. As shown in Figure 5.3 our target 1532bp DNA fragment within the *UGT1A* locus overlaps one of the VDR/RXR binding motifs highlighted in tracks based on VDR/Chip-seq data. Additionally, H3K27ac marks are present in this region and signify active enhancer activity (Pradeepa *et al.,* 2016). The targeted sequence also harbours *UGT1A4* distal enhancers and is rich in transcription factor (TF) binding sites (See Figure 5.3). Upon scanning the region for potential VDREs, 10 potential VDREs were identified (AGGTCA). If functional, the VDREs will also explain the dramatic *UGT1A4* mRNA expression (See Figure 5.4). It is possible that results from our CRISPRi approach can be explained by these binding motifs clustered within the 1532bp *UGT1A* fragment, which can act as supportive sites, and as such compensate for the CRISPRi interrogated direct site. Nonetheless, the putative VDREs will need to be characterized to better understand this mechanism. What is crucial at this stage is that our findings suggest a unique and complex *UGT1A4* regulatory mechanism by VDR ligands that may involve distal VDREs located within the *UGT1A1* promoter region. The involvement of these elements together with those within the *UGT1A4* promoter region itself could explain the significantly enhanced *UGT1A4* gene expression.

We also evaluated yet another role of VDR in *UGT1A* regulation; that is, its ability to work in conjunction with the oxidative stress (OS) sensor, nuclear factor erythroid 2-related factor 2 (NRF2) (Vomund *et al.,* 2017). NRF2 is a TF that has gained its recognition in neutralization of OS, but also in detoxification pathways (Vomund *et al.,* 2017; Zhang *et al.,* 2009). Numerous studies have associated NRF2 with VDR. Particularly, Chen *et al.,* (2019) who identified that 1,25D activates NRF2 signalling, increasing the expression of p16, p53 and p21 which all regulate the cell cycle and function as tumour suppressors. Additionally, Nakai *et al.,* (2014) identified that 1,25D activates the NRF2/ARE signaling pathway, which in turn combats nephropathy in diabetic rats. Zhang *et al.,* (2009) identified that NRF2 increased the

level of *UGT1A* in cells. Kalthof *et al.*, (2010) further confirmed that expression of *UGT1A8* and *UGT1A10* can be enhanced by NRF2 and more significantly in conjunction with AhR, in KYSE70 colonic cells. These findings support the previously stated 'phenotypic stability hypothesis that states that 1,25D activates induces Klotho and NRF2 which are both important for an extensive cellular health, functioning as an anti-aging, OS neutralization and mineral health regulator (Berridge, 2015).

We here hypothesized that both VDR and NRF2 significantly enhance *UGT1A* gene expression in LS180 cells. We confirmed that, 1,25D enhances (anti-oxidant response element) ARE signaling in both LS180 and LNCaP cell. Exogenous VDR only slightly increases this signaling in both LS180 and HEK293 cells. Sulforaphane (SFN) and *tert*-butlyhydroquione (*t*BHQ) are effectors of ARE/NRF2 signaling. Additionally, 3kLCA also significantly increased NRF2/ARE signaling, although minor compared to SFN and tBHQ responses. In a colonic context, NRF2/ARE signaling affects secondary bile acid reabsorption through regulation of the apical sodium-dependent bile acid transporter (ASBT) (Weerahayapom *et al.,* 2012). 3kLCA, by enhancing ARE activity may be able to facilitate a feedback system that ensures its own metabolism and excretion through increased expression of NRF2 expressing detoxification-related genes (Kamisako *et al.*, 2014). What is not certain from our data is whether 3kLCA modulation of ARE activity is a direct or indirect effect. Additionally, whether VDR is directly implicated in 3kLCA effects in this manner will also need to be investigated further.

Surprisingly our site-directed mutagenesis experiment suggest that rather than a dependency of NRF2-directed signaling on an intact VDR pathway, we find that modulation of *UGT1A* expression by VDR ligands is dependent upon an intact ARE, also present within the promoter fragment that contains the VDRE. In our colonic context, this suggests that the antioxidant system is the primary defense mechanism against toxic endogenous and exogenous compounds, together with reactive oxygen species that may disrupt cellular integrity. Although we analyzed the expression of numerous VDR and NRF2 target genes, inhibitory effects of SFN were consistently observed on the 1,25D-driven responses of VDR targets *CYP24A1*, *CYP3A4*, *UGT1A4*

and *VDR*. In the case of UGT1A however, its protein expression became notably increased following such co-treatments. The mechanisms that underpin the inhibitory properties of SFN upon VDR signaling were not investigated, however our speculation is that SFN competes with the VDR binding site, or is involved indirectly through competition for binding to co-regulatory proteins recruited to the VDR/RXR heterodimer, thus suppressing overall gene expression. Use of the mammalian-two hybrid assay or assessment of the impact of the exogenous expression of candidate shared accessory protein factors could be used to help explain these inhibitory events.

The NRF2 target genes, *HMOX1, NQO1* and *GCLC* were not affected by 1,25D exposure in our LS180 and LNCaP cells although Jain and Micinski, (2013) had previously shown that *GCLC* and *GR* expression are increased by 1,25D in U937 monocytes. The differences may suggest that 1,25D modulates these NRF2 target genes in a cell-specific manner. What we did confirm in both LS180 cells and LNCaP cells were the potential anti-apoptotic properties of both VDR and NRF2 signaling pathways through the suppression of *BIRC5* gene expression. Our data also point to the fact that 1,25D and SFN elicit growth inhibitory properties in both a colonic and prostatic cellular context; however, the effects will require further examination at functional level to observe whether these ligands increase apoptosis. Additionally, further use of animal models will confirm these compounds as potential use as a chemotherapeutic measure, that is, to inhibit tumor growth. Whilst our data on the interplay of NRF2 and VDR is somewhat encouraging, the approaches are not enough to support the proposed hypothesis.

6.2 Clinical relevance

This study establishes 1,25D/VDR signaling as critical in maintaining overall cellular health. The human body is constantly exposed to various exogenous substances in addition to endogenous components such as bilirubin, bile acids and hormones, which need to be excreted (Haas *et al.,* 2006; Wang *et al.,* 2016; Amandito *et al.,* 2019). In this thesis, we seek to translate our findings into a clinical context, whereby, maintenance of optimal 1,25D levels will further maintain a healthy equilibrium of these substances through an increase in *UGT1A* expression.

UGT1A1 expression is delayed in new-borns, hence over 80% present with abnormally high levels of serum bilirubin, causing a benign condition clinically known as neonatal jaundice, characterized by yellowing of the skin, whites of eyes, inside the mouth, soles of feet and palm of hands (Fujiwara *et al.*, 2015). This manifests because of the delayed *UGT1A1* expression, (*UGT1A1* is the only isoform involved in the homeostatic control of bilirubin (See Figure 6.1)) (de Souza *et al.*, 2017). Neonatal jaundice is usually managed by invasive intense phototherapy or exchange transfusion (Mitra and Rennie, 2017). Severe cases, usually observed in neonates lead to a fatal condition known as kernicterus, characterized by brain damage (Fujiwara *et al.*, 2015). Breast-feeding also contributes to neonatal jaundice by suppressing *UGT1A1* expression (Fujiwara *et al.*, 2012). Previous studies by Kumral *et al.*, (2009) Apaydin *et al.*, (2012) and Wilson *et al.*, (1992) suggested that the presence of steroids, fats, cytokines and β-glucuronidase in breast milk correlates with an increased bilirubin re-uptake through enterohepatic circulation, decreased bilirubin excretion from the body and the inhibitory effects on UGT1A1 enzymatic activity. These effects are disadvantageous as breast-feeding comes with developmental benefits, maternal-infant bonding and a rich nutritional gain. Our findings suggest that vitamin D or its synthetic analogue (EB1089) could be used to revive *UGT1A1* expression, leading to efficient bilirubin metabolism, therefore preventing kernicterus development or neonatal jaundice altogether. Additionally the VDR may counter-act the *UGT1A1* inhibitory effects from breast milk.

UGT1A1 genetic polymorphisms have been linked with impaired enzymatic activity and are associated with hereditary hyperbilirubinemia (serum bilirubin levels above 5ml/dL) (Sanchez-Dominguez *et al.*, (2017). More specifically, Gilbert's Syndrome (GS), caused by a *UGT1A1*28* promoter polymorphism and Crigler Najjar Syndrome (CNS: type I and type II). (Wagner *et al.*, 2018). CNS I and CNS II are commonly linked with *UGT1A1*34* and *UGT1A1*35* genetic polymorphisms (Ciotti *et al.*, 1999). GS presents as a benign form, with symptoms (jaundice) manifesting well in to adolescence usually triggered by stress or fasting (Fujiwara *et al.*, 2015). By comparison, individuals with mutations that cause CNS II also present with mild symptoms and moderate to high hyperbilirubinemia. However, mutations that cause

CNS I lead to complete loss of UGT1A1 acitivity (Maruo *et al.,* 2015). This results in serum levels ranging between 30 to 50mg/dL, which often lead to the fatal encephalopathy (Maruo *et al.,* 2015). If our findings translate to a functional context, vitamin D/VDR could be used to manage hereditary hyperbilirubinemia and prevent fatal encephalopathy in individuals with CNS I.

So far, efforts to revive *UGT1A* expression were attempted by Aoshima *et al.,* (2014) who observed that glucose administration enhanced extrahepatic *UGT1A* expression. This also correlated with a decrease in unconjugated bilirubin. Studies by Fujiwara *et al.,* (2012) and Sumida *et al.,* (2013) identified that extrahepatic (small intestinal and skin) *UGT1A1* expression are involved in bilirubin metabolism. More importantly, these findings are a reinforcement to our study, implying that extrahepatic *UGT1A*, can be involved in bilirubin metabolism. Furthermore, VDR agonists could be an alternative treatment measure for neonatal jaundice and hyperbilirubinemia-related conditions.

UGT1A polymorphisms are also typically correlated with reduced capacity of glucuronidation (Mehboob *et al.,* 2017). As such, *UGT1A* gene polymorphism usually present a potential marker for cancer susceptibility (Strassburg *et al.,* 1998 and Garcia *et al.,* 2018). For example, colorectal cancer, which develops due to altered exposure to dietary or harmful exogenous factors (Wang *et al.,* 2013 and Angstadt *et al.,* 2014). Reduced *UGT1A6* activity is linked to lung cancer and its polymorphism is a biomarker for high risk in its development (Kua *et al.,* 2012). Moreover, low levels of *UGT1A7* and *UGT1A10* expression are linked to the development oesophageal and oestrogen related cancers respectively (Vogel *et al.,* 2002 and Staland-Davenport *et al.,* 2007). Our findings link vitamin D to chemotherapy and chemoprevention through UGT1A enhanced expression.

The role of drug-metabolism is well documented with over 50% of clinically administered drugs being metabolised by *UGT1A* genes (Sanchez-Dominguez *et al.,* 2018). Numerous studies have linked *UGT1A* expression with the metabolism of chemotherapeutic compounds in cancer model systems (Chen *et al.,* 2013 and Takano *et al.,* 2017). The most commonly studied is irinotecan, which, upon glucuronidation

leads to an active metabolite 7-ethyl-10-hydroxycamptothecin, (SN-38), finally leading to an inactive glucuronide, SN-38-G (Tanaka *et al.,* 2013). GS patients are usually susceptible to irinotecan-induced toxicity and present with diarrhoea, diaphoresis and abdominal pain (Takano *et al.,* 2017). Defective clearance results in cancer development (Takano *et al,* 2017). Normal clearance of drugs susceptible to glucuronidation facilitated by normal *UGT1A* expression will prevent drug-toxicity (Wang *et al.,* 2016; Konaka *et al.,* 2019) (See Table 1.3). Our *UGT1A* expression profile implies that co-administration of vitamin D with these drugs should be carefully considered to avoid drug-drug interactions. Whilst this study encourages the use of vitamin D, it is noteworthy that its synthetic analogue EB1089 enhanced *UGT1A* expression more potently and may be a better therapeutic measure in conditions where *UGT1A* expression is compromised. Compared to vitamin D, EB1089 has low calcaemic activity and as such, hypercalcemia, which causes kidney failure, abnormal heart rhythms and coma can be avoided (Abdaimi *et al.,* 1999 and Ghous *et al.,* 2008). The synthetic analogue has already shown promising therapeutic effects in mice models with c-MET-β-catenin driven hepatocellular cancer (Matsuda *et al.,* 2019).

SFN is equally an inducer of *UGT1A1* as 1,25D, however did not significantly affect other *UGT1A* isoforms (Wang *et al.,* 2005). From this study, we can deduce that SFN is a significantly potent chemo protective agent, through its growth inhibition properties observed both in LNCaP and LS180 cell lines. The co-treatment of both SFN and 1,25D does not increase this effect as anticipated. However, the inhibitory effects between SFN and 3kLCA do imply that the ARE/NRF2 signalling is involved in BA homeostatic control or may act indirectly to bind 3kLCA, supressing its carcinogenic properties. Further studies into the interplay between NRF2 and VDR will need to be addressed, perhaps more in-depth in various extrahepatic cell lines. What was possibly a challenge in this thesis to be able to translate these findings clinically were the negligible NRF2 levels in LS180 cells.

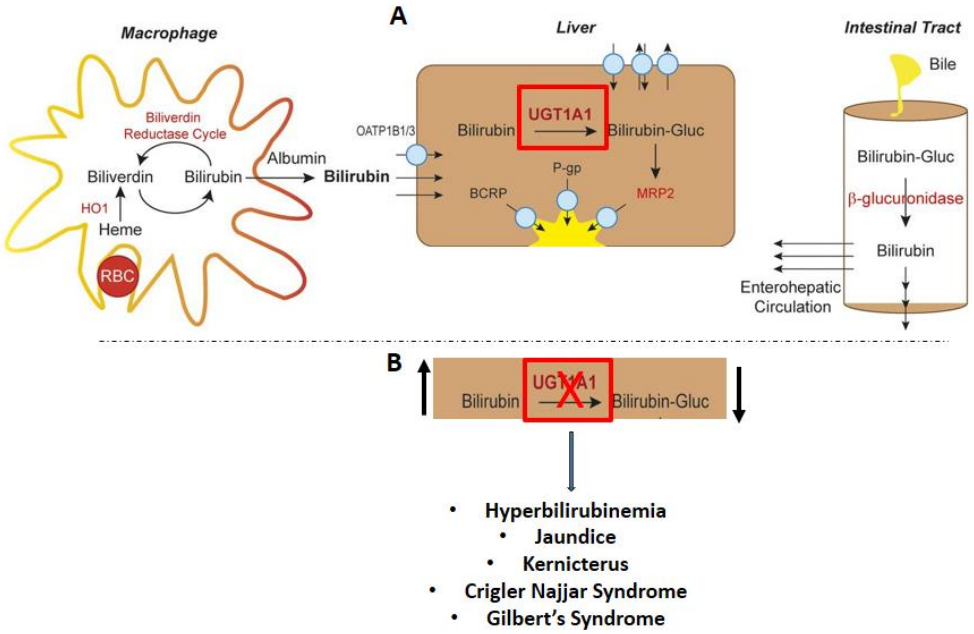

Figure 6.1: Bilirubin metabolism by UGT1A1. **(A)***The breakdown on red blood cells produces biliverdin, which is further metabolized by biliverdin reductase, producing bilirubin. Bilirubin binds to albumin protein as is transported throughout the body. In the liver, it is metabolized by UGT1A1, forming mono-/di-bilirubin glucuronides that are secreted via the biliary tract. The glucuronides are susceptible to hydroxylation by β-glucuronidates in the intestinal tract which facilitates its enterohepatic circulation. (**B**) UGT1A1 is the sole enzyme capable to metabolizing bilirubin, therefore, inactive or suppressed enzymatic activity results in devastative consequences including hyperbilirubinemia, GS and CNS.* (*Image edited from Chen and Tukey, 2018)*

6.3 Limitations of this study

This study had a number of limitations, particularly due to the time constraints and the availability of resources. Experimentally, the thesis would have been more informative with successful assay approaches to detect glucuronidation, possibly the use of LC-MS/MS where the glucuronidation of specific compounds (e.g. bilirubin) could be measured in our chosen cell line. Furthermore, the implementation of *ex-vivo* samples, i.e. patient colonic biopsies to measure impact of vitamin D exposures on UGT1A expressions, would have extended the relevance of our cell based *in-vitro* data. Evaluating the correlation between *UGT1A* and *VDR* gene expression levels in

normal colonic biopsies will clinically determine the relevance of *UGT1A* gene expression by VDR ligands. In addition, the use of previously generated transgenic *UGT1A* (*hUGT1A*) mice models that express the entire *UGT1A* locus and *Ugt1*-null background would have provided the first appropriate animal model to study the mechanisms associated with 1,25D/VDR signalling (Chen and Tukey, 2018). There are a number of conclusions to draw from using *hUGT1A* mice models. Firstly, whether at functional level the *UGT1A* induction is enhanced by VDR signalling, and secondly, the clinical consequences can be critically examined, such as the involvement of intestinal *UGT1A* expression in bilirubin metabolism, tumour inhibitory properties and redox signalling were NRF2 and VDR ligands are co-administered. Furthermore, comparative analysis of other *UGT1A* regulating TFs can be fully evaluated. Altogether, data from transgenic mice will have favourable human relevance.

Another major challenge in this study was the difficulty in cloning the promoter region that we postulated to mediate regulation of *UGT1A4* due to many technical/optimisation challenges within the ligation stage. The findings in this experiment would have been crucial in identifying additional functional cistromes and their effects on each *UGT1A* isoform expression. The CRISPRi approach was an excellent choice; however, the limited resources and the expense of this approach meant we were limited in optimization in our LS180 cells. Examining successful transfection is a challenge but is critical for this kind of approach, or fusing the ribonucleic protein (RNP) with repressor domains (SID and KRAB) that completely block co-regulatory complex formation. Lastly, our experiments were predominantly in LS180 cells, although in other experiments were included HEK293, CaCo-2 and LNCaP cell line models. It is unclear how each cell line may relate to the actual physiological relevance of an *UGT1A* gene regulation by VDR and the interplay with NRF2.

6.4 Future experiments

This thesis added valued knowledge into understanding one of the many roles of VDR, primarily the regulation of extrahepatic *UGT1A* gene family members. As already

mentioned, numerous studies have investigated individual isoforms, we here considered all the gene family members. However, with a few limitations and a number of gaps to fill, the experiments proposed below will further strengthen our findings. These include exposing VDR (and NRF2) ligands to cells together with *UGT1A* susceptible compounds. Measurement of glucuronidation activity through quantification of metabolite formation by LC-MS/MS will confirm that VDR does enhance *UGT1A* gene and protein expression level, but also functional activity will determine the physiological relevance of this regulation. The quantification of metabolites upon co-treatment of VDR and NRF2 ligands will also be useful in determining cross-talk between the two signalling pathways at functional level.

Another important approach to strengthen this study is the use of humanized *UGT1A* mice models with *Ugt*1-null background. Previously, Cai *et al.,* (2010) successfully used this transgenic mouse model expressing the *UGT1A1*28* allele for assessing drug clearance by *UGT1A1*-dependant glucuronidation. The transgenic mice presented with a hyperbilirubinemia phenotype. The use of these models in our study, particularly, the ingestion of Vitamin D or its synthetic analogues and monitoring physiological changes, including the presence of or rescue of UGT1A1 enzymatic activity, reduction in hyperbilirubinemia symptoms and measurement of serum bilirubin will further confirm that extrahepatic *UGT1A1*, regulated by VDR is physiologically relevant and can be used as a treatment option where *UGT1A1* expression is compromised. In the same manner, the glucuronidation substrate metabolites, including irinotecan, total serum bilirubin and various homornes (e.g estrogen) can be measured upon ingestion of Vitamin D or its analogues by transgenic mice. Examination of 1,25D side effects compared to that of other VDR ligands (e.g. EB1089) will determine suitable treatment option in diseases where UGT1A expression is compromised.

Other approaches to strenghthen this study include:

- *Ex-vivo* experiments on extra-hepatic biopsies, measure mRNA, protein and functional tests to observe a correlation with our data.

- Identify a specific cell line with significant VDR and NRF2 levels to reliably examine the interplay of the two signalling pathways.
- Investigate protein-protein interactions that may cause inhibitory effects between VDR and NRF2 ligands.
- Silence the VDR to examine 3kLCA effects in ARE/NRF2 signaling.
- Targeting more UGT1A isoforms to examine the involvement of the range of VDR/RXR binding sites within the UGT1A locus identified by Chip-Seq data.
- Manipulate each individual binding site from the ChIP-seq data (Pike's laboratory) to identify functional VDREs that contribute to the regulation of each isoform.
- Include repression domains in CRISPRi approach to suppress H3K24ac marks and heterochromatin formation.

6.5 Summary of key findings

- VDR activation induces the expression of *UGT1A1, UGT1A3, UGT1A4, UGT1A5 and UGT1A7*
- *UGT1A1* is the most abundant and *UGT1A4* is the most sensitive isoform in response to VDR ligands
- VDR directly influences UGT1A protein expression
- The putative DR3-type element within the *UGT1A1* promoter region is VDR specific
- A functional VDRE was identified within the *UGT1A1* (within position -3483/-3194) promoter region.
- VDR activity relies on an intact VDRE and ARE but the same is not true for NRF2
- 1,25D and co-treatment of NRF2 and VDR ligands does not significantly enhance gene expression/activity
- SFN has more potent growth inhibition properties than 1,25D in both a colonic and prostate cancer cellular context.

6.6 Concluding Remarks

The key focus for this study was to determine extrahepatic *UGT1A* regulation by VDR. We successfully define the gene family members induced in this manner and subsequently confirmed this regulation at protein and functional level. We also observed modest to absent interaction between VDR and NRF2 signaling in enhancing detoxification genes including *UGT1As*, although VDR depended on an intact NRF2/ARE signalling. This study has shed some light into extrahepatic detoxification pathways. The multiple VDR/RXR binding sites within the *UGT1A* locus potentially contribute to the robust response of *UGT1A4* to VDR ligands. Clinically, these findings are advantageous in cases where *UGT1A* expression is crucial (i.e. hyperbilirubinemia, drug metabolism and chemoprevention).

7: Chapter 7

References

1. Abbaoui, B., Telu, K.H., Lucas, C.R., Thomas-Ahner, J.M., Schwartz, S.J., Clinton, S.K., Freitas, M.A. and Mortazavi, A. (2017) The impact of cruciferous vegetable isothiocyanates on histone acetylation and histone phosphorylation in bladder cancer. *Journal of Proteomics,* 156, 94-103.
2. Adzemovic, M.Z., Zeitelhofer, M., Hochmeister, S., Gustafsson, S.A. and Jagodic, M. (2013) Efficacy of vitamin D in treating multiple sclerosis-like neuroinflammation depends on developmental stage. *Experimental Neurology,* 249, 39-48.
3. Aguilera, O., Pena, C., Garcia, J.M., Larriba, M.J., Ordonez-Moran, P., Navarro, D., Barbachano, A., Lopez de Silanes, I., Ballestar, E., Fraga, M.F., Esteller, M., Gamallo, C., Bonilla, F., Gonzalez-Sancho, J.M. and Munoz, A. (2007) The Wnt antagonist DICKKOPF-1 gene is induced by 1alpha,25-dihydroxyvitamin D3 associated to the differentiation of human colon cancer cells. *Carcinogenesis,* 28(9), 1877-1884.
4. Agusa, T., Iwata, H., Fujihara, J., Kunito, T., Takeshita, H., Minh, T.B., Trang, P.T., Viet, P.H. and Tanabe, S. (2010) Genetic polymorphisms in glutathione S-transferase (GST) superfamily and arsenic metabolism in residents of the Red River Delta, Vietnam. *Toxicology and Applied Pharmacology*, 242(3), 352-362.
5. Agyeman, A.S., Chaerkady, R., Shaw, P.G., Davidson, N.E., Visvanathan, K., Pandey, A. and Kensler, T.W. (2012) Transcriptomic and proteomic profiling of KEAP1 disrupted and sulforaphane-treated human breast epithelial cells reveals common expression profiles. *Breast Cancer Research and Treatment,* 132(1), 175-187.
6. Ahmed, S.M., Luo, L., Namani, A., Wang, X.J. and Tang, X. (2017) Nrf2 signaling pathway: Pivotal roles in inflammation. *Biochimica Et Biophysica Acta.Molecular Basis of Disease,* 1863(2), 585-597.
7. Ahn, J., Park, S., Zuniga, B., Bera, A., Song, C.S. and Chatterjee, B. (2016) Vitamin D in Prostate Cancer. *Vitamins and Hormones,* 100, 321-355.
8. Ali, N.S. & Nanji, K., 2017. A Review on the Role of Vitamin D in Asthma. *Cureus*.
9. Alvarez-Diaz, S., Valle, N., Ferrer-Mayorga, G., Lombardia, L., Herrera, M., Dominguez, O., Segura, M.F., Bonilla, F., Hernando, E. and Munoz, A. (2012) MicroRNA-22 is induced by vitamin D and contributes to its antiproliferative,

antimigratory and gene regulatory effects in colon cancer cells. *Human Molecular Genetics*, 21(10), 2157-2165.

10. Al-Zoughool, M. and Talaska, G. (2006) 4-Aminobiphenyl N-glucuronidation by liver microsomes: optimization of the reaction conditions and characterization of the UDP-glucuronosyltransferase isoforms. *Journal of Applied Toxicology : JAT*, 26(6), 524-532.
11. Amandito, R., Rohsiswatmo, R., Carolina, E., Maulida, R., Kresnawati, W. and Malik, A. (2019) Profiling of UGT1A1(*)6, UGT1A1(*)60, UGT1A1(*)93, and UGT1A1(*)28 Polymorphisms in Indonesian Neonates With Hyperbilirubinemia Using Multiplex PCR Sequencing. *Frontiers in Pediatrics*, 7, 328.
12. Anderson, P.H., O'Loughlin, P.D., May, B.K. and Morris, H.A. (2004) Determinants of circulating 1,25-dihydroxyvitamin D3 levels: the role of renal synthesis and catabolism of vitamin D. *The Journal of Steroid Biochemistry and Molecular Biology*, 89-90(1-5), 111-113.
13. Angstadt, A.Y., Hartman, T.J., Lesko, S.M., Muscat, J.E., Zhu, J., Gallagher, C.J. and Lazarus, P. (2014) The effect of UGT1A and UGT2B polymorphisms on colorectal cancer risk: haplotype associations and gene-environment interactions. *Genes, Chromosomes & Cancer*, 53(6), 454-466.
14. Aoshima, N., Fujie, Y., Itoh, T., Tukey, R.H. and Fujiwara, R. (2014) Glucose induces intestinal human UDP-glucuronosyltransferase (UGT) 1A1 to prevent neonatal hyperbilirubinemia. *Scientific Reports*, 4, 6343.
15. Aueviriyavit, S., Furihata, T., Morimoto, K., Kobayashi, K. and Chiba, K. (2007) Hepatocyte nuclear factor 1 alpha and 4 alpha are factors involved in interindividual variability in the expression of UGT1A6 and UGT1A9 but not UGT1A1, UGT1A3 and UGT1A4 mRNA in human livers. *Drug Metabolism and Pharmacokinetics*, 22(5), 391-398.
16. Bacchetta, J., Sea, J.L., Chun, R.F., Lisse, T.S., Wesseling-Perry, K., Gales, B., Adams, J.S., Salusky, I.B. and Hewison, M. (2013) Fibroblast growth factor 23 inhibits extrarenal synthesis of 1,25-dihydroxyvitamin D in human monocytes. *Journal of Bone and Mineral Research : The Official Journal of the American Society for Bone and Mineral Research*, 28(1), 46-55.

17. Barbarino, J.M., Haidar, C.E., Klein, T.E. and Altman, R.B. (2014) PharmGKB summary: very important pharmacogene information for UGT1A1. *Pharmacogenetics and Genomics,* 24(3), 177-183.
18. Barbier, O., Villeneuve, L., Bocher, V., Fontaine, C., Torra, I.P., Duhem, C., Kosykh, V., Fruchart, J.C., Guillemette, C. and Staels, B. (2003) The UDP-glucuronosyltransferase 1A9 enzyme is a peroxisome proliferator-activated receptor alpha and gamma target gene. *The Journal of Biological Chemistry,* 278(16), 13975-13983.
19. Bedi, S., Hostetler, H.A. and Rider, S.D.,Jr. (2017) Mutations in Liver X Receptor Alpha that Impair Dimerization and Ligand Dependent Transactivation. *Nuclear Receptor Research,* 4, 10.11131/2017/101302.
20. Bellemare, J., Rouleau, M., Harvey, M., Tetu, B. and Guillemette, C. (2010) Alternative-splicing forms of the major phase II conjugating UGT1A gene negatively regulate glucuronidation in human carcinoma cell lines. *The Pharmacogenomics Journal,* 10(5), 431-441.
21. Bellezza, I. (2018) Oxidative Stress in Age-Related Macular Degeneration: Nrf2 as Therapeutic Target. *Frontiers in Pharmacology,* 9, 1280.
22. Bellezza, I., Scarpelli, P., Pizzo, S.V., Grottelli, S., Costanzi, E. and Minelli, A. (2017) ROS-independent Nrf2 activation in prostate cancer. *Oncotarget,* 8(40), 67506-67518.
23. Berridge, M.J. (2015) Vitamin D: a custodian of cell signalling stability in health and disease. *Biochemical Society Transactions,* 43(3), 349-358.
24. Berridge, M.J. (2016) Vitamin D, reactive oxygen species and calcium signalling in ageing and disease. *Philosophical Transactions of the Royal Society of London.Series B, Biological Sciences,* 371(1700), 10.1098/rstb.2015.0434.
25. Beurel, E., Grieco, S.F. and Jope, R.S. (2015) Glycogen synthase kinase-3 (GSK3): regulation, actions, and diseases. *Pharmacology & Therapeutics,* 148, 114-131.
26. Bischoff-Ferrari, H.A., Giovannucci, E., Willett, W.C., Dietrich, T. and Dawson-Hughes, B. (2006) Estimation of optimal serum concentrations of 25-hydroxyvitamin D for multiple health outcomes. *The American Journal of Clinical Nutrition,* 84(1), 18-28.

27. Bishayee, A., Bhatia, D., Thoppil, R.J., Darvesh, A.S., Nevo, E. and Lansky, E.P. (2011) Pomegranate-mediated chemoprevention of experimental hepatocarcinogenesis involves Nrf2-regulated antioxidant mechanisms. *Carcinogenesis,* 32(6), 888-896.
28. Blaine, J., Chonchol, M. and Levi, M. (2015) Renal control of calcium, phosphate, and magnesium homeostasis. *Clinical Journal of the American Society of Nephrology : CJASN,* 10(7), 1257-1272.
29. Boucher, B.J. (2018) Vitamin D status and its management for achieving optimal health benefits in the elderly. *Expert Review of Endocrinology & Metabolism,* 13(6), 279-293.
30. Boyce, B.F. and Xing, L. (2008) Functions of RANKL/RANK/OPG in bone modeling and remodeling. *Archives of Biochemistry and Biophysics,* 473(2), 139-146.
31. Buckley, D.B. and Klaassen, C.D. (2009) Induction of mouse UDP-glucuronosyltransferase mRNA expression in liver and intestine by activators of aryl-hydrocarbon receptor, constitutive androstane receptor, pregnane X receptor, peroxisome proliferator-activated receptor alpha, and nuclear factor erythroid 2-related factor 2. *Drug Metabolism and Disposition: The Biological Fate of Chemicals,* 37(4), 847-856.
32. Campbell, M.J. (2014) Vitamin D and the RNA transcriptome: more than mRNA regulation. *Frontiers in Physiology,* 5, 181.
33. Campos, L.T., Brentani, H., Roela, R.A., Katayama, M.L., Lima, L., Rolim, C.F., Milani, C., Folgueira, M.A. and Brentani, M.M. (2013) Differences in transcriptional effects of 1alpha,25 dihydroxyvitamin D3 on fibroblasts associated to breast carcinomas and from paired normal breast tissues. *The Journal of Steroid Biochemistry and Molecular Biology,* 133, 12-24.
34. Canning, P., Sorrell, F.J. and Bullock, A.N. (2015) Structural basis of Keap1 interactions with Nrf2. *Free Radical Biology & Medicine,* 88(Pt B), 101-107.
35. Canu, G., Minucci, A., Zuppi, C. and Capoluongo, E. (2013) Gilbert and Crigler Najjar syndromes: an update of the UDP-glucuronosyltransferase 1A1 (UGT1A1) gene mutation database. *Blood Cells, Molecules & Diseases,* 50(4), 273-280.

36. Carlberg, C. and Campbell, M.J. (2013) Vitamin D receptor signaling mechanisms: integrated actions of a well-defined transcription factor. *Steroids*, 78(2), 127-136.
37. Carlberg, C., Seuter, S. and Heikkinen, S. (2012) The first genome-wide view of vitamin D receptor locations and their mechanistic implications. *Anticancer Research*, 32(1), 271-282.
38. Carleton, J.B., Berrett, K.C. and Gertz, J. (2017) Multiplex Enhancer Interference Reveals Collaborative Control of Gene Regulation by Estrogen Receptor alpha-Bound Enhancers. *Cell Systems*, 5(4), 333-344.e5.
39. Cattaneo, D., Ripamonti, D., Baldelli, S., Cozzi, V., Conti, F. and Clementi, E. (2010) Exposure-related effects of atazanavir on the pharmacokinetics of raltegravir in HIV-1-infected patients. *Therapeutic Drug Monitoring*, 32(6), 782-786.
40. Cengiz, B., Yumrutas, O., Bozgeyik, E., Borazan, E., Igci, Y.Z., Bozgeyik, I. and Oztuzcu, S. (2015) Differential expression of the UGT1A family of genes in stomach cancer tissues. *Tumour Biology : The Journal of the International Society for Oncodevelopmental Biology and Medicine*, 36(8), 5831-5837.
41. Chai, X., Zeng, S. and Xie, W. (2013) Nuclear receptors PXR and CAR: implications for drug metabolism regulation, pharmacogenomics and beyond. *Expert Opinion on Drug Metabolism & Toxicology*, 9(3), 253-266.
42. Chandrasekar, V. and John, S., 2020. *Gilbert Syndrome*. [online] Statpearls.com. Available at: <https://www.statpearls.com/kb/viewarticle/22249> [Accessed 9 April 2020].
43. Chen, L., Yang, R., Qiao, W., Zhang, W., Chen, J., Mao, L., Goltzman, D. and Miao, D. (2019) 1,25-Dihydroxyvitamin D exerts an antiaging role by activation of Nrf2-antioxidant signaling and inactivation of p16/p53-senescence signaling. *Aging Cell*, 18(3), e12951.
44. Chen, S., Beaton, D., Nguyen, N., Senekeo-Effenberger, K., Brace-Sinnokrak, E., Argikar, U., Remmel, R.P., Trottier, J., Barbier, O., Ritter, J.K. and Tukey, R.H. (2005) Tissue-specific, inducible, and hormonal control of the human UDP-glucuronosyltransferase-1 (UGT1) locus. *The Journal of Biological Chemistry*, 280(45), 37547-37557.

45. Chen, S., Yueh, M.F., Evans, R.M. and Tukey, R.H. (2012) Pregnane-x-receptor controls hepatic glucuronidation during pregnancy and neonatal development in humanized UGT1 mice. *Hepatology (Baltimore, Md.),* 56(2), 658-667.
46. Chen, X., Duan, N., Zhang, C. and Zhang, W. (2016) Survivin and Tumorigenesis: Molecular Mechanisms and Therapeutic Strategies. *Journal of Cancer,* 7(3), 314-323.
47. Chen, Y., Rao, X., Huang, K., Jiang, X., Wang, H. and Teng, L. (2017) FH535 Inhibits Proliferation and Motility of Colon Cancer Cells by Targeting Wnt/beta-catenin Signaling Pathway. *Journal of Cancer,* 8(16), 3142-3153.
48. Chen, Z., Ye, X., Tang, N., Shen, S., Li, Z., Niu, X., Lu, S. and Xu, L. (2014) The histone acetylranseferase hMOF acetylates Nrf2 and regulates anti-drug responses in human non-small cell lung cancer. *British Journal of Pharmacology,* 171(13), 3196-3211.
49. Cheng, J., Fang, Z.Z., Kim, J.H., Krausz, K.W., Tanaka, N., Chiang, J.Y. and Gonzalez, F.J. (2014) Intestinal CYP3A4 protects against lithocholic acid-induced hepatotoxicity in intestine-specific VDR-deficient mice. *Journal of Lipid Research,* 55(3), 455-465.
50. Chiang, T.C., Koss, B., Su, L.J., Washam, C.L., Byrum, S.D., Storey, A. and Tackett, A.J. (2019) Effect of Sulforaphane and 5-Aza-2'-Deoxycytidine on Melanoma Cell Growth. *Medicines (Basel, Switzerland),* 6(3), 10.3390/medicines6030071.
51. Choi, K.C. and Jeung, E.B. (2008) Molecular mechanism of regulation of the calcium-binding protein calbindin-D9k, and its physiological role(s) in mammals: a review of current research. *Journal of Cellular and Molecular Medicine,* 12(2), 409-420.
52. Choi, M., Yamamoto, K., Masuno, H., Nakashima, K., Taga, T. and Yamada, S. (2001) Ligand recognition by the vitamin D receptor. *Bioorganic & Medicinal Chemistry,* 9(7), 1721-1730.
53. Chorley, B.N., Campbell, M.R., Wang, X., Karaca, M., Sambandan, D., Bangura, F., Xue, P., Pi, J., Kleeberger, S.R. and Bell, D.A. (2012) Identification of novel NRF2-regulated genes by ChIP-Seq: influence on retinoid X receptor alpha. *Nucleic Acids Research,* 40(15), 7416-7429.

54. Chouinard, S., Barbier, O. and Belanger, A. (2007) UDP-glucuronosyltransferase 2B15 (UGT2B15) and UGT2B17 enzymes are major determinants of the androgen response in prostate cancer LNCaP cells. *The Journal of Biological Chemistry,* 282(46), 33466-33474.
55. Chowdhry, S., Zhang, Y., McMahon, M., Sutherland, C., Cuadrado, A. and Hayes, J.D. (2013) Nrf2 is controlled by two distinct beta-TrCP recognition motifs in its Neh6 domain, one of which can be modulated by GSK-3 activity. *Oncogene,* 32(32), 3765-3781.
56. Chowdhury, A.M.M.A., Katoh, H., Hatanaka, A., Iwanari, H., Nakamura, N., Hamakubo, T., Natsume, T., Waku, T. and Kobayashi, A. (2017) Multiple regulatory mechanisms of the biological function of NRF3 (NFE2L3) control cancer cell proliferation. *Scientific Reports,* 7(1), 12494-017-12675-y.
57. Christakos, S., Dhawan, P., Porta, A., Mady, L. and Seth, T., 2011. *Vitamin D And Intestinal Calcium Absorption*.
58. Ciotti, M., Basu, N., Brangi, M. and Owens, I.S. (1999) Glucuronidation of 7-ethyl-10-hydroxycamptothecin (SN-38) by the human UDP-glucuronosyltransferases encoded at the UGT1 locus. *Biochemical and Biophysical Research Communications,* 260(1), 199-202.
59. Court, M.H. (2010) Interindividual variability in hepatic drug glucuronidation: studies into the role of age, sex, enzyme inducers, and genetic polymorphism using the human liver bank as a model system. *Drug Metabolism Reviews,* 42(1), 209-224.
60. Cox, A.J., Ng, M.C., Xu, J., Langefeld, C.D., Koch, K.L., Dawson, P.A., Carr, J.J., Freedman, B.I., Hsu, F.C. and Bowden, D.W. (2013) Association of SNPs in the UGT1A gene cluster with total bilirubin and mortality in the Diabetes Heart Study. *Atherosclerosis,* 229(1), 155-160.
61. Danoff, T.M., Campbell, D.A., McCarthy, L.C., Lewis, K.F., Repasch, M.H., Saunders, A.M., Spurr, N.K., Purvis, I.J., Roses, A.D. and Xu, C.F. (2004) A Gilbert's syndrome UGT1A1 variant confers susceptibility to tranilast-induced hyperbilirubinemia. *The Pharmacogenomics Journal,* 4(1), 49-53.
62. de Souza, M.M., Vaisberg, V.V., Abreu, R.M., Ferreira, A.S., daSilvaFerreira, C., Nasser, P.D., Paschoale, H.S., Carrilho, F.J. and Ono, S.K. (2017) UGT1A1*28

relationship with abnormal total bilirubin levels in chronic hepatitis C patients: Outcomes from a case-control study. *Medicine*, 96(11), e6306.

63. Delanghe, J.R., Speeckaert, R. and Speeckaert, M.M. (2015) Behind the scenes of vitamin D binding protein: more than vitamin D binding. *Best Practice & Research.Clinical Endocrinology & Metabolism*, 29(5), 773-786.
64. Dluzen, D.F., Sun, D., Salzberg, A.C., Jones, N., Bushey, R.T., Robertson, G.P. and Lazarus, P. (2014) Regulation of UDP-glucuronosyltransferase 1A1 expression and activity by microRNA 491-3p. *The Journal of Pharmacology and Experimental Therapeutics*, 348(3), 465-477.
65. Doherty, D., Dvorkin, S.A., Rodriguez, E.P. and Thompson, P.D. (2014) Vitamin D receptor agonist EB1089 is a potent regulator of prostatic "intracrine" metabolism. *The Prostate*, 74(3), 273-285.
66. Donate-Correa, J., Martin-Nunez, E., Hernandez-Carballo, C., Ferri, C., Tagua, V.G., Delgado-Molinos, A., Lopez-Castillo, A., Rodriguez-Ramos, S., Cerro-Lopez, P., Lopez-Tarruella, V.C., Felipe-Garcia, R., Arevalo-Gomez, M.A., Perez-Delgado, N., Mora-Fernandez, C. and Navarro-Gonzalez, J.F. (2019) Fibroblast growth factor 23 expression in human calcified vascular tissues. *Aging*, 11(18), 7899-7913.
67. Dong, J., Wong, S.L., Lau, C.W., Lee, H.K., Ng, C.F., Zhang, L., Yao, X., Chen, Z.Y., Vanhoutte, P.M. and Huang, Y. (2012) Calcitriol protects renovascular function in hypertension by down-regulating angiotensin II type 1 receptors and reducing oxidative stress. *European Heart Journal*, 33(23), 2980-2990.
68. Du, P., Wang, A., Ma, Y. and Li, X. (2019) Association between the UGT1A1*28 allele and hyperbilirubinemia in HIV-positive patients receiving atazanavir: a meta-analysis. *Bioscience Reports*, 39(5), 10.1042/BSR20182105. Print 2019 May 31.
69. Duguay, Y., McGrath, M., Lepine, J., Gagne, J.F., Hankinson, S.E., Colditz, G.A., Hunter, D.J., Plante, M., Tetu, B., Belanger, A., Guillemette, C. and De Vivo, I. (2004) The functional UGT1A1 promoter polymorphism decreases endometrial cancer risk. *Cancer Research*, 64(3), 1202-1207.
70. Echchgadda, I., Song, C.S., Roy, A.K. and Chatterjee, B. (2004) Dehydroepiandrosterone sulfotransferase is a target for transcriptional induction by the vitamin D receptor. *Molecular Pharmacology*, 65(3), 720-729.

71. Edwards, P.A., Kennedy, M.A. and Mak, P.A. (2002) LXRs; oxysterol-activated nuclear receptors that regulate genes controlling lipid homeostasis. *Vascular Pharmacology,* 38(4), 249-256.
72. Eeckhoute, J., Formstecher, P. and Laine, B. (2004) Hepatocyte nuclear factor 4alpha enhances the hepatocyte nuclear factor 1alpha-mediated activation of transcription. *Nucleic Acids Research,* 32(8), 2586-2593.
73. Ehmer, U., Kalthoff, S., Fakundiny, B., Pabst, B., Freiberg, N., Naumann, R., Manns, M.P. and Strassburg, C.P. (2012) Gilbert syndrome redefined: a complex genetic haplotype influences the regulation of glucuronidation. *Hepatology (Baltimore, Md.),* 55(6), 1912-1921.
74. Erichsen, T.J., Aehlen, A., Ehmer, U., Kalthoff, S., Manns, M.P. and Strassburg, C.P. (2010) Regulation of the human bile acid UDP-glucuronosyltransferase 1A3 by the farnesoid X receptor and bile acids. *Journal of Hepatology,* 52(4), 570-578.
75. Fan, Z., Wirth, A.K., Chen, D., Wruck, C.J., Rauh, M., Buchfelder, M. and Savaskan, N. (2017) Nrf2-Keap1 pathway promotes cell proliferation and diminishes ferroptosis. *Oncogenesis,* 6(8), e371.
76. Ferrer-Mayorga, G., Gomez-Lopez, G., Barbachano, A., Fernandez-Barral, A., Pena, C., Pisano, D.G., Cantero, R., Rojo, F., Munoz, A. and Larriba, M.J. (2017) Vitamin D receptor expression and associated gene signature in tumour stromal fibroblasts predict clinical outcome in colorectal cancer. *Gut,* 66(8), 1449-1462.
77. Fetahu, I.S., Hobaus, J. and Kallay, E. (2014) Vitamin D and the epigenome. *Frontiers in Physiology,* 5, 164.
78. Finel, M., Li, X., Gardner-Stephen, D., Bratton, S., Mackenzie, P.I. and Radominska-Pandya, A. (2005) Human UDP-glucuronosyltransferase 1A5: identification, expression, and activity. *The Journal of Pharmacology and Experimental Therapeutics,* 315(3), 1143-1149.
79. Fishilevich, S., Nudel, R., Rappaport, N., Hadar, R., Plaschkes, I., Iny Stein, T., Rosen, N., Kohn, A., Twik, M., Safran, M., Lancet, D. and Cohen, D. (2017) GeneHancer: genome-wide integration of enhancers and target genes in GeneCards. *Database : The Journal of Biological Databases and Curation,* 2017, 10.1093/database/bax028.
80. Fleet, J.C. (2017) The role of vitamin D in the endocrinology controlling calcium homeostasis. *Molecular and Cellular Endocrinology,* 453, 36-45.

81. Fleet, J.C. and Schoch, R.D. (2010) Molecular mechanisms for regulation of intestinal calcium absorption by vitamin D and other factors. *Critical Reviews in Clinical Laboratory Sciences,* 47(4), 181-195.
82. Flores, O., Wang, Z., Knudsen, K.E. and Burnstein, K.L. (2010) Nuclear targeting of cyclin-dependent kinase 2 reveals essential roles of cyclin-dependent kinase 2 localization and cyclin E in vitamin D-mediated growth inhibition. *Endocrinology,* 151(3), 896-908.
83. Fujiwara, R., Chen, S., Karin, M. and Tukey, R.H. (2012) Reduced expression of UGT1A1 in intestines of humanized UGT1 mice via inactivation of NF-kappaB leads to hyperbilirubinemia. *Gastroenterology,* 142(1), 109-118.e2.
84. Fujiwara, R., Nakajima, M., Oda, S., Yamanaka, H., Ikushiro, S., Sakaki, T. and Yokoi, T. (2010) Interactions between human UDP-glucuronosyltransferase (UGT) 2B7 and UGT1A enzymes. *Journal of Pharmaceutical Sciences,* 99(1), 442-454.
85. Fujiwara, R., Nguyen, N., Chen, S. and Tukey, R.H. (2010) Developmental hyperbilirubinemia and CNS toxicity in mice humanized with the UDP glucuronosyltransferase 1 (UGT1) locus. *Proceedings of the National Academy of Sciences of the United States of America,* 107(11), 5024-5029.
86. Fujiwara, R., Yokoi, T. and Nakajima, M. (2016) Structure and Protein-Protein Interactions of Human UDP-Glucuronosyltransferases. *Frontiers in Pharmacology,* 7, 388.
87. Furue, M., Fuyuno, Y., Mitoma, C., Uchi, H. and Tsuji, G. (2018) Therapeutic Agents with AHR Inhibiting and NRF2 Activating Activity for Managing Chloracne. *Antioxidants (Basel, Switzerland),* 7(7), 10.3390/antiox7070090.
88. Garland, C.F., Kim, J.J., Mohr, S.B., Gorham, E.D., Grant, W.B., Giovannucci, E.L., Baggerly, L., Hofflich, H., Ramsdell, J.W., Zeng, K. and Heaney, R.P. (2014) Meta-analysis of all-cause mortality according to serum 25-hydroxyvitamin D. *American Journal of Public Health,* 104(8), e43-50.
89. Gil, A., Plaza-Diaz, J. and Mesa, M.D. (2018) Vitamin D: Classic and Novel Actions. *Annals of Nutrition & Metabolism,* 72(2), 87-95.
90. Glerup, H., Mikkelsen, K., Poulsen, L., Hass, E., Overbeck, S., Thomsen, J., Charles, P. and Eriksen, E., 2000. Commonly Recommended Daily Intake Of Vitamin D Is Not Sufficient If Sunlight Exposure Is Limited.

91. Goeman, F., De Nicola, F., D'Onorio De Meo, P., Pallocca, M., Elmi, B., Castrignano, T., Pesole, G., Strano, S., Blandino, G., Fanciulli, M. and Muti, P. (2014) VDR primary targets by genome-wide transcriptional profiling. *The Journal of Steroid Biochemistry and Molecular Biology*, 143, 348-356.
92. Gombart, A.F. (2009) The vitamin D-antimicrobial peptide pathway and its role in protection against infection. *Future Microbiology*, 4(9), 1151-1165.
93. Green, M. (2011) Cod liver oil and tuberculosis. *BMJ (Clinical Research Ed.)*, 343, d7505.
94. Gregory, P.A., Gardner-Stephen, D.A., Lewinsky, R.H., Duncliffe, K.N. and Mackenzie, P.I. (2003) Cloning and characterization of the human UDP-glucuronosyltransferase 1A8, 1A9, and 1A10 gene promoters: differential regulation through an interior-like region. *The Journal of Biological Chemistry*, 278(38), 36107-36114.
95. Grishkan, I.V., Fairchild, A.N., Calabresi, P.A. and Gocke, A.R. (2013) 1,25-Dihydroxyvitamin D3 selectively and reversibly impairs T helper-cell CNS localization. *Proceedings of the National Academy of Sciences of the United States of America*, 110(52), 21101-21106.
96. Guo, G.L., Lambert, G., Negishi, M., Ward, J.M., Brewer, H.B.,Jr, Kliewer, S.A., Gonzalez, F.J. and Sinal, C.J. (2003) Complementary roles of farnesoid X receptor, pregnane X receptor, and constitutive androstane receptor in protection against bile acid toxicity. *The Journal of Biological Chemistry*, 278(46), 45062-45071.
97. Haas, S., Pierl, C., Harth, V., Pesch, B., Rabstein, S., Bruning, T., Ko, Y., Hamann, U., Justenhoven, C., Brauch, H. and Fischer, H.P. (2006) Expression of xenobiotic and steroid hormone metabolizing enzymes in human breast carcinomas. *International Journal of Cancer*, 119(8), 1785-1791.
98. Hanel, A., Malmberg, H.R. and Carlberg, C. (2020) Genome-wide effects of chromatin on vitamin D signaling. *Journal of Molecular Endocrinology*,
99. Hanioka, N., Iwabu, H., Hanafusa, H., Nakada, S. and Narimatsu, S. (2012) Expression and inducibility of UDP-glucuronosyltransferase 1As in MCF-7 human breast carcinoma cells. *Basic & Clinical Pharmacology & Toxicology*, 110(3), 253-258.

100. Haq, A., Wimalawansa, S.J., Pludowski, P. and Anouti, F.A. (2018) Clinical practice guidelines for vitamin D in the United Arab Emirates. *The Journal of Steroid Biochemistry and Molecular Biology*, 175, 4-11.

101. Hashizume, T., Xu, Y., Mohutsky, M.A., Alberts, J., Hadden, C., Kalhorn, T.F., Isoherranen, N., Shuhart, M.C. and Thummel, K.E. (2008) Identification of human UDP-glucuronosyltransferases catalyzing hepatic 1alpha,25-dihydroxyvitamin D3 conjugation. *Biochemical Pharmacology*, 75(5), 1240-1250.

102. Haussler, M., Saini, R., Sabir, M., Dussik, C., Khan, Z., Whitfield, G., Griffin, K., Kaneko, I. and Jurutka, P., 2020. *Vitamin D Nutrient-Gene Interactions And Healthful Aging*.

103. Haussler, M.R., Whitfield, G.K., Kaneko, I., Forster, R., Saini, R., Hsieh, J.C., Haussler, C.A. and Jurutka, P.W. (2012) The role of vitamin D in the FGF23, klotho, and phosphate bone-kidney endocrine axis. *Reviews in Endocrine & Metabolic Disorders*, 13(1), 57-69.

104. Hayes, J.D. and Dinkova-Kostova, A.T. (2017) Epigenetic Control of NRF2-Directed Cellular Antioxidant Status in Dictating Life-Death Decisions. *Molecular Cell*, 68(1), 5-7.

105. Hayes, J.D. and McMahon, M. (2009) NRF2 and KEAP1 mutations: permanent activation of an adaptive response in cancer. *Trends in Biochemical Sciences*, 34(4), 176-188.

106. Hirotsu, Y., Katsuoka, F., Funayama, R., Nagashima, T., Nishida, Y., Nakayama, K., Engel, J.D. and Yamamoto, M. (2012) Nrf2-MafG heterodimers contribute globally to antioxidant and metabolic networks. *Nucleic Acids Research*, 40(20), 10228-10239.

107. Hirschmann, F., Krause, F. and Papenbrock, J. (2014) The multi-protein family of sulfotransferases in plants: composition, occurrence, substrate specificity, and functions. *Frontiers in Plant Science*, 5, 556.

108. Hoenderop, J.G., Nilius, B. and Bindels, R.J. (2005) Calcium absorption across epithelia. *Physiological Reviews*, 85(1), 373-422.

109. Holick, M.F. (1981) The cutaneous photosynthesis of previtamin D3: a unique photoendocrine system. *The Journal of Investigative Dermatology*, 77(1), 51-58.

110. Holick, M.F. (2004) Vitamin D: importance in the prevention of cancers, type 1 diabetes, heart disease, and osteoporosis. *The American Journal of Clinical Nutrition,* 79(3), 362-371.

111. Holick, M.F., Biancuzzo, R.M., Chen, T.C., Klein, E.K., Young, A., Bibuld, D., Reitz, R., Salameh, W., Ameri, A. and Tannenbaum, A.D. (2008) Vitamin D2 is as effective as vitamin D3 in maintaining circulating concentrations of 25-hydroxyvitamin D. *The Journal of Clinical Endocrinology and Metabolism,* 93(3), 677-681.

112. Holick, M.F., Binkley, N.C., Bischoff-Ferrari, H.A., Gordon, C.M., Hanley, D.A., Heaney, R.P., Murad, M.H., Weaver, C.M. and Endocrine Society. (2011) Evaluation, treatment, and prevention of vitamin D deficiency: an Endocrine Society clinical practice guideline. *The Journal of Clinical Endocrinology and Metabolism,* 96(7), 1911-1930.

113. Holick, M.F., Smith, E. and Pincus, S. (1987) Skin as the site of vitamin D synthesis and target tissue for 1,25-dihydroxyvitamin D3. Use of calcitriol (1,25-dihydroxyvitamin D3) for treatment of psoriasis. *Archives of Dermatology,* 123(12), 1677-1683a.

114. Hollis, B.W. (1984) Comparison of equilibrium and disequilibrium assay conditions for ergocalciferol, cholecalciferol and their major metabolites. *Journal of Steroid Biochemistry,* 21(1), 81-86.

115. Hu, D.G., Mackenzie, P.I., Lu, L., Meech, R. and McKinnon, R.A. (2015) Induction of human UDP-Glucuronosyltransferase 2B7 gene expression by cytotoxic anticancer drugs in liver cancer HepG2 cells. *Drug Metabolism and Disposition: The Biological Fate of Chemicals,* 43(5), 660-668.

116. Hustert, E., Zibat, A., Presecan-Siedel, E., Eiselt, R., Mueller, R., Fuss, C., Brehm, I., Brinkmann, U., Eichelbaum, M., Wojnowski, L. and Burk, O. (2001) Natural protein variants of pregnane X receptor with altered transactivation activity toward CYP3A4. *Drug Metabolism and Disposition: The Biological Fate of Chemicals,* 29(11), 1454-1459.

117. Ichiki, A., Miyazaki, T., Nodera, M., Suzuki, H. and Yanagisawa, H. (2008) Ascorbate inhibits apoptosis of Kupffer cells during warm ischemia/reperfusion injury. *Hepato-Gastroenterology,* 55(82-83), 338-344.

118. Iizuka, T., Ishii, Y., Itoh, K., Kiwamoto, T., Kimura, T., Matsuno, Y., Morishima, Y., Hegab, A.E., Homma, S., Nomura, A., Sakamoto, T., Shimura, M., Yoshida, A., Yamamoto, M. and Sekizawa, K. (2005) Nrf2-deficient mice are highly susceptible to cigarette smoke-induced emphysema. *Genes to Cells : Devoted to Molecular & Cellular Mechanisms,* 10(12), 1113-1125.

119. Ikushiro, S., Emi, Y., Kato, Y., Yamada, S. and Sakaki, T. (2006) Monospecific antipeptide antibodies against human hepatic UDP-glucuronosyltransferase 1A subfamily (UGT1A) isoforms. *Drug Metabolism and Pharmacokinetics,* 21(1), 70-74.

120. Itoh, K., Wakabayashi, N., Katoh, Y., Ishii, T., Igarashi, K., Engel, J.D. and Yamamoto, M. (1999) Keap1 represses nuclear activation of antioxidant responsive elements by Nrf2 through binding to the amino-terminal Neh2 domain. *Genes & Development,* 13(1), 76-86.

121. Iyanagi, T. (2007) Molecular mechanism of phase I and phase II drug-metabolizing enzymes: implications for detoxification. *International Review of Cytology,* 260, 35-112.

122. Izukawa, T., Nakajima, M., Fujiwara, R., Yamanaka, H., Fukami, T., Takamiya, M., Aoki, Y., Ikushiro, S., Sakaki, T. and Yokoi, T. (2009) Quantitative analysis of UDP-glucuronosyltransferase (UGT) 1A and UGT2B expression levels in human livers. *Drug Metabolism and Disposition: The Biological Fate of Chemicals,* 37(8), 1759-1768.

123. Jain, S.K. and Micinski, D. (2013) Vitamin D upregulates glutamate cysteine ligase and glutathione reductase, and GSH formation, and decreases ROS and MCP-1 and IL-8 secretion in high-glucose exposed U937 monocytes. *Biochemical and Biophysical Research Communications,* 437(1), 7-11.

124. Jean, G., Souberbielle, J. and Chazot, C., 2020. *Vitamin D In Chronic Kidney Disease And Dialysis Patients*.

125. Jelinek, G.A., Marck, C.H., Weiland, T.J., Pereira, N., van der Meer, D.M. and Hadgkiss, E.J. (2015) Latitude, sun exposure and vitamin D supplementation: associations with quality of life and disease outcomes in a large international cohort of people with multiple sclerosis. *BMC Neurology,* 15, 132-015-0394-1.

126. Jiang, L., Liang, S.C., Wang, C., Ge, G.B., Huo, X.K., Qi, X.Y., Deng, S., Liu, K.X. and Ma, X.C. (2015) Identifying and applying a highly selective probe to

simultaneously determine the O-glucuronidation activity of human UGT1A3 and UGT1A4. *Scientific Reports*, 5, 9627.

127. Jiraskova, A., Bortolussi, G., Dostalova, G., Eremiasova, L., Golan, L., Danzig, V., Linhart, A. and Vitek, L. (2017) Serum Bilirubin Levels and Promoter Variations in HMOX1 and UGT1A1 Genes in Patients with Fabry Disease. *Oxidative Medicine and Cellular Longevity*, 2017, 9478946.

128. Jones, G., Prosser, D.E. and Kaufmann, M. (2014) Cytochrome P450-mediated metabolism of vitamin D. *Journal of Lipid Research*, 55(1), 13-31.

129. Kadakol, A., Ghosh, S.S., Sappal, B.S., Sharma, G., Chowdhury, J.R. and Chowdhury, N.R. (2000) Genetic lesions of bilirubin uridine-diphosphoglucuronate glucuronosyltransferase (UGT1A1) causing Crigler-Najjar and Gilbert syndromes: correlation of genotype to phenotype. *Human Mutation*, 16(4), 297-306.

130. Kaeding, J., Belanger, J., Caron, P., Verreault, M., Belanger, A. and Barbier, O. (2008) Calcitrol (1alpha,25-dihydroxyvitamin D3) inhibits androgen glucuronidation in prostate cancer cells. *Molecular Cancer Therapeutics*, 7(2), 380-390.

131. Kahlon, T.S., Chiu, M.C. and Chapman, M.H. (2008) Steam cooking significantly improves in vitro bile acid binding of collard greens, kale, mustard greens, broccoli, green bell pepper, and cabbage. *Nutrition Research (New York, N.Y.)*, 28(6), 351-357.

132. Kalousova, M., Dusilova-Sulkova, S., Zakiyanov, O., Kostirova, M., Safranek, R., Tesar, V. and Zima, T., 2020. *Vitamin D Binding Protein Is Not Involved In Vitamin D Deficiency In Patients With Chronic Kidney Disease*

133. Kalthoff, S., Ehmer, U., Freiberg, N., Manns, M.P. and Strassburg, C.P. (2010) Interaction between oxidative stress sensor Nrf2 and xenobiotic-activated aryl hydrocarbon receptor in the regulation of the human phase II detoxifying UDP-glucuronosyltransferase 1A10. *The Journal of Biological Chemistry*, 285(9), 5993-6002.

134. Kalthoff, S., Ehmer, U., Freiberg, N., Manns, M.P. and Strassburg, C.P. (2010) Coffee induces expression of glucuronosyltransferases by the aryl hydrocarbon receptor and Nrf2 in liver and stomach. *Gastroenterology*, 139(5), 1699-710, 1710.e1-2.

135. Kansanen, E., Kuosmanen, S.M., Leinonen, H. and Levonen, A.L. (2013) The Keap1-Nrf2 pathway: Mechanisms of activation and dysregulation in cancer. *Redox Biology,* 1, 45-49.

136. Keppler, D. (2014) The roles of MRP2, MRP3, OATP1B1, and OATP1B3 in conjugated hyperbilirubinemia. *Drug Metabolism and Disposition: The Biological Fate of Chemicals,* 42(4), 561-565.

137. Kerner, S.A., Scott, R.A. and Pike, J.W. (1989) Sequence elements in the human osteocalcin gene confer basal activation and inducible response to hormonal vitamin D3. *Proceedings of the National Academy of Sciences of the United States of America,* 86(12), 4455-4459.

138. Keum, Y.S., Owuor, E.D., Kim, B.R., Hu, R. and Kong, A.N. (2003) Involvement of Nrf2 and JNK1 in the activation of antioxidant responsive element (ARE) by chemopreventive agent phenethyl isothiocyanate (PEITC). *Pharmaceutical Research,* 20(9), 1351-1356.

139. Khan, A.A., Dragt, B.S., Porte, R.J. and Groothuis, G.M. (2010) Regulation of VDR expression in rat and human intestine and liver--consequences for CYP3A expression. *Toxicology in Vitro : An International Journal Published in Association with BIBRA,* 24(3), 822-829.

140. Khedkar, S.A., Samad, M.A., Choudhury, S., Lee, J.Y., Zhang, D., Thadhani, R.I., Karumanchi, S.A., Rigby, A.C. and Kang, P.M. (2017) Identification of Novel Non-secosteroidal Vitamin D Receptor Agonists with Potent Cardioprotective Effects and devoid of Hypercalcemia. *Scientific Reports,* 7(1), 8427-017-08670-y.

141. Khurana, N. and Sikka, S.C. (2018) Targeting Crosstalk between Nrf-2, NF-kappaB and Androgen Receptor Signaling in Prostate Cancer. *Cancers,* 10(10), 10.3390/cancers10100352.

142. Khurana, N., Talwar, S., Chandra, P.K., Sharma, P., Abdel-Mageed, A.B., Mondal, D. and Sikka, S.C. (2016) Sulforaphane increases the efficacy of anti-androgens by rapidly decreasing androgen receptor levels in prostate cancer cells. *International Journal of Oncology,* 49(4), 1609-1619.

143. Kim, S., Yamazaki, M., Zella, L.A., Shevde, N.K. and Pike, J.W. (2006) Activation of receptor activator of NF-kappaB ligand gene expression by 1,25-

dihydroxyvitamin D3 is mediated through multiple long-range enhancers. *Molecular and Cellular Biology*, 26(17), 6469-6486.

144. Kim, S., Yamazaki, M., Zella, L.A., Shevde, N.K. and Pike, J.W. (2006) Activation of receptor activator of NF-kappaB ligand gene expression by 1,25-dihydroxyvitamin D3 is mediated through multiple long-range enhancers. *Molecular and Cellular Biology*, 26(17), 6469-6486.

145. Kim, S.G., Kim, B.K., Kim, K. and Fang, S. (2016) Bile Acid Nuclear Receptor Farnesoid X Receptor: Therapeutic Target for Nonalcoholic Fatty Liver Disease. *Endocrinology and Metabolism (Seoul, Korea)*, 31(4), 500-504.

146. Kiran, K., Ansari, S.A., Srivastava, R., Lodhi, N., Chaturvedi, C.P., Sawant, S.V. and Tuli, R. (2006) The TATA-box sequence in the basal promoter contributes to determining light-dependent gene expression in plants. *Plant Physiology*, 142(1), 364-376.

147. Kitamura, H. and Motohashi, H. (2018) NRF2 addiction in cancer cells. *Cancer Science*, 109(4), 900-911.

148. Koenig, G. and Seneff, S., 2015. *Gamma-Glutamyltransferase: A Predictive Biomarker Of Cellular Antioxidant Inadequacy And Disease Risk*.

149. Konaka, K., Sakurada, T., Saito, T., Mori, S., Imanishi, M., Kakiuchi, S., Fushitani, S. and Ishizawa, K. (2019) Study on the Optimal Dose of Irinotecan for Patients with Heterozygous Uridine Diphosphate-Glucuronosyltransferase 1A1 (UGT1A1). *Biological & Pharmaceutical Bulletin*, 42(11), 1839-1845.

150. Kraft, A.D., Johnson, D.A. and Johnson, J.A. (2004) Nuclear factor E2-related factor 2-dependent antioxidant response element activation by tert-butylhydroquinone and sulforaphane occurring preferentially in astrocytes conditions neurons against oxidative insult. *The Journal of Neuroscience : The Official Journal of the Society for Neuroscience*, 24(5), 1101-1112.

151. Kraichely, D.M., Collins, J.J.,3rd, DeLisle, R.K. and MacDonald, P.N. (1999) The autonomous transactivation domain in helix H3 of the vitamin D receptor is required for transactivation and coactivator interaction. *The Journal of Biological Chemistry*, 274(20), 14352-14358.

152. Krasowski, M.D., Ai, N., Hagey, L.R., Kollitz, E.M., Kullman, S.W., Reschly, E.J. and Ekins, S. (2011) The evolution of farnesoid X, vitamin D, and pregnane

X receptors: insights from the green-spotted pufferfish (Tetraodon nigriviridis) and other non-mammalian species. *BMC Biochemistry*, 12, 5-2091-12-5.

153. Krasowski, M.D., Yasuda, K., Hagey, L.R. and Schuetz, E.G. (2005) Evolutionary selection across the nuclear hormone receptor superfamily with a focus on the NR1I subfamily (vitamin D, pregnane X, and constitutive androstane receptors). *Nuclear Receptor*, 3, 2-1336-3-2.

154. Krishnan, A.V., Shinghal, R., Raghavachari, N., Brooks, J.D., Peehl, D.M. and Feldman, D. (2004) Analysis of vitamin D-regulated gene expression in LNCaP human prostate cancer cells using cDNA microarrays. *The Prostate*, 59(3), 243-251.

155. Kubo, E., Chhunchha, B., Singh, P., Sasaki, H. and Singh, D.P. (2017) Sulforaphane reactivates cellular antioxidant defense by inducing Nrf2/ARE/Prdx6 activity during aging and oxidative stress. *Scientific Reports*, 7(1), 14130-017-14520-8.

156. Kutsuno, Y., Itoh, T., Tukey, R.H. and Fujiwara, R. (2014) Glucuronidation of drugs and drug-induced toxicity in humanized UDP-glucuronosyltransferase 1 mice. *Drug Metabolism and Disposition: The Biological Fate of Chemicals*, 42(7), 1146-1152.

157. Kutuzova, G.D. and DeLuca, H.F. (2007) 1,25-Dihydroxyvitamin D3 regulates genes responsible for detoxification in intestine. *Toxicology and Applied Pharmacology*, 218(1), 37-44.

158. Lacko, M., Oude Ophuis, M.B., Peters, W.H. and Manni, J.J. (2009) Genetic polymorphisms of smoking-related carcinogen detoxifying enzymes and head and neck cancer susceptibility. *Anticancer Research*, 29(2), 753-761.

159. Lagishetty, V., Liu, N. and Hewison, M., 2011. *Vitamin D Metabolism And Innate Immunity*.

160. Lazarus, P., Blevins-Primeau, A.S., Zheng, Y. and Sun, D. (2009) Potential role of UGT pharmacogenetics in cancer treatment and prevention: focus on tamoxifen. *Annals of the New York Academy of Sciences*, 1155, 99-111.

161. Lee, W.C., Mokhtar, S.S., Munisamy, S., Yahaya, S. and Rasool, A.H.G. (2018) Vitamin D status and oxidative stress in diabetes mellitus. *Cellular and Molecular Biology (Noisy-Le-Grand, France)*, 64(7), 60-69.

162. Lehmann, J.M.(.1.)., Watson, M.A.(.1.)., Kliewer, S.A. (1,4), McKee, D.D.(.2.)., Moore, J.T.(.2.). and Willson, T.M.(.3.). (1998) The human orphan nuclear receptor PXR is activated by compounds that regulate CYP3A4 gene expression and cause drug interactions. *Journal of Clinical Investigation*, 102(5), 1016-1023.

163. Levesque, E., Girard, H., Journault, K., Lepine, J. and Guillemette, C. (2007) Regulation of the UGT1A1 bilirubin-conjugating pathway: role of a new splicing event at the UGT1A locus. *Hepatology (Baltimore, Md.)*, 45(1), 128-138.

164. Levresse, V., Marek, L., Blumberg, D. and Heasley, L.E. (2002) Regulation of platinum-compound cytotoxicity by the c-Jun N-terminal kinase and c-Jun signaling pathway in small-cell lung cancer cells. *Molecular Pharmacology*, 62(3), 689-697.

165. Li, F., Ling, X., Huang, H., Brattain, L., Apontes, P., Wu, J., Binderup, L. and Brattain, M.G. (2005) Differential regulation of survivin expression and apoptosis by vitamin D3 compounds in two isogenic MCF-7 breast cancer cell sublines. *Oncogene,* 24(8), 1385-1395.

166. Linus Pauling Institute. 2020. *Vitamin D*. [online] Available at: <https://lpi.oregonstate.edu/mic/vitamins/vitamin-D> [Accessed 8 April 2020].

167. Littlejohns, T.J., Henley, W.E., Lang, I.A., Annweiler, C., Beauchet, O., Chaves, P.H., Fried, L., Kestenbaum, B.R., Kuller, L.H., Langa, K.M., Lopez, O.L., Kos, K., Soni, M. and Llewellyn, D.J. (2014) Vitamin D and the risk of dementia and Alzheimer disease. *Neurology,* 83(10), 920-928.

168. Liu, G.H., Qu, J. and Shen, X. (2008) NF-kappaB/p65 antagonizes Nrf2-ARE pathway by depriving CBP from Nrf2 and facilitating recruitment of HDAC3 to MafK. *Biochimica Et Biophysica Acta,* 1783(5), 713-727.

169. Liu, Y. and Coughtrie, M.W.H. (2017) Revisiting the Latency of Uridine Diphosphate-Glucuronosyltransferases (UGTs)-How Does the Endoplasmic Reticulum Membrane Influence Their Function? *Pharmaceutics,* 9(3), 10.3390/pharmaceutics9030032.

170. Liu, Z., Zhou, T., Ziegler, A.C., Dimitrion, P. and Zuo, L. (2017) Oxidative Stress in Neurodegenerative Diseases: From Molecular Mechanisms to Clinical Applications. *Oxidative Medicine and Cellular Longevity,* 2017, 2525967.

171. Liu, Z.G., Jiang, G., Tang, J., Wang, H., Feng, G., Chen, F., Tu, Z., Liu, G., Zhao, Y., Peng, M.J., He, Z.W., Chen, X.Y., Lindsay, H., Xia, Y.F. and Li, X.N. (2016) c-Fos over-expression promotes radioresistance and predicts poor prognosis in malignant glioma. *Oncotarget,* 7(40), 65946-65956.

172. Loboda, A., Damulewicz, M., Pyza, E., Jozkowicz, A. and Dulak, J. (2016) Role of Nrf2/HO-1 system in development, oxidative stress response and diseases: an 73(17), 3221-3247.

173. Lou, H., Du, S., Ji, Q. and Stolz, A. (2006) Induction of AKR1C2 by phase II inducers: identification of a distal consensus antioxidant response element regulated by NRF2. *Molecular Pharmacology,* 69(5), 1662-1672.

174. Lu, K., Alcivar, A.L., Ma, J., Foo, T.K., Zywea, S., Mahdi, A., Huo, Y., Kensler, T.W., Gatza, M.L. and Xia, B. (2017) NRF2 Induction Supporting Breast Cancer Cell Survival Is Enabled by Oxidative Stress-Induced DPP3-KEAP1 Interaction. *Cancer Research,* 77(11), 2881-2892.

175. Luo, G., Cunningham, M., Kim, S., Burn, T., Lin, J., Sinz, M., Hamilton, G., Rizzo, C., Jolley, S., Gilbert, D., Downey, A., Mudra, D., Graham, R., Carroll, K., Xie, J., Madan, A., Parkinson, A., Christ, D., Selling, B., LeCluyse, E. and Gan, L.S. (2002) CYP3A4 induction by drugs: correlation between a pregnane X receptor reporter gene assay and CYP3A4 expression in human hepatocytes. *Drug Metabolism and Disposition: The Biological Fate of Chemicals,* 30(7), 795-804.

176. Luo, Y., Eggler, A.L., Liu, D., Liu, G., Mesecar, A.D. and van Breemen, R.B. (2007) Sites of alkylation of human Keap1 by natural chemoprevention agents. *Journal of the American Society for Mass Spectrometry*, 18(12), 2226-2232.

177. Ma, J.Q., Tuersun, H., Jiao, S.J., Zheng, J.H., Xiao, J.B. and Hasim, A. (2015) Functional Role of NRF2 in Cervical Carcinogenesis. *PloS One*, 10(8), e0133876.

178. Maguire, O., Pollock, C., Martin, P., Owen, A., Smyth, T., Doherty, D., Campbell, M.J., McClean, S. and Thompson, P. (2012) Regulation of CYP3A4 and CYP3A5 expression and modulation of "intracrine" metabolism of androgens in prostate cells by liganded vitamin D receptor. *Molecular and Cellular Endocrinology,* 364(1-2), 54-64.

179. Makishima, M., Lu, T.T., Xie, W., Whitfield, G.K., Domoto, H., Evans, R.M., Haussler, M.R. and Mangelsdorf, D.J. (2002) Vitamin D receptor as an intestinal bile acid sensor. *Science (New York, N.Y.),* 296(5571), 1313-1316.

180. Malfatti, M.A., Ubick, E.A. and Felton, J.S. (2005) The impact of glucuronidation on the bioactivation and DNA adduction of the cooked-food carcinogen 2-amino-1-methyl-6-phenylimidazo[4,5-b]pyridine in vivo. *Carcinogenesis,* 26(11), 2019-2028.

181. Marton, M., Tihanyi, N., Gyulavari, P., Banhegyi, G. and Kapuy, O. (2018) NRF2-regulated cell cycle arrest at early stage of oxidative stress response mechanism. *PloS One,* 13(11), e0207949.

182. Masuno, H., Ikura, T., Morizono, D., Orita, I., Yamada, S., Shimizu, M. and Ito, N. (2013) Crystal structures of complexes of vitamin D receptor ligand-binding domain with lithocholic acid derivatives. *Journal of Lipid Research,* 54(8), 2206-2213.

183. Mattevi, V.S. and Tagliari, C.F. (2017) Pharmacogenetic considerations in the treatment of HIV. *Pharmacogenomics,* 18(1), 85-98.

184. McMullan, C.J., Borgi, L., Curhan, G.C., Fisher, N. and Forman, J.P. (2017) The effect of vitamin D on renin-angiotensin system activation and blood pressure: a randomized control trial. *Journal of Hypertension,* 35(4), 822-829.

185. Meyer, M.B., Goetsch, P.D. and Pike, J.W. (2012) VDR/RXR and TCF4/beta-catenin cistromes in colonic cells of colorectal tumor origin: impact on c-FOS and c-MYC gene expression. *Molecular Endocrinology (Baltimore, Md.),* 26(1), 37-51.

186. Morelli, S., Buitrago, C., Boland, R. and de Boland, A.R. (2001) The stimulation of MAP kinase by 1,25(OH)(2)-vitamin D(3) in skeletal muscle cells is mediated by protein kinase C and calcium. *Molecular and Cellular Endocrinology,* 173(1-2), 41-52.

187. Morris, H.A. and Anderson, P.H. (2010) Autocrine and paracrine actions of vitamin d. *The Clinical Biochemist.Reviews,* 31(4), 129-138.

188. Mottino, A.D. and Rodriguez Garay, E.A. (1987) Influence of uridine diphosphoglucuronic acid on bilirubin glucuronidation in liver microsomes from normal and spironolactone-treated rats. *Acta Physiologica Et Pharmacologica Latinoamericana : Organo De La Asociacion Latinoamericana De Ciencias Fisiologicas y De La Asociacion Latinoamericana De Farmacologia,* 37(4), 479-484.

189. Mundy, G. and Guise, T., 2020. *Hormonal Control Of Calcium Homeostasis*. [online] Indiana University School of Medicine. Available at: <https://indiana.pure.elsevier.com/en/publications/hormonal-control-of-calcium-homeostasis> [Accessed 9 April 2020].

190. Murphy, J.F., Hughes, I., Verrier Jones, E.R., Gaskell, S. and Pike, A.W. (1981) Pregnanediols and breast milk jaundice. *Archives of Disease in Childhood,* 56(6), 474-476.

191. Myzak MC, Hardin K, Wang R, Dashwood RH, Ho E. Sulforaphane inhibits histone deacetylase in BPH-1, LNCaP and PC-3 prostate epithelial cells. Carcinogenesis. 2006;27:811–9.

192. Myzak MC, Karplus PA, Chung FL, Dashwood RH. A novel mechanism of chemoprotection by sulforaphane: inhibition of histone deacetylase. Cancer Res. 2004;64:5767–74.

193. Nakai, K., Fujii, H., Kono, K., Goto, S., Kitazawa, R., Kitazawa, S., Hirata, M., Shinohara, M., Fukagawa, M. and Nishi, S. (2014) Vitamin D activates the Nrf2-Keap1 antioxidant pathway and ameliorates nephropathy in diabetic rats. *American Journal of Hypertension*, 27(4), 586-595.

194. Nakamura, A., Nakajima, M., Yamanaka, H., Fujiwara, R. and Yokoi, T. (2008) Expression of UGT1A and UGT2B mRNA in human normal tissues and various cell lines. *Drug Metabolism and Disposition: The Biological Fate of Chemicals*, 36(8), 1461-1464.

195. Narvaez, C.J., Matthews, D., LaPorta, E., Simmons, K.M., Beaudin, S. and Welsh, J. (2014) The impact of vitamin D in breast cancer: genomics, pathways, metabolism. *Frontiers in Physiology*, 5, 213.

196. Nguyen, T.T., Ung, T.T., Kim, N.H. and Jung, Y.D. (2018) Role of bile acids in colon carcinogenesis. *World Journal of Clinical Cases,* 6(13), 577-588.

197. Nioi, P., McMahon, M., Itoh, K., Yamamoto, M. and Hayes, J.D. (2003) Identification of a novel Nrf2-regulated antioxidant response element (ARE) in the mouse NAD(P)H:quinone oxidoreductase 1 gene: reassessment of the ARE consensus sequence. *The Biochemical Journal,* 374(Pt 2), 337-348.

198. Nioi, P., Nguyen, T., Sherratt, P.J. and Pickett, C.B. (2005) The carboxy-terminal Neh3 domain of Nrf2 is required for transcriptional activation. *Molecular and Cellular Biology*, 25(24), 10895-10906.

199. Norman, A.W. (2008) From vitamin D to hormone D: fundamentals of the vitamin D endocrine system essential for good health. *The American Journal of Clinical Nutrition,* 88(2), 491S-499S.

200. Nutrition classics from The Journal of Biological Chemistry 15:167-175, 1913. The necessity of certain lipins in the diet during growth. By E. V. McCollum and Marguerite Davis. (1973) *Nutrition Reviews,* 31(9), 280-281.

201. Oda, S., Kato, Y., Hatakeyama, M., Iwamura, A., Fukami, T., Kume, T., Yokoi, T. and Nakajima, M. (2017) Evaluation of expression and glycosylation status of UGT1A10 in Supersomes and intestinal epithelial cells with a novel specific UGT1A10 monoclonal antibody. *Drug Metabolism and Disposition: The Biological Fate of Chemicals,* 45(9), 1027-1034.

202. Ohri, S., Sharma, D. and Dixit, A. (2002) Modulation of c-myc and c-fos gene expression in regenerating rat liver by 2-mercaptopropionylglycine. *Cell Biology International,* 26(2), 187-192.

203. Onal, M., St John, H.C., Danielson, A.L., Markert, J.W., Riley, E.M. and Pike, J.W. (2016) Unique Distal Enhancers Linked to the Mouse Tnfsf11 Gene Direct Tissue-Specific and Inflammation-Induced Expression of RANKL. *Endocrinology,* 157(2), 482-496.

204. Osanai, M. and Lee, G.H. (2016) CYP24A1-induced vitamin D insufficiency promotes breast cancer growth. *Oncology Reports,* 36(5), 2755-2762.

205. Palmer, S.C., McGregor, D.O., Craig, J.C., Elder, G., Macaskill, P. and Strippoli, G.F. (2009) Vitamin D compounds for people with chronic kidney disease requiring dialysis. *The Cochrane Database of Systematic Reviews,* (4):CD005633. doi(4), CD005633.

206. Pan, H., Wang, H., Wang, X., Zhu, L. and Mao, L. (2012) The absence of Nrf2 enhances NF-kappaB-dependent inflammation following scratch injury in mouse primary cultured astrocytes. *Mediators of Inflammation,* 2012, 217580.

207. Papageorgiou, I. and Court, M.H. (2017) Identification and validation of microRNAs directly regulating the UDP-glucuronosyltransferase 1A subfamily enzymes by a functional genomics approach. *Biochemical Pharmacology,* 137, 93-106.

208. Pascussi, J.M., Drocourt, L., Fabre, J.M., Maurel, P. and Vilarem, M.J. (2000) Dexamethasone induces pregnane X receptor and retinoid X receptor-alpha

expression in human hepatocytes: Synergistic increase of CYP3A4 induction by pregnane X receptor activators. *Molecular Pharmacology*, 58(2), 361-372.

209. Paul, S., Ghosh, S., Mandal, S., Sau, S. and Pal, M. (2018) NRF2 transcriptionally activates the heat shock factor 1 promoter under oxidative stress and affects survival and migration potential of MCF7 cells. *The Journal of Biological Chemistry,* 293(50), 19303-19316.

210. Pena, C., Garcia, J.M., Silva, J., Garcia, V., Rodriguez, R., Alonso, I., Millan, I., Salas, C., de Herreros, A.G., Munoz, A. and Bonilla, F. (2005) E-cadherin and vitamin D receptor regulation by SNAIL and ZEB1 in colon cancer: clinicopathological correlations. *Human Molecular Genetics,* 14(22), 3361-3370.

211. Penner, N., Xu, L. and Prakash, C. (2012) Radiolabeled absorption, distribution, metabolism, and excretion studies in drug development: why, when, and how? *Chemical Research in Toxicology,* 25(3), 513-531.

212. Penning, T.M. (2017) Aldo-Keto Reductase Regulation by the Nrf2 System: Implications for Stress Response, Chemotherapy Drug Resistance, and Carcinogenesis. *Chemical Research in Toxicology,* 30(1), 162-176.

213. Petschnigg, J., Groisman, B., Kotlyar, M., Taipale, M., Zheng, Y., Kurat, C.F., Sayad, A., Sierra, J.R., Mattiazzi Usaj, M., Snider, J., Nachman, A., Krykbaeva, I., Tsao, M.S., Moffat, J., Pawson, T., Lindquist, S., Jurisica, I. and Stagljar, I. (2014) The mammalian-membrane two-hybrid assay (MaMTH) for probing membrane-protein interactions in human cells. *Nature Methods*, 11(5), 585-592.

214. Pike, J.W. (2011) Genome-wide principles of gene regulation by the vitamin D receptor and its activating ligand. *Molecular and Cellular Endocrinology,* 347(1-2), 3-10.

215. Pike, J.W. and Meyer, M.B. (2012) The vitamin D receptor: new paradigms for the regulation of gene expression by 1,25-dihydroxyvitamin D3. *Rheumatic Diseases Clinics of North America,* 38(1), 13-27.

216. Pike, J.W., Meyer, M.B., Benkusky, N.A., Lee, S.M., St John, H., Carlson, A., Onal, M. and Shamsuzzaman, S. (2016) Genomic Determinants of Vitamin D-Regulated Gene Expression. *Vitamins and Hormones*, 100, 21-44.

217. Prevostel, C., Rammah-Bouazza, C., Trauchessec, H., Canterel-Thouennon, L., Busson, M., Ychou, M. and Blache, P. (2016) SOX9 is an atypical intestinal

tumor suppressor controlling the oncogenic Wnt/ss-catenin signaling. *Oncotarget,* 7(50), 82228-82243.

218. Priemel, M., von Domarus, C., Klatte, T.O., Kessler, S., Schlie, J., Meier, S., Proksch, N., Pastor, F., Netter, C., Streichert, T., Puschel, K. and Amling, M. (2010) Bone mineralization defects and vitamin D deficiency: histomorphometric analysis of iliac crest bone biopsies and circulating 25-hydroxyvitamin D in 675 patients. *Journal of Bone and Mineral Research : The Official Journal of the American Society for Bone and Mineral Research,* 25(2), 305-312.

219. Protiva, P., Cross, H.S., Hopkins, M.E., Kallay, E., Bises, G., Dreyhaupt, E., Augenlicht, L., Lipkin, M., Lesser, M., Livote, E. and Holt, P.R. (2009) Chemoprevention of colorectal neoplasia by estrogen: potential role of vitamin D activity. *Cancer Prevention Research (Philadelphia, Pa.),* 2(1), 43-51.

220. Rachez, C., Gamble, M., Chang, C.P., Atkins, G.B., Lazar, M.A. and Freedman, L.P. (2000) The DRIP complex and SRC-1/p160 coactivators share similar nuclear receptor binding determinants but constitute functionally distinct complexes. *Molecular and Cellular Biology,* 20(8), 2718-2726.

221. Radominska-Pandya, A., Bratton, S.M., Redinbo, M.R. and Miley, M.J. (2010) The crystal structure of human UDP-glucuronosyltransferase 2B7 C-terminal end is the first mammalian UGT target to be revealed: the significance for human UGTs from both the 1A and 2B families. *Drug Metabolism Reviews,* 42(1), 133-144.

222. Ramagopalan, S.V., Heger, A., Berlanga, A.J., Maugeri, N.J., Lincoln, M.R., Burrell, A., Handunnetthi, L., Handel, A.E., Disanto, G., Orton, S.M., Watson, C.T., Morahan, J.M., Giovannoni, G., Ponting, C.P., Ebers, G.C. and Knight, J.C. (2010) A ChIP-seq defined genome-wide map of vitamin D receptor binding: associations with disease and evolution. *Genome Research,* 20(10), 1352-1360.

223. Ramchandani, R.P., Wang, Y., Booth, B.P., Ibrahim, A., Johnson, J.R., Rahman, A., Mehta, M., Innocenti, F., Ratain, M.J. and Gobburu, J.V. (2007) The role of SN-38 exposure, UGT1A1*28 polymorphism, and baseline bilirubin level in predicting severe irinotecan toxicity. *Journal of Clinical Pharmacology,* 47(1), 78-86.

224. Raynal, C., Pascussi, J.M., Leguelinel, G., Breuker, C., Kantar, J., Lallemant, B., Poujol, S., Bonnans, C., Joubert, D., Hollande, F., Lumbroso, S., Brouillet, J.P.

and Evrard, A. (2010) Pregnane X Receptor (PXR) expression in colorectal cancer cells restricts irinotecan chemosensitivity through enhanced SN-38 glucuronidation. *Molecular Cancer,* 9, 46-4598-9-46.

225. Reschly, E.J. and Krasowski, M.D. (2006) Evolution and function of the NR1I nuclear hormone receptor subfamily (VDR, PXR, and CAR) with respect to metabolism of xenobiotics and endogenous compounds. *Current Drug Metabolism,* 7(4), 349-365.

226. Ribeiro, L.F., Ribeiro, L.F.C., Barreto, M.Q. and Ward, R.J. (2018) Protein Engineering Strategies to Expand CRISPR-Cas9 Applications. *International Journal of Genomics,* 2018, 1652567.

227. Riera, P., Salazar, J., Virgili, A.C., Tobena, M., Sebio, A., Gallano, P., Barnadas, A. and Paez, D. (2018) Relevance of CYP3A4*20, UGT1A1*37 and UGT1A1*28 variants in irinotecan-induced severe toxicity. *British Journal of Clinical Pharmacology,* 84(6), 1389-1392.

228. Roizen, J.D., Casella, A., Lai, M., Long, C., Tara, Z., Caplan, I., O'Lear, L. and Levine, M.A. (2018) Decreased Serum 25-Hydroxyvitamin D in Aging Male Mice Is Associated With Reduced Hepatic Cyp2r1 Abundance. *Endocrinology,* 159(8), 3083-3089.

229. Rondini, E.A., Fang, H., Runge-Morris, M. and Kocarek, T.A. (2014) Regulation of human cytosolic sulfotransferases 1C2 and 1C3 by nuclear signaling pathways in LS180 colorectal adenocarcinoma cells. *Drug Metabolism and Disposition: The Biological Fate of Chemicals,* 42(3), 361-368.

230. Rouleau, M., Collin, P., Bellemare, J., Harvey, M. and Guillemette, C. (2013) Protein-protein interactions between the bilirubin-conjugating UDP-glucuronosyltransferase UGT1A1 and its shorter isoform 2 regulatory partner derived from alternative splicing. *The Biochemical Journal,* 450(1), 107-114.

231. Rowland, n., Miners, J. and Mackenzie, P., 2020. *UDP-Glucuronosyltransferases : Their Role In Drug Metabolism And Etoxification*. [online] Semanticscholar.org. Available at: <https://www.semanticscholar.org/paper/UDP-glucuronosyltransferases-%3A-Their-role-in-drug-Rowland-Miners/0bcac0834e700540f016229dce7c14dd0f641e3e> [Accessed 9 April 2020].

232. Royalsocietypublishing.org. 2020. *Crystalline Vitamin D | Proceedings Of The Royal Society Of London. Series B, Containing Papers Of A Biological Character*. [online] Available at: <https://royalsocietypublishing.org/doi/10.1098/rspb.1932.0008> [Accessed 9 April 2020].

233. Ryan, J.W., Anderson, P.H. and Morris, H.A. (2015) Pleiotropic Activities of Vitamin D Receptors - Adequate Activation for Multiple Health Outcomes. *The Clinical Biochemist.Reviews,* 36(2), 53-61.

234. Ryan, J.W., Reinke, D., Kogawa, M., Turner, A.G., Atkins, G.J., Anderson, P.H. and Morris, H.A. (2013) Novel targets of vitamin D activity in bone: action of the vitamin D receptor in osteoblasts, osteocytes and osteoclasts. *Current Drug Targets,* 14(14), 1683-1688.

235. Ryu, H., Lee, J., Zaman, K., Kubilis, J., Ferrante, R.J., Ross, B.D., Neve, R. and Ratan, R.R. (2003) Sp1 and Sp3 are oxidative stress-inducible, antideath transcription factors in cortical neurons. *The Journal of Neuroscience : The Official Journal of the Society for Neuroscience,* 23(9), 3597-3606.

236. Saeki, M., Kurose, K., Tohkin, M. and Hasegawa, R. (2008) Identification of the functional vitamin D response elements in the human MDR1 gene. *Biochemical Pharmacology,* 76(4), 531-542.

237. Saini, S.P., Mu, Y., Gong, H., Toma, D., Uppal, H., Ren, S., Li, S., Poloyac, S.M. and Xie, W. (2005) Dual role of orphan nuclear receptor pregnane X receptor in bilirubin detoxification in mice. *Hepatology (Baltimore, Md.),* 41(3), 497-505.

238. Sakakibara, Y., Katoh, M., Imai, K., Kondo, Y., Asai, Y., Ikushiro, S. and Nadai, M. (2016) Expression of UGT1A subfamily in rat brain. *Biopharmaceutics & Drug Disposition,* 37(5), 314-319.

239. Sampietro, M. and Iolascon, A. (1999) Molecular pathology of Crigler-Najjar type I and II and Gilbert's syndromes. *Haematologica,* 84(2), 150-157.

240. Sanchez-Dominguez, C.N., Gallardo-Blanco, H.L., Salinas-Santander, M.A. and Ortiz-Lopez, R. (2018) Uridine 5'-diphospho-glucronosyltrasferase: Its role in pharmacogenomics and human disease. *Experimental and Therapeutic Medicine,* 16(1), 3-11.

241. Sanchez-Dominguez, C.N., Gallardo-Blanco, H.L., Salinas-Santander, M.A. and Ortiz-Lopez, R. (2018) Uridine 5'-diphospho-glucronosyltrasferase: Its role in

pharmacogenomics and human disease. *Experimental and Therapeutic Medicine,* 16(1), 3-11.

242. Santoro, A.B., Vargens, D.D., Barros Filho Mde, C., Bulzico, D.A., Kowalski, L.P., Meirelles, R.M., Paula, D.P., Neves, R.R., Pessoa, C.N., Struchine, C.J. and Suarez-Kurtz, G. (2014) Effect of UGT1A1, UGT1A3, DIO1 and DIO2 polymorphisms on L-thyroxine doses required for TSH suppression in patients with differentiated thyroid cancer. *British Journal of Clinical Pharmacology,* 78(5), 1067-1075.

243. Schmiedlin-Ren, P., Thummel, K.E., Fisher, J.M., Paine, M.F., Lown, K.S. and Watkins, P.B. (1997) Expression of enzymatically active CYP3A4 by Caco-2 cells grown on extracellular matrix-coated permeable supports in the presence of 1alpha,25-dihydroxyvitamin D3. *Molecular Pharmacology,* 51(5), 741-754.

244. Schwab, M., Reynders, V., Loitsch, S., Steinhilber, D., Schroder, O. and Stein, J. (2008) The dietary histone deacetylase inhibitor sulforaphane induces human beta-defensin-2 in intestinal epithelial cells. *Immunology,* 125(2), 241-251.

245. Seldon, M.P., Silva, G., Pejanovic, N., Larsen, R., Gregoire, I.P., Filipe, J., Anrather, J. and Soares, M.P. (2007) Heme oxygenase-1 inhibits the expression of adhesion molecules associated with endothelial cell activation via inhibition of NF-kappaB RelA phosphorylation at serine 276. *Journal of Immunology (Baltimore, Md.: 1950),* 179(11), 7840-7851.

246. Seo, Y.K., Mirkheshti, N., Song, C.S., Kim, S., Dodds, S., Ahn, S.C., Christy, B., Mendez-Meza, R., Ittmann, M.M., Abboud-Werner, S. and Chatterjee, B. (2013) SULT2B1b sulfotransferase: induction by vitamin D receptor and reduced expression in prostate cancer. *Molecular Endocrinology (Baltimore, Md.),* 27(6), 925-939.

247. Seuter, S., Neme, A. and Carlberg, C. (2017) Epigenomic PU.1-VDR crosstalk modulates vitamin D signaling. *Biochimica Et Biophysica Acta.Gene Regulatory Mechanisms,* 1860(4), 405-415.

248. Shen, G. and Kong, A.N. (2009) Nrf2 plays an important role in coordinated regulation of Phase II drug metabolism enzymes and Phase III drug transporters. *Biopharmaceutics & Drug Disposition,* 30(7), 345-355.

249. Shen, J., Rasmussen, M., Dong, Q.R., Tepel, M. and Scholze, A. (2017) Expression of the NRF2 Target Gene NQO1 Is Enhanced in Mononuclear Cells in

Human Chronic Kidney Disease. *Oxidative Medicine and Cellular Longevity,* 2017, 9091879.

250. Shigematsu, T., Horiuchi, N., Ogura, Y., Miyahara, T. and Suda, T. (1986) Human parathyroid hormone inhibits renal 24-hydroxylase activity of 25-hydroxyvitamin D3 by a mechanism involving adenosine 3',5'-monophosphate in rats. *Endocrinology,* 118(4), 1583-1589.

251. Shin, J. et al., 2010. Vitamin D effects on pregnancy and the placenta. *Placenta*, 31(12), pp.1027–1034.

252. Singh, R.P. and Agarwal, R. (2005) Prostate cancer and inositol hexaphosphate: efficacy and mechanisms. *Anticancer Research,* 25(4), 2891-2903.

253. Sita, G., Hrelia, P., Tarozzi, A. and Morroni, F. (2016) Isothiocyanates Are Promising Compounds against Oxidative Stress, Neuroinflammation and Cell Death that May Benefit Neurodegeneration in Parkinson's Disease. *International Journal of Molecular Sciences,* 17(9), 10.3390/ijms17091454.

254. Sonoda, J., Pei, L. and Evans, R.M. (2008) Nuclear receptors: decoding metabolic disease. *FEBS Letters,* 582(1), 2-9.

255. Spiro, A. and Buttriss, J.L. (2014) Vitamin D: An overview of vitamin D status and intake in Europe. *Nutrition Bulletin,* 39(4), 322-350.

256. Sridar, C., Hanna, I. and Hollenberg, P.F. (2013) Quantitation of UGT1A1 in human liver microsomes using stable isotope-labelled peptides and mass spectrometry based proteomic approaches. *Xenobiotica; the Fate of Foreign Compounds in Biological Systems,* 43(4), 336-345.

257. Stees, J.S., Varn, F., Huang, S., Strouboulis, J. and Bungert, J. (2012) Recruitment of transcription complexes to enhancers and the role of enhancer transcription. *Biology*, 1(3), 778-793.

258. Strassburg, C.P., Manns, M.P. and Tukey, R.H. (1998) Expression of the UDP-glucuronosyltransferase 1A locus in human colon. Identification and characterization of the novel extrahepatic UGT1A8. *The Journal of Biological Chemistry*, 273(15), 8719-8726.

259. Strassburg, C.P., Nguyen, N., Manns, M.P. and Tukey, R.H. (1998) Polymorphic expression of the UDP-glucuronosyltransferase UGT1A gene locus in human gastric epithelium. *Molecular Pharmacology*, 54(4), 647-654.

260. Strassburg, C.P., Oldhafer, K., Manns, M.P. and Tukey, R.H. (1997) Differential expression of the UGT1A locus in human liver, biliary, and gastric tissue: identification of UGT1A7 and UGT1A10 transcripts in extrahepatic tissue. *Molecular Pharmacology,* 52(2), 212-220.

261. Strassburg, C.P., Strassburg, A., Kneip, S., Barut, A., Tukey, R.H., Rodeck, B. and Manns, M.P. (2002) Developmental aspects of human hepatic drug glucuronidation in young children and adults. *Gut,* 50(2), 259-265.

262. Strassburg, C.P., Strassburg, A., Nguyen, N., Li, Q., Manns, M.P. and Tukey, R.H. (1999) Regulation and function of family 1 and family 2 UDP-glucuronosyltransferase genes (UGT1A, UGT2B) in human oesophagus. *The Biochemical Journal,* 338 (Pt 2)(Pt 2), 489-498.

263. Strassburg, C.P., Vogel, A., Kneip, S., Tukey, R.H. and Manns, M.P. (2002) Polymorphisms of the human UDP-glucuronosyltransferase (UGT) 1A7 gene in colorectal cancer. *Gut,* 50(6), 851-856.

264. Sueyoshi, T. and Negishi, M. (2001) Phenobarbital response elements of cytochrome P450 genes and nuclear receptors. *Annual Review of Pharmacology and Toxicology,* 41, 123-143.

265. Sugatani, J., Mizushima, K., Osabe, M., Yamakawa, K., Kakizaki, S., Takagi, H., Mori, M., Ikari, A. and Miwa, M. (2008) Transcriptional regulation of human UGT1A1 gene expression through distal and proximal promoter motifs: implication of defects in the UGT1A1 gene promoter. *Naunyn-Schmiedeberg's Archives of Pharmacology,* 377(4-6), 597-605.

266. Sugatani, J., Sueyoshi, T., Negishi, M. and Miwa, M. (2005) Regulation of the human UGT1A1 gene by nuclear receptors constitutive active/androstane receptor, pregnane X receptor, and glucocorticoid receptor. *Methods in Enzymology,* 400, 92-104.

267. Sugatani, J., Uchida, T., Kurosawa, M., Yamaguchi, M., Yamazaki, Y., Ikari, A. and Miwa, M. (2012) Regulation of pregnane X receptor (PXR) function and UGT1A1 gene expression by posttranslational modification of PXR protein. *Drug Metabolism and Disposition: The Biological Fate of Chemicals,* 40(10), 2031-2040.

268. Sugatani, J., Yamakawa, K., Tonda, E., Nishitani, S., Yoshinari, K., Degawa, M., Abe, I., Noguchi, H. and Miwa, M. (2004) The induction of human UDP-

glucuronosyltransferase 1A1 mediated through a distal enhancer module by flavonoids and xenobiotics. *Biochemical Pharmacology,* 67(5), 989-1000.

269. Sumida, K., Kawana, M., Kouno, E., Itoh, T., Takano, S., Narawa, T., Tukey, R.H. and Fujiwara, R. (2013) Importance of UDP-glucuronosyltransferase 1A1 expression in skin and its induction by UVB in neonatal hyperbilirubinemia. *Molecular Pharmacology,* 84(5), 679-686.

270. Sun, L., Li, M., Zhang, L., Teng, X., Chen, X., Zhou, X., Ma, Z., Qi, L. and Wang, P. (2017) Differences in UGT1A1 gene mutations and pathological liver changes between Chinese patients with Gilbert syndrome and Crigler-Najjar syndrome type II. *Medicine,* 96(45), e8620.

271. Sutiman, N., Lim, J.S.L., Muerdter, T.E., Singh, O., Cheung, Y.B., Ng, R.C.H., Yap, Y.S., Wong, N.S., Ang, P.C.S., Dent, R., Schroth, W., Schwab, M., Khor, C.C. and Chowbay, B. (2016) Pharmacogenetics of UGT1A4, UGT2B7 and UGT2B15 and Their Influence on Tamoxifen Disposition in Asian Breast Cancer Patients. *Clinical Pharmacokinetics,* 55(10), 1239-1250.

272. Suzuki, T., Mihara, K., Nagai, G., Kagawa, S., Nakamura, A., Nemoto, K. and Kondo, T. (2019) Relationship Between UGT1A4 and UGT2B7 Polymorphisms and the Steady-State Plasma Concentrations of Lamotrigine in Patients With Treatment-Resistant Depressive Disorder Receiving Lamotrigine as Augmentation Therapy. *Therapeutic Drug Monitoring,* 41(1), 86-90.

273. Swami, S., Raghavachari, N., Muller, U.R., Bao, Y.P. and Feldman, D. (2003) Vitamin D growth inhibition of breast cancer cells: gene expression patterns assessed by cDNA microarray. *Breast Cancer Research and Treatment,* 80(1), 49-62.

274. Takahashi, N., Udagawa, N. and Suda, T. (2014) Vitamin D endocrine system and osteoclasts. *BoneKEy Reports,* 3, 495.

275. Tan, J.S., Mohandas, N. and Conboy, J.G. (2006) High frequency of alternative first exons in erythroid genes suggests a critical role in regulating gene function. *Blood,* 107(6), 2557-2561.

276. Tan, K.P., Yang, M. and Ito, S. (2007) Activation of nuclear factor (erythroid-2 like) factor 2 by toxic bile acids provokes adaptive defense responses to enhance cell survival at the emergence of oxidative stress. *Molecular Pharmacology,* 72(5), 1380-1390.

277. Tang, W., Fu, Y.P., Figueroa, J.D., Malats, N., Garcia-Closas, M., Chatterjee, N., Kogevinas, M., Baris, D., Thun, M., Hall, J.L., De Vivo, I., Albanes, D., Porter-Gill, P., Purdue, M.P., Burdett, L., Liu, L., Hutchinson, A., Myers, T., Tardon, A., Serra, C., Carrato, A., Garcia-Closas, R., Lloreta, J., Johnson, A., Schwenn, M., Karagas, M.R., Schned, A., Black, A., Jacobs, E.J., Diver, W.R., Gapstur, S.M., Virtamo, J., Hunter, D.J., Fraumeni, J.F.,Jr, Chanock, S.J., Silverman, D.T., Rothman, N. and Prokunina-Olsson, L. (2012) Mapping of the UGT1A locus identifies an uncommon coding variant that affects mRNA expression and protects from bladder cancer. *Human Molecular Genetics,* 21(8), 1918-1930.

278. Tebay, L.E., Robertson, H., Durant, S.T., Vitale, S.R., Penning, T.M., Dinkova-Kostova, A.T. and Hayes, J.D. (2015) Mechanisms of activation of the transcription factor Nrf2 by redox stressors, nutrient cues, and energy status and the pathways through which it attenuates degenerative disease. *Free Radical Biology & Medicine,* 88(Pt B), 108-146.

279. Tebben, P.J., Singh, R.J. and Kumar, R. (2016) Vitamin D-Mediated Hypercalcemia: Mechanisms, Diagnosis, and Treatment. *Endocrine Reviews,* 37(5), 521-547.

280. Tebben, P.J., Singh, R.J. and Kumar, R. (2016) Vitamin D-Mediated Hypercalcemia: Mechanisms, Diagnosis, and Treatment. *Endocrine Reviews,* 37(5), 521-547.

281. Teichert, A., Arnold, L.A., Otieno, S., Oda, Y., Augustinaite, I., Geistlinger, T.R., Kriwacki, R.W., Guy, R.K. and Bikle, D.D. (2009) Quantification of the vitamin D receptor-coregulator interaction. *Biochemistry,* 48(7), 1454-1461.

282. Teixeira, T.M., da Costa, D.C., Resende, A.C., Soulage, C.O., Bezerra, F.F. and Daleprane, J.B. (2017) Activation of Nrf2-Antioxidant Signaling by 1,25-Dihydroxycholecalciferol Prevents Leptin-Induced Oxidative Stress and Inflammation in Human Endothelial Cells. *The Journal of Nutrition,* 147(4), 506-513.

283. Thimmulappa, R.K., Lee, H., Rangasamy, T., Reddy, S.P., Yamamoto, M., Kensler, T.W. and Biswal, S. (2006) Nrf2 is a critical regulator of the innate immune response and survival during experimental sepsis. *The Journal of Clinical Investigation,* 116(4), 984-995.

284. Thompson, P.D., Jurutka, P.W., Whitfield, G.K., Myskowski, S.M., Eichhorst, K.R., Dominguez, C.E., Haussler, C.A. and Haussler, M.R. (2002) Liganded VDR induces CYP3A4 in small intestinal and colon cancer cells via DR3 and ER6 vitamin D responsive elements. *Biochemical and Biophysical Research Communications,* 299(5), 730-738.

285. Thompson, P.D., Jurutka, P.W., Whitfield, G.K., Myskowski, S.M., Eichhorst, K.R., Dominguez, C.E., Haussler, C.A. and Haussler, M.R. (2002) Liganded VDR induces CYP3A4 in small intestinal and colon cancer cells via DR3 and ER6 vitamin D responsive elements. *Biochemical and Biophysical Research Communications,* 299(5), 730-738.

286. Thummel, K.E., Brimer, C., Yasuda, K., Thottassery, J., Senn, T., Lin, Y., Ishizuka, H., Kharasch, E., Schuetz, J. and Schuetz, E. (2001) Transcriptional control of intestinal cytochrome P-4503A by 1alpha,25-dihydroxy vitamin D3. *Molecular Pharmacology,* 60(6), 1399-1406.

287. Tian, H., Li, X., Jiang, W., Lv, C., Sun, W., Huang, C. and Chen, R. (2016) High expression of AKR1C1 is associated with proliferation and migration of small-cell lung cancer cells. *Lung Cancer (Auckland, N.Z.),* 7, 53-61.

288. To, C., Ringelberg, C.S., Royce, D.B., Williams, C.R., Risingsong, R., Sporn, M.B. and Liby, K.T. (2015) Dimethyl fumarate and the oleanane triterpenoids, CDDO-imidazolide and CDDO-methyl ester, both activate the Nrf2 pathway but have opposite effects in the A/J model of lung carcinogenesis. *Carcinogenesis,* 36(7), 769-781.

289. Tong, K.I., Kobayashi, A., Katsuoka, F. and Yamamoto, M. (2006) Two-site substrate recognition model for the Keap1-Nrf2 system: a hinge and latch mechanism. *Biological Chemistry,* 387(10-11), 1311-1320.

290. Torino, C., Pizzini, P., Cutrupi, S., Tripepi, R., Vilasi, A., Tripepi, G., Mallamaci, F. and Zoccali, C. (2017) Effect of Vitamin D Receptor Activation on the AGE/RAGE System and Myeloperoxidase in Chronic Kidney Disease Patients. *Oxidative Medicine and Cellular Longevity,* 2017, 2801324.

291. Tripkovic, L., Lambert, H., Hart, K., Smith, C.P., Bucca, G., Penson, S., Chope, G., Hypponen, E., Berry, J., Vieth, R. and Lanham-New, S. (2012) Comparison of vitamin D2 and vitamin D3 supplementation in raising serum 25-

hydroxyvitamin D status: a systematic review and meta-analysis. *The American Journal of Clinical Nutrition,* 95(6), 1357-1364.

292. Tsujikawa, H., Kurotaki, Y., Fujimori, T., Fukuda, K. and Nabeshima, Y., 2003. *Klotho, A Gene Related To A Syndrome Resembling Human Premature Aging, Functions In A Negative Regulatory Circuit Of Vitamin D Endocrine System*.

293. Tukey, R.H. and Strassburg, C.P. (2000) Human UDP-glucuronosyltransferases: metabolism, expression, and disease. *Annual Review of Pharmacology and Toxicology,* 40, 581-616.

294. Turgeon, D., Carrier, J.S., Levesque, E., Hum, D.W. and Belanger, A. (2001) Relative enzymatic activity, protein stability, and tissue distribution of human steroid-metabolizing UGT2B subfamily members. *Endocrinology,* 142(2), 778-787.

295. Ullah, S., Rahman, K. and Hedayati, M. (2016) Hyperbilirubinemia in Neonates: Types, Causes, Clinical Examinations, Preventive Measures and Treatments: A Narrative Review Article. *Iranian Journal of Public Health,* 45(5), 558-568.

296. Valko, M., Leibfritz, D., Moncol, J., Cronin, M.T., Mazur, M. and Telser, J. (2007) Free radicals and antioxidants in normal physiological functions and human disease. *The International Journal of Biochemistry & Cell Biology,* 39(1), 44-84.

297. VanWagner, L.B. and Green, R.M. (2015) Evaluating elevated bilirubin levels in asymptomatic adults. *Jama,* 313(5), 516-517.

298. Veldurthy, V., Wei, R., Oz, L., Dhawan, P., Jeon, Y.H. and Christakos, S. (2016) Vitamin D, calcium homeostasis and aging. *Bone Research,* 4, 16041.

299. Verreault, M., Senekeo-Effenberger, K., Trottier, J., Bonzo, J.A., Belanger, J., Kaeding, J., Staels, B., Caron, P., Tukey, R.H. and Barbier, O. (2006) The liver X-receptor alpha controls hepatic expression of the human bile acid-glucuronidating UGT1A3 enzyme in human cells and transgenic mice. *Hepatology (Baltimore, Md.),* 44(2), 368-378.

300. Vomund, S., Schafer, A., Parnham, M.J., Brune, B. and von Knethen, A. (2017) Nrf2, the Master Regulator of Anti-Oxidative Responses. *International Journal of Molecular Sciences,* 18(12), 10.3390/ijms18122772.

301. Vukic, M., Neme, A., Seuter, S., Saksa, N., de Mello, V.D., Nurmi, T., Uusitupa, M., Tuomainen, T.P., Virtanen, J.K. and Carlberg, C. (2015) Relevance of vitamin D receptor target genes for monitoring the vitamin D responsiveness of primary human cells. *PloS One,* 10(4), e0124339.

302. Vukovic, M., Radlovic, N., Lekovic, Z., Vucicevic, K., Maric, N., Kotur, N., Gasic, V., Ugrin, M., Stojiljkovic, M., Dokmanovic, L., Zukic, B. and Pavlovic, S. (2018) UGT1A1 (TA)n Promoter Genotype: Diagnostic and Population Pharmacogenetic Marker in Serbia. *Balkan Journal of Medical Genetics : BJMG,* 21(1), 59-68.

303. Wagner, K.H., Shiels, R.G., Lang, C.A., Seyed Khoei, N. and Bulmer, A.C. (2018) Diagnostic criteria and contributors to Gilbert's syndrome. *Critical Reviews in Clinical Laboratory Sciences,* 55(2), 129-139.

304. Wagner, M., Halilbasic, E., Marschall, H.U., Zollner, G., Fickert, P., Langner, C., Zatloukal, K., Denk, H. and Trauner, M. (2005) CAR and PXR agonists stimulate hepatic bile acid and bilirubin detoxification and elimination pathways in mice. *Hepatology (Baltimore, Md.),* 42(2), 420-430.

305. Wakabayashi, N., Chartoumpekis, D.V. and Kensler, T.W. (2015) Crosstalk between Nrf2 and Notch signaling. *Free Radical Biology & Medicine,* 88(Pt B), 158-167.

306. Wakabayashi, N., Dinkova-Kostova, A.T., Holtzclaw, W.D., Kang, M.I., Kobayashi, A., Yamamoto, M., Kensler, T.W. and Talalay, P. (2004) Protection against electrophile and oxidant stress by induction of the phase 2 response: fate of cysteines of the Keap1 sensor modified by inducers. *Proceedings of the National Academy of Sciences of the United States of America,* 101(7), 2040-2045.

307. Wallace, B.D., Betts, L., Talmage, G., Pollet, R.M., Holman, N.S. and Redinbo, M.R. (2013) Structural and functional analysis of the human nuclear xenobiotic receptor PXR in complex with RXRalpha. *Journal of Molecular Biology,* 425(14), 2561-2577.

308. Walle, T., Otake, Y., Galijatovic, A., Ritter, J.K. and Walle, U.K. (2000) Induction of UDP-glucuronosyltransferase UGT1A1 by the flavonoid chrysin in the human hepatoma cell line hep G2. *Drug Metabolism and Disposition: The Biological Fate of Chemicals,* 28(9), 1077-1082.

309. Wang, H., Bian, T., Jin, T., Chen, Y., Lin, A. and Chen, C. (2014) Association analysis of UGT1A genotype and haplotype with SN-38 glucuronidation in human livers. *Pharmacogenomics,* 15(6), 785-798.

310. Wang, L., Zhou, S. and Guo, B. (2020) Vitamin D Suppresses Ovarian Cancer Growth and Invasion by Targeting Long Non-Coding RNA CCAT2. *International Journal of Molecular Sciences,* 21(7), 10.3390/ijms21072334.

311. Wang, M., Li, Y.Q., Zhong, N., Chen, J., Xu, X.Q. and Yuan, M.B. (2005) Induction of uridine 5'-diphosphate-glucuronosyltransferase gene expression by sulforaphane and its mechanism: experimental study in human colon cancel cells. *Zhonghua Yi Xue Za Zhi,* 85(12), 819-824.

312. Wang, M., Li, Y.Q., Zhong, N., Chen, J., Xu, X.Q. and Yuan, M.B. (2005) Induction of uridine 5'-diphosphate-glucuronosyltransferase gene expression by sulforaphane and its mechanism: experimental study in human colon cancel cells. *Zhonghua Yi Xue Za Zhi,* 85(12), 819-824.

313. Wang, T.T., Tavera-Mendoza, L.E., Laperriere, D., Libby, E., MacLeod, N.B., Nagai, Y., Bourdeau, V., Konstorum, A., Lallemant, B., Zhang, R., Mader, S. and White, J.H. (2005) Large-scale in silico and microarray-based identification of direct 1,25-dihydroxyvitamin D3 target genes. *Molecular Endocrinology (Baltimore, Md.),* 19(11), 2685-2695.

314. Wang, X., Wang, H., Shen, B., Overholser, B.R., Cooper, B.R., Lu, Y., Tang, H., Zhou, C., Sun, X., Zhong, L., Favus, M.J., Decker, B.S., Liu, W. and Peng, Z. (2016) 1-Alpha, 25-dihydroxyvitamin D3 alters the pharmacokinetics of mycophenolic acid in renal transplant recipients by regulating two extrahepatic UDP-glucuronosyltransferases 1A8 and 1A10. *Translational Research : The Journal of Laboratory and Clinical Medicine,* 178, 54-62.e6.

315. Wang, Y., Shen, L., Xu, N., Wang, J.W., Jiao, S.C., Liu, Z.Y. and Xu, J.M. (2012) UGT1A1 predicts outcome in colorectal cancer treated with irinotecan and fluorouracil. *World Journal of Gastroenterology,* 18(45), 6635-6644.

316. Wang, Z., Schuetz, E.G., Xu, Y. and Thummel, K.E. (2013) Interplay between vitamin D and the drug metabolizing enzyme CYP3A4. *The Journal of Steroid Biochemistry and Molecular Biology,* 136, 54-58.

317. Wang, Z., Wong, T., Hashizume, T., Dickmann, L.Z., Scian, M., Koszewski, N.J., Goff, J.P., Horst, R.L., Chaudhry, A.S., Schuetz, E.G. and Thummel, K.E.

(2014) Human UGT1A4 and UGT1A3 conjugate 25-hydroxyvitamin D3: metabolite structure, kinetics, inducibility, and interindividual variability. *Endocrinology,* 155(6), 2052-2063.

318. Wardyn, J.D., Ponsford, A.H. and Sanderson, C.M. (2015) Dissecting molecular cross-talk between Nrf2 and NF-kappaB response pathways. *Biochemical Society Transactions,* 43(4), 621-626.

319. Watai, Y., Kobayashi, A., Nagase, H., Mizukami, M., McEvoy, J., Singer, J.D., Itoh, K. and Yamamoto, M. (2007) Subcellular localization and cytoplasmic complex status of endogenous Keap1. *Genes to Cells : Devoted to Molecular & Cellular Mechanisms,* 12(10), 1163-1178.

320. Webb, A.R., DeCosta, B.R. and Holick, M.F. (1989) Sunlight regulates the cutaneous production of vitamin D3 by causing its photodegradation. *The Journal of Clinical Endocrinology and Metabolism,* 68(5), 882-887.

321. Weerachayaphorn, J., Mennone, A., Soroka, C.J., Harry, K., Hagey, L.R., Kensler, T.W. and Boyer, J.L. (2012) Nuclear factor-E2-related factor 2 is a major determinant of bile acid homeostasis in the liver and intestine. *American Journal of Physiology.Gastrointestinal and Liver Physiology,* 302(9), G925-36.

322. Wong, C.H. and Ko, W.H. (2002) Stimulation of Cl- secretion via membrane-restricted Ca2+ signaling mediated by P2Y receptors in polarized epithelia. *The Journal of Biological Chemistry,* 277(11), 9016-9021.

323. Wu, K.C., McDonald, P.R., Liu, J. and Klaassen, C.D. (2014) Screening of natural compounds as activators of the keap1-nrf2 pathway. *Planta Medica,* 80(1), 97-104.

324. Wu, R.P., Hayashi, T., Cottam, H.B., Jin, G., Yao, S., Wu, C.C., Rosenbach, M.D., Corr, M., Schwab, R.B. and Carson, D.A. (2010) Nrf2 responses and the therapeutic selectivity of electrophilic compounds in chronic lymphocytic leukemia. *Proceedings of the National Academy of Sciences of the United States of America,* 107(16), 7479-7484.

325. Xiang, W., Kong, J., Chen, S., Cao, L.P., Qiao, G., Zheng, W., Liu, W., Li, X., Gardner, D.G. and Li, Y.C. (2005) Cardiac hypertrophy in vitamin D receptor knockout mice: role of the systemic and cardiac renin-angiotensin systems. *American Journal of Physiology.Endocrinology and Metabolism,* 288(1), E125-32.

326. Xie, W., Yeuh, M.F., Radominska-Pandya, A., Saini, S.P., Negishi, Y., Bottroff, B.S., Cabrera, G.Y., Tukey, R.H. and Evans, R.M. (2003) Control of steroid, heme, and carcinogen metabolism by nuclear pregnane X receptor and constitutive androstane receptor. *Proceedings of the National Academy of Sciences of the United States of America,* 100(7), 4150-4155.

327. Xu, C., Li, C.Y. and Kong, A.N. (2005) Induction of phase I, II and III drug metabolism/transport by xenobiotics. *Archives of Pharmacal Research,* 28(3), 249-268.

328. Xue, D., Zhou, C., Shi, Y., Lu, H., Xu, R. and He, X. (2016) Nuclear transcription factor Nrf2 suppresses prostate cancer cells growth and migration through upregulating ferroportin. *Oncotarget,* 7(48), 78804-78812.

329. Yang, G., Ge, S., Singh, R., Basu, S., Shatzer, K., Zen, M., Liu, J., Tu, Y., Zhang, C., Wei, J., Shi, J., Zhu, L., Liu, Z., Wang, Y., Gao, S. and Hu, M. (2017) Glucuronidation: driving factors and their impact on glucuronide disposition. *Drug Metabolism Reviews,* 49(2), 105-138.

330. Yang, H., Magilnick, N., Lee, C., Kalmaz, D., Ou, X., Chan, J.Y. and Lu, S.C. (2005) Nrf1 and Nrf2 regulate rat glutamate-cysteine ligase catalytic subunit transcription indirectly via NF-kappaB and AP-1. *Molecular and Cellular Biology,* 25(14), 5933-5946.

331. Yang, Y., Zhou, M., Hu, M., Cui, Y., Zhong, Q., Liang, L. and Huang, F. (2018) UGT1A1*6 and UGT1A1*28 polymorphisms are correlated with irinotecan-induced toxicity: A meta-analysis. *Asia-Pacific Journal of Clinical Oncology*, 14(5), e479-e489.

332. Yilmaz, L., Borazan, E., Aytekin, T., Baskonus, I., Aytekin, A., Oztuzcu, S., Bozdag, Z. and Balik, A. (2015) Increased UGT1A3 and UGT1A7 expression is associated with pancreatic cancer. *Asian Pacific Journal of Cancer Prevention : APJCP*, 16(4), 1651-1655.

333. Yueh, M.F. and Tukey, R.H. (2007) Nrf2-Keap1 signaling pathway regulates human UGT1A1 expression in vitro and in transgenic UGT1 mice. *The Journal of Biological Chemistry,* 282(12), 8749-8758.

334. Zagorski, J.W., Turley, A.E., Dover, H.E., VanDenBerg, K.R., Compton, J.R. and Rockwell, C.E. (2013) The Nrf2 activator, tBHQ, differentially affects early

events following stimulation of Jurkat cells. *Toxicological Sciences : An Official Journal of the Society of Toxicology,* 136(1), 63-71.

335. Zanardo, V., Golin, R., Amato, M., Trevisanuto, D., Favaro, F., Faggian, D. and Plebani, M. (2007) Cytokines in human colostrum and neonatal jaundice. *Pediatric Research,* 62(2), 191-194.

336. Zella, L.A., Kim, S., Shevde, N.K. and Pike, J.W. (2006) Enhancers located within two introns of the vitamin D receptor gene mediate transcriptional autoregulation by 1,25-dihydroxyvitamin D3. *Molecular Endocrinology (Baltimore, Md.),* 20(6), 1231-1247.

337. Zella, L.A., Meyer, M.B., Nerenz, R.D., Lee, S.M., Martowicz, M.L. and Pike, J.W. (2010) Multifunctional enhancers regulate mouse and human vitamin D receptor gene transcription. *Molecular Endocrinology (Baltimore, Md.),* 24(1), 128-147.

338. Zhang, D.D., Lo, S.C., Cross, J.V., Templeton, D.J. and Hannink, M. (2004) Keap1 is a redox-regulated substrate adaptor protein for a Cul3-dependent ubiquitin ligase complex. *Molecular and Cellular Biology,* 24(24), 10941-10953.

339. Zhang, L., Huang, M., Blair, I.A. and Penning, T.M. (2013) Interception of benzo[a]pyrene-7,8-dione by UDP glucuronosyltransferases (UGTs) in human lung cells. *Chemical Research in Toxicology,* 26(10), 1570-1578.

340. Zhang, Z.M., Yang, X.Y., Yuan, J.H., Sun, Z.Y. and Li, Y.Q. (2009) Modulation of NRF2 and UGT1A expression by epigallocatechin-3-gallate in colon cancer cells and BALB/c mice. *Chinese Medical Journal,* 122(14), 1660-1665.

341. Zhao, C., Wang, X., Cong, Y., Deng, Y., Xu, Y., Chen, A. and Yin, Y. (2014) Effects of bile acids and the bile acid receptor FXR agonist on the respiratory rhythm in the in vitro brainstem medulla slice of neonatal Sprague-Dawley rats. *PloS One,* 9(11), e112212.

342. Zheng, Z., Park, J.Y., Guillemette, C., Schantz, S.P. and Lazarus, P. (2001) Tobacco carcinogen-detoxifying enzyme UGT1A7 and its association with orolaryngeal cancer risk. *Journal of the National Cancer Institute,* 93(18), 1411-1418.

343. Zhou, C., Poulton, E.J., Grun, F., Bammler, T.K., Blumberg, B., Thummel, K.E. and Eaton, D.L. (2007) The dietary isothiocyanate sulforaphane is an

antagonist of the human steroid and xenobiotic nuclear receptor. *Molecular Pharmacology*, 71(1), 220-229.

344. Zundorf, G. and Reiser, G. (2011) Calcium dysregulation and homeostasis of neural calcium in the molecular mechanisms of neurodegenerative diseases provide multiple targets for neuroprotection. *Antioxidants & Redox Signaling*, 14(7), 1275-1288.

8: Appendix

ORAL PRESENTATIONS

21st Vitamin D Workshop, Barcelona, Spain AND Biomedical Science Post graduate Society Conference, Coleraine :

- Regulation of *Regulation of UDP-glucuronosyltransferase 1A gene family members by Vitamin D Receptor*. **Dube, K.,**Goodman, R., Rodriguez E.P., Pike,W., Meyer B., Thompson, P.D., 2018

SUPERVISION EXPERIENCE

- **Laboratory Demonstrator to Undergraduate Students of :**
  Clinical Biochemistry
  Clinical Haemotology
  Clinical and Molecular Genetics

AWARDS

- Trainee Travel Award ($500) - 21st Vitamin D Workshop, Barcelona, Spain
- ILM Level 5 Diploma in Leadership and Management
- 3MT (3 minute thesis) Semi- Finalist